
# An Investigation of the Bioactivity of Cyanobacterial Exometabolites in Plant Stress Tolerance

**Alysha Chua BSc, MRes**

This thesis is submitted to Waterford Institute *of* Technology in fulfilment of the thesis requirement for the degree of Doctor of Philosophy.

Based on research undertaken in the School of Science and Computing, Waterford Institute *of* Technology, Waterford

under the supervision of:

Dr. Cara Daly and Dr. Laurence Fitzhenry

Submitted to Waterford Institute *of* Technology July, 2019

I hereby declare that I am the sole author of this thesis. I authorise Waterford Institute of Technology to lend or photocopy this thesis in whole or part to other institutions or individuals for the purposes of scholarly research.

_____

Alysha Chua

# Acknowledgements

There are so many people to thank and words can never convey the depth of gratefulness I have. But I shall try. To my incredible family back home who always believed in me, it's been nine long years since I left home shores and I miss you guys so much. It's been a long road, but it's finally done. Thank you, thank you, thank you, for always being there. Please don't worry about me anymore, it's my turn to take care of you now! Up next are my amazing supervisors, Cara and Larry. Thanks for taking a chance on me all those years ago, you changed the life trajectory of a small-town girl. Thank you for always encouraging me when work got me down and having faith in me to pursue all the strange twist and turns this project took. Your unwavering confidence and kind words helped to drive me over the finish line and I'm forever indebted for that.

Big shout-outs to my fellow PhD comrades, who were always there for a quick chat and laugh. I've never met such a nice bunch of folks in a lab before, it was almost unsettling how quick everyone was to offer a hand whenever a problem cropped up. Who knew that trouble-shooting could be fun, when you're doing it with friends? Thank you and best of luck in your own journeys. Up next are the wonderful WIT lab technicians and porters. Thanks for giving me leeway when I needed extra reagents and not losing your tempers when I got locked in the campus. I'm out of your hair now, so you'll be free of my shenanigans!

I can't forget the wonderful friends I've met over the years, especially the folks of Bramble Grove. Thank you for the late-night conversations and encouragement given over the years. Lifelong friendships are hard to build, but we somehow managed it. Lastly, to Kong Kong. I am sorry you couldn't get to see this. But I did it. It feels strange dedicating a thesis to someone not around anymore, but I will anyhow. This thesis is for you, in remembrance of all that you've done for the family. Our lives would not be the same, without all the sacrifices you took. So, thank you. This is for you.

# Abbreviations

AAAP = Amino acid/auxin permease

ABA = Abscisic acid

ABFs = ABRE-binding factors

ACC = 1-aminocyclopropane-1-carboxylate

AGEs = Advanced glycation end products

AL-PCD = Apoptotic-like programmed cell death

APX = Ascorbate peroxidase

AREBPs = ABA-response-element-binding proteins

ARFs = Auxin response factors

Asp = Aspartic acid

ATF = Amino acid transporter

BG11 = Blue-Green 11 medium

BI-1 = Bax inhibitor-1

BNF = Biological nitrogen fixation

C1P = Ceramide-1-phosphate

CAT = Catalase

CDPK = Calcium-dependent protein kinase

CEF = Cyclic electron flow

CerK = Ceramidases kinase

CLPs = Caspase-like proteases

CM = Conditioned medium

CPS = Capsulated polysaccharides

Cyt *c* = Cytochrome *c*

Cys = Cysteine

DHAR = Dehydroascorbate reductase

DREB1A = Dehydration-responsive transcription factor

DW = Deionised water

EC = European Commission

ETC = Electron transport chain

EPS = exopolysaccharide

ER = Endoplasmic reticulum

erd genes = Early response to dehydration genes

ESI = Early-salt-induced

FDA = Fluorescein diacetate

GAs = Gibberellins

GC-MS = Gas chromatography-mass spectrometry

GlcNAc = 1,4-$\beta$-linked N-acetyl-D-glucosamine

GlcP = Glucose permease

Gly I = Glyoxalase I

Gly II = Glyoxalase II

Gly III = Glyoxalase III

GPOX = Guaiacol peroxidase

GPX = Glutathione peroxidase

GR = Glutathione reductase

GS = Glutamine synthetase

GS-GOGAT = Glutamine synthetase-glutamine synthase

GSH = Glutathione

GST = Glutathione S-transferase

HIF = Hormogonia-inducing factors

HPLC = High performance liquid chromatography

HR = Hypersensitive response

HSPs = Heat shock proteins

HSFs = Heat-shock factors

IAA = Indole-3-acetic acid

IMS = Intermembrane space

ISR = Induced systemic resistance

LCBs = Long-chain bases

LCB-Ps = Phosphorylated forms of long-chain bases

LCO = Lipo-chitooligosaccharide

LEA = Late embryogenesis abundant

LHT = Lysine-histidine transporter

MAPK = Mitogen-activated protein kinase

MDHAR = Monodehydroascorbate reductase

MET = Mitochondria electron transport

MG = Methylglyoxal

MMP = Mitochondrial membrane permeabilisation

MnSOD = Manganese superoxide dismutase

MS = Murashige and Skoog

MW = Molecular weight

NSAPs = Non-specific acid phosphatases

OEC = Oxygen-evolving complex

ORAC = Oxygen radical absorbance capacity

OsOAT = Ornithine ı-aminotransferase

P5C = Δ1-pyrroline-5-carboxlyate

P5CS1 = Pyrroline-5-carboxylate synthetase

PCD = Programmed cell death

PES = Polyethersulfone

PGPR = Plant growth promoting rhizobacteria

PITC = Phenyl isothiocyanate

PLGA = Poly (lactic-co-glycolic acid)

POD = Peroxidase

POX = Peroxidase

ProDH = Proline dehydrogenase

ProT = Proline transporter

PS I = Photosystem I

PSII = Photosystem II

PSM = Phosphate solubilising microorganisms

PTC = Phenylthiocarbamyl

PTP = Permeability transition pore

PVA = Polyvinyl alcohol

QTL = Quantitative trait loci

RAS/RT = Root adhering soil per root tissue

RFLP = Restriction fragment length polymorphism

RHA = Root hair assay

ROS = Reactive oxygen species

RPS = Released polysaccharide

RubisCO = Ribulose 1,5-bisphosphate carboxylase–oxygenase

RWC = Relative water content

S1P = Sphingosine-1-phosphate

SAR = Systematic acquired resistance

SB = Spring barley

SDW = Sterilised deionised water

sHSp = Small Hsps

SnRK2 = Sucrose non-fermenting 1-related protein kinase 2

SOD = Superoxide dismutase

SOS = Salt Overly Sensitive

SW = Spring wheat

TCP = Tricalcium phosphate

TEB = Tebuconazole

TPP = Tripolyphosphate

UF = Urea–formaldehyde

UPR = Unfolded protein response

VPEs = Vacuolar processing enzymes

VRN = Vernalization-responsive

WB = Winter barley

W/O = Water-in-oil

W/O/W = Water-in-oil-in-water

WW = Winter wheat

# Abstract

As the global population expands and climates rapidly change, reliable access to enough inexpensive, nutritious food is already a major problem. The challenge of enhancing food security cannot be at the expense of environmental damage, therefore sustainable agriculture must be a central tenet. Around the world, $N_2$-fixing inoculants like cyanobacteria are used in sustainable agriculture programmes to enhance yields and mitigate plant responses to stress. Presently, assessment of novel cereal varieties focuses mostly on high yields while screening for stress tolerance is an expensive, time-consuming process. However, it is proposed here that cell death modes, especially programmed cell death (PCD), can be used as a marker of plant stress tolerance. PCD is a normal facet of plant growth and development, but plant cells also activate environmentally-induced PCD as a protective mechanism during stress exposure and it is possible to limit stress-induced PCD to minimise crop yield losses. Here, it is shown that medium conditioned by the cyanobacteria *Nostoc muscorum* reduces PCD in stressed plant cells, and a further investigation identified proline as the major bioactive *N. muscorum*-derived compound.

To start, a root hair assay (RHA) was used as an *in vivo* tool to enumerate the overall plant stress response in *Arabidopsis thaliana* and to characterise the bioactivity of cyanobacteria *N. muscorum* conditioned medium (CM). Heat stressed *A. thaliana* exhibited reduced PCD when treated with *N. muscorum* CM fractions. Proline emerged as a bioactive candidate of interest and was confirmed in *N. muscorum* CM using the ninhydrin assay and HPLC. Furthermore, proline feeding experiments revealed a similar performance to CM but with marginally lower PCD suppression levels. Confirmation of proline as the main bioactive candidate was attained by treating mutant *Arabidopsis* lines with impaired proline transporters with exogenous proline and CM fractions.

The RHA was also successfully used as a high-throughput screening tool to pinpoint stress-tolerant and susceptible *Triticum aestivum* and *Hordeum vulgare* varieties. Heat stress experiments showed that winter and spring barley varieties could be subdivided into their seasonal groups based on their PCD susceptibility. Furthermore, stress-induced PCD levels were used to investigate basal, induced and cross-stress tolerance of eight wheat varieties to heat and salt stress. The RHA identified varieties with high basal tolerance based on their performance after single and combined stress exposure. However, these varieties also had an unexpectedly slower cross-stress tolerance response than their stress-susceptible counterparts, demonstrating slower flexibility against recurrent stress exposure.

Finally, to relate findings back to applications in sustainable agricultural practices, preliminary work to encapsulate proline in slow-release microspheres found that the maximum safe dosage of proline was 8 µM in *Arabidopsis*, 10 µM in barley and 100 µM in wheat; however, proline bioactivity was only effective at a narrow stress range. Collectively, this thesis demonstrates that cyanobacteria-derived proline elevates plant stress tolerance by inhibiting PCD and that by using the RHA, PCD is a convenient marker of plant stress tolerance and susceptibility. This offers preliminary evidence of a novel biofertiliser mechanism for enhancing plant stress tolerance independent of the existing mechanisms cited in the literature.

# Table of Contents

# Chapter 1 - Plant Growth Promoting (PGPR) Biofertilisers

With approximately 7.5 billion citizens in this world, a figure expected to increase to 9.7 billion by 2050 (United Nations 2017), agriculture must constantly evolve to meet the rising demands for food, while maintaining food security standards. This has broad implications in future crop production methods as improvement in yields must not come at the expense of the environment. However, conventional synthetic fertilisation methods have raised sustainability concerns as prolonged application without natural replenishment of organic matter in soils affect long-term soil fertility and soil water holding capacity (Choudhury *et al.* 2014). The unimpeded advancement of global warming increases the flooding incidences of rivers and lakes, which substantially increases the risk of nitrogen fertiliser run-off into watercourses (Levy *et al.* 2016).

Biofertilisers provide an interesting alternative to this problem; unlike conventional chemical fertilisation strategies, biofertilisers contain little macro and micro-nutrients themselves. Instead, the inoculants act as a catalyst for mobilising nutrients into metabolically accessible forms, which are otherwise not available to plants (Kennedy 2008). Depending on the functional characteristics of the inoculants, biofertilisers can either provide direct or indirect yield gains in crops. Direct benefits include making essential macronutrients for plant growth available through nitrogen fixation and phosphate solubilisation (Barreto *et al.* 2011). Conversely, indirect benefits rely on an assortment of mechanisms to protect against abiotic and biotic stresses: production of phytohormones, hydrolytic enzymes, siderophores, exopolysaccharide release, and upregulation of 1-aminocyclopropane-1-carboxylate (ACC) deaminase (Barreto *et al.* 2011). Bacteria with one or more of these functional characteristics are known as plant growth promoting rhizobacteria (PGPR) and are members of the phyla *Cyanobacteria*, *Actinobacteria*, *Bacteroidetes*, *Firmicutes*, and *Proteobacteria* (Barreto *et al.* 2011).

This chapter will explore the definition of biofertilisers and its legal discrepancies (Section 1.1) and the mechanisms of direct (Section 1.2) and indirect effects of biofertilisers on crop yield (Section 1.3). Following that, Section 1.4 details the usage of cyanobacteria biofertilisers, the mechanism of cyanobacteria and plant symbiosis (Section 1.4.1) and a literature review of all known *Nostoc muscorum* exometabolites

(Section 1.4.2) which are the subject of research in this thesis. Lastly, this chapter will explain the modes and hallmarks of plant cell death (Section 1.5*)* in the context of their use in the further development of the root hair assay (Section 1.5.3) to assess the *in vivo* effects of stress treatments.

# 1.1 Biofertiliser definition

The term 'biofertiliser' hints at a wide range of beneficial effects but in academic literature and legal frameworks, the term has a diverse array of definitions. Agriculture-centric countries have made a substantial effort to generate legislation to standardise biofertilisers and quality control of the biofertiliser products on the market. For example, the Vietnam Standard TCVN 6169-1996 legislation defines biofertilisers as a '…product containing a selected living micro-organism with a density that meets the requirement of the promulgated standard. Through the living activity of inoculated micro-organisms, nutrients like N, P, K and S can be available for plants, or biological substances can be produced that contribute to increasing plant yield or improving the quality of agricultural products' (Pham *et al.* 2008). India has the most comprehensive framework, first established under the Essentials Commodities Act of 1966 and Fertilizer Control Act 1985, and subsequently amended in 2006 and 2009 following new research developments (Sekar *et al.* 2016). In India, biofertilisers are legally defined as '…product(s) containing carrier base (solid or liquid) living microorganisms which are agriculturally useful in terms of nitrogen fixation, phosphorus solubilisation or nutrient mobilisation to increase the productivity of the soil and/or crop' (Sekar *et al.* 2016).

However, developed markets such as the European Union (EU) and USA do not have legal frameworks in place for biofertilisers (Malusá and Vassilev 2014). Under the European Union Commission Regulation 889/2008, all microbial products are classified as biological control agents, regardless of the mode of action (Malusá and Vassilev 2014). In efforts to clarify the regulatory proceedings, a report from the European Commission (EC) in 2014 by Amat *et al.* (2014) proposed distinguishing between biofertilisers, biostimulants and biocontrol agents. In the EC report, biofertilisers are proposed to be 'any substance or microorganism, in the form in which it is supplied to the user, added to a fertiliser, soil improver, growing medium with the intention to improve the agronomic efficacy of the final product and/or to modify the environmental fate of the nutrients released by the fertiliser, the soil improver or the growing medium, or any combination

of such substances and/or microorganisms intended for this use' (Amat *et al.* 2014). Biostimulants was proposed as the new umbrella term for biofertilisers and biocontrol agents, which Amat *et al.* (2014) defines as 'any substance or microorganism, in the form in which it is supplied to the user, applied to plants, seeds or the root environment with the intention to stimulate natural processes of plants to benefit their nutrient use efficiency and/or their tolerance to abiotic stress, regardless of its nutrients content, or any combination of such substances and/or microorganisms intended for this use'. Further details on the proposed reclassification of biofertilisers and biostimulants can be found in du Jardin (2015), written by the co-authors of the European Commission report.

However, redefining these terms requires a great deal of work, as most of the published literature does not adhere to the terms proposed by the EC (Amat *et al.* 2014) and du Jardin (2015). In the landmark review published by Vessey (2003), a biofertiliser is described as a 'substance which contains living microorganisms which, when applied to seed, plant surfaces, or soil, colonizes the rhizosphere or the interior of the plant and promotes growth by increasing the supply or availability of primary nutrients to the host plant'. However, this definition has a limited scope that focuses on macronutrient availability; it does not account for the indirect benefits of PGPR inoculation, such as phytohormone exudation, enhanced soil structure or higher micronutrient density that also stimulates plant growth. Therefore, until academics and legislators can come to a shared consensus, this thesis refers to the simple definition given by Barreto *et al.* (2011) who describes biofertilisers as 'biological products which contain microorganisms providing direct and indirect gains in yield from crops' as they encompass a wide range of responses not merely limited to improving macronutrient availability.

# 1.2 Direct benefits of PGPR inoculation to soils and plants

## 1.2.1 Nitrogen Fixation

Nitrogen (N) is an essential macronutrient for plant growth but its severe misuse in developed nations and inaccessibility within developing countries has led to a myriad of environmental and economic issues (Oldroyd and Dixon 2014). The rigorous application of N-fertilisers has raised significant concerns over their negative environmental impact and is a growing problem faced by China, Northern India, the United States of America

and Western Europe (Fowler *et al.* 2013). Crop plants only assimilate around 50% of the N fertiliser applied, as 25% is lost to terrestrial, aquatic and atmospheric ecosystems by denitrification, leaching and ammonia volatilisation (Saikia and Jain 2007). Losing reactive N causes substantial damage to the environment (eutrophication, acidification of ecosystems, biodiversity loss, modification of soil properties and microbiota, and coastal dead zones), human health (respiratory illness and groundwater pollution) and climate (stratospheric ozone depletion and greenhouse emissions) (Erisman *et al.* 2013). In contrast to the nutrient excesses in developed countries, a large majority of sub-Saharan Africa smallholder farms have limited access to N-fertilisers which severely limits crop yields (Rogers and Oldroyd 2014). Bohlool *et al.* (1992) estimate that the construction of a medium sized N- fertiliser factory requires a capital investment of ~$100 million, an unfeasible cost for most developing countries. Due to the lack of infrastructure and resources, sub-Saharan Africa relies heavily on imported fertilisers, but most countries are landlocked and do not have coastline access (Kelly 2006). This causes an artificial inflation of N-fertiliser prices, making them further inaccessible to smallholder farmers (Kelly 2006).

To close the fixed N-yield gap, biological nitrogen fixation (BNF) is considered a long-term supplementary fertilisation strategy to reduce the dependency on its synthetic counterparts (Herridge *et al.* 2008). BNF is the conversion of unreactive $N_2$ gas to ammonia ($NH_3$) and while there are other global sources of fixed N (e.g. lightning, fossil fuel combustion and the Haber–Bosch process), BNF is the primary non-anthropogenic source of fixed N for plants (Fowler *et al.* 2013; Oldroyd and Dixon 2014). Agricultural BNF is estimated to contribute 50–70 teragrams (Tg) of fixed N per year, with the largest contribution coming from the symbiotic legume-rhizobia relationship (18.5 Tg for oilseed and 2.95 Tg for pulse legumes) (Herridge *et al.* 2008). With the advances in synthetic biology, researchers are attempting to overcome BNF limitations via two strategies: transfer of the rhizobium-legume symbiosis to cereals or engineering the direct expression of nitrogenase into plant cells (Rogers and Oldroyd 2014). Both approaches have the potential to change the agriculture landscape but have many complex internal challenges that need to be overcome. In the meantime, existing BNF approaches can be optimised for increased efficiency as modest fixed N gains can cause significant crop yield gains in areas with limited N-fertiliser access (Rogers and Oldroyd 2014). For example, the N-fertiliser application rates in maize fields of sub-Saharan Africa are a mere

3-5 kg/ha and increasing fixed N levels to 25-50 kg/ha is predicted to double or triple yield gains (Rogers and Oldroyd 2014).

Atmospheric nitrogen remains inaccessible to plants because of the stability of its triple bond and electron configuration (Cherkasov *et al.* 2015). Only diazotrophic bacteria and archaea have evolved the ability to fix $N_2$ via the nitrogenase enzyme (Oldroyd and Dixon 2014). Considering the conditions required by the Haber-Bosch process (350–550 °C, 150-350 atm), the ability of nitrogenase to fix nitrogen under normal atmospheric conditions is remarkable (Schrock 2005). The Haber-Bosch process is so resource intensive that it consumes approximately 2% of global energy and 3-5% of the world's annual natural gas production (Licht *et al.* 2014). Nevertheless, BNF is not without its weakness. First, BNF requires 16 ATP and 8 electrons to reduce a single $N_2$ to 2 $NH_3$ molecules (Saikia and Jain 2007). As this poses a significant metabolic burden on the cell, BNF is inhibited when other N sources are available (Issa *et al.* 2014). Second, N fixation only occurs in specialised, microoxic niches, as nitrogenase is highly sensitive to $O_2$. This is problematic for aerobic diazotrophs as oxygenic photosynthesis and $N_2$ fixation are two incompatible processes: photosynthesis generates $O_2$ which irreversibly inactivates nitrogenase (Issa *et al.* 2014). To circumvent the $O_2$-incompatibility problem, some diazotrophs like rhizobia only fix $N_2$ within the microoxic root nodules of their symbiotic legume partners. While the symbiotic rhizobia-legume partnership are the biggest BNF contributors in agriculture, the specificity of the Nod-factor signalling pathway severely limits the host range of rhizobia (Herridge *et al.* 2008). For these reasons, there is a growing interest in using cyanobacteria as BNF inoculants as they are not limited to a narrow host range; certain heterocystous cyanobacteria can differentiate into hormogonia, which are transient motile filaments required for infecting a non-legume symbiotic partner (Flores and Herrero 2010; Khamar *et al.* 2010; Christman *et al.* 2011).

#### 1.2.1.1 Adaptations of heterocystous cyanobacteria for protecting nitrogenase against $O_2$-inactivation

Cyanobacteria are the original pioneers of oxygenic photosynthesis as the modern-day plant chloroplast are derived from the endosymbiosis of ancient cyanobacteria (Issa *et al.* 2014). Filamentous and heterocystous strains (e.g. *Nostoc* and *Anabaena*) have evolved a unique strategy for protecting the $O_2$-sensitive nitrogenase. Members in this family rely on the spatial separation of the two incompatible processes into different cells: $N_2$-fixing

heterocysts and carbon-fixing photosynthetic vegetative cells (Flores and Herrero 2010). Under low N conditions, *Nostoc* filaments exist as vegetative cells that are regularly interspaced with $N_2$-fixing heterocysts. Heterocysts are easily distinguishable because of their thick envelope that limits $O_2$ diffusion; they have significant morphological and physiological differences for maintaining low $O_2$ concentrations (Flores and Herrero 2010). For example, *Anabaena* sp. PCC 7120 has two alternative oxidases (*Cox2* and *Cox3*) not found in vegetative cells that maintain a microoxic environment for continued nitrogenase activity. Similarly, Ow *et al.* (2009) detected a 4-fold increase in photosystem I (PS I) centers in *Nostoc punctiforme* heterocysts, without significant changes in photosystem II (PSII) levels. The elevated PSI:PSII ratio is estimated to increase respiration rates for higher $O_2$ consumption (Ow *et al.* 2009). $N_2$-fixation has a substantial energy expenditure, but heterocysts have evolved a unique process for meeting the high energy demands of nitrogenase. In five heterocysts-forming species, a divergent PsaB2 reaction center protein for PSI was identified (Magnuson *et al.* 2011). Homology modelling shows that PsaB2 alters the structure of PS I near key electron cofactor sites (PhyQA, PhyQB and F) (Magnuson *et al.* 2011). The subsequent shifting of the redox potential cofactors is hypothesised to form alternative PS I center specially optimised for cyclic electron flow (CEF) to meet the high energy demands of nitrogenase; CEF produces ATP without NADPH formation and is more efficient than linear electron flow in ATP generation (Kramer and Evans 2011; Nogales *et al.* 2012).

#### 1.2.1.2 N-kinetics during heterocystous cyanobacteria-plant symbiosis

Nitrogen metabolism and carbon (C) fixation are two closely intertwined processes; the reductants generated from the photosynthetic light reaction are used to incorporate ammonium into carbon skeletons through the glutamine synthetase-glutamine synthase (GS-GOGAT) cycle (Bhaya *et al.* 2002). The nitrogen metabolism in these symbiotically associated strains differs significantly from their free-living counterparts. In free-living *Nostoc* strains, only 5-10% of vegetative cells terminally differentiate into heterocysts under N-limiting conditions (Meeks and Elhai 2002). Heterocysts cannot fix $CO_2$ as they lack ribulose 1,5-bisphosphate carboxylase–oxygenase (RubisCO), the key enzyme of the Calvin-Benson-Bassham cycle (Flores and Herrero 2010). Instead, they form a mutual relationship with neighbouring vegetative cells: heterocysts supply vegetative cells with fixed $N_2$ and receive fixed C in return. This relationship enables vegetative cells to grow

continually under N-limiting conditions and heterocysts to function normally with imported carbon (Flores and Herrero 2010). While free-living *Nostoc* strains produce enough photosynthate reductants for nitrogen fixation, it is impossible for symbiotic cyanobacteria (cyanobionts) to sustain the highly elevated nitrogen fixation rates, considering their reduced photosynthetic capacity (Adams *et al.* 2013). Instead, cyanobionts rely on the oxidation of plant-derived hexoses to generate reductants for nitrogenase and oxidative respiration (Meeks and Elhai 2002).

Another marked difference between symbiotic and free-living *Nostoc* strains is the capacity to assimilate ammonium. Free-living cyanobacteria assimilates most of its fixed nitrogen and releases a limited amount (6-20%) into the environment under variable growth conditions (Meeks and Elhai 2002). In contrast, symbiotic *Nostoc* colonies make a substantial amount of their fixed nitrogen available to the host plant, e.g. 80% in *Anthoceros* (Meeks *et al.* 1985) and 90% in *Gunnera* (Silvester *et al.* 1996). The uncoupling between nitrogen fixation and ammonium assimilation in a cyanobiont results from downregulated glutamine synthetase (GS) activity either by catalytic or biosynthesis repression depending on the involved host plant (Bhaya *et al.* 2002). Impairing the cyanobionts ammonium assimilation system leads to substantial ammonium release, which the host plant absorbs and uses for plant growth and development (Bhaya *et al.* 2002).

### 1.2.2 Phosphate solubilisation

Phosphorus (P) makes up 0.2% of plant dry mass and is only behind nitrogen as the second biggest limiting factor for plant growth (Schachtman *et al.* 1998). P is a key building block for essential macromolecules such as nucleic acids (DNA and RNA), phospholipids and energy storage intermediates (ATP) (Arif *et al.* 2017). Consequently, P is present in all plant cells and involved in many key processes such as energy transfer, cell division, respiration, photosynthesis, signal transduction, and enzyme activation (Arif *et al.* 2017). Soil P is available in organic and inorganic forms but the majority remains inaccessible to plants as they are insoluble or fixed (Khan *et al.* 2014), the average soil P content is 0.05% (w/w), but approximately 0.1% of the P-pool is available for plant use (Illmer and Schinner 1995). To address the shortage of soluble P, modern agricultural practices rely on chemical P-fertiliser and manure application. Common forms of chemical P-fertiliser include monocalcium phosphate and monopotassium phosphate;

their application to soil forms a P-saturated patch suitable for plant assimilation (Shen *et al.* 2011). Likewise, manure application is a rich P-source as ~70% of total P is labile, with concentrated levels of phospholipids and nucleic acids (Shen *et al.* 2011). However, chemical P-fertiliser has low efficiency rates as most applied P becomes fixed or immobilised upon soil application, rendering them unsuitable for plant assimilation (Chen *et al.* 2006). Therefore, phosphate solubilising microorganisms (PSM) play an important role in the soil P cycle by releasing bound P through inorganic P-solubilisation and organic P-mineralisation.

#### 1.2.2.1 Mechanism of inorganic phosphate solubilisation

Depending on the soil type, the levels of inorganic P can vary from 35 to 70% (Shen *et al.* 2011). Inorganic P can exist in three forms: primary P minerals (apatites, strengite and variscite), secondary P minerals (Ca, Fe and Al phosphates), and adsorbed P (clay particles, organic matter and Fe/Al oxides) (Khan *et al.* 2014). Primary P minerals and adsorbed P particles have high stability and their slow release of bio-available P makes them unsuitable for meeting the high demands of modern agriculture (Shen *et al.* 2011). While secondary P have higher dissolution rates, their solubility differs according to soil type; fixed Fe and Al phosphates are more soluble under basic conditions, while Ca phosphates have higher solubility in acidic soil (Khan *et al.* 2014). All three forms of inorganic P exist in equilibrium with each other and are sparingly available to plants compared to organic P. Consequently, plants are heavily reliant on arbuscular fungi and PSM to solubilise inorganic P. Mobilisation of this P-pool occurs by the extracellular release of $H_2S$, organic and inorganic acids, siderophores and chelating substances (Sharma *et al.* 2013). Of all these compounds, organic acids are primarily responsible for releasing bound P; the list of involved organic acids includes: oxalic, 2-ketogluconic, citric, tartaric, fumaric, gluconic, malic, glycolic, lactic, succinic, propionic, butyric, acetic, isobutyric, glyoxalic, isovaleric, itaconic, 2-ketobutyric, propionic, aspartic, malic and glutamic acid (Alori *et al.* 2017). Gluconic acid is considered the primary organic acid responsible for inorganic P-solubilisation (Alori *et al.* 2017), but the organic acid profile differs according to the organism and its ecological niche. For example, P-solubilising strains (*Bacillus*, *Rhodococcus*, *Arthrobacter*, *Serratia*, *Chryseobacterium*, *Delftia*, *Gordonia* and *Phyllobacterium)* from subtropical soils in Central Taiwan exuded citric acid, gluconic acid, lactic acid, succinic acid and propionic acid (Chen *et al.* 2006). In contrast, nineteen *Pseudomonas* strains isolated from the cold trans-Himalayan deserts

released gluconic acid, oxalic acid, 2-ketogluconic acid, lactic acid, succinic acid, formic acid, citric acid and malic acid (Vyas and Gulati 2009). The organic acid profile was not consistent as cluster analysis showed large intra-species variations between the nineteen examined strains (Vyas and Gulati 2009).

Organic acids are generated within the microbial periplasm but once released into the extracellular environment, their carboxyl and hydroxyl groups chelate P-bound cations (Ca, Al and Fe) to increase P-bioavailability (Sharma *et al.* 2013). Organic acids also solubilise inorganic P by decreasing soil pH and competing with P for soil adsorption sites (Sharma *et al.* 2013). Acidification induces P-release from insoluble complexes by proton substitution for $Ca^{2+}$. In addition, exopolysaccharide (EPS) release augments the efficiency of organic acids to solubilise inorganic P as EPS binds to metal cations by their organic and inorganic substituents (Arif *et al.* 2017). This was reflected in the synergistic effect shared by organic acids and EPS in *Azotobacter*, *Arthrobacter* and *Enterobacter*; exogenous EPS could not solubilise tricalcium phosphate (TCP) by itself, but had a dose-dependent effect on TCP solubilisation rates in the presence of citric acid (Yi *et al.* 2008).

#### 1.2.2.2 Mechanism of organic phosphorus mineralisation

Organic P content constitutes 30-65% of total soil P and comes primarily from organic matter (Shen *et al.* 2011). The primary source of organic P comes from inositol phosphates, but additional sources of organic P include phosphonates, phospholipids, nucleic acids, orthophosphate diesters, labile orthophosphate monoesters and phosphotriesters (Khan *et al.* 2014). As these compounds have high molecular weights (MW), organic P are mostly resistant to hydrolysis but can be mineralised to make them bio-available (Alori *et al.* 2017). PSM catalyses P-mineralisation through three enzyme groups: phosphatases, phytases and phosphonatases (Sharma *et al.* 2013). Phosphatases are hydrolytic enzymes that cleave phosphate esters and anhydride bonds of organic P to release assimilable forms of inorganic P ($H_2PO_4^-$ and $HPO_4^{2-}$) (Dodor and Tabatabai 2003). They are divided into two groups based on their optimum pH performance: non-specific acid phosphatases (NSAPs) in acidic soil and substrate-specific alkaline phosphatases in alkaline to neutral soil conditions (Duff *et al.* 1994). Acid phosphatases play a larger role in organic P-mineralisation than alkaline phosphatases (Rodríguez and Fraga 1999) as the plant rhizosphere tends to be acidic (Duff *et al.* 1994) and NSAPs can

dephosphorylate structurally diverse compounds (e.g. nucleotides, sugar phosphates and phytic acid) (Gandhi and Chandra 2012).

The importance of NSAPs is further underscored by the fact that plants secrete acid phosphatases into outer surface cells and the apical meristems, even though both acid and alkaline phosphatases are generated *in vivo* (Duff *et al.* 1994). However, plant-based acid phosphatases are unlikely to contribute as much as their microbial counterparts towards soil P recycling (Duff *et al.* 1994) as PSM-based acid phosphatases make up the majority of soil phosphatases (Tabatabai 1994) and are significantly more efficient than plant-based phosphatases (Tarafdar *et al.* 2001). This was demonstrated by Tarafdar *et al.* (2001) who investigated the differences in efficiency between plant- and fungal-based acid phosphatases: fungal *Aspergillus niger*, *A. terreus* and *A. rugulosus* had a greater 2-3-fold efficiency in hydrolysing lecithin and phytin, compared to plant-based phosphatases found in *Sorghum bicolor*, *Vigna unguiculata* and *Phaseolus radiatus*. Other enzymes involved in organic P-mineralisation include phosphonatases and phytase. Phosphonatases are enzymes that hydrolyse the C–P bond of organophosphonates, while phytases hydrolyse insoluble phytate into *myo*-inositol phosphate and inorganic phosphate derivatives (Singh and Satyanarayana 2011). Phytates constitute up to 60% of organic P and are the predominant source of soil organic P, but plants cannot assimilate phytate without undergoing mineralisation because of its insolubility and adsorption to soil particles (Singh and Satyanarayana 2011).

# 1.3 Indirect benefits of PGPR inoculation

## 1.3.1 ACC deaminase and its influence on deleterious ethylene levels

Ethylene is a gaseous phytohormone that regulates many plant development and growth processes such as flowering, fruit ripening, root and shoot primordial formation, seed germination and root initiation, elongation and branching (Saraf *et al.* 2010). However, ethylene is also a stress hormone as its biosynthesis is accelerated in response to abiotic (temperature, gravity, light, heavy metals, drought and nutrient deprivation) and biotic (pathogen, insect and nematode damage) stresses (Glick 2012, 2014). During stress onset, plants generate two ethylene peaks of varying amplitudes (Figure 1.1). The first ethylene peak occurs a few hours after stress onset (Glick *et al.* 2007) and stimulates the transcription of multiple stress-response genes such as hydrolytic enzymes (chitinases, *β*-

1,3-glucanases) (Deikman 1997), defensin (Penninckx *et al.* 1996), hydroxyproline-rich glycoproteins (Ecker and Davis 1987) and various enzymes of the phenylpropanoid and flavonoid glycoside pathways (Ecker and Davis 1987). However, if the stress response is inadequate, ethylene levels continue to rise disproportionately, days after the initial stress encounter (Glick *et al.* 2007). This second ethylene peak causes many detrimental effects that lower plant survival rates, such as the inhibition of shoot and root development, chlorophyll destruction, leaf abscission, chlorosis, epinasty, leaf and flower senescence (Nadeem *et al.* 2010).

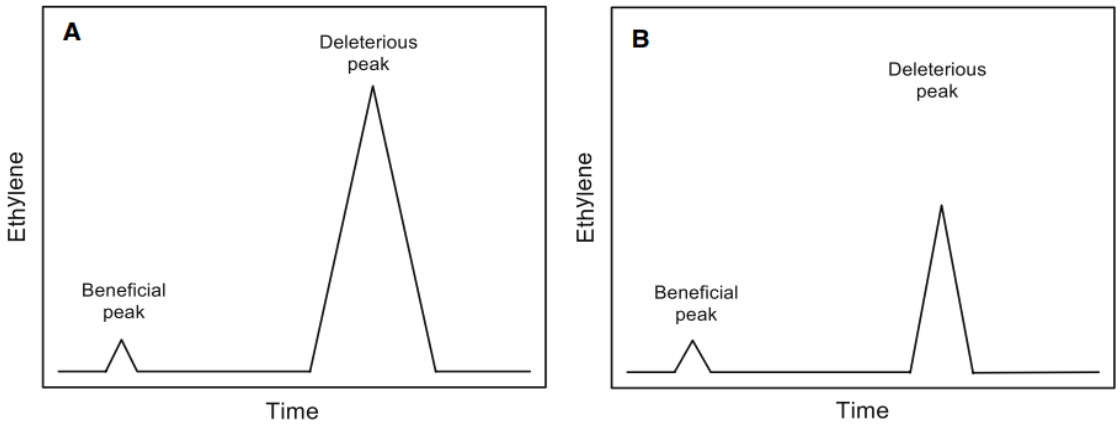


**Figure 1.1** - Ethylene peaks in stressed plants with (A) no PGPR inoculation and (B) ACC-deaminase expressing PGPR strains. The first beneficial ethylene peak activates stress-response genes, but the second deleterious peak induces cellular damage and lower plant survival rates. With inoculation (2B), the amplitude of the second deleterious peak is smaller as PGPR converts plant-derived ACC into α-ketobutyrate and ammonia. Image adapted from Glick et al. 2007.

To avoid premature death, plants must regulate ethylene to manageable levels as overly high ethylene has deleterious effects that outweigh benefits conferred at lower concentrations. The precursor of ethylene is 1-aminocyclopropane-1-carboxylate (ACC) and inoculation with ACC deaminase-expressing PGPR strains lower plant ethylene levels by converting ACC into $\alpha$-ketobutyrate and ammonia (Saraf *et al.* 2010). Many studies have showed the ability of such PGPR strains to ease the stress-induced effects of ethylene to sustain plant growth under unfavourable conditions. For example, two *Pseudomonas* strains (*P. fluorescens* YsS6 and *P. migulae* 8R6) with ACC deaminase activity facilitated tomato plant growth even under high salt stress (Ali *et al.* 2014). Compared to their ACC deaminase deficient mutants, plants inoculated with *P. fluorescens* YsS6 and *P. migulae* 8R6 were more resistant to salt stress and had higher

biomass, chlorophyll concentration and more flowers and buds compared to the control plants after 11 weeks (Ali *et al.* 2014). In a separate study, Saikia *et al.* (2018) examined the synergistic effect of three ACC-deaminase-producing strains (*Ochrobactrum pseudogrignonense*, *Pseudomonas* sp RJ15 and *Bacillus subtilis*) in drought-stressed *Vigna mungo* and *Pisum sativum* plants. Microbial consortium pre-treated plants had higher seed germination rates, enhanced root and shoot length, and chlorophyll levels compared to control samples (Saikia *et al.* 2018). Inoculated plants also had elevated cellular osmolytes (proline and phenolics) levels, and antioxidant enzymatic activity (catalase and peroxidase) (Saikia *et al.* 2018).

ACC-deaminase expressing strains lower the amplitude of the second deleterious ethylene peak as the first ethylene peak consumes most of the ACC pool (Robison *et al.* 2001). The initial bacterial ACC deaminase expression is low and its transcription only upregulated in response to increasing ACC being exuded by the stressed plant (Glick *et al.* 2007). The second ethylene peak can never be fully annulled as bacterial ACC deaminase has a significantly lower ACC affinity than plant ACC oxidase which catalyses ACC conversion into ethylene. Glick (2005) estimates that ACC deaminase levels need to be 100 to 1000-fold higher than ACC oxidase to be effective at lowering ethylene levels. ACC deaminase expression is relatively common in soil microorganisms and is found in multiple proteobacterial strains across the genera *Azospirillum*, *Rhizobium*, *Agrobacterium*, *Achromobacter*, *Burkholderia, Ralstonia*, *Pseudomonas*, *Enterobacter. Kluyvera, Alcaligenes, Bacillus, Variovorax, Sinorhizobium, Methylobacterium, Ralstonia* and *Rhodococcus* (Belimov *et al.* 2001, 2005; Blaha *et al.* 2006; Stiens *et al.* 2006; Madhaiyan *et al.* 2006). Despite its prevalence across a broad spectrum of bacteria species, there are two main groups of ACC-deaminase expressing bacteria: free-living and rhizobia strains (Glick 2005). Free-living strains bind non-specifically to host plants and have greater ACC deaminase activity than rhizobia strains; the former can be further sub-divided into endophytes that reside within plant tissue, rhizospheric (binds to roots and seed surfaces) and phyllospheric (binds to leaf and stem surfaces) organisms (Glick 2014). Conversely, symbiotic rhizobia only inhabit the nodules of specific host partners and do not lower overall *in planta* ethylene levels, but inhibit localised ethylene spikes (Glick 2005).The model for understanding how microbial ACC deaminase lowers plant ethylene levels is illustrated in Figure 1.2. Soil microorganisms are chemo-attracted towards roots or seeds in response to the nutrient-rich exudates which are high in sugars,

amino acids and organic acids (Nadeem *et al.* 2010). The build-up of ethylene in stressed plants is caused by rapid expansion of the ACC pool because of increased ACC synthase activity (Ecker and Davis 1987). Stressed plants exude a significant amount of the newly synthesised ACC (Penrose and Glick 2001, 2003), along with other compounds such as tryptophan (Glick *et al.* 1998). ACC-deaminase expressing PGPR strains assimilate plant-derived ACC as an additional N-source for growth to outcompete the surrounding soil microbiota lacking the enzyme (Jacobson *et al.* 1994; Belimov *et al.* 2005).

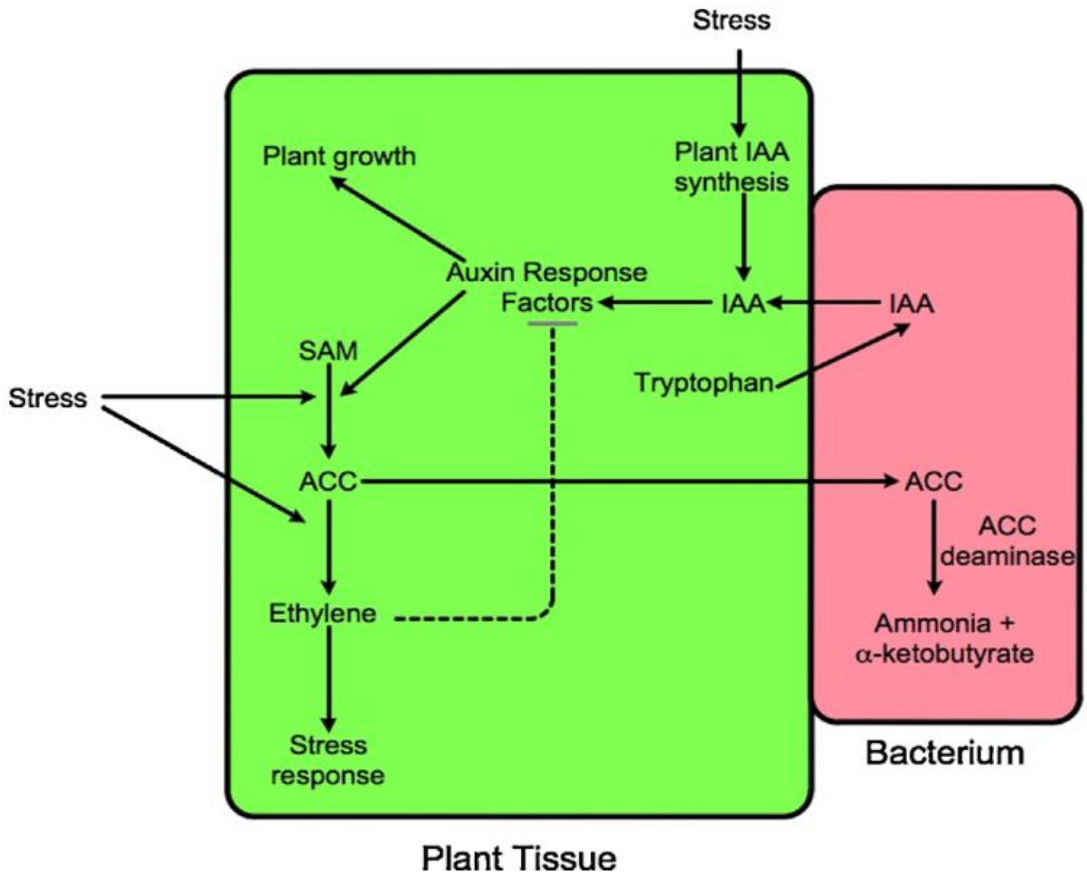


**Figure 1.2** - Model of ACC-deaminase expressing PGPR strains in reducing plant ethylene levels for enhanced stress tolerance. Without inoculation, the deleterious second ethylene peak inhibits transcription of auxin response factors (ARFs), which represses auxin-stimulated plant growth and ACC synthase transcription. PGPR inoculation serves as an external ACC sink to prevent excessive ethylene build-up and reduces ARFs transcription suppression to facilitate plant growth under stress conditions. Abbreviations: ACC, 1-aminocyclopropane-l-carboxylate; IAA, indole-3-acetic acid; SAM, S-adenosyl methionine. Image from Glick (2014).

Besides regulating *in planta* ethylene levels, microbial ACC deaminase also influences the cross-talk between ethylene and the auxin indole-3-acetic acid (IAA). In response to assimilation of certain root exudates (especially tryptophan) PGPR strains synthesise and

release IAA to the rhizosphere, that plants can assimilate (Glick *et al.* 1998). IAA is a growth hormone that stimulates plant growth and increasing the internal IAA pool positively impacts cell proliferation and elongation. Moreover, microbial IAA weakens the structural integrity of plant cell walls and increases the efflux of root exudates such as ACC into the rhizosphere (Saraf *et al.* 2010). IAA also induces stressed plants to generate more ACC by upregulating ACC synthase activity (Kende 1993) but as PGPR strains are acting as an ACC-sink, the rapid microbial consumption of ACC ensures plants avoid an excessive build-up of ethylene (Saraf *et al.* 2010). Sustained microbial reduction of *in planta* ethylene levels brings the added benefit of lifting the transcription suppression of auxin response factors (ARFs) as high ethylene levels dampen the IAA signalling network (Glick *et al.* 2007). This enables IAA to stimulate cell division without accumulating excessive ethylene, which facilitates plant growth despite unfavourable conditions (Glick *et al.* 2007).

### 1.3.2 Phytohormones and their role in modulating plant stress tolerance

Phytohormones are signalling molecules that regulate plant growth and development but are also found in algae, fungi and bacteria (Lu and Xu 2015). The modern phytohormone pathways in higher plants are evolutionary artefacts from ancient microalgae, as reflected by the highly conserved phytohormone chemical structures shared between prokaryotes (bacteria, cyanobacteria) and eukaryotes (algae, fungi, ferns and seed plants) (Lu and Xu 2015). This section will cover the effect of microbial-derived phytohormones and their role in modulating plant stress tolerance. For each phytohormone, brief explanations for its relevant function, mechanism of action and appropriate PGPR inoculation case studies will be examined. The phytohormones detailed in this section include auxin, abscisic acid, cytokinin, and gibberellins. Ethylene has been covered in detail in Section 1.3.1.

#### 1.3.2.1 Abscisic acid

Abscisic acid (ABA) is a sesquiterpene signalling hormone that regulates many growth and developmental processes such as embryo maturation, seed dormancy and germination, cell division and elongation, flowering, and senescence (Finkelstein 2013). In addition, ABA plays a critical role during osmotic stress as it is a long-distance messenger that controls the plant water-regulation status (Tuteja 2007). Osmotic stresses such as drought, salinity and chilling share common signalling pathway elements and downstream symptoms (e.g. cellular desiccation and osmotic imbalance) and ABA acts

as a central hub that integrates and transduces osmotic stress signals by activating ABA-dependent stress response genes (Tuteja 2007). In *Arabidopsis*, ABA regulates ~10% of protein-coding genes, a much higher percentage than other phytohormones (Nemhauser *et al.* 2006). ABA induces two waves of gene expression; an early (0.5-6 hours) transient response encodes multiple transcription factors (e.g. AREB/ABF, bZIP and MYB), protein kinases (SnRK2s) and *early response to dehydration* (*erd*) genes (Fujita *et al.* 2011; Finkelstein 2013). The second response is sustained and late (> 10 hours from stress onset), and it upregulates stress-responsive genes such as osmolytes (proline, sugars, and glycine-betaine) to correct the cellular osmotic imbalance, ion and water-channel proteins to re-establish the plant-water homeostasis and enzymatic antioxidants to decrease reactive oxygen species (ROS) levels (Ingram and Bartels 1996; Finkelstein 2013).

ABA also targets guard cells for stomatal closure to reduce transpiration rates and limit gaseous exchange by transiently increasing cytoplasmic $Ca^{2+}$ levels (Finkelstein 2013). PGPR inoculation increases osmotic stress tolerance by increasing *in planta* ABA levels (Cohen *et al.* 2008, 2009, 2015; Park *et al.* 2017) and regulating ABA-mediated signalling pathways (Bharti *et al.* 2016). Inoculation with *Bacillus aryabhattai* SRB02, *Azospirillum lipoferum* and *Azospirillum brasilense* 245 increases ABA levels in soybean (Park *et al.* 2017), maize (Cohen *et al.* 2009) and *Arabidopsis* (Cohen *et al.* 2015), respectively. SRB02-inoculated soybean plants succeeded in maintaining green leaves and continuous ABA production under heat stress, while control plants suffered from medium to severe leaf chlorosis (Park *et al.* 2017). Similarly, inoculation with *Azospirillum brasilense* 245 increased endogenous ABA levels, leaf area, root length and lateral root numbers in *Arabidopsis* (Col-0 wild type and *aba2-1* mutant) seedlings (Cohen *et al.* 2015). *Azospirillum*-inoculated plants displayed enhanced drought resistance, with greater levels of proline, photosynthetic pigments and leaf relative water content (RWC) than control plants. Inoculated seedlings also had less oxidative damage, as evidenced by lower malondialdehyde concentrations, and reduced water loss from decreased stomatal conductance (Cohen *et al.* 2015). In a separate study, Bharti *et al.* (2016) showed that inoculation with the halotolerant *Dietzia natronolimnaea* STR1 strain enhanced the salt tolerance of wheat plants by modulating the ABA-signalling cascade; upregulation of *TaABARE* and *TaOPR1* led to the expression of stress-response genes such as TaST, a salt-inducible gene that lowers intracellular $Na^+$ levels, elevates $K^+$ levels and sustains a high $K^+/Na^+$ ratio for enhanced salt tolerance (Bharti *et al.* 2016). Inoculated wheat plants

also had increased flux through the Salt Overly Sensitive (SOS) pathway, elevated proline levels and higher expression of tissue-specific ion transporters (TaNHX1, TaHAK, and TaHKT1) and enzymatic (ascorbate peroxidase, manganese superoxide dismutase, catalase, peroxidase, glutathione peroxidase and glutathione reductase) antioxidant activity (Bharti *et al.* 2016).

#### 1.3.2.2 Cytokinin

Cytokinin is a positive regulator of shoot growth, nutrient acquisition (nitrogen, phosphorus and sulphur), stress defence (respiration, photosynthesis and antioxidant network), but a negative regulator of senescence and root growth (Pavlů *et al.* 2018). The phytohormone is primarily synthesised in roots, but virtually all plant cells contain traces of cytokinin as it regulates cytokinesis during cell division (Salamone *et al.* 2005). A long-range signalling messenger, cytokinin travels from roots to other tissue sections and interacts with other phytohormones to regulate plant growth and development such as vascular bundle differentiation, secondary metabolite biosynthesis, suppression of lateral root formation and senescence delay (Salamone *et al.* 2005; Zwack and Rashotte 2015). However, cytokinin also plays a prominent role during the stress response as it interacts with multiple abiotic stress signalling pathways and other stress phytohormones, such as jasmonic acid, salicylic acid and ABA (Zwack and Rashotte 2015; Pavlů *et al.* 2018). The cytokinin signalling cascade in plants occurs through a modified bacterial two-component signalling system (Keshishian and Rashotte 2015)*;* detection of stress cues (e.g. drought, heat, nutrient deficiency) by histidine kinase receptors is transduced into transcription factor biosynthesis, cell wall expansion and macronutrient acquisition (Sakakibara *et al.* 2006). Cytokinin levels fluctuate according to the encountered stress intensity as illustrated in Figure 1.3. Initial stress exposure induces a transient cytokinin burst (< 3 hours) that activates stress-responsive genes (Zwack and Rashotte 2015). If moderate stress levels persist, cytokinin levels will steadily decline but plants will maintain elevated cytokinin levels if stress intensity continues to rise (Zwack and Rashotte 2015)

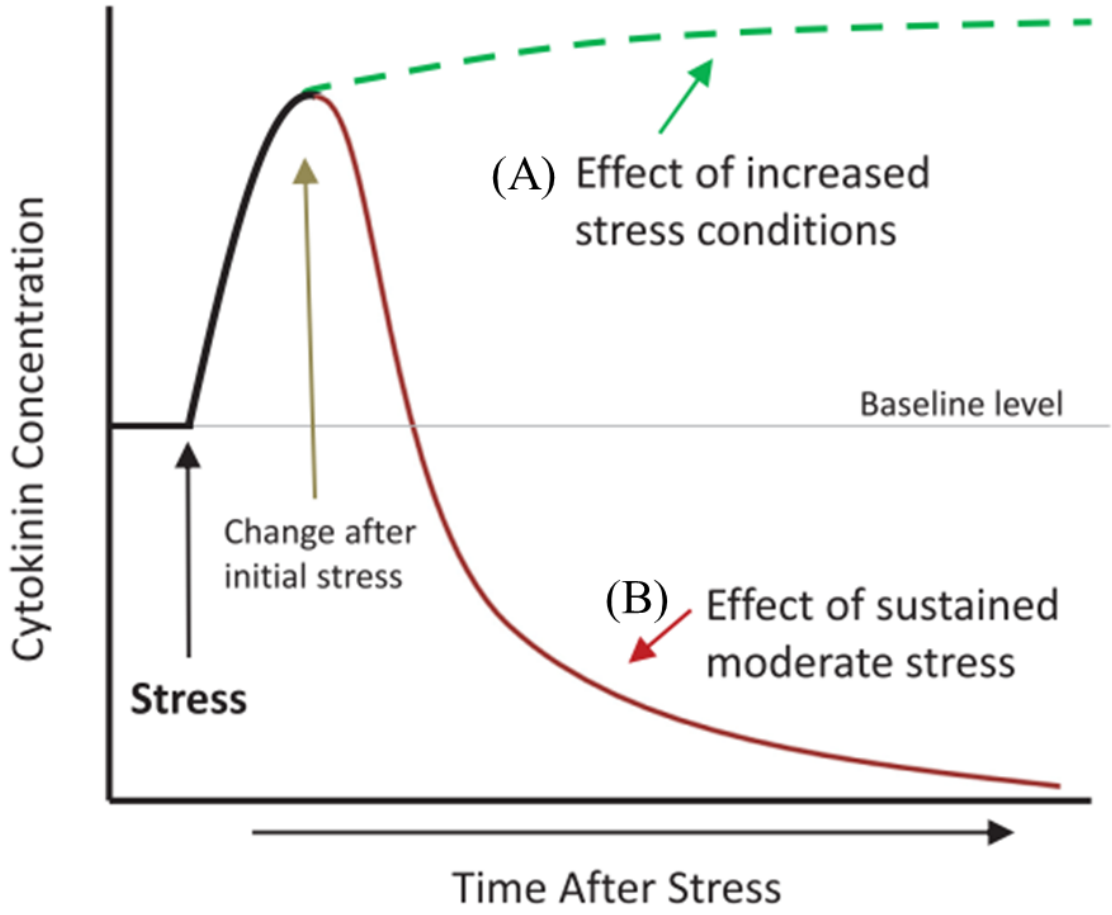


**Figure 1.3** - Effects of (A) increased or (B) sustained moderate stress on plant cytokinin levels. Following stress onset, the initial transient cytokinin spike (< 3 hours) activates various stress-responsive genes and will steadily decrease under moderate stress, but elevated cytokinin levels will be maintained if high stress intensities persist. Image adapted from Zwack and Rashotte (2015).

Under water-limiting conditions, plants reduce cytokinin levels to promote root elongation and inhibit stomata opening and shoot growth (Hare *et al.* 1997). These are essential drought adaptations as stomata closure prevents excessive water loss by transpiration, while root growth enables higher water extraction rates from soil (Hare *et al.* 1997). However, cytokinin-producing PGPR strains are still effective at strengthening plant tolerance against drought stress (Arkhipova *et al.* 2007; Liu *et al.* 2013). Inoculation of *Platycladus orientalis* seedlings with *Bacillus subtilis* alleviated effects of drought stress as inoculated seedlings had higher RWC and lower electrolyte leakage than uninoculated seedlings, the latter being an indication of reduced cell death levels (Liu *et al.* 2013). Inoculated seedlings also had higher shoot cytokinin levels as the majority of microbial-derived cytokinin was transported into shoots (Liu *et al.* 2013). Under normal

conditions, this would be detrimental to droughted plants as high shoot cytokinin levels cause elevated transpiration rates. However, the researchers noted that *B. Subtilis* inoculation did not significantly increase stomata conductance as drought-stressed shoot tissue had elevated ABA levels, compared to the uninoculated control. Both phytohormones acted synergistically under drought stress as cytokinin stimulated cell division and expansion (inoculated shoots experienced higher growth-stimulating properties than roots) while elevated ABA levels increased stomata closure and prevented excessive water loss (Liu *et al.* 2013). Arkhipova *et al.* (2007) observed similar effects when drought-stressed *Lactuca sativa* L seedlings were inoculated with *Bacillus* (strain IB-22). Inoculated seedlings had higher shoot cytokinin levels as they exported most of the microbial-derived cytokinin to leaves, resulting in 50% higher shoot biomass than non-inoculated controls. Like *Bacillus*-inoculated *P. orientalis* seedlings (Liu *et al.* 2013), inoculated *Lactuca sativa* L seedlings had elevated ABA shoot levels, which exerted a stronger stomata-closure force over the stomata-opening properties of cytokinin, causing no net effect on stomata conductance (Arkhipova *et al.* 2007).

#### 1.3.2.3 Gibberellins

Gibberellins (GAs) regulate many developmental and physiological processes such as seed dormancy and germination, floral and trichome initiation, lateral shoot growth, leaf expansion, stem elongation, pollen maturation and cell senescence (Fahad *et al.* 2015; Salazar-Cerezo *et al.* 2018). Plants have many types of gibberellin and as of now, 136 forms have been identified in higher plants, but the most common bioactive forms are $GA_1$, $GA_3$ and $GA_4$ (Hedden and Thomas 2012). Many bacteria species have been reported to synthesise these bioactive forms, such as *Acetobacter* (Bastián *et al.* 1998), *Acinetobacter* (Kang *et al.* 2009), *Azospirillum* (Bottini *et al.* 1989), *Leifsonia* (Kang *et al.* 2017), *Pseudomonas* (Kang *et al.* 2014a), *Bacillus* (Gutierrez-Manero *et al.* 2001), and *Burkholderia* (Joo *et al.* 2009). Apart from direct gibberellin biosynthesis, PGPR strains can also indirectly modulate plant gibberellin levels by deconjugating glucosyl gibberellins and converting inactive GAs into bioactive forms (Kang *et al.* 2014b). Under abiotic stress, gibberellin enables plants to continue plant growth and development as it modulates other phytohormones and the source-sink relationship to initiate the stress response and increase photosynthetic efficiency (Fahad *et al.* 2015; Egamberdieva *et al.* 2017). Various studies have reported the beneficial effects of GA-producing PGPR strains

in alleviating abiotic stress (Salazar-Cerezo *et al.* 2018). For example, under drought and salt stress, inoculation of soybean seedlings with *Pseudomonas putida* H-2-3 increased the shoot length, fresh weight, chlorophyll content and decreased stress phytohormone (ABA and jasmonic acid) levels compared to uninoculated controls (Kang *et al.* 2014a). The stress-protection effects conferred by *P. putida* H-2-3 was attributed to the bioactive $GA_1$ and $GA_4$ forms present in the cultural filtrate as it helped to maintain cellular ionic balance by decreasing $Na^+$ levels in drought and salt stressed plants.

Kang *et al.* (2017) have also demonstrated the effectiveness of GA-producing strains in alleviating copper (Cu) toxicity symptoms. Cu toxicity stunts plant growth as it causes significant cellular oxidative damage and inhibits many pathways, including photosynthesis, nutrient uptake, nitrogen assimilation and carbohydrate synthesis (Kang *et al.* 2017). However, inoculation of tomato seedlings with *Leifsonia xyli* SE134 enabled plants to maintain growth despite elevated Cu levels; *L. xyli* SE134 improved the nutrient profile (P and Fe) and growth parameters (shoot and root biomass, stem diameter and chlorophyll levels) of inoculated plants over controls (Kang *et al.* 2017). *L. xyli* SE134 inoculation also reduced oxidative damage under elevated Cu stress by increasing polyphenol and flavonoid levels. Interestingly, *L. xyli* SE134 not only modulated *in planta* proline levels, an important osmolyte, but other endogenous amino acids such as glutamic acid, threonine, phenylalanine, glycine and arginine. Kang *et al.* (2017) speculates that elevated amino acid levels sustained plant growth under $Cu^{2+}$ toxicity, by driving metabolic flux into the photosynthetic and nitrogen fixation pathways.

#### 1.3.2.4 Auxin

The auxin indole-3-acetic acid (IAA) regulates many developmental processes such as cell division and elongation, vascular tissue differentiation, apical dominance, delaying senescence, and root and shoot growth in response to phototropism and gravitropism (Kurepin *et al.* 2014; Fahad *et al.* 2015; Egamberdieva *et al.* 2017). Plants produce excess IAA as a strategy to shorten the time needed to reach the flowering stage, but IAA production consumes metabolic resources that plants would otherwise utilise for growth (Yurekli *et al.* 2004). Plants have a diminished capacity to synthesise phytohormones during high stress, but PGPR inoculants can supplement *in planta* levels by acting as an external source of phytohormones to lessen the plant metabolic load (Salamone *et al.* 2005). For example, co-inoculation of IAA-producing *Rhizobium* and *Pseudomonas*

strains improved total dry matter and salt tolerance index of salt stressed-mung bean plants compared to controls (Ahmad *et al.* 2013). Higher seedling biomass is a marker for salt tolerance as high salt results in lower biomass as plants must devote significant metabolic resources to make osmotic adjustments for continued survival. In a separate study, Marulanda *et al.* (2009) identified *Pseudomonas putida,* and *Bacillus megaterium* as osmotic tolerant strains that adapted to water-limiting conditions by increasing internal proline and IAA levels. Colonisation of droughted *Trifolium repens* L. seedlings with these IAA-producing strains resulted in stronger root growth and higher RWC, shoot and root biomass compared to control plants (Marulanda *et al.* 2009). Nevertheless, high IAA producing bacterial inoculants may not always be the best candidates for improving stress tolerance (Bresson *et al.* 2013). For example, *Phyllobacterium brassicacearum* STM196 is not a high auxin producer compared to other characterised strains, but inoculated *Arabidopsis* seedlings displayed significant physiological adjustments for enhanced drought tolerance (Bresson *et al.* 2013). By delaying plant reproductive development, STM196 prolonged vegetative growth, which gave rise to higher plant biomass and water-use efficiency. Bresson *et al.* (2013) also observed significant changes in the auxin distribution of inoculated root tissues, resulting in improvements in root architecture, higher lateral root length and ABA levels, traits that enhanced their drought tolerance.

### 1.3.3 Hydrolytic enzymes in phytopathogen stress tolerance

Selected PGPR strains are used as bio-control agents to suppress fungal pathogen growth by secreting four types of hydrolytic enzymes: chitinase, glucanase, protease and cellulase (Sayyed and Jadhav 2016). Chitinases degrade the chitin homopolymer, a polysaccharide composed of 1,4-$\beta$-linked N-acetyl-D-glucosamine (GlcNAc) monomers. There are three types of chitinase enzymes, each with different modes of action: (1) $\beta$-1,4-N-acetyl-glucosaminidase hydrolyses chitin into GlcNAc monomers in an exo-type pattern, (2) endochitinases randomly cleave glycosidic linkages in chitin to generate chitooligosaccharides, and (3) exochitinases progressively cleaves the chitin non-reducing end to release GlcNAc or chitobiose units (Felse and Panda 2000). On the other hand, glucanase weaken cell walls and create holes in fungal mycelium by breaking down $\beta$-1,3(1,6)-glucans, another prominent fungal cell wall component (Fridlender *et al.* 1993). Two types of glucanase exist: exo-1,3-glucanases, which sequentially cleaves $\beta$-D-glucose units from the non-reducing ends to release $\alpha$-glucose monomers, and endo-

1,3-glucanases, which randomly cleaves *β*-1,3(1,6)-glucans chains (Jadhav *et al.* 2017). Proteases degrade the protein gel-like matrix encasing chitin and *β*-1,3(1,6)-glucans chains by hydrolysing peptide bonds to release amino acid residues; proteases can also inhibit fungal growth by inactivating the extracellular enzymes of phytopathogens (Jadhav *et al.* 2017).

Cellulose is the most abundant natural polymer but is resistant to hydrolysis because of the strong intra- and inter-molecular hydrogen bonds between chains (Jadhav *et al.* 2017). Degradation of cellulose relies on cellulase which hydrolyses the 1,4-*β*-D-glycosidic linkages to release *β*-glucose monomers. PGPR secretes three types of cellulases: (1) endoglucanases that hydrolyse the 1,4-*β*-D-glycosidic linkages in cellulose in an endo-type pattern, (2) exo-glucanases (cellobiohydrolases), which cleave glycosidic linkages from non-reducing ends, and (3) *β*-glucosidases (cellobioses) that hydrolyse the terminal, non-reducing beta-D-glucosyl residues (Zhang and Zhang 2013). Due to the unique composition of the fungal cell wall, bacterial hydrolytic enzymes do not affect the cell walls of inoculated host plants (Jadhav *et al.* 2017). The fungal cell wall is distinctive from higher plants and bacteria as approximately 80% of the cell wall components are made up of polysaccharides (e.g. chitin, *β*-glucans, mannans and chitosan), with lipids and glycoproteins making up the remaining components (Bowman and Free 2006). Consequently, fungal cell walls present a unique target for extracellular degradation as weakening the fungal cell wall integrity causes the hyphae to swell, curl and burst, thus inhibiting phytopathogen growth (Sayyed and Jadhav 2016)

Prasanna *et al.* (2008) have identified many cyanobacteria strains with hydrolytic enzyme activity; 35 *Anabaena* strains exhibited varying fungicidal activity against pathogenic fungi such as *Fusarium monoliforme*, *Alternaria solani*, *Aspergillus candida*, *Drechslera oryzae* and *Fusarium solani.* The authors of the study attributed the antagonistic ability of *Anabaena* to a wide-range of secreted hydrolytic enzymes, such as protease, *β*-1,4-endoglucanases, *β*-1,3-glucanase, chitosanase, carboxymethyl cellulase and *β*-glucosidases. High chitosanase activity was detected in all 35 extracellular filtrates, ranging from 0.040-0.482 U/ml. This led to the development of *Anabaena torulosa* biofilms as a bio-control matrix for embedding beneficial PGPR consortia strains (Prasanna *et al.* 2013).The rich mucilage of biofilms offer a favourable environment for PGPR growth and they observed synergistic interactions between *A. torulosa* and their

various biofilm-based partners (*Bacillus*, *Pseudomonas*, *Azotobacter*, *Xanthomonas*, *Aspergillus* and *Trichoderma*). Compared to axenic individual cultures, Prasanna *et al.* (2013) also noted heightened anti-fungal activity in cyanobacteria-bacteria biofilms, with high *β*-1,3-glucanase, endoglucanase and chitosanase activity against *Pythium debaryanum*, *Macrophomina phaseolina* and *Fusarium moniliforme*.

Other studies have also demonstrated the effectiveness of using *Bacillus* inoculation to inhibit phytopathogen growth (Kumar *et al.* 2012; Rais *et al.* 2016, 2017). For example, *Bacillus* sp. BPR7 lysed phytopathogen mycelium filaments (*Fusarium oxysporum*, *F. solani*, *M. Phaseolina, Sclerotinia sclerotiorum*, *Rhizoctonia solani* and *Colletotrichum* sp.) by secreting *β*-chitinase, *β*-1,3-glucanase and *β*-1,4-glucanase (Kumar *et al.* 2012). In another study, five *Bacillus* strains (KFP-5, KFP-7, KFP-12, KFP- 17 and KFP-18) inhibited 63-65% fungal growth of *Pyricularia oryzae,* the rice blast pathogen (Rais *et al.* 2016). Through the secretion of protease, *β*-1,3 glucanase and cellulase, *Bacillus*-inoculated rice plants were more resistant against *P. oryzae* infection than control plants (Rais *et al.* 2017). Interestingly, extracellular hydrolytic enzymes also stimulated the antioxidant defence system as inoculated plants had higher (1.7 to 4.4-fold) antioxidant (superoxide dismutase, polyphenol oxidase and phenylalanine ammonia-lyase) activity compared to control plants (Rais *et al.* 2017). These concur with past reports regarding the ability of PGPR-derived hydrolytic enzymes to induce systemic resistance in host plants (Naureen *et al.* 2009; Gill and Tuteja 2010; Sharma *et al.* 2012). Sugars are not merely metabolic precursors but are signalling molecules closely tied with the antioxidant network; cleavage of cell wall polysaccharides generates signals that upregulate anthocyanin and phenolic production, which lowers ROS levels for improved stress tolerance (Bolouri-Moghaddam *et al.* 2010). Therefore, hydrolytic enzymes can enhance phytopathogen stress resistance by direct (fungal cell wall degradation) or indirect (stimulation of antioxidant enzyme activity) processes (Bolouri-Moghaddam *et al.* 2010; Rais *et al.* 2017).

### 1.3.4 Exopolysaccharide production and the protective role of biofilms

Exopolysaccharide (EPS) production by PGPR can make up 40-95% of microbial mass as it forms a protective mucus membrane over cells under inhospitable conditions (Naseem and Bano 2014). Known as biofilms, these protective membranes are composed

of complex multicellular (algae, fungal and bacteria) communities anchored to an extracellular organic matrix via cellular appendages (Swarnalakshmi *et al.* 2013; Angus and Hirsch 2013). Biofilms promote microbial survival but also improve soil structure and root development by encasing root hairs in a mucilage layer of soil particles and microbial cells (Seneviratne *et al.* 2009; Triveni *et al.* 2013). EPS are released by PGPR in the form of capsular and slime materials; a protective capsule around soil aggregates is formed from the adsorption of EPS onto clay surfaces through cation bridges, hydrogen bonding and Van der Waals force (Sandhya *et al.* 2009; Vurukonda *et al.* 2016). Consequently, many studies have demonstrated the protective role of EPS during drought stress. For example, *Proteus penneri*, *Pseudomonas aeruginosa* and *Alcaligenes faecalis* were identified as high EPS-producing strains based on mucoid colony formation (Naseem and Bano 2014). Individual and consortia strain inoculation of droughted maize seedlings resulted in higher soil moisture content, protein and sugar levels, and enhanced growth parameters (root and shoot dry weight and leaf area) compared to controls (Naseem and Bano 2014). Inoculated plants also had higher RWC as the protective mucilage layer around roots was highly hygroscopic. By maintaining the water potential levels around roots, EPS protected against desiccation and regulated soil nutrient diffusion to support growth despite water-limiting conditions (Naseem and Bano 2014).

In another study, droughted *Helianthus annuus* L. seedlings were inoculated with an EPS-producing *Pseudomonas putida* strain GAPP45 strain; inoculated plants had higher survival rates and displayed significant enhancements to the root adhering soil per root tissue (RAS/RT) ratio over control plants (Sandhya *et al.* 2009). Inoculation with *P. putida* eased drought stress symptoms by secreting EPS that bind to soil particles to form micro- (< 250µm diameter) and macro-aggregates (>250µm diameter). Soil aggregates are composed of organic matter and pores; unstable soil aggregates have low organic matter content and require additional supplementation from root exudates and microbial EPS (Sandhya *et al.* 2009). Formation of stable soil aggregates from *P. putida* EPS release had a positive effect on water retention and nutrient diffusion, enabling plant growth in spite of drought stress (Sandhya *et al.* 2009). Alami *et al.* (2000) made similar observations in sunflower plants inoculated with *Rhizobium* sp. strain YAS34 as treated plants had a higher RAS/RT ratio, soil macroporosity and biomass than controls. EPS release positively impacted RAS by increasing soil aggregate ability and soil adhesion to roots, which modulated root suction of water and nutrients. Consequently, *Rhizobium* inoculated

seedlings had higher N-uptake and growth rates than uninoculated plants (Alami *et al.* 2000).

EPS-producing PGPR strains can also alleviate metal toxicity (Upadhyay *et al.* 2017) and salt stress (Qurashi and Sabri 2012) by binding metal cations to negatively charged EPS functional groups. Identified EPS functional groups with metal cation binding abilities include alginate, uronic acids, glucose, mannose, carboxyl and phosphoryl groups (Upadhyay *et al.* 2017). However, metal biosorption by microbial EPS varies across species as metal biosorption depends on many factors, such as cell surface properties, functional group charge and metal speciation (Upadhyay *et al.* 2017). Under $Zn^{2+}$ stress, *Pseudomonas* strains increased alginate production in a stress dose-dependent manner and had altered morphology (thickened membranes and increased protuberances) to increase $Zn^{2+}$ binding sites, resulting in enhanced wheat seedling and root hair growth (Upadhyay *et al.* 2017). *Pseudomonas alg8* deletion mutants with impaired alginate production had significantly less EPS and biofilm formation; inoculated wheat plants with these mutants strains displayed no differences from uninoculated controls (Upadhyay *et al.* 2017).

Similarly in salt-stressed wheat seedlings, EPS-producing *Bacillus* and *Enterobacter* sp. strains increased salt tolerance by binding metal cations ($Na^+$, $K^+$ and $Ca^{2+}$); treated seedlings had up to an 6.3% decrease in $Na^+$ uptake compared to controls (Upadhyay *et al.* 2011). Qurashi and Sabri (2012) also showed that *Halomonas variabilis* and *Planococcus* strains increased EPS production in proportion to increasing NaCl concentrations. Inoculation of salt-stressed *Cicer arietinum* seedlings with these halotolerant strains lead to enhanced plant growth parameters (seedling length and biomass), osmolyte levels (sugar and proline) and soil structure. Both strains also increased soil aggregation by helping soil particles to stick together and maintaining a mucilage-water rich layer around seeds for enhanced germination rates compared to controls (Qurashi and Sabri 2012).

In addition, EPS secretion protects the $O_2$-sensitive nitrogenase enzyme in *Medicago* plants from oxidative damage; this was especially important during the early symbiotic establishment phase as host plants respond to *Sinorhizobium meliloti* infection with a protracted oxidative burst (Santos *et al.* 2001). Lehman and Long (2013) demonstrated a

positive correlation between succinoglycan (EPS-I) and galactoglucan (EPS-II) production with $H_2O_2$ reduction; *S. melilot* mutants lacking EPS-I production were sensitive to oxidative damage, but EPS-I overproducing mutants were resistant to $H_2O_2$. EPS-I is synthesised in high- and low-molecular weight forms, and the latter form was especially effective in lowering intracellular $H_2O_2$ levels (Lehman and Long 2013).

### 1.3.5 Fe-chelating siderophores in soil phytoremediation and pathogen resistance

Iron is an essential micronutrient for plant growth and is an integral component in many cellular reactions such as oxygen metabolism, electron transport, and DNA and RNA synthesis (Schalk *et al.* 2011). It is the second must abundant cation found in metal-dependant enzymes as it is heavily involved in the catalysis of redox reactions (Andreini *et al.* 2008). However, iron has low soil bio-availability as iron is commonly present as insoluble oxide hydrate complexes (Schalk *et al.* 2011). Soil microbes use siderophores to chelate and assimilate iron from the environment, either to the benefit or detriment of surrounding plants, depending on the microbe involved. Siderophores are low MW (200-2000 Da) metal-chelating enzymes with a strong $Fe^{3+}$ affinity of around 1030 $M^{-1}$ (Schalk *et al.* 2011). Bacteria assimilate the microbial Fe-siderophore complex using a common transport system comprising the TonB complex, TonB-dependent transporters and an inner TonB-ExbB-ExbD membrane complex, but once in the periplasm, Gram-positive and -negative bacteria utilise different mechanisms for translocating $Fe^{2+}$ into the cytoplasm (Schalk *et al.* 2011; Ahmed and Holmström 2014). Certain phytopathogens need siderophores to obtain iron for full virulence expression, but siderophores from PGPR strains can impart growth-promoting and stress resistance to host plants (Aznar and Dellagi 2015). Microbial siderophores have higher iron affinity than fungal counterparts and can outcompete fungal pathogens for limited $Fe^{3+}$ to limit phytopathogen survival (Hassen *et al.* 2016). In addition, microbial siderophores can also provide host plants with additional iron to boost growth under iron-limiting conditions (Masalha *et al.* 2000; Katiyar and Goel 2004; Radzki *et al.* 2013). It is unclear how this transfer occurs, but two current hypotheses exist: (i) the microbial ferric-siderophore complex is transported to the root apoplast via diffusion and mass flow, where the subsequent reduction of $Fe^{3+}$ siderophores traps $Fe^{2+}$ in the apoplastic fluid or (ii) microbial $Fe^{3+}$

siderophores perform a ligand exchange with plant-derived phytosiderophores, which plant roots then assimilate for iron uptake (Masalha *et al.* 2000; Ahmed and Holmström 2014).

External (soil $Fe^{3+}$) and internal (cytoplasmic $Fe^{3+}$) levels regulate microbial siderophore biosynthesis but recent evidence shows that other metals (e.g. molybdenum and aluminium) can also induce siderophore biosynthesis (Schalk *et al.* 2011). There are four types of microbial siderophores based on their different functional groups: carboxylate, hydroxamates, catecholates and pyoverdines (Ahmed and Holmström 2014). Siderophores have a great diversity of chemical structures; *Pseudomonas* produces over 50 types of pyoverdine siderophores but also synthesises many secondary low-affinity siderophores such as pyochelin, pseudomonin, corrugatins and ornicorrugatins, yersiniabactin, and thioquinolobactin (Boukhalfa and Crumbliss 2002; Cornelis 2010).

#### 1.3.5.1 Microbial siderophores in phytoremediation of heavy metal soils

Heavy metal stress causes significant plant growth retardation by causing excessive oxidative damage, but microbial siderophores can aid in the phytoremediation of heavy metal-laden soils (Dimkpa *et al.* 2009). While siderophores have a strong preference for iron, they can also chelate other metals with varying affinities (Schalk *et al.* 2011). For example, *Pseudomonas aeruginosa* secretes two types of siderophore (pyoverdine and pyochelin) which can bind to 16 metals collectively (Braud *et al.* 2009, 2010). Both siderophores had different metal binding affinities as pyoverdine was more effective at inhibiting non-biological metals ($Eu^{3+}$, $Ga^{3+}$, $Pb^{2+}$, $Sn^{2+}$ and $Tb^{3+}$) uptake, while pyochelin was more effective at reducing biological metal ($Co^{2+}$, $Fe^{3+}$, $Ni^{2+}$ and $Zn^{2+}$) uptake (Braud *et al.* 2009, 2010). Pyoverdine exerted a stronger protective effect as it was more efficient than pyochelin at sequestering extracellular metal cations; pyoverdine inhibited ~80% uptake for $Al^{3+}$ and $Cu^{2+}$ and ~40% uptake for $Co^{2+}$, $Eu^{3+}$, $Ni^{2+}$, $Pb^{2+}$, $Tb^{3+}$ and $Zn^{2+}$, while pyochelin approximately reduced 80% uptake for $Al^{3+}$, $Co^{2+}$, $Cu^{2+}$ and $Zn^{2+}$ (Braud *et al.* 2010). Consequently, *P. aeruginosa* was more tolerant against heavy metal stress than siderophore-impaired mutants as the siderophore-metal complex was too large to pass through microbial porins to enter cells (Braud *et al.* 2010). Inoculation also protects host plants against heavy metal stress as metal-bound siderophores decrease the extracellular levels of free metal cations in the surrounding rhizosphere (Tripathi *et al.* 2005). For example, *Pseudomonas putida* KNP9 significantly increased the height and

weight of mung bean seedlings despite high cadmium and lead stress (Tripathi *et al.* 2005). As *P. putida* KNP9 inoculation reduced the accumulation of cadmium in roots (52.6%) and shoots (37.5%), host plants experienced significantly less chlorophyll loss compared to uninoculated controls.

Another study examined the effects of inoculating cowpea plants in heavy metal-contaminated soil with the extracellular filtrate of *Streptomyces acidiscabies* E13, a nickel-resistant strain that secretes hydroxamate siderophores and auxin (Dimkpa *et al.* 2009). Uninoculated metal-stressed cowpea plants experienced severe growth retardation and reductions to leaf pigmentation, RNA and protein levels. However, treatment with *Streptomyces* extracellular filtrate alleviated these symptoms as treated plants had lower lipid peroxidation damage and greater plant biomass, chlorophyll and carotenoid levels compared to untreated controls (Dimkpa *et al.* 2009). Interestingly, metal chelation by the siderophores also protected *Streptomyces*-derived auxins from free radical degradation, enabling microbial auxin to exert its growth-promoting effects despite heavy metal stress. Dimkpa *et al.* (2009) also observed that treated plants had higher trace metal (Al, Cd, Cr, Cu, Mn, Ni and U) levels in the root tissue compared to untreated controls, but the cytotoxic effects was diluted in treated plants as they had significantly higher biomass. The researchers also noted that metal-chelated siderophores accumulated primarily in the root apoplast and had limited release into the symplast. Thus, most of the root-localised metal cations were not translocated into shoots, thereby reducing the metal toxicity effects (Dimkpa *et al.* 2009).

#### 1.3.5.2 Microbial siderophores and induced systemic resistance (ISR)

Microbial siderophores trigger induced systemic resistance (ISR) in plants against phytopathogen by iron scavenging or siderophore perception by host plants (Aznar and Dellagi 2015). ISR stimulates the plant defensive mechanisms, which primes plants to respond faster against pathogen infections (Van Loon and Bakker 2005). ISR is not a pathogen-specific response as it increases plant basal tolerance to make them more resistant against multiple pathogens (Van Loon and Bakker 2005). ISR shares phenotypic similarities with systematic acquired resistance (SAR) as the key NPR1 protein regulates both downstream signalling cascades (Annapurna *et al.* 2013; Hassen *et al.* 2016). However, ISR is regulated by jasmonic acid and ethylene signalling, while SAR is modulated by salicylic acid. Therefore, there is only a partial overlap in the spectrum of diseases that ISR and SAR protects against, e.g. ISR-primed plants have elevated

resistance against pathogens susceptible to jasmonic acid- or ethylene-dependent defence mechanisms (Annapurna *et al.* 2013). For example, *Pseudomonas aeruginosa* 7NSK2 produces three types of siderophores under Fe-limiting conditions and triggers ISR against pathogenic *Botrytis cinerea* (Audenaert *et al.* 2002) *and Pythium splendens* in tomato plants (Buysens *et al.* 1996), as well as against *Colletotrichum lindemuthianum* in bean plants (Bigirimana and Höfte 2002).

Audenaert *et al.* (2002) investigated the protective ISR effect of pyoverdine and pyochelin by generating three mutant strains defective in either (*pyoverdine*$^{+}$ *pyochelin*$^{-}$; *pyoverdine*$^{-}$ *pyochelin*$^{+}$) or both (*pyoverdine*$^{-}$ *pyochelin*$^{-}$) siderophores from the parental strain. Compared to the wild-type strain, all three mutants were considerably less efficient at inhibiting *Pythium*-induced seed and radicle rot. Pyoverdine and pyochelin have overlapping functions and are mutually exchangeable as both single mutants had similar antagonistic activity. (Audenaert *et al.* 2002). Further investigations by Audenaert *et al.* (2002) showed that pyochelin complementation enabled the double negative mutant to attain comparable protection levels against *Pythium* as the parental strain but could not trigger ISR in plants by itself. Instead, *P. aeruginosa* required synergistic actions between the Fe-pyochelin complex and pyocyanin (a phenazine compound)*;* both compounds act concertedly to deprive *B. cinerea* from iron assimilation, while simultaneously triggering ISR in tomato plants (Audenaert *et al.* 2002).

# 1.4 Cyanobacteria biofertilisers

Cyanobacteria biofertilisers have been primarily used for their direct effects as nitrogen-fixers. The most frequent cyanobacteria inoculants are heterocystous strains belonging to the *Nostocales* and *Stigonematales* orders, and the *Nostoc*, *Anabaena*, *Tolypothrix*, *Aulosira*, *Cylindrospermum,* and *Scytonema* genera (Kaushik 2014; Issa *et al.* 2014). However, non-heterocystous cyanobacteria can also form loose associations with crop plants. For example, *Chroococcidiopsis* sp. MMG-5 and *Leptolyngbya* sp. MMG-1 penetrated into the root epidermal cells of *Triticum aestivum*, *Vigna radiata* and *Pisum sativum* (Ahmed *et al.* 2010). These non-heterocystous strains were fixing $N_2$ as plant roots consumed surrounding $O_2$ through respiration, creating a microoxic environment suitable for nitrogenase expression (Ahmed *et al.* 2010). Nevertheless, this section will focus on heterocystous strains as they constitute the primary bulk of cyanobacteria

biofertiliser inoculants. Heterocystous cyanobacteria exist as photosynthetic vegetative cells under normal conditions but will differentiate into three cell types ($N_2$-fixing heterocysts, akinetes, and motile hormogonia) upon nutrient limitation or specific environmental signals (Flores and Herrero 2010), see Figure 1.4.

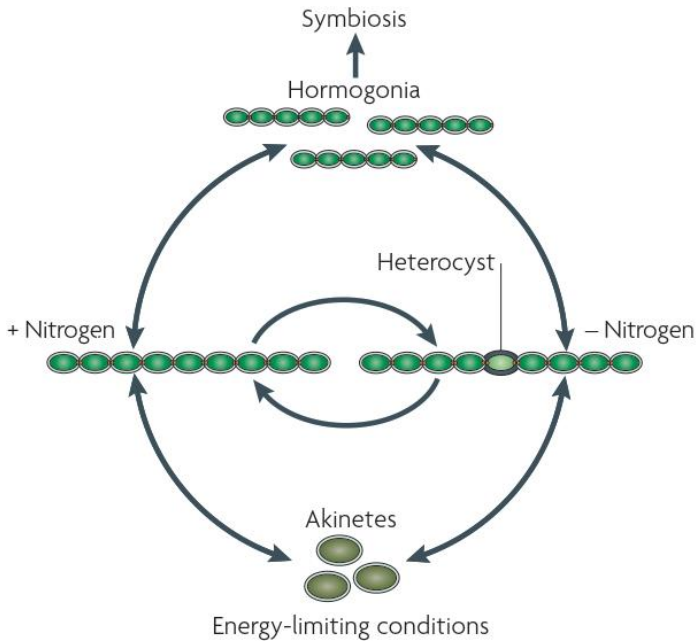


**Figure 1.4** - Lifecycle of certain heterocystous-forming cyanobacteria: heterocyst formation is induced under N-limiting conditions. Akinetes are induced under stress or energy-limiting conditions, while motile hormogonia filaments are dispersal units for entering plants to establish a symbiotic relationship. Image and information adapted from Flores and Herrero (2010).

Heterocyst formation is induced in response to N-deficiency; heterocysts have distinct morphological features that enable maintenance of a microoxic site for continued nitrogenase activity (Golden and Yoon 2003). Filamentous strains like *Nostoc* spp. spatially separate $N_2$-fixing heterocysts from photosynthetic vegetative cells; heterocysts provide fixed N to photosynthetic cells and receive sugars from vegetative cells in return (Flores and Herrero 2010). On the other hand, akinetes are spore-like cells induced in response to stress and energy-limiting conditions (Flores and Herrero 2010). Akinetes are more resistant towards cold and desiccation than vegetative cells, and only germinate once conditions become favourable again (Kumar *et al.* 2010). Motile hormogonia filaments have gliding motility and enter plants to establish a symbiotic relationship (Khamar *et al.* 2010).

### 1.4.1 Mechanism of cyanobacteria and plant symbiosis

#### 1.4.1.1 Infecting the host plant

$N_2$-fixing heterocystous cyanobacteria can associate with an extensive range of plants, such as bryophytes, ferns, gymnosperms and angiosperms (Khamar *et al.* 2010). The symbiotic relationship offers benefits to both parties as host plants receive fixed N from cyanobacteria strains in exchange for sugars, which supplements their growth under N-limiting conditions. In return, cyanobacteria gain access to the enclosed symbiotic cavities of the host plant which protects against predation, microflora competition and harsh environmental conditions (e.g. high light intensity and desiccation) (Adams *et al.* 2013). To infect their symbiotic partner, photosynthetic vegetative cells differentiate into hormogonia, which are transient, non-growing motile filaments required for infecting a symbiotic partner (Flores and Herrero 2010; Khamar *et al.* 2010). For example, *Nostoc punctiforme* mutants with inactivated pilus-forming genes (*pilT* and *pilD*) had diminished symbiotic competency with its host bryophyte *Blasia pusilla* because of impaired motility (Duggan *et al.* 2007). Various environmental cues induce hormogonia formation such as N-starvation, excess phosphate, changes in osmolarity, exposure to red light, and hormogonia-inducing factors (HIFs) released from N-stressed host plants (Khamar *et al.* 2010; Christman *et al.* 2011; Adams *et al.* 2013). Smaller than vegetative cells with unique, tapered ends, hormogonia filaments are remain mobile, up to 48 hours after induction (Christman *et al.* 2011). During this period, hormogonia gravitate towards chemoattractants released by host plants (Figure 1.5).

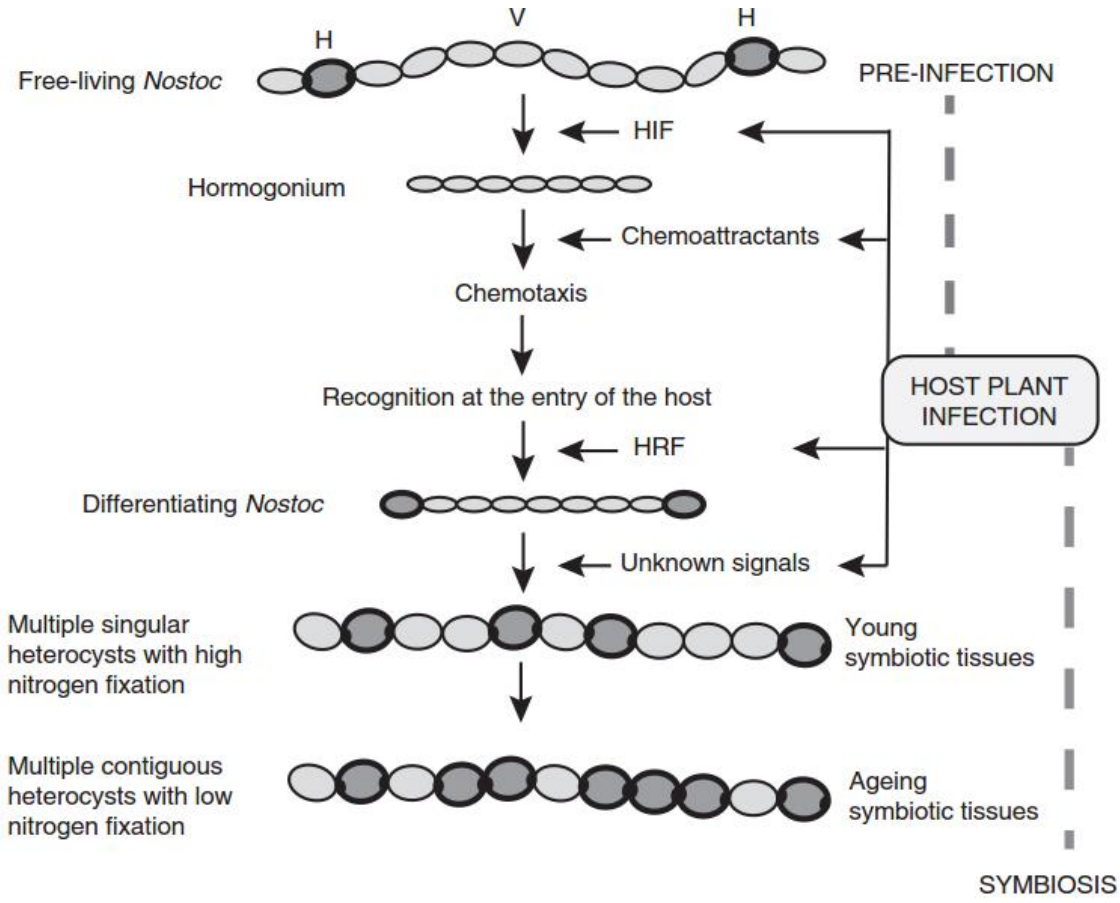


**Figure 1.5** - Mechanism of cyanobacteria and plant symbiosis. In N-free medium, Nostoc filaments exist as vegetative cells (V) that are regularly interspaced with N2-fixing heterocysts (H); heterocysts are easily distinguishable because of their thick envelope that limits O2 diffusion. N-stressed host plants releases hormogonia-inducing factors (HIF), triggering filament differentiation into motile hormogonia that are chemo-attracted towards the host plant. Upon penetrating the host symbiotic cavities, hormogonia revert to vegetative filaments with elevated heterocysts levels. N2 fixation is highest where single heterocysts predominate around young symbiotic tissue and drops among older symbiotic tissues with contiguous heterocysts. Image adapted from Santi et al. (2013).

However, hormogonia formation is not the sole factor in establishing symbiosis as certain *Nostoc* strains can form hormogonia but cannot infect the angiosperm *Gunnera* (Rasmussen *et al.* 1994). Instead, a successful symbiotic partnership involves a combination of hormogonia motility and the release of plant chemoattractants (Santi *et al.* 2013). Soluble sugars such as arabinose, glucose and galactose are hormogonia chemoattractants that play an important role in establishing plant-cyanobacteria symbiosis (Nilsson *et al.* 2006); *N. punctiforme* mutants that could not assimilate glucose because of inactivation of glucose permease (GlcP) were unable to infect its symbiotic partner, the hornwort *Anthoceros punctatus* (Ekman *et al.* 2013). As GlcP inactivation did not affect hormogonia motility, this demonstrated the importance of glucose in the

chemotaxis response (Ekman *et al.* 2013). As a result, heterocystous cyanobacteria can associate with a broad range of host plants as the chemo-attraction between hormogonia and plants is considerably less specific, unlike the stringent Nod-factor signalling pathway between rhizobia and legumes. For example, hormogonium of *Nostoc* strains (8964:3 and PCC 73102) were chemoattracted towards extracts of unconventional host plants like *Trifolium repens*, *Arabidopsis thaliana* and *Oryza sativa*, suggesting a unique capacity to associate with a wide host range (Nilsson *et al.* 2006).

#### 1.4.1.2 Establishment of symbiotic colony

Upon successfully entering the host plant, the tapered end cells of the hormogonia filament differentiates into heterocysts, while the remaining cells in the filament revert to vegetative cells. The vegetative cells show altered morphology as they are bigger and more irregular-shaped compared to their free-living counterparts (Santi *et al.* 2013). It is interesting to note that heterocyst differentiation within host plants occurs at substantially higher frequencies than in free-living cells. In free-living *Nostoc* filaments, the average heterocyst frequency is 5-10%, but increases to 25-80% in symbiotic filaments, depending on the host association and maturity status of the colony (Meeks 1990). The frequency of heterocysts increases in a gradient-like manner along maturing tissue. For example, around 5-10% of heterocysts are found in the young glands of *Gunnera*, while older glands have up to 75% (Santi *et al.* 2013). While the rate of $N_2$ fixation parallels increasing heterocyst frequency, it peaks at intermediate heterocyst frequencies of around 25-35%, when single heterocysts predominate around young symbiotic tissue (Meeks and Elhai 2002). $N_2$ fixation rates decline in older symbiotic tissue as most heterocysts are entering senescence (Adams *et al.* 2013). Older symbiotic tissue also has elevated frequencies of contiguous heterocysts, which develop over time as new heterocysts form adjacent to senescent heterocysts (Santi *et al.* 2013). Contiguous heterocysts have significantly lower $N_2$-fixing activity compared to a singlet heterocyst as fixed carbon has to diffuse longer distances from vegetative cells to reach functional heterocysts in a contiguous group (Meeks and Elhai 2002; Meeks *et al.* 2002).

Symbiotic cyanobacteria colonies, henceforth termed cyanobiont, have to adapt to their new intracellular conditions (Santi *et al.* 2013). These physiological adaptations include the transition to heterotrophic growth, elevated heterocyst frequency, and $N_2$ fixation

rates, and downregulation of growth rate, carbon fixation, and ammonium assimilation (Meeks and Elhai 2002). As cyanobionts are fixing $N_2$ in exchange for reduced carbon compounds, genes involved in $N_2$ fixation and the oxidative pentose phosphate pathway are highly upregulated; the latter oxidises carbohydrates in the dark and is vital for heterotrophic growth (Stal 2012). In contrast, enzymes involved in the carbon fixing Calvin cycle are downregulated (Meeks and Elhai 2002). Cyanobionts also have slowed growth (e.g. doubling time of *Nostoc-Anthoceros* is 240 hours compared to 45 hours in its free-living state) to match the growth rate of its host plant (Meeks 1990). Symbiotic *Nostoc* colonies also experience changes related to EPS synthesis and expression of surface- and membrane-associated proteins, signifying adaptations that facilitate efficient nutrient exchange between the partners (Santi *et al.* 2013). The composition of light harvesting phycobiliproteins are also altered, e.g. allophycocyanin and phycocyanin are upregulated, while phycoerythrin is downregulated, suggesting adaptation to the dark interior of symbiotic cavities (Santi *et al.* 2013).

### 1.4.2 *Nostoc muscorum* exometabolites

Cyanobacteria are versatile organisms found in aquatic and terrestrial ecosystems; their unique capacity to inhabit most environments is attributed to the diverse range of exuded metabolites, henceforth termed exometabolites. These bioactive exometabolites have assorted properties ranging from antiviral, antibacterial, antifungal, antitumoral and anti-inflammatory, that enable their proliferation in spite of harsh environments (Singh *et al.* 2005; Jaiswal *et al.* 2008; Prasanna *et al.* 2010). This thesis aims to investigate the bioactive exometabolites released by *Nostoc muscorum* sp. 7120, hereafter *N. muscorum.* Considered the model organism for studying heterocyst differentiation, *N. muscorum* has undergone many name changes over the years. *Nostoc* sp. strain PCC 7120 was originally named *Nostoc muscorum*, before being classified as *Anabaena* and finally renamed as *Nostoc* sp. strain PCC 7120 based on DNA–DNA hybridization data and short tandem repeated repetitive fingerprinting (Svenning *et al.* 2005). However, *N. muscorum* cannot differentiate into akinetes nor hormogonia, and have a more limited phenotype than any taxonomically defined *Nostoc* species (Meeks *et al.* 2002). The following section details all the known *N. muscorum* exometabolites documented in literature, as summarised in Table 1.1.

**Table 1.1:** Exometabolites detected in *N. muscorum* in conditioned medium.

| Exometabolites | Description |
|---|---|
| Exoproteins | 139 identified exoproteins belonging to 16 different functional categories (Oliveira *et al.* 2015) |
| Exopolysaccharides | 10% TCA extract contained arabinose, glucose, galactose, rhamnose, xylose, ribose, and two unidentified components (Mehta and Vaidya 1978) |
| Amino acids | Aspartate, glutamic acid, glutamine, asparagine, serine, glycine, histidine, threonine, alanine, arginine, proline, tyrosine, valine, methionine, cysteine, isoleucine, leucine, phenylalanine and lysine detected (Picossi *et al.* 2005; Pernil *et al.* 2008) |
| Phytohormones | Auxin (Mirsa and Kaushik 1989; Karthikeyan *et al.* 2009) and ABA (Maršálek *et al.* 1992) |
| Bioactive compounds | High concentrations of phenolic and alkaloids present (Abdel-Hafez *et al.* 2015) |
| | Fatty acids and derivatives (Abdel-Hafez *et al.* 2015) |
| | Long-chain base sphingolipids (sphingosine$^{\Delta 4}$ and phytosphingosine) (Daly 2013) |

### 1.4.2.1 *N. muscorum* exoproteome

The exoproteome comprises a selected subset of proteins found in the extracellular environment of a biological system (Armengaud *et al.* 2012). Their extracellular presence results from active (protein translocation and secretion) or passive (cell lysis and membrane diffusion) transport (Armengaud *et al.* 2012; Christie-Oleza *et al.* 2015). Exoproteins are characterised by long half-lives that allow them to remain stable under sub-optimal extracellular conditions (Christie-Oleza *et al.* 2015). Analysis of the exoproteome of *N. muscorum* under different nitrogen sources identified 139 proteins belonging to 16 different functional categories (Oliveira *et al.* 2015). A large subset of the identified exoproteins is associated with ROS detoxification, indicating the importance of maintaining redox homeostasis even outside the cell (Oliveira *et al.* 2015). Proteins were profiled under nitrogen-fixing conditions ($BG11_0$), where the heaviest protein mass was 80.8 kDa (Alr2887 protein) and the lightest, 9.8 kDa (fragment of phycocyanin A subunit).

### 1.4.2.2 Exopolysaccharide release from *N. muscorum*

Exopolysaccharides are biopolymers secreted by cyanobacteria and are the main constituents of the extracellular polymeric matrix, otherwise known as biofilms (Swarnalakshmi *et al.* 2013). Biofilms provide structural support and microbial protection for survival under unfavourable conditions, such as dehydration, UV radiation, fluctuating pH levels, antimicrobial resistance and protozoan predation (Seneviratne *et al.* 2009; Triveni *et al.* 2013). Mehta and Vaidya (1978) investigated the EPS composition in *N. muscorum* and detected arabinose, glucose, galactose, rhamnose, xylose and ribose. The most recurrent monosaccharides found in cyanobacterial EPS are fucose, rhamnose, arabinose, galactose, glucose, mannose, xylose, galacturonic acid and glucuronic acid, but EPS composition varies according to species (Rossi and De Philippis 2015).

### 1.4.2.3 Amino acid exudates from *N. muscorum*

The release of amino acids into culture medium has been reported in cyanobacteria (Watanabe 1951; Fogg 1952; Stewart 1963; Flynn and Gallon 1990). The mechanism of amino acid release has not been fully elucidated, but evidence strongly indicates that spontaneous diffusion has a greater influence than cellular lysis (Montesinos *et al.* 1995; Picossi *et al.* 2005; Pernil *et al.* 2008). Cell lysis is not considered the primary route of amino release as extracellular amino acid levels would correspond with the most abundant intracellular amino acids, which was not observed by Picossi *et al.* (2005). Moreover, *N. muscorum* strains with impaired neutral amino acid transport systems (N-I, N-II and N-III) have elevated concentrations of extracellular hydrophobic amino acids in their conditioned medium (CM), the liquid medium in which cultures are grown in, as cells are unable to import leaked amino acids back into the cell (Montesinos *et al.* 1995; Picossi *et al.* 2005; Pernil *et al.* 2008, 2015). In wild-type *N. muscorum* CM, the following amino acids were detected using high performance liquid chromatography (HPLC): aspartate, glutamic acid, glutamine, asparagine, serine, glycine, histidine, threonine, alanine, arginine, proline, tyrosine, valine, methionine, cysteine, isoleucine, leucine, phenylalanine and lysine (Picossi *et al.* 2005; Pernil *et al.* 2008).

### 1.4.2.4 Phytohormone production by *N. muscorum*

The ability of PGPR inoculants to produce phytohormones is vital in establishing symbiotic relationships with host plants, but free-living microbes are also capable of phytohormone biosynthesis (Tsavkelova *et al.* 2006). The extracellular presence of auxin in *N. muscorum* CM has been reported (Mirsa and Kaushik 1989; Karthikeyan *et al.* 2009), treatment of rice and wheat seedlings with culture filtrate resulted in an increase of coleoptile and radicle length (Mirsa and Kaushik 1989; Karthikeyan *et al.* 2009). In addition, the extracellular production of ABA occurred in a dose-dependent manner against salt stress in *N. muscorum* (Maršálek *et al.* 1992). Both auxin and ABA can be exploited for improvement of plant stress tolerance (Lu and Xu 2015); overexpression of *AtEDT1*/*HDG11* (a protein of the class IV HD-Zip family) in *Brassica oleracea* var. *alboglabra* exhibited auxin-overproduction phenotypes and hypersensitivity to ABA, leading to significantly improved drought and osmotic stress tolerance (Zhu *et al.* 2016). Similarly, transgenic ABA-overexpressing tobacco lines displayed enhanced drought tolerance levels, showing that maximum stress tolerance occurs when ABA levels were elevated before stress application (Qin and Zeevaart 2002).

### 1.4.2.5 Bioactive compounds derived from *N. muscorum* growth medium.

The extracellular filtrate of *N. muscorum* exhibited antimicrobial activity against Gram-positive (*B. subtilis, B. cereus* and *S. aureus*), and Gram-negative bacteria (*E. coli* and *S. typhi*) and filamentous fungi (*Aspergillus niger, Aspergillus flavous and Penicillium* sp.) (El-Sheekh *et al.* 2006). The identity of the bioactive compound was not fully elucidated, but infrared and nuclear magnetic resonance work indicated that it was a phenolic compound (El-Sheekh *et al.* 2006). In addition, *N. muscorum* CM also displayed anti-fungal activity against *Alternaria porri*, the carrier of onion purple blotch, by inhibiting linear mycelial growth by 20.37% (Abdel-Hafez *et al.* 2015). The fungicidal activity was attributed to the high concentrations of phenols (145.0 mg/L) and alkaloids (378.12 mg/L) present in *N. muscorum* CM (Abdel-Hafez *et al.* 2015) and this corresponds to previous antimicrobial activity reported in other cyanobacteria CM (*Anabaena subcylindrica, Oscillatoria angusta* and *Spirulina platensis*) that also contained high concentrations of phenolic, saponins and alkaloid compounds (de Cano *et al.* 1990; Zulpa *et al.* 2003; Hussien *et al.* 2009; Zeeshan *et al.* 2010). Gas chromatography-mass spectrometry (GC-MS) analysis identified 22 compounds, constituting 58.15% of total analytes, in *N. muscorum* CM, including various fatty acids and methyl ester forms (Abdel-Hafez *et al.*

2015). Some of the more notable identified compounds include oleic acid, a long-chain unsaturated fatty acid with antibacterial activity (Zheng *et al.* 2005) and linoleic acid methyl esters that inhibit *Ehrlich* tumour growth in mice (Zhu *et al.* 1989). Additionally, the presence of two free long-chain base sphingolipids (sphingosine$^{\Delta 4}$ and phytosphingosine) were detected in *N. muscorum* CM (Daly 2013). Sphingolipids are major constituents of cell membranes and are putative secondary messengers in many signalling activities, including plant stress tolerance and programmed cell death regulation (Berkey *et al.* 2012).

# 1.5 Modes of cell death and their hallmarks

Cell death is an important component of the cell life cycle and it is essential to make distinctions between its different modes as the timing and severity of an insult governs the final cell fate (Lockshin and Zakeri 2004). The importance of stress dosage in determining cell fate has been demonstrated across animal and plant cell cultures. For example, HaCaT keratinocyte (Mammone *et al.* 2000) and human tumour (HL-60, U937, Molt-4 and Daudi) (Lennon *et al.* 1991) cell lines underwent apoptosis under medium stress encounters, but died predominantly by necrosis under high stress stimuli. A similar biphasic cell death motif was observed in carrot (*Daucus carota*, cell line S12) cell suspension cultures (McCabe *et al.* 1997) and *Arabidopsis* seedlings (Hogg *et al.* 2011). In animal systems, researchers have grouped cell death into three categories based on distinctive corpse morphologies: apoptosis, autophagy, and necrosis (Lockshin and Zakeri 2004). Apoptosis in animal cells is characterised by cell shrinkage, nuclear condensation (pyknosis) and fragmentation (karyorrhexis), and plasma membrane blebbing; the integrity of the plasma membrane is maintained up to the point the cell breaks up into apoptotic bodies, which are removed by phagocytes (Savill and Fadok 2000; Rock and Kono 2008; Taylor *et al.* 2008). Apoptotic death avoids inducing an inflammatory response as cells die quickly and are rapidly cleared before they can spill their cellular contents (Rock and Kono 2008). In contrast to apoptosis, necrosis is associated with uncontrolled cell death when cells cannot withstand overwhelming cellular stress (Hogg *et al.* 2011). Necrotic death is characterised by the loss of plasma membrane integrity, resulting in impaired osmoregulation and the influx of water and ions into the cell; this causes cells to rupture and release their cellular contents, eliciting an inflammatory reaction (Lockshin and Zakeri 2004). Finally, autophagy is a recycling pathway that serves as a survival response to nutrient starvation (Van Doorn and

Woltering 2005). Double-membrane vesicles encapsulate obsolete organelles and long-lived proteins (known as autophagosomes) and fuse with a lysosomal vacuole for the degradation and recycling of nutrients (Edinger and Thompson 2004).

### 1.5.1 Key differences between animal cell apoptosis and plant AL-PCD

Programmed cell death (PCD) in plant cells shares many hallmarks of apoptosis in animal cells but key differences exist between them. Some commonalities exist because of shared ancestry with an ancient unicellular ancestor, but evolution of the apoptotic sequence, following the divergence of plant and animal lineages, has resulted in very distinctive attributes of their respective cell death programmes (Reape and McCabe 2010). Hence, apoptotic-like (AL-PCD) is used to describe PCD in plants to accentuate its morphological differences from the mammalian apoptotic programme; this makes it easier to compare plant PCD studies across different research groups (Reape *et al.* 2008; Reape and McCabe 2013). AL-PCD exhibits a different death profile than animal cell apoptosis as plant cells have unique cellular architectures, e.g. cell walls that inhibit phagocytosis (Kacprzyk *et al.* 2011) and a large vacuole that constitutes up to 80% of cell volume (da Silva Conceicão *et al.* 1999). Hence, overlapping death pathways may display mixed hallmarks in plant cells. For example, the *Papaver* self-incompatibility pollen tube response exhibits a mixture of vacuolar and necrotic hallmarks (Bosch and Franklin-Tong 2008).

A key difference between AL-PCD and apoptosis is the lack of apoptotic bodies and phagocytic cells in plants (van Doorn *et al.* 2011). There have been reports of 'apoptotic-like' bodies in plants, such as the sloughing root cap of onion cells (Wang *et al.* 1996) and the hypersensitive response (HR) in soybean leaves with *Pseudomonas syringae* (Levine *et al.* 1996), and wheat infected with *Puccinia graminis tritici* (Bolton *et al.* 2008). However, it is difficult to make unambiguous claims on whether the protoplast had fragmented into apoptotic bodies or if the masses had simply fused together out of plane, and it is highly unlikely that apoptotic-like bodies is a universal feature of plant cells (McCabe *et al.* 1997; Van Doorn and Woltering 2005). That being said, the corpse morphology of AL-PCD in plant cells is remarkably similar to canonical apoptotic animal cells (e.g. cell shrinkage, membrane blebbing, nuclear condensation and fragmentation, and cytoplasm retraction) and a growing body of evidence indicates that plants share certain evolutionary conserved parts of the cell death machinery with animal systems

(Watanabe and Lam 2008). In any case, the term AL-PCD used for plant cells, will henceforth be referred to as PCD, unless specified otherwise.

## 1.5.2 Cell death machinery in plant AL-PCD

### 1.5.2.1 Caspase-like proteases (CLPs)

Caspases are a family of proteases that play a key role in animal apoptosis; the name caspase is derived from the critical cysteine (Cys) residue in the active site of the enzyme and the cleavage of specific aspartic acid (Asp) residues at the C-terminus of target proteins (Lord and Gunawardena 2012). During apoptosis, activation of the caspase cascade occurs through two routes: (1) the intrinsic pathway is initiated by release of pro-apoptotic mitochondria intermembrane space (IMS) proteins into the cytoplasm or (2) the extrinsic pathway which involves death/Fas ligand receptors (Reape and McCabe 2008). The animal caspase system is considered absent in plants as evidenced by the lack of caspase homologues in the sequenced *Arabidopsis* genome, but two caspase-like proteases (CLPs) have been detected in plants: cysteine endopeptidases (Rojo *et al.* 2004) and serine endopeptidases (Coffeen and Wolpert 2004).

Cysteine endopeptidases are further sub-divided into groups: vacuolar processing enzymes (VPEs) and metacaspases (Lord and Gunawardena 2012). VPEs are plant cysteine proteases belonging to the legumain C13 protein family also found in animals (Watanabe and Lam 2009). VPE-mediated PCD occurs not only in response to stress (pathogen, heat, oxidative, salt, UV radiation and heavy metal), but is also involved in plant development processes, such as hybrid lethality, reproductive development, bud development and senescence (Hatsugai *et al.* 2006). VPEs share many structural and functional similarities with animal caspase-1 such as the histidine-cysteine catalytic dyad in the active site (Hatsugai *et al.* 2006; Hara-Nishimura and Hatsugai 2011). Moreover, key residues (Arg179, Arg341 and Ser 347) of the caspase-1 substrate-binding pocket are conserved in over 20 VPEs, implying a similar binding pocket (Piszczek and Gutman 2007; Hara-Nishimura and Hatsugai 2011) and substrate activity as VPEs also cleaves YVAD, a synthetic caspase-1 substrate (Piszczek and Gutman 2007). Finally, *Arabidopsis* leaves exhibit caspase-1 and VPE activity, but both enzyme activities are absent in the *VPE*-null quadruple mutant (*αvpe-3*, *βvpe-5*, *γvpe-1*, *δvpe-1*) (Kuroyanagi *et al.* 2005). However unlike their cytosol-localised animal caspase-1 counterparts, VPEs are localised

in the vacuole and can also cleave asparagine (Hatsugai *et al.* 2006). Metacaspases are divided into Type I and II groups, based on their sequence and domain similarity to true caspases: Type I originates from fungi and plants, while Type II are found exclusively in plants (Lord and Gunawardena 2012). While metacaspases share many structural similarities with animal caspases, it is unlikely they are involved in plant caspase-like activities; metacaspases have different substrate specificity (cleaves arginine and lysine, but not aspartic acid) and cannot degrade synthetic caspase substrates (Piszczek and Gutman 2007; Watanabe and Lam 2009).

Saspases belong to the serine endopeptidase family and exhibits caspase-6 like activities by cleaving Asp residues across a range of caspase substrates (VAD-, VKMD-, VNLD-, and VEHD-AFC) and are inhibited by caspase inhibitors (Watanabe and Lam 2009; Hatsugai *et al.* 2015). However, saspases are not strict CLPs as they have a serine residue active-site, instead of the typical Cys residue (Sanmartín *et al.* 2005). Similar to caspases, saspases have unusual characteristics that suggest a role as a processive instead of a degradative protease, such as: (1) inactivity against general protease and non-caspase specific substrates (casein, bovine serum albumin and purified RubisCO), (2) unconventional Asp requirement in substrate $P_1$ position and (3) early involvement in the signalling cascade leading to RubisCO proteolysis and eventual PCD (Coffeen and Wolpert 2004; Vartapetian *et al.* 2011). Unlike animal caspases though, saspases are constitutively expressed and secreted into the apoplast to avoid cell proteolysis (Vartapetian *et al.* 2011). Upon PCD-induced stress, saspase activity in the extracellular fluid increases greatly, possibly from the 'de-tethering' or unmasking of saspase activity in the extracellular space (Vartapetian *et al.* 2011). It is unclear how the extracellular saspase signal is transduced back to the cytosol, but saspase extracellular activity is detected one hour after PCD-inducing victorin treatment and at least seven hours before PCD-markers, e.g. RubisCO proteolysis and DNA laddering, appear (Coffeen and Wolpert 2004).

#### 1.5.2.2 Cytochrome *c*

The intrinsic pathway of apoptosis is initiated by the release of cytochrome c (cyt *c*) from the mitochondrial IMS into the cytoplasm. Cyt *c* activates the apoptotic protease activating factor that oligomerizes into a heptameric apoptosome, which recruits and

activates initiator procaspase-9 proteins. Activated procaspase-9 cleaves downstream executioner procaspases to initiate an amplifying proteolytic cascade that leads to apoptosis. As cyt *c* release is a common feature of AL-PCD in plant research (Balk *et al.* 1999; Curtis and Wolpert 2002; Vacca *et al.* 2006; Contran *et al.* 2007), cyt *c* was initially believed to play a similar role in plants as it did in animal apoptosis. However, Balk *et al.* (2003) demonstrated that cyt *c* did not directly activate AL-PCD proteases: in a cell-free system containing purified *Arabidopsis* nuclei, the addition of broken mitochondria displayed typical AL-PCD hallmarks. However, addition of purified plant cyt *c* could not induce the same AL-PCD symptoms, indicating that alternative mitochondrial proteins were initiating AL-PCD in plants (Balk *et al.* 2003). Instead of directly activating AL-PCD proteases, release of cyt *c* amplified the original PCD-inducing signal by disrupting the mitochondrial electron transport chain (ETC) and generating lethal ROS levels (Jabs 1999).

#### 1.5.2.3 Sphingolipids

Sphingolipids are fatty acids that are major constituents of cell membranes and account for up to 40% of the plasma membrane and tonoplast lipids in plants (Kacprzyk *et al.* 2011). In plants, there are four classes of sphingolipids: free long-chain bases (LCBs), ceramides, glycosylceramides and (glycosyl) inositol phosphoceramides (G)IPCs (Berkey *et al.* 2012). Great structural diversity exists between these different classes, but all are composed of a sphingoid long-chain base bounded to an N-acylated fatty acid chain via an amide link. As illustrated in Figure 1.6, the structural diversity of sphingolipids is attributed to many factors, e.g. length of the LCB and N-acylated fatty acid chain, degree of hydroxylation, desaturation, number and position of double bonds in the LCB and degree of saturation and hydroxylation of the fatty acid chain (Berkey *et al.* 2012). Over 200 sphingolipids have been identified in *Arabidopsis* leaves (Markham *et al.* 2006) and its structural diversity plays an important role as putative second messengers in signalling networks, including plant stress tolerance and AL-PCD regulation (Berkey *et al.* 2012). Two classes of sphingolipids and their respective phosphorylated derivatives appear to be key regulators of plant PCD (Figure 1.7).

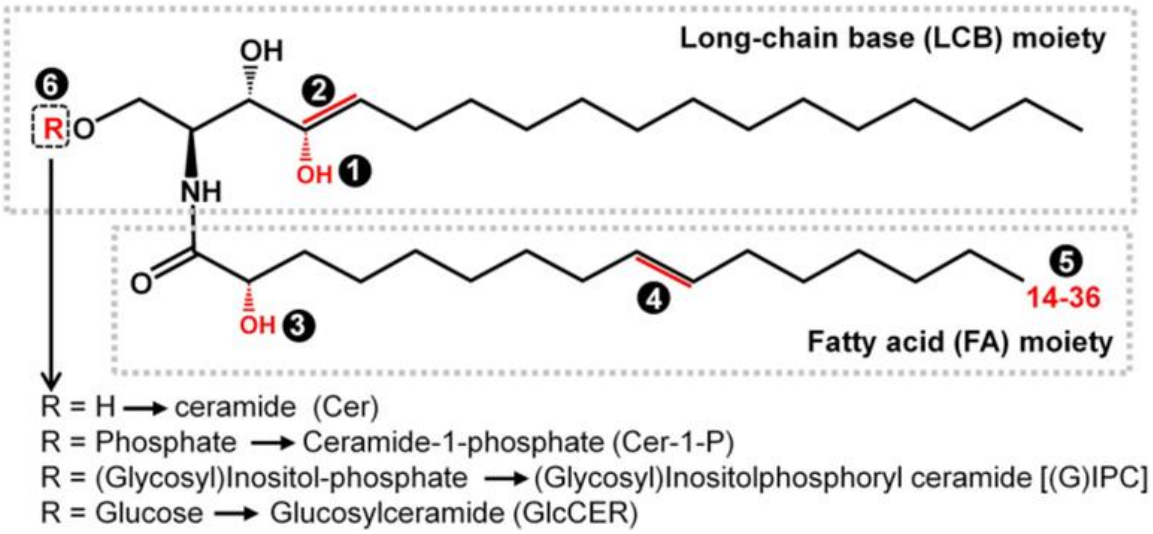


**Figure 1.6** - Four classes of plant sphingolipids: free LCBs, ceramides, glycosylceramides and (glycosyl) inositol phosphoceramides. All sphingolipids comprise a hydrophobic ceramide core and a hydrophilic head group. The ceramide core is composed of a sphingoid LCB linked to a fatty acid (FA) moiety. Sources of structural diversity can be generated from: (1) modification of the LCB by hydroxylation at 4-position or (2) double bond formation at $C_4$ or $C_8$, (3) modification of the FA moiety by hydroxylation at the $\alpha$-position, (4) double bond formation at the ω9-position or (5) variation in FA chain length and (6) substitution of the hydrophilic head group with a phosphoryl group (ceramide phosphates), mono- or pluri-hexose (glycosylceramides) or (glycosyl) inositol phosphate group [(G)IPC]. Image adapted from Berkey *et al.* (2012) and text adapted from Berkey *et al.* (2012) and Pata *et al.* (2010).

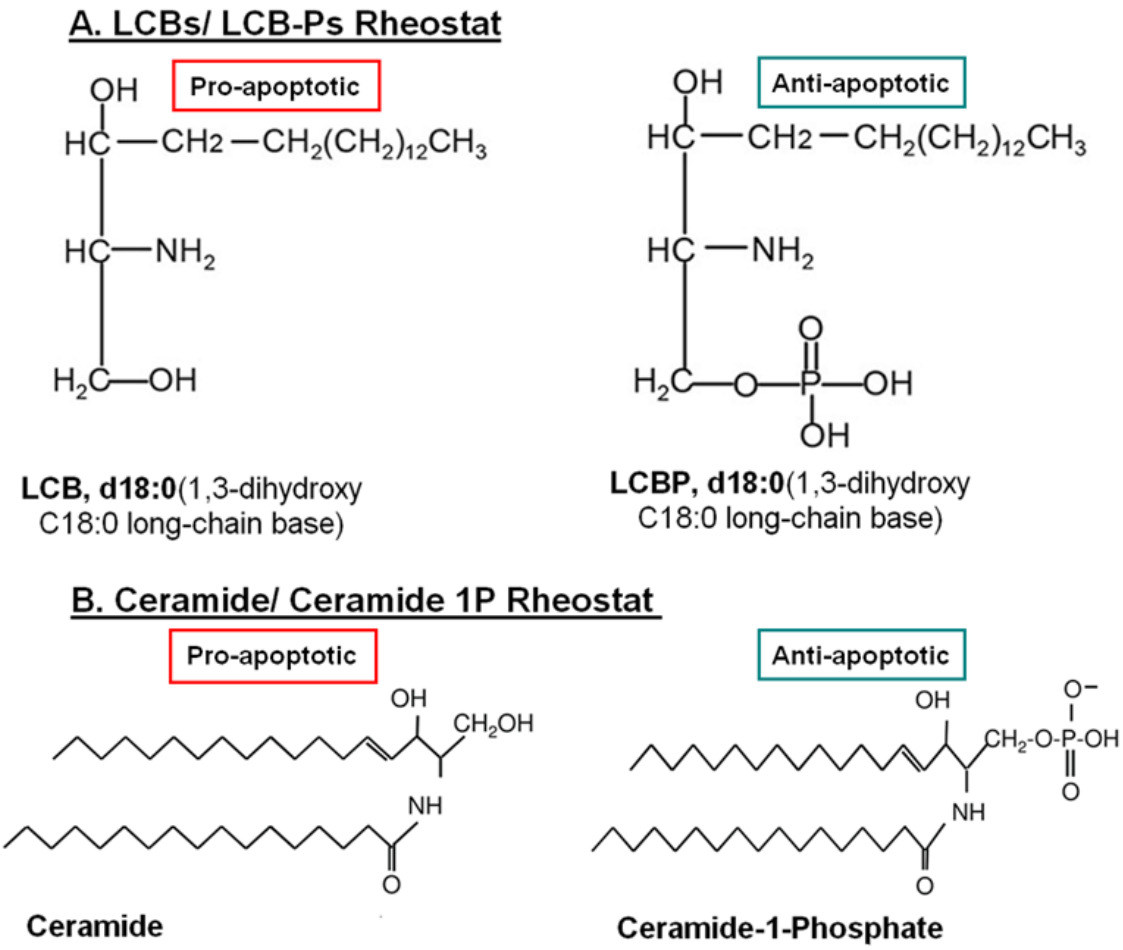


**Figure 1.7** - Two sphingolipid pairs that act as a rheostat to control plant PCD: (A) LCBs and LCB-Ps and (2) ceramide and ceramide-1-phosphate. Images adapted from Li *et al.* (2014).

The first pair is composed of LCBs and their phosphorylated forms (LCB-Ps) (Berkey *et al.* 2012). Mammalian studies show that LCB-Ps suppresses PCD and similar observations are seen in plants: exogenous application of LCBs (dihydrosphingosine, phytosphingosine and sphingosine) induced ROS production and PCD in *Arabidopsis* leaves, while their phosphorylated forms (dihydrosphingosine-1-phosphate, phytosphingosine-1-phosphate, and sphingosine-1-phosphate) could not induce PCD (Shi *et al.* 2007). Interestingly, the PCD-inducing effects of these LCBs were dose-dependent (Shi *et al.* 2007). Coupled with further studies showing that LCB accumulation, via LCB lyase mutation (Tsegaye *et al.* 2007) and sphingosine kinase inhibitors (Alden *et al.* 2011), triggers PCD in *Arabidopsis*, these observations suggest that homeostatic maintenance of LCBs and LCB-Ps acts as a rheostat to control plant PCD (Shi *et al.* 2007; Berkey *et al.* 2012).

The second rheostat pair consists of ceramides and their phosphorylated form, ceramide-1-phosphate (C1P). CerK (ceramidases kinase) is responsible for phosphorylating ceramides (a pro-apoptotic signal) into C1P (pro-survival signal). *Arabidopsis* CerK mutants (*acd5*) with only 10% of wild-type activity, accumulated non-phosphorylated ceramides and displayed elevated PCD levels upon pathogen infection (Liang *et al.* 2003). Ceramide treatment induced higher PCD levels in *acd5* protoplasts than wild-type plants, while C1P partially alleviated the PCD-inducing effects of ceramide (Liang *et al.* 2003). Like the LCB/LCB-P rheostat, these results suggest that maintaining the balance between ceramides and C1P regulates plant PCD. It is also of note that ceramides and sphingosine-1-phosphate (S1P) can also counteract one another, Alden *et al.* (2011) demonstrated that ceramide induces AL-PCD in a dose-dependent manner which S1P application could attenuate. An interesting 1:1 relationship existed between both compounds: 10 μM S1P protected *Arabidopsis* cells from PCD by 10 μM ceramide, but could not protect against PCD induced by 100 μM ceramide (Alden *et al.* 2011). Similarly, 100 μM S1P completely attenuated 100 μM ceramide-induced PCD. This unique dose-dependent ceramide/S1P effect is consistent with the existence of a sphingolipid rheostat in regulating plant PCD (Alden *et al.* 2011).

#### 1.5.2.4 'BCL2-like' family members

The release of mitochondrial proteins into the cytoplasm results from mitochondrial membrane permeabilisation (MMP), a key feature shared between apoptosis and AL-PCD. In mammalian cells, MMP ocurs via the Bax/Bcl-2 controlled pore (Shimizu *et al.* 1999; Youle and Strasser 2008). Composed of pro-apoptotic (Bax, Bak, Bad and Bid) and anti-apoptotic (Bcl-2 and Bcl-$x_L$) proteins, the Bcl-2 protein family regulates the intrinsic pathway of apoptosis (Youle and Strasser 2008). Under normal growth conditions, the integrity of the outer mitochondrial membrane is maintained through a balance of pro- and anti-apoptotic proteins, but disruption of the balance releases mitochondrial IMS proteins into the cytoplasm (Wang 2001; Adrain and Martin 2001). While no Bcl-2 homologues have been identified in plants, divergent sequences can produce similar catalytic active sites: mammalian Bcl-2 and *C. elegans* ced-9 genes only share 25% sequence similarity but can functionally substitute for one another (Lord and Gunawardena 2012). Therefore, the inability of sequence alignments to detect plant Bcl-2 homologues does not necessarily mean they are absent (Lord and Gunawardena 2012).

It is of note that transgenic expression of mammalian Bcl-2 proteins in plants can regulate PCD induction/inhibition. For example, PCD in stress-induced (UV-B irradiation, paraquat treatment, and *tobacco mosaic virus* infection) tobacco plants was inhibited by overexpression of anti-apoptotic Bcl-$x_L$ and ced-9 (*C. elegans* homolog) proteins (Mitsuhara *et al.* 1999). Similarly, overexpression of pro-apoptotic Bax protein triggered rapid cell death in tobacco plants, reminiscent of a hypersensitive response (Lacomme and Santa Cruz 1999). In addition, Bax inhibitor-1 (BI-1) homologues have been identified in various plants such as *Arabidopsis*, rice, tobacco and barley (Ishikawa *et al.* 2011). BI-1 is one of the most intensively characterised cell death suppressors conserved between plants and mammals (Ishikawa *et al.* 2011); mammalian Bax-induced cell death could be suppressed by BI-1 (AtBI-1) overexpressing *Arabidopsis* lines (Kawai-Yamada *et al.* 2001). These results suggest that in spite of the apparent lack of plant Bcl-2 homologs, there is a highly conserved PCD mechanism being targeted and shared across both kingdoms.

Plant BI-1 resides in the endoplasmic reticulum (ER) and interacts with other ER-based proteins (calmodulin, cb5-interacting and cb5lD-containing proteins) to regulate intracellular $Ca^{2+}$ flux and sphingolipid levels (Ihara-Ohori *et al.* 2007; Kawai-Yamada *et al.* 2009; Ishikawa *et al.* 2011). The ER plays a key role in lipid and protein biosynthesis, with specific mechanisms for protein sorting, post-translational modifications (N-glycosylation) and protein folding (Petrov *et al.* 2015). The ER also functions as an intracellular $Ca^{2+}$ source which is accessed for signalling purposes: $Ca^{2+}$ is a secondary messenger common to animal apoptosis and plant PCD as rapid $Ca^{2+}$ release from the ER into the cytoplasm takes place in response to stress perception (Kacprzyk *et al.* 2011). When a cell is subjected to increasing stress levels, cellular function becomes impaired and misfolded proteins accumulate inside the ER, thus instigating ER stress (Lam 2008). The cell tries to overcome ER stress by activating the unfolded protein response (UPR), which activates a specific suite of genes (e.g. isomerases and chaperones) to increase the protein folding capacity of the cell (Lam 2008). If UPR is insufficient for restoring protein conformation, the cell undergoes PCD because of the inability to withstand prolonged ER stress (Kacprzyk *et al.* 2011). Taking this into consideration along with the interacting partners of plant BI-1, there is substantial evidence suggesting that the ER-localised BI-1 acts as a rheostat for determining the ER stress threshold at which PCD is initiated

(Watanabe and Lam 2009; Ishikawa *et al.* 2011). Figure 1.8 provides a summary on the mechanism of AL-PCD and the role of plant BI-1 in regulating plant stress tolerance.

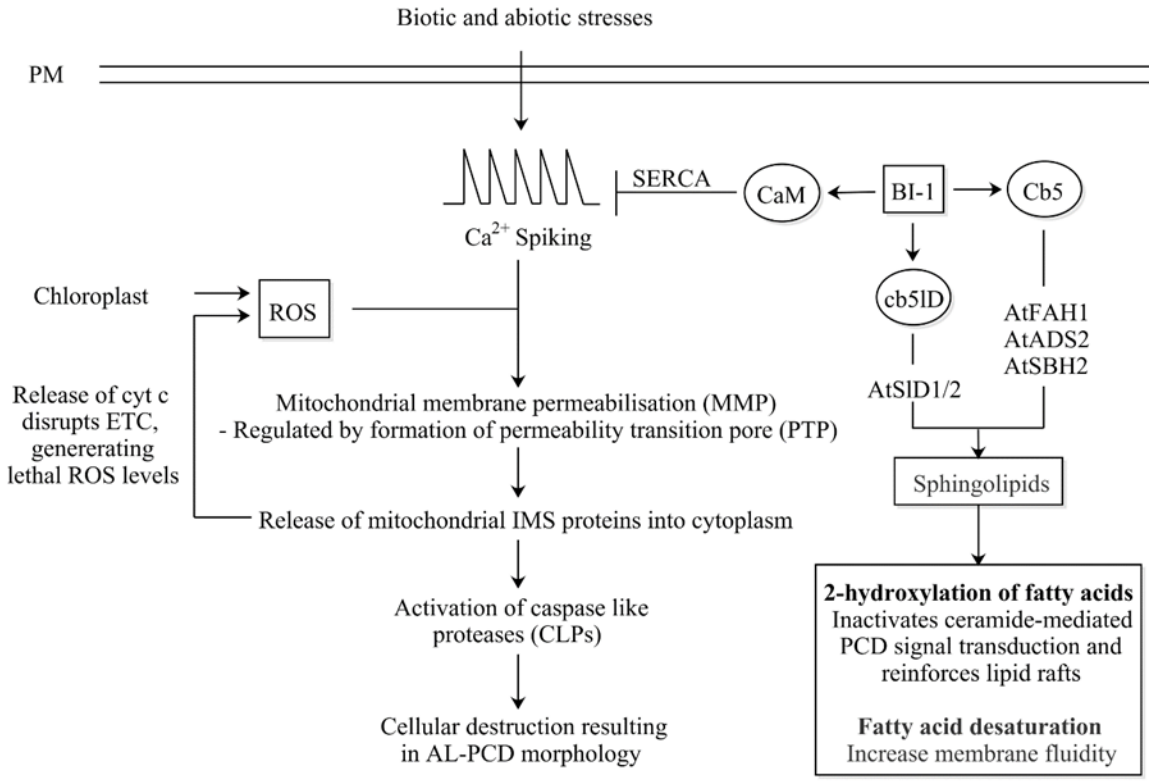


**Figure 1.8** - Mechanism of AL-PCD and the role of plant BI-1 and its interacting partners in plant stress tolerance. A PCD-inducing stress signal causes a $Ca^{2+}$ spike in plant cells and induces the formation of a permeability transition pore (PTP) and subsequent release of mitochondrial IMS proteins, including cyt *c*, into the cytoplasm. Cyt *c* release disrupts the mitochondrial ETC and generates lethal ROS levels. The chloroplast is also a source of ROS that generates a feedback loop that amplifies the initial PCD-inducing stress signal. Activation of CLPs initiates an amplifying proteolytic cascade that leads to cell death. Plant BI-1 is a rheostat that determines the ER stress threshold at which PCD is initiated. Interaction studies have shown that BI-1 has three binding partners: calmodulin, cb5-interacting (AtFAH1, AtADS2 and AtSBH2) and cb5lD-containing (AtSLD1) proteins. Information adapted from (Ihara-Ohori *et al.* 2007; Kawai-Yamada *et al*, 2009; Ishikawa *et al*, 2011). Image author's own.

### 1.5.3 Root Hair Assay: Examining AL-PCD morphology in seedling root hairs

Plant AL-PCD shares many features with animal apoptosis: cell shrinkage, membrane blebbing, nuclear condensation and fragmentation, and cytoplasm retraction (Reape and McCabe 2008). This specific corpse morphology is observed in both plant suspension cultures and cells of whole plants, including the single-celled root hairs (Hogg *et al.* 2011). As microscopic extensions of root epidermal cells, root hairs provide a rapid *in vivo* model for quantifying AL-PCD using the corpse morphology as a visual indicator (Hogg *et al.* 2011). The viability of root hairs is determined using a novel root hair assay (RHA) that relies on fluorescein diacetate (FDA) staining (Hogg *et al.* 2011). FDA is a cell permeable acetylated derivative of fluorescein, a green fluorescent dye. FDA is de-acetylated by esterases to form fluorescein in the cytoplasm of living cells; the charged groups of fluorescein promotes retention within the cell (Boyd *et al.* 2008). The severity of an insult determines the fate of the cell (Lockshin and Zakeri 2004) and Figure 1.9 illustrates the dose-dependent relationship between stress intensity and modes of cell death. Under low stress intensities, root hairs remain viable and can cleave FDA to form fluorescein, which fluoresces green when excited by light with a wavelength of 485 nm (Hogg *et al.* 2011). When stress levels are increased, root hairs undergo AL-PCD which are characterised by a negative FDA stain and retracted cytoplasm, leaving a distinct gap between the cell wall and plasma membrane. At even higher stress levels, root hairs undergo necrotic death which has a negative FDA stain but no cytoplasm retraction.

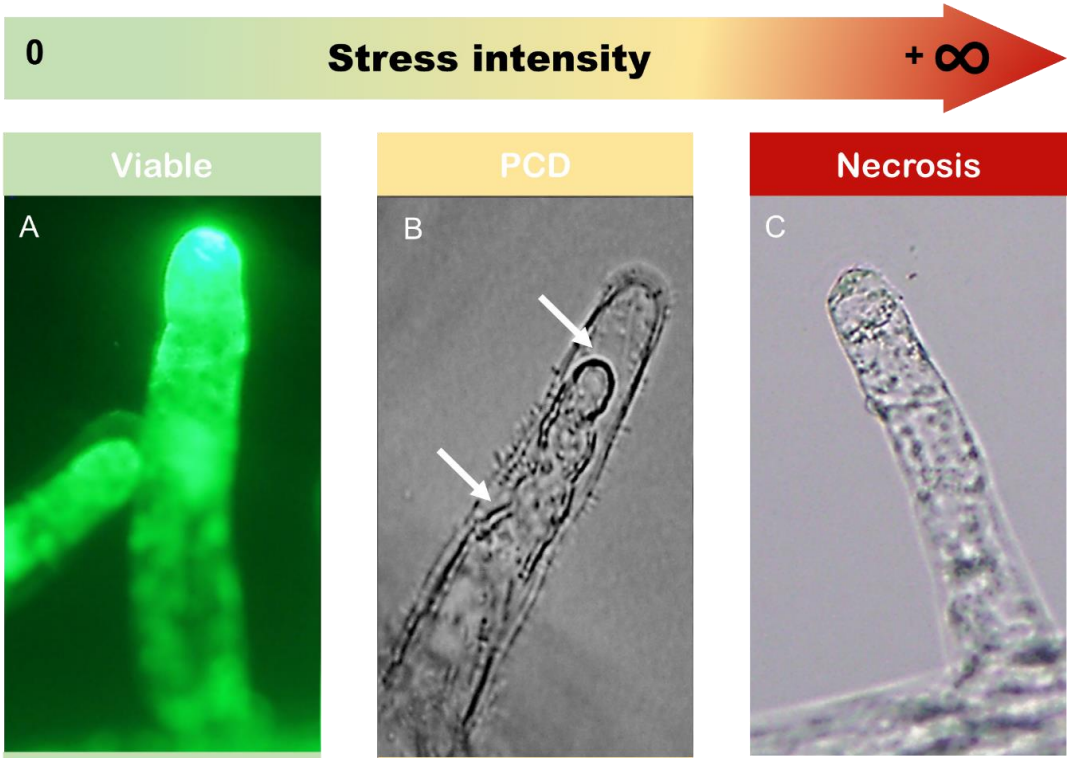


**Figure 1.9** – Appearance of FDA-stained *Arabidopsis thaliana* root hairs in response to increasing stress: A) Viable cells are FDA positive and exhibit fluorescence at low stress intensities, (B) after low-to-medium stress treatment, PCD cells are FDA negative and have a retracted cytoplasm (as shown by arrows) and (C) necrotic cells are FDA negative but do not have a retracted cytoplasm after exposure to high stress intensities. Images authors own and captured using an Olympus BX61 microscope under 1000X magnification.

The RHA holds several advantages over conventional model systems for investigating plant PCD. First, it allows rapid enumeration of the stress response as root hairs grow abundantly and are easily accessible. Moreover, the easy accessibility allows treatment of root hairs with a wide range of elicitor treatments to assess their PCD-modulating effects (Kacprzyk *et al.* 2014). In contrast, restrictive conventional methods are limited by difficult tissue sectioning as PCD cells are usually embedded within surrounding viable tissue, such as tapetal cell PCD in *Helianthus annuus* anther tissues (Balk and Leaver 2001). Second, the RHA can be used across different species as the PCD morphology is a universal feature across monocotyledon and dicotyledon plant species; to date, researchers have employed the RHA to investigate the stress-response in *Arabidopsis*, *Medicago truncatula*, *Zea mays* and *Quercus robur* seedlings (Hogg *et al.* 2011). In the third instance, results can be obtained quickly as the RHA is an *in vivo* technique and

avoids the time-consuming and fastidious process of establishing and maintaining axenic plant suspension cultures.

The RHA also holds an important advantage over single end-point measurements as it can simultaneously quantify cell viability, PCD, and necrosis levels. Alternative assays that only measure a single variable do not capture the complete, intricate processes behind stress treatment and the corresponding plant response. For example, viability assays (e.g. TTC, NBT, Evans blue, and neutral red) that only measure cell viability do not account for the differences between PCD and necrotic death, while the RHA allows distinct measurement of these two separate cell death modes. Finally, it is important to stress that plants are complex organisms and have many signalling pathways acting concertedly to regulate the PCD network. The reduced complexity of suspension cultures makes it easy to assess how single cells respond to PCD modulators. However, it is also important to assess the effects of these modulators in the whole plant context, as tissue-specific cells will not respond in a synchronised manner as it would in homogenous plant cell cultures (Reape *et al.* 2015). Therefore, using *in vivo* plants as a model system for investigating plant PCD offers a more accurate representation than artificially controlled reconstructions using *in vitro* methods.

## 1.6 Aims and objectives of the study

- Characterise *N. muscorum* CM for bioactivity in *Arabidopsis* seedlings.
- Identification of pro-survival compound(s) in *N. muscorum* CM.
- Develop the root hair assay (RHA) so it can be used to screen for stress tolerance in cereals.
- Use stress-induced PCD levels to investigate basal, induced and cross-stress tolerance in wheat varieties.
- Evaluate PCD-suppressing effects of exogenous proline in plant stress tolerance.

# Chapter 2 - Screening *N. muscorum* conditioned medium for bioactivity

## 2.1 Introduction

$N_2$-fixing heterocystous cyanobacteria are used as biofertiliser inoculants to stimulate plant growth but can also elevate plant stress tolerance by secreting exometabolites. Previous work showed that the liquid medium in which *N. muscorum* are grown, termed conditioned medium (CM), inhibit stress-induced PCD in root hairs of the model plant organism *A. thaliana* (Daly 2013). However, attempts to discern the bioactive compounds involved is difficult as a wide array of compounds are exuded. To date, no one has attempted to assess their effects on plant stress tolerance as a function of organised PCD or uncontrolled necrotic death, even though it is important to distinguish between both death modes. PCD is a genetically controlled and conserved mechanism in the plant life cycle that is activated by a combination of developmental and environmental factors (Huysmans *et al.* 2017). For example, PCD plays an important role in vegetative tissue development (xylogenesis, lateral root cap formation, leaf morphogenesis, trichome and aerenchyma differentiation), and reproductive tissue development (gametophyte development, anther dehiscence and pollen self-incompatibility) (Kacprzyk *et al.* 2011; Daneva *et al.* 2016). However, plant cells also undergo PCD to mitigate the effects of abiotic and biotic stress, such as hypoxia (Lenochová *et al.* 2009), salt (Shabala 2009), drought (Nguyen *et al.* 2009), UV overexposure (Ferreyra *et al.* 2016), heavy metal exposure (Xu *et al.* 2013), heat (Vacca *et al.* 2004) and pathogen infection (Lam *et al.* 2001).

PCD is a methodical process of cellular destruction characterised by the distinctive retraction of the cytoplasm which is an active and interruptible process driven by cellular $Ca^{2+}$ influx (Kacprzyk *et al.* 2017). Conversely, necrosis is associated with uncontrolled cell death that occurs when cells cannot withstand overwhelming cellular stress (Reape *et al.* 2008). Inhibition of $Ca^{2+}$ influx modulates PCD but not necrotic death (Kacprzyk *et al.* 2017). Necrotic cells are characterised by a loss of plasma membrane integrity that impairs osmoregulation. This leads to an influx of water and ions into the cell causing the cell to swell and rupture, releasing their cellular contents (Burbridge *et al.* 2007). Considering the substantial differences between PCD and necrosis, e.g. in terms of

signalling, morphology and regulation, it is essential to distinguish between both death modes to generate an accurate picture of plant cell death studies across different research groups (Reape *et al.* 2008; Reape and McCabe 2013). If a stress response is only quantified through viability levels, it loses context as to whether cells are dying in a controlled process (PCD), or uncontrollably (necrosis) because of the inability to cope with overwhelming cellular stress. However, conventional *in vitro* and *in vivo* techniques for studying plant PCD have constraints that limit their widespread use, but the RHA holds several advantages over conventional model systems for investigating plant PCD as explained in Section 1.5.3. Given these points, the RHA was utilised as a preliminary tool for characterising *N. muscorum* CM bioactivity and its effect in modifying the PCD activation threshold in treated seedlings.

### 2.1.1 Aims and Objectives

The primary aim of this research was to identify the PCD-suppressing compound(s) present in *N. muscorum* CM. In this chapter, a work-flow involving the RHA as a rapid screening tool for characterising *N. muscorum* CM bioactivity is described: *Arabidopsis* seedlings were pre-treated with *N. muscorum* CM fractions, heat stress applied and the RHA used to quantify the plant stress response in terms of cell viability, PCD, and necrosis based on specific cell morphologies. This was done to test if the bioactive compound was affecting the PCD pathway or modulating a general stress response. Based on documented *N. muscorum* exometabolites, a framework was developed to narrow the list of bioactive candidates and identified proline, a stress-responsive amino acid, as a compound of interest. Proline was detected in *N. muscorum* CM using the ninhydrin assay and HPLC. Confirmation of proline bioactivity was achieved by carrying out experiments with mutant *Arabidopsis* lines with impaired proline transporters.

**Chapter aims:**

- Establish baseline heat stress response in *A. thaliana.*
- Sample preparation and screening of *N. muscorum* CM for bioactive effects by measuring *in vivo* levels of cell viability, PCD, and necrosis after pre-treatment with CM.
- Development of a literature review-derived framework to narrow the list of putative bioactive candidates.

- Identification and quantification of the main PCD-suppressing compound of interest.
- Assess the effect of exogenous proline on wild-type *Arabidopsis* seedlings.
- Evaluate the effect of *N. muscorum* and exogenous proline on mutant *Arabidopsis* lines with impaired proline transporters (*lht1*, *aap1* and *atprot1-1::atprot2-3::atprot3-2* mutants).

# 2.2 Materials and Methods

## 2.2.1 Growth and sterilisation procedures for seedlings

*Arabidopsis thaliana* L. ecotype Columbia (Col-0) seeds were soaked in a 20% bleach solution (Domestos® disinfectant: sodium hypochlorite - 4.5g per 100g) and gently shaken for 10 minutes under aseptic conditions. All work was performed in a horizontal laminar flow hood (Esco Airstream® Class II Biological Safety Cabinet), which was turned on 15 minutes prior to use and its work surfaces wiped down with 70% ethanol in advance to maintain a sterile environment. The bleach solution was removed, and the seeds rinsed five times with sterilised deionised water (SDW) until all suds were removed. Sterilised seeds (15-20) were placed in a straight line on plates of germination medium comprising ½ Murashige and Skoog (MS) agar (2.15 g/L MS basal salt mixture, 10 g/L sucrose, 6 g/L Duchefa® plant agar, adjusted to pH 5.8 with NaOH). For stratification, plates were wrapped in aluminium foil and stored at 4 °C for 24 hours to synchronise germination. Plates were placed vertically under light (33 µmol/$m^2$/s, 16-hour light: 8-hour darkness) in a 21 °C growth chamber to germinate seeds. *Arabidopsis* seedlings developed sufficient root hair density after five days of growth and were used for stress assays (Figure 2.1).

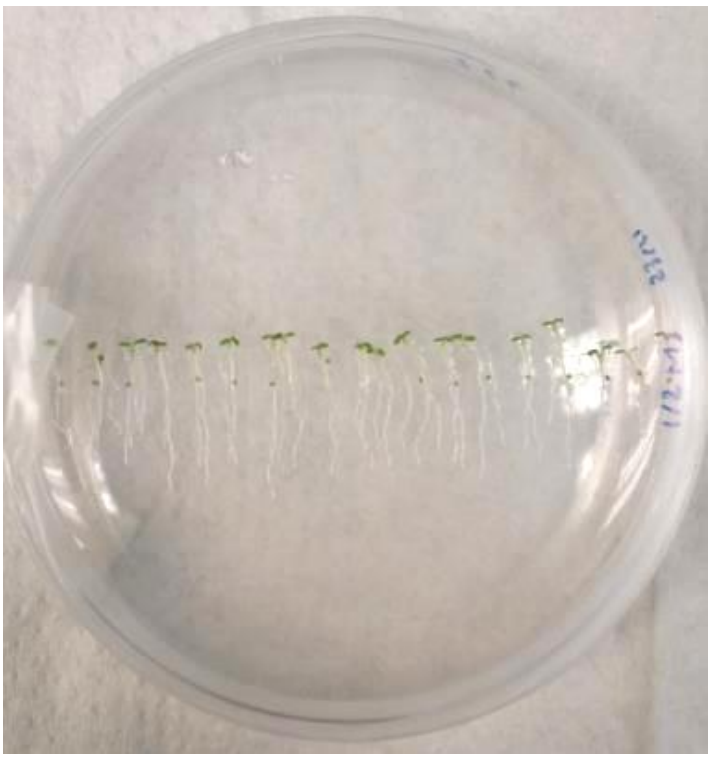

**Figure 2.1** – 5-day-old *Arabidopsis* seedlings ready for heat stress experiments.

### 2.2.2 Heat stressing of *A. thaliana* seedlings

To apply heat stress, 5-day old *A. thaliana* seedlings were transferred using sterile forceps into individual wells of a sterile 24-well plate (Sarstedt© Tissue Culture Plate) containing 1 mL SDW. Seedlings were handled with care during the transfer process to avoid root hair mechanical damage and elevated background death levels. The lid of the 24-well plate was sealed using autoclave tape to prevent accidental water leakage during transport. The 24-well plates were placed in a Grant SUB Aqua Pro 26 water bath already stabilised at the desired heat stress temperature, and each plate was heat stressed for 10 minutes. Seedlings were returned to the 21 °C growth chamber and scored 14-16 hours after stress application to allow PCD morphology to fully develop. The RHA was used to quantify the stress response in terms of viability, PCD and necrosis. At least 4 seedlings were scored per treatment ($n \geq 4$) and the data from three experiment replicas merged into a single dataset to yield a final sample size of $n \geq 12$.

### 2.2.3 Assessing the plant stress response using PCD morphology and viability stain

Direct scoring of root hairs relied on a combination of the FDA viability stain and cell corpse morphology (PCD and necrotic root hairs) as visual indicators. FDA is an acetylated derivative of fluorescein, a green fluorescent dye that enters cells via passive diffusion. Only viable root hairs will be able to de-acetylate FDA using cell-localised esterases to form fluorescein, whose charged groups promotes retention within the cytoplasm (Boyd *et al.* 2008). Upon excitation by a 485 nm wavelength, fluorescein-containing root hairs fluoresce green and are scored as FDA positive. A 0.1 % (w/v) FDA (Sigma©) stock solution was stored at -20 °C for up to 1 year. To stain root hairs, a diluted FDA staining solution (0.001% w/v) was prepared by mixing 10 µL FDA stock solution to 1 mL SDW. *Arabidopsis* seedlings were placed on microscope slides and the root hairs stained with the diluted FDA solution for two minutes and examined under fluorescent light using an Olympus BX61 microscope with an FITC filter. Images were captured using the Cell$^F$ 3.4 software program. Figure 1.9 depicts the key markers exhibited by the different cell modes. Root hairs were scored viable, PCD or necrotic, based on the method developed by Hogg *et al*. (2011). At least 100 root hairs were scored per seedling to give an accurate representation of viable and total cell death (PCD + necrosis) levels. Each cell

mode is represented as the percentage of cell mode over total number of root hairs, where viability% + PCD% + necrosis% = 100%

### 2.2.4 Profiling bioactive *N. muscorum* spp. exometabolites in conditioned medium (CM)

#### 2.2.4.1 Maintenance of sterile conditions for cell culture experiments

Sterile conditions for *N. muscorum* growth experiments were maintained using pre-autoclaved reagents and apparatus (conical flask, cotton stoppers and pipette tips) and sterile petri dishes. Autoclaving was carried out at 121 °C for 15 minutes, while thermolabile components were filter-sterilised either using a 0.2 or 0.45 µm polyethersulfone (PES) membrane syringe filter. Metal equipment such as forceps and inoculation loops were sterilised in the Bunsen burner flame and cooled by pressing to the inside of the agar plate or liquid flask before use. All work was carried out in a horizontal laminar flow hood that was switched on 15 minutes prior to use and wiped down with 70% ethanol both before and in between experiments.

#### 2.2.4.2 Sub-culturing and growth monitoring of *N. muscorum* cultures

*N. muscorum* cultures were provided by Dr Carl Ng from University College Dublin, formerly purchased from the Pasteur Culture Collection of Cyanobacteria Paris, France (strain passport number: ATCC 27347). *N. muscorum* cultures were grown in liquid BG11 (Blue-Green) medium at 25 °C (light regiment: 30 µmol/$m^2$/s, 16-hour light: 8-hour darkness) and shaken at 110 rpm to maintain uniformly mixed cultures. Sub-culturing of *N. muscorum* cultures was done in a laminar flow hood and involved transferring 25 mL of 3-week-old culture into 125 mL fresh BG11 medium. Stock strains were maintained on BG11 agar plates at 25 °C under a similar light regime (Figure 2.2).

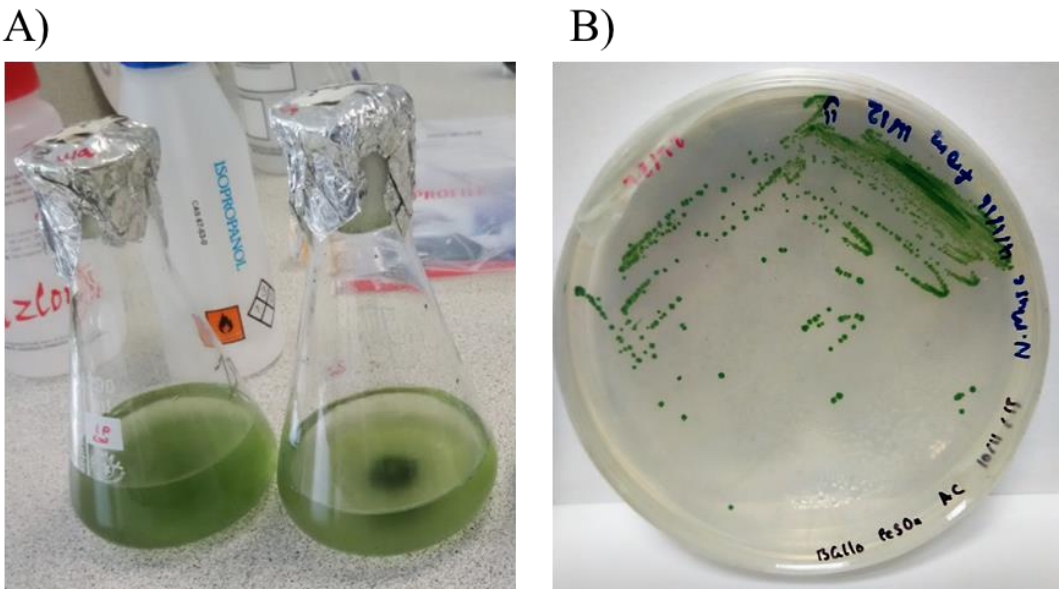


**Figure 2.2** - *N. muscorum* cultures: (A) Suspension cultures in BG11 liquid medium, (B) stock cells maintained on BG11 agar plates.

To prepare BG11 liquid medium concentrated stock solutions were made up as outlined in Table 2.1A and stored at 4 °C. Appropriate aliquots of the stock solutions (Table 2.1B) were combined, the solution was made up to 1 L with deionised water (DW), and the pH adjusted to 7.1 using NaOH. Then, 125 mL of the BG11 medium was aliquoted into conical flasks sealed with cotton stoppers and autoclaved at 121 °C for 15 minutes. Unused BG11 medium was stored at 4 °C for up to 3 weeks only. For solid BG11 agar, BG11 liquid medium (containing $Na_2S_2O_3$ to prevent photobleaching) and Bacto® agar (BD Diagnostic Systems®) were separately autoclaved and mixed just before solidification to prevent ROS formation which occurs when agar is directly autoclaved with phosphate-containing medium (Tanaka *et al.* 2014). The agar mixture was cooled to ~45 °C before it was poured into sterile plates. BG11 plates were stored at 4 °C for a maximum of 3 months and were checked for contamination before use.

*N. muscorum* culture growth was monitored by measuring optical density, chl-*a*, and carotenoid concentration (Myers *et al.* 2013; Zavřel *et al.* 2015). To measure chl-*a* and carotenoid content, 1 mL of cyanobacterial cells were centrifuged (Eppendorf Centrifuge 5810®) at 15000 *x* g for 7 minutes and the supernatant discarded. Precooled methanol (1mL) was added to the pellet, samples were vortexed and incubated at 4 °C for 20 minutes in the dark. Samples were re-centrifuged at 15000 g at 4 °C for 7 minutes and supernatant absorbance was measured at 470, 665 and 720 nm using a Ultrospec 2000®

spectrophotometer and plastic cuvettes.

Photosynthetic pigment concentrations were determined using the following equations:

- **chl-*a* [µg/mL]** = 12.9447 ($A_{665} - A_{720}$)
- **carotenoids [µg/mL]** = $\frac{1{,}000\ (A_{470} - A_{720}) - 2.86\ (\text{chl-}a\ [\mu g/mL])}{221}$

Culture growth was also monitored by measuring the optical density of 1mL cyanobacteria cells at 730 nm as it provides a good estimate of biomass concentration in suspension cultures (Myers *et al.* 2013).

**Table 2.1** - A) Stock solution concentrations and (B) final recipe for BG11 *N. muscorum* growth medium.

**(A) Concentration of BG11 stock solutions**

*1000x Stock solutions*

| Salt | Concentration (g/L) |
|---|---|
| $Na_2MG$ EDTA | 0.01 |
| Ferric ammonium citrate | 0.06 |
| Citric acid | 0.06 |
| $CaCl_2$. $2H_2O$ | 0.36 |
| $MgSO_4$. $7H_2O$ | 0.75 |
| $K_2HPO_4$. $3H_2O$ | 0.4 |

*1000x Trace metal mix A5*

| Salt | Concentration (g/L) |
|---|---|
| $H_3BO_3$ | 2.86 |
| $MnCl_2 \cdot 4H_2O$ | 1.81 |
| $ZnSO_4 \cdot 7H_2O$ | 0.222 |
| $NaMoO_4 \cdot 2H_2O$ | 0.39 |
| $CuSO_4 \cdot 5H_2O$ | 0.079 |
| $Co(NO_3)_2 \cdot 6H_2O$ | 0.05 |

**(B) Recipe for 1 L liquid BG11 medium**

| Stocks | Per L |
|---|---|
| $Na_2MG$ EDTA | 1 mL |
| Ferric ammonium citrate | 1 mL |
| Citric acid | 1 mL |
| $CaCl_2$. $2H_2O$ | 1 mL |
| $MgSO_4$. $7H_2O$ | 1 mL |
| $K_2HPO_4$. $3H_2O$ | 1 mL |
| Trace metal mix | 1 mL |
| $Na_2CO_3$ | 0.02 g |

**C) Recipe for BG11 agar plates**

| Stocks | Per L |
|---|---|
| BG11 liquid medium | 1 L |
| Bacto® agar | 15 g |
| Sodium thiosulfate | 4.5 g |

#### 2.2.4.2 Screening *N. muscorum* CM for PCD-suppressing bioactivity

*N. muscorum* CM was harvested in the deceleration phase ($OD_{730}$ = 1.17, chl-*a* = 14.14 µg/mL and carotenoid = 3 µg/mL) after two cycles of centrifugation (Eppendorf Centrifuge 5810®) at 3000 *x* g for 20 minutes. After each cycle, the supernatant was collected, and the pellet discarded. The resulting supernatant was sterile-filtered through a 0.45 µm PES filter; half of the filtered supernatant was autoclaved in a loosely-stoppered glass McCartney bottle at 121 °C for 15 minutes, while the other half remained unautoclaved. When not in use, both fractions were stored at 4 °C for up to 3 weeks. *N. muscorum* CM fractions (autoclaved, and non-autoclaved) diluted in BG11 at various concentrations were screened for PCD-suppressing bioactivity by pre-treating *Arabidopsis* seedlings with CM fractions for 3 hours in 24-well plates, followed by 50 °C exposure for 10 minutes in the water bath. Viability, PCD, and necrosis levels were scored 14-16 hours later as described in Section 2.2.3.

### 2.2.5 Identification and quantification of proline in *N. muscorum* CM using ninhydrin assay

A modified ninhydrin-based protocol adapted from Bates *et al.* (1973) was used to quantify proline levels in autoclaved and non-autoclaved CM. A mixture containing 400 µL of CM, 400 µL of glacial acetic acid, and 400 µL ninhydrin mixture (2.5% ninhydrin dissolved in 6:3:1 ratios of glacial acetic acid, SDW and 85% orthophosphoric acid) were vortexed and heated at 100 °C for 1 hour in a block heater (Stuart® SBH130D). The reaction was terminated by incubation at 21 °C for 5 minutes, followed by quantification at 546 nm using an Ultrospec 2000® spectrophotometer. The concentration of proline (purchased from TCI Chemicals©) was determined from a proline standard curve (Figure 2.6).

### 2.2.6 Identification and quantification of proline in *N. muscorum* CM using HPLC

Modified protocols from Heinrikson and Meredith (1984) and Kwanyuen and Burton (2010) were adapted to detect amino acids in *N. muscorum* CM. Phenyl isothiocyanate (PITC) was chosen as the precolumn derivatization agent as it reacts with both primary and secondary amines such as proline and hydroxyproline, unlike other derivatizing agents such as o-phthalaldehyde (Walker and Mills 1995). At the start of the method

development process, a proline standard curve (10-100 µM, 7 µL injection volume) was performed to determine if PITC-derivatized proline can be detected linearly. The resultant proline standard curve (Figure 2.7) confirmed that proline could be detected linearly ($R^2$ = 0.984). Following this, the method was revised across a series of parameters (injection volume, PITC derivatization mixture ratio, *N. muscorum* CM sample volume and impact of guard column) until an optimum protocol was developed. Using the final protocol, a new proline standard curve was performed, and proline successfully quantified in *N. muscorum* CM. Amino acid standards (TCI Chemicals®), each corresponding to 1.5 mM, were prepared individually and in a mixture in 0.1 M HCl (Table 2.2). HPLC-grade water was used throughout the sample preparation process.

**Table 2.2** – Amino acid standards used. Each amino acid was established at a concentration of 1.5 mM in 0.1 M HCl. Individual standards were used to determine the elution time of each amino acid peak, while the mixed standard was used to separate the 20 amino acids peaks

| | **Amino acid** |
|---|---|
| 1 | L-Proline |
| 2 | L-Phenylalanine |
| 3 | L-Glutamine |
| 4 | L-Methionine |
| 5 | L-Arginine |
| 6 | L-Glycine |
| 7 | L-cysteine |
| 8 | L-Aspartic acid |
| 9 | L-Histidine |
| 10 | L-Glutamic acid |
| 11 | L-Alanine |
| 12 | L-Serine |
| 13 | L-Tyrosine |
| 14 | L-Valine |
| 15 | L-Tryptophan |
| 16 | L-Leucine |
| 17 | L-Threonine |
| 18 | L-Isoleucine |
| 19 | L-Lysine monohydrochloride |
| 20 | L-Asparagine Monohydrate |

*N. muscorum* CM was harvested in the deceleration phase ($OD_{730}$: 1.67, chl-*a*: 33.19 µg/mL and carotenoid: 9.77 µg/mL) after two cycles of centrifugation at 3000 *x* g

(Eppendorf Centrifuge 5810®) for 20 minutes. After each cycle, the pellet was discarded, and the supernatant collected and sterile-filtered through a 0.45 µm PES filter. Following that, 40 µL of the amino acid mixture or 200 µL of filtered *N. muscorum* CM sample was added to 100 µL of coupling buffer (acetonitrile: pyridine: triethylamine: $H_2O$ in a ratio of 10:5:2:3) and dried under vacuum by rotary evaporation (ScanSpeed 32®) at 85 °C. Derivatization was performed by adding 20 µL of a 7:1:1:1 ratio mixture of ethanol: $H_2O$: triethylamine: PITC (v/v). The resultant mixture was incubated for 20 minutes in the dark at room temperature to form phenylthiocarbamyl derivatives (PTC-amino acid) that were quantified using reverse-phase HPLC. Samples were then dried under vacuum (ScanSpeed 32®) at 35 °C because of PTC-amino acid sensitivity to light and high temperature. The pellet was re-suspended in 100 µL of suspension buffer (4 mM sodium phosphate (pH 7.4) and 2% (v/v) acetonitrile) and injected into a Symmetry® C18 column (3.99 x 150 mm, 5 µM particle size) in a HPLC system (Agilent Technologies 1200 Series: G1379B Degasser, G1330B Autosampler Thermostat, G13929B Automatic Liquid Sampler, G1316B Thermostatted Column Compartment and G1315C Diode-array Detector). An injection volume of 14 µL was used for the amino acid mixture, while 70 µL was injected for the *N. muscorum* CM sample. The mobile phase consisted of two solvents: Solvent A was 70 mM sodium phosphate (pH 6.55, adjusted by NaOH) and 2% acetonitrile (v/v); Solvent B comprised 50% (v/v) water: acetonitrile. The following step-wise gradient was used to separate the amino acid peaks: 0-1 min (0% Solvent B); 5.5-7 min (15% B); 8.5-13.5 min (30% B); 14 min (35% B); 15.5 min (42% B); 16 min (43% B); 20 min (60%); 22 min 0% B). Absorbance of the PTC-amino acid adducts was monitored at 254 nm.

### 2.2.6.1 Investigation of HPLC process development parameters

For all process development steps, a Symmetry® C18 (4.6 x 75 mm, 3.5 µm particle size) guard-column and mobile phase step-wise gradient was used: 0 min (0% Solvent B); 0.5 min (0% B); 5-7 min (15% B); 12-13 min (30% B); 13.5 min (40% B); 15 min (42% B); 18.5 min (60% B); 21.5-24.5 (0% B). The impact of using larger injection volumes on peak resolution was investigated by using 7, 10 and 15 µL injection volumes. A similar protocol to Section 2.2.6 was used, but with the following amendments: 30 µL each of proline and alanine standards were vacuum-dried and samples injected into a Symmetry® C18 column (3.99 x 150 mm, 5 µm particle size), preceded by the guard column. Absorbance of the PTC-amino acid adducts was again monitored at 254 nm. The next

parameter to be examined was the PITC dose-dependent effect on peak resolution. Increasing concentrations of PITC derivatization mixture, 1X (20 µL), 2X (40 µL), 5X (100 µL), 10X (200µL) and 12X (240µL), were added to the proline and alanine pellet, and the mixture dried at 35 °C for three days. A 15 µL injection volume was used. Lastly, the impact of changing the sample of volume of *N. muscorum* CM was inspected using two controls (200 µL *N. muscorum* CM and 30 µL proline standard) and four 30 µL proline-spiked *N. muscorum* CM samples of varying volumes (80, 100, 150 and 200 µL). A 14 µL injection volume was used. A summary of the changes made in the method development process is illustrated in Table 2.3.

**Table 2.3** – Summary of HPLC method development process.

| Method development | Sample volume | PITC derivatization mixture (µL) | Guard column | Injection Volume | Mobile Phase |
|---|---|---|---|---|---|
| Impact of injection volume at peak resolution | 30 µL amino acid standard | 20 | Yes | 7, 10 and 15 µL | **G1:** 0 min (0% Solvent B); 0.5 min (0% B); 5-7 min (15% B); 12-13 min (30% B); 13.5 min (40% B); 15 min (42% B); 18.5 min (60% B); 21.5-24.5 (0% B). |
| Impact of PITC ratio on peak resolution between proline and alanine | 30 µL amino acid standard | 20, 40, 100, 200 and 240 | Yes | 15 µL | **G1:** 0 min (0% Solvent B); 0.5 min (0% B); 5-7 min (15% B); 12-13 min (30% B); 13.5 min (40% B); 15 min (42% B); 18.5 min (60% B); 21.5-24.5 (0% B). |
| Impact of *N. muscorum* CM sample volume on proline resolution | Controls (200 µL *N. muscorum* CM and 30 µL proline standard) and 30 µL proline-spiked *N. muscorum* CM samples (80, 100, 150 and 200 µL) | 20 | Yes | 14 µL | **G1:** 0 min (0% Solvent B); 0.5 min (0% B); 5-7 min (15% B); 12-13 min (30% B); 13.5 min (40% B); 15 min (42% B); 18.5 min (60% B); 21.5-24.5 (0% B). |
| Amino acid standard mixture | 40 µL amino acid mixture | 20 | Yes | 14 µL | **G2:** 0-2 min (0% Solvent B); 5-13 min (8% B); 14-15 min (35% B); 17 min (37% B); 19-22 min (42% B); 23-24 min (45% B); 25-26 (50% B); 27-28 (55% B); 29-30 min (60% B) and 31-33 min (0% B) |
| Final method | 40 µL amino acid mixture | 20 | No | 14 µL for amino acid mixture | **G3:** 0-1 min (0% Solvent B); 5.5-7 min (15% B); 8.5-13.5 min (30% B); 14 min (35% B); 15.5 min (42% B); 16 min (43% B); 20 min (60%); 22 min 0% B |
| | Standard curve: 40 µL proline (1, 3, 30, 40, 60, 70, 80 and 100 µM) | | | 70 µL for CM sample and standard curve | |
| | 200 µL *N. muscorum* CM sample | | | | |

### 2.2.7 Evaluating the effect of exogenous proline and *N. muscorum* CM in wild-type and mutant *Arabidopsis* lines

Two proline solutions were established in BG11 at identical concentrations previously measured in autoclaved CM (1.94 µM) and non-autoclaved CM (1.83 µM), with the former solution autoclaved at 121 °C for 15 minutes. A similar protocol to Section 2.2.4.2 was used, where 5-day-old *Arabidopsis* seedlings were incubated for 3 hours in the proline solutions and seedlings were then heat stressed at 50 °C for 10 minutes. A temperature of 50 °C was chosen here because (as explained in Section 2.4.1) it is a stress intensity that can either give rise to high levels of PCD or cell survival, depending on the elicitor treatment. Therefore, stress exposure at this viability/PCD 'inflection point' informs on the effect of various treatments on the perturbation of cell death or survival signalling pathways. Seedlings were returned to the 21 °C growth chamber and scored for viability, and death via necrosis or PCD 14-16 hours after heat stress application. This protocol was repeated with mutant *Arabidopsis* lines with impaired proline transporters (*lht1*, *aap1* and *atprot1-1::atprot2-3::atprot3-2*). *lht1* and *aap1* mutants were provided by Professor Mechthild Tegeder (Washington State University, USA), while the *atprot1-1::atprot2-3::atprot3-2* mutant was a kind gift of Professor Doris Rentsch (University of Bern, Switzerland). Seeds were germinated as per Section 2.2.1, and 5-day-old *Arabidopsis* mutant seedlings were treated with exogenous proline (1, 2, 5 or 100 µM) or fresh 100% *N. muscorum* CM ($OD_{730}$ = 1.43, chl-*a* = 18.9 µg/mL and carotenoid = 4.67 µg/mL) for 3 hours, heat stressed at the 50 °C 'inflection point' for 10 minutes and returned to the 21 °C growth chamber. The RHA was used to score viable, PCD and necrotic root hairs of the mutants after 14-16 hours of stress application.

### 2.2.8 Statistical analysis

IBM® SPSS® (Version 24) was used to analyse results for significant changes ($p<0.05$) across elicitor treatment and mutant *Arabidopsis* lines. Statistical tests used include one-way ANOVA (Tukey or Dunnett Post-hoc Test) and linear regression analysis. Most statistics tables are included in the chapters at the relevant points, but larger tables are provided in the Appendix as supplementary material.

## 2.3 Results

### 2.3.1 Three stress-response phases identified in heat-shocked *Arabidopsis* seedlings

Baseline heat stress responses were established in *A. thaliana* and three distinctive stress-response phases were detected: 1) the stress tolerant/high viability phase, 2) the PCD zone and 3) the necrotic zone (Figure 2.3). During the stress tolerant phase (25-45 °C), the majority of root hairs remained viable (65-75%) and resisted incremental rises in temperature through cellular protective mechanisms. In the PCD zone (50-65 °C), cell death accumulated at greater rates, with PCD being the predominant form of cell death. Under overwhelming heat stress (75-85 °C) in the necrotic zone, root hairs died primarily by necrosis, instead of PCD. Based on the dose-dependent response, 50 °C was identified as the viable/PCD inflection point, as it was located at the thresholds of both the stress-tolerant and PCD zones.

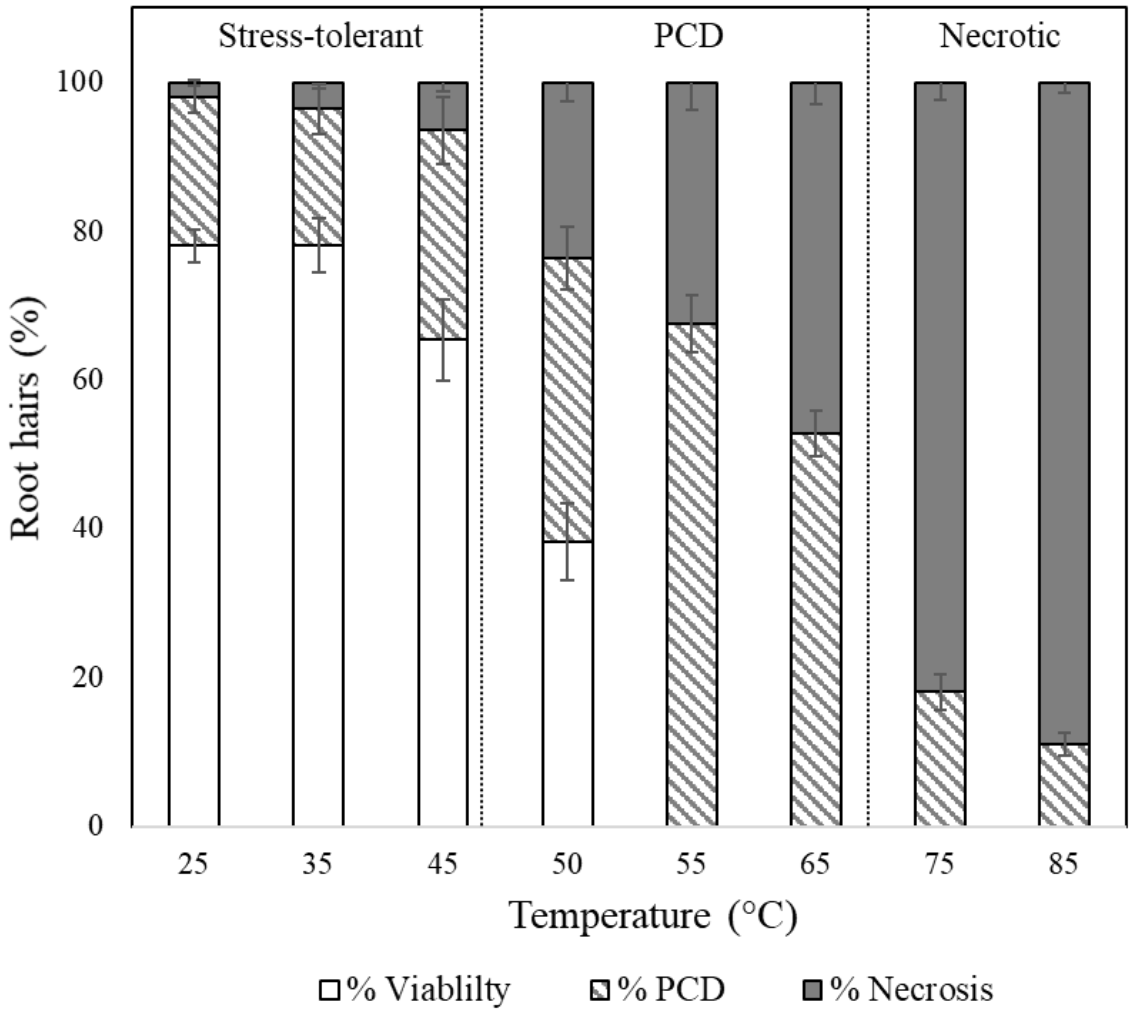


**Figure 2.3** - Effect of heat stress on root hair viability and cell death (PCD and necrosis) levels of 5-day-old *Arabidopsis* seedlings. Values are means ±SE (n ≥ 12) and represent the merged results of 3 experiments. Each cell mode is represented as the percentage of cell mode over total number of root hairs, where viability% + PCD% + necrosis% = 100%.

### 2.3.2 *N. muscorum* culture growth rate

*N. muscorum* was cultured in a closed batch system; cell growth was monitored for optimisation of bioactive exometabolite production (Section 2.4.1) and to ensure cultures remained free from microbial or cyanophage contamination. Culture growth was monitored by measuring optical density, chl-*a* and carotenoid concentration (Figure 2.4). Optical density is an indicator of growth rates (Myers *et al.* 2013), while chl-*a* and carotenoid levels are linked to cellular stress and physiological states (Zavřel *et al.* 2015). There are seven chlorophyll isoforms (*a-f*) but as chl-*a* is the most common isoform in cyanobacteria, it was the ideal photosynthetic pigment for tracking *N. muscorum* growth rates (Wada *et al.* 2013). Optical density and chl-*a* concentration increased over time, while carotenoid concentration remained relatively constant. No discernible lag phase

was detected when cells were first sub-cultured (days 0-3) and cells appeared to be growing in the deceleration phase as a linear optical density plot was observed across the 27 day time-course experiment. Data was not collected past the 27 day time-point because of the limited cell culture volume. However, preliminary observations (data not shown) suggest that *N. muscorum* cultures can grow continuously for at least 3.5 months without addition of fresh growth medium before entering senescence.

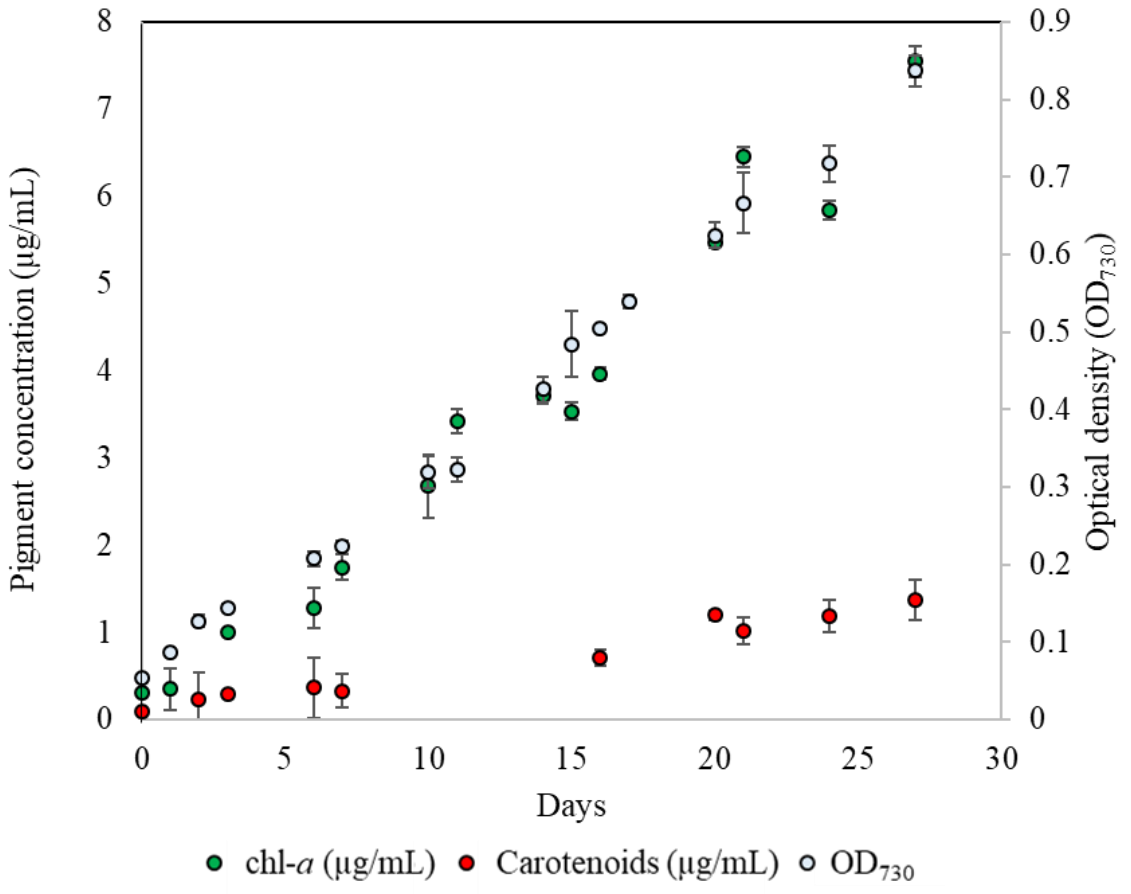


**Figure 2.4** - N. muscorum growth rate monitored by measuring optical density ($OD_{730}$), chl-*a* (µg/mL) and carotenoid levels (µg/mL). Values are the average of $n \geq 3$ of a single experiment over 27 days.

### 2.3.3 Screening *N. muscorum* CM for PCD-suppression activity

The secretion of pro-survival signals into extracellular filtrate have been observed in animal (Barres *et al.* 1992) and plant cells (McCabe *et al.* 1997), and similar observations by Daly (2013) suggest that *N. muscorum* CM contains pro-survival signals that can inhibit stress-induced PCD levels in treated *Arabidopsis* root hairs. Attempts to identify the bioactive exometabolites released by *N. muscorum* is difficult as a broad array of

compounds are exuded, so the high-throughput RHA was used to screen *N. muscorum* CM for PCD-suppressing action. *N. muscorum* was cultured in a closed batch system and harvested in the deceleration phase. The harvested CM was then diluted in fresh BG11 to generate a concentration range (20-100%) to determine the optimum CM% for the strongest PCD-inhibiting effect at the 50 °C inflection point. Unless noted otherwise, 50 °C was used for all subsequent heat shock experiments as it reflects the viable/PCD inflection point, where elicitor treatments induced the largest stress-induced PCD levels in treated plants.

There were three key takeaways from the initial *N. muscorum* CM screening experiments. Firstly, PCD was inhibited dose-dependently (Figure 2.5), with 60-100% non-autoclaved CM offering the highest protection against 50 °C heat stress (38-42% PCD), an approximate 30% decrease in PCD levels compared to SDW and BG11 (75-78% PCD) controls. Secondly, apart from the 20% autoclaved treatment, PCD levels of all tested *N. muscorum* CM fractions were significantly different ($p<0.05$) from the BG11 control. As outlined in Figure 2.5 and Table 2.4, autoclaved and non-autoclaved CM fractions were tested to determine if the PCD-suppressing compound was thermolabile. Both treatments suppressed PCD in root hairs, thus demonstrating the main bioactive compound was thermostable. However, the PCD-suppression effect in autoclaved *N. muscorum* CM was consistently lower than non-autoclaved CM across all five tested CM concentrations (20-100%). Autoclaved *N. muscorum* CM treated seedlings had significantly ($p<0.05$) higher PCD levels, with an average difference of 10.3%, compared to their non-autoclaved treated counterparts. Lastly, *N. muscorum* CM treatment made seedlings more tolerant to heat stress by shifting the deleterious threshold because a portion of treated seedlings normally dying by PCD were now viable. There were negligible changes in necrosis levels across all tested CM concentrations, as improvements in viability levels corresponded to increasing PCD suppression.

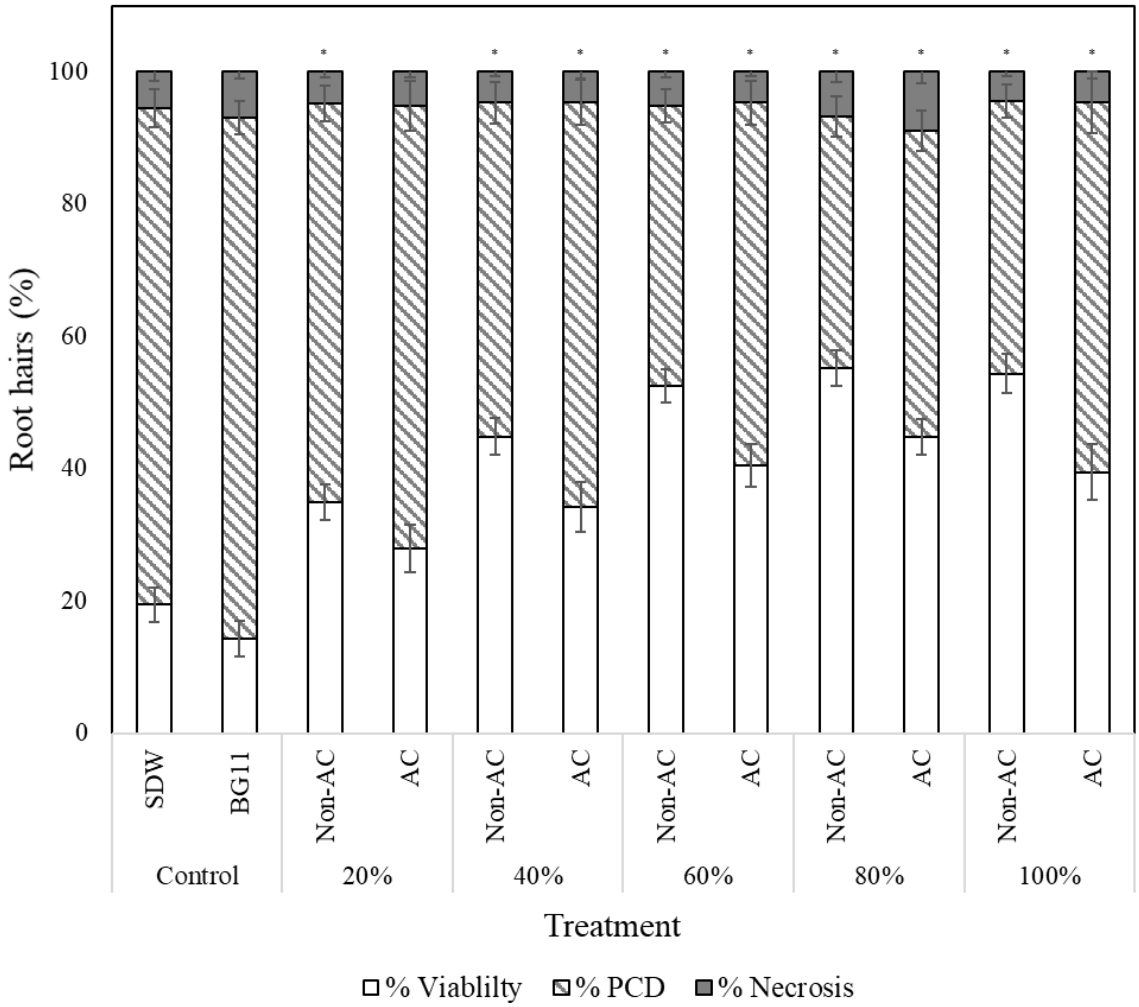


**Figure 2.5** - Effect of autoclaved (AC) and non-autoclaved *N. muscorum* CM on *Arabidopsis* root hair viability and death (PCD and necrosis) levels at 50 °C heat stress. (*) indicates PCD results significantly ($p$<0.05) different from the BG11 control. Values are the average of n ≥ 12 (± SE) and represent the merged results of 3 experiments. *N. muscorum* CM properties: $OD_{730}$ (1.17), chl-a (14.14 µg/mL), carotenoid (3 µg/mL). Each cell mode is represented as the percentage of cell mode over total number of root hairs, where viability% + PCD% + necrosis% = 100%.

**Table 2.4** - Effect of autoclaved and non-autoclaved *N. muscorum* CM fractions on *Arabidopsis* root hair viability at 50° C heat stress. Values are the average of n ≥ 8 (± SE) and represent the merged results of 3 experiments. A Dunnett *t*-test was used for statistical analysis which treated the BG11 dataset as a control and compared all other group datasets against it. (*) The mean difference is significant at the 0.05 level.

| ***N. muscorum* CM Treatments** | | **PCD (%)** | **Mean difference from BG11 control (%)** | ***p*-value** |
|---|---|---|---|---|
| Controls | BG11 | 75.1 ± 2.93 | N/A | N/A |
| | SDW | 78.7 ± 2.51 | 3.6 | 0.989 |
| 20% | Non-autoclaved | 60.3 ± 2.66 | -18.5* | 0.001 |
| | Autoclaved | 67.0 ± 3.73 | -11.8 | 0.079 |
| 40% | Non-autoclaved | 50.5 ± 3.09 | -28.3* | 0.000 |
| | Autoclaved | 61.2 ± 3.51 | -17.5* | 0.002 |
| 60% | Non-autoclaved | 42.4 ± 2.48 | -36.3* | 0.000 |
| | Autoclaved | 54.9 ± 3.31 | -23.9* | 0.000 |
| 80% | Non-autoclaved | 38.1 ± 3.01 | -40.7* | 0.000 |
| | Autoclaved | 46.3 ± 3.01 | -32.4* | 0.000 |
| 100% | Non-autoclaved | 41.2 ± 2.54 | -37.5* | 0.000 |
| | Autoclaved | 56.0 ± 4.64 | -22.7* | 0.000 |

### 2.3.3.1 Additional statistical analysis – Linear regression model

Linear regression analysis (Table 2.5) was used to assess if increasing the *N. muscorum* CM concentration and autoclaving fractions would decrease PCD levels of treated *Arabidopsis* seedlings. The % CM fraction variable had a *p*-value (sig) of 0.000, showing that PCD levels decreased in proportion to *N. muscorum* CM concentration in a statistically significant manner. Its coefficient (B) value of -0.221 estimates that for every 1% increase in % CM fraction, the regression model predicts a 0.22% decrease in PCD levels, i.e. increasing the CM dosage by 40% decreases PCD levels by approximately 8%. Similarly, the coefficient for the autoclave treatment variable was 10.3 and statistically different (*p*-value = 0.00). The positive coefficient confirms that autoclaved *N. muscorum* CM treated seedlings had higher PCD levels, with an average difference of 10.3%, compared to their non-autoclaved treated counterparts. Finally, the R-squared value of the regression model was 0.297, indicating that approximately 29.7% of the variability in stress-induced PCD levels were accounted by both % CM fractions and autoclave treatment variables.

**Table 2.5** - *N. muscorum* CM linear regression model predicting the dependent variable (% PCD) from two independent variables (% CM fractions and autoclave treatment). (A) Model summary reporting the overall model fit and (B) Parameter estimates of coefficients of the dependent variables.

**(A) Model Summary[a]**

| Model | R | R Square | Adjusted R Square | Std. Error of the Estimate |
|---|---|---|---|---|
| 1 | .545[a] | 0.297 | 0.286 | 12.3 |

a. Predictors: (Constant), Autoclave treatment, % CM fraction

**(B) Coefficients[b]**

| Model | Unstandardized Coefficients | | t | Sig. |
|---|---|---|---|---|
| | B | Std. Error | | |
| (Constant) | 49.8 | 3.98 | 12.5 | 0.000 |
| Autoclave treatment | 10.3 | 2.16 | 4.77 | 0.000 |
| % CM fraction | -0.221 | 0.038 | -5.83 | 0.000 |

b. Dependent Variable: Stress-induced PCD levels

### 2.3.4 Identification of proline in *N. muscorum* CM using the ninhydrin assay

The initial *N. muscorum* CM screening process showed that the bioactive compound was thermostable and directly modulating the PCD pathway, as elaborated in Section 2.4.2. This information was cross-referenced with data from a literature review on *N. muscorum* exometabolites (Table 1.1) and used as input for building a framework to identify possible bioactive candidates (Section 2.4.3). The resultant framework highlighted proline as a candidate of interest as proline is a stress-responsive amino acid that accumulates in plants under abiotic and biotic stress (Abrahám *et al.* 2010). A proline standard curve was generated using the ninhydrin assay, which detected proline linearly ($R^2$ = 0.9991) from 1-300 µM (Figure 2.6). Following that, proline was detected in autoclaved and non-autoclaved CM at concentrations of 1.94 µM and 1.83 µM, respectively (Table 2.6).

**Table 2.6** - Quantification of proline in autoclaved and non-autoclaved *N. muscorum* CM [$OD_{730}$ (1.17), chl-a (14.14 µg/mL) and carotenoid (3 µg/mL)]. Values are the average of n=16 (± SE) and represent the merged results of 2 experiments.

| ***N. muscorum* CM** | **Proline concentration (µM)** |
|---|---|
| Autoclaved | 1.83 ± 0.26 |
| Non-autoclaved | 1.94 ± 0.22 |

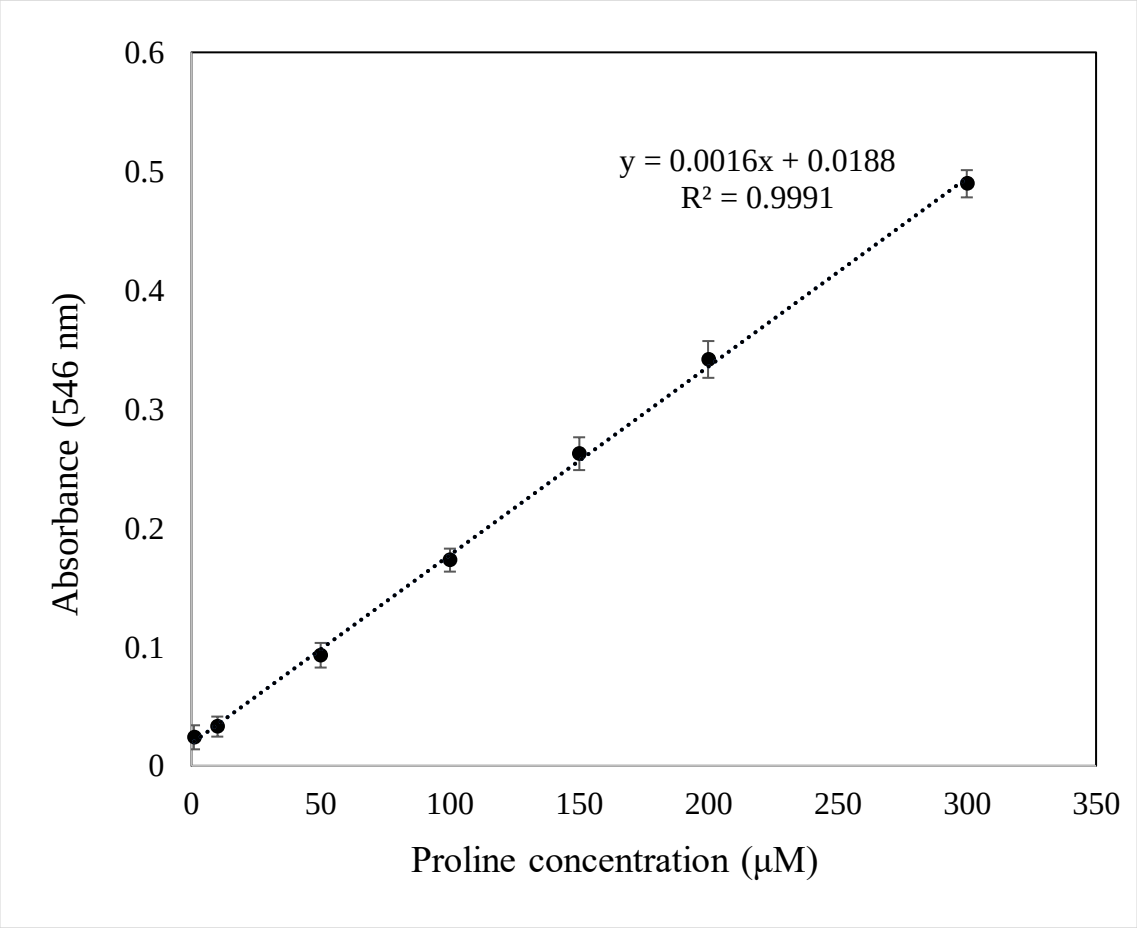


**Figure 2.6** – Proline standard curve ($R^2$ = 0.9991) generated using the ninhydrin assay, where n = 4.

## 2.3.5 HPLC Method development process

Pernil *et al.* (2008) identified 19 amino acids in *N. muscorum* extracellular filtrates, but the published method lacked key details that limited its reproducibility as discussed in Section 2.4.4. A protocol was initially adapted from Heinrikson and Meredith (1984) and Kwanyuen and Burton (2010) to identify the amino acids in *N. muscorum* CM. Under this initial protocol, proline, when treated with PITC, responded linearly ($R^2$ = 0.984) from a

10-100 µM concentration (Figure 2.7). After demonstrating this linearity response, four variables were investigated in the method development process: sample injection volume, PITC ratio, *N. muscorum* CM concentration factor and guard column usage. By monitoring the process development steps, an optimum method was found for separating the amino acid mixtures; a final proline standard curve was generated using the optimized configurations and proline successfully quantified in *N. muscorum* CM (Section 2.3.6).

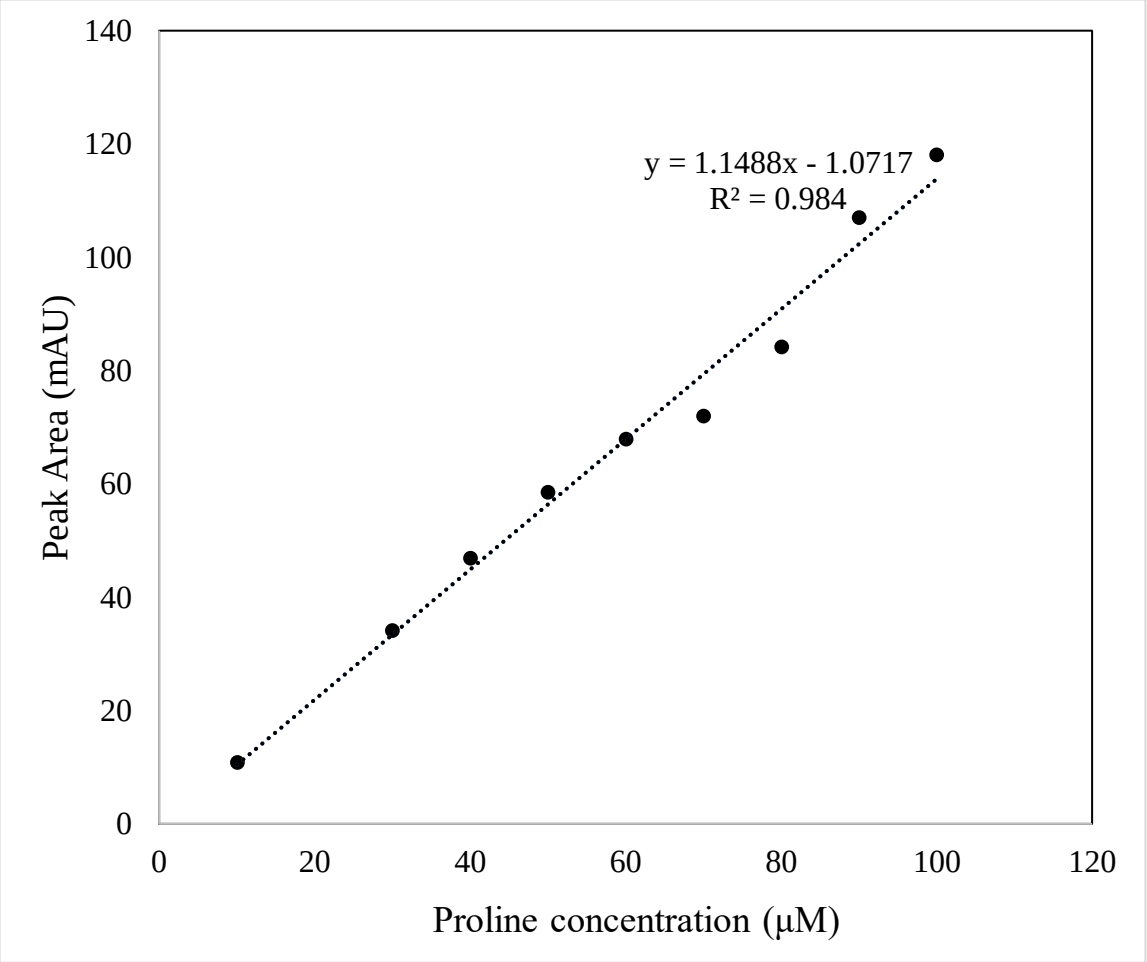


**Figure 2.7** - Proline standard curve generated from the initial protocol adapted from Heinrikson and Meredith (1984) and Kwanyuen and Burton (2010). Note the linear detection of proline from 10-100 µM. Run configurations: guard column, G1 gradient and 7 µL injection volume. Readings are from a single replicate.

### 2.3.5.1 Impact of injection volume on the resolution between alanine and proline

Proline and alanine peak areas increased linearly ($R^2$ = 0.9992 and 0.9931, respectively) as injection volume increased from 7, 10 and 15 µL (Table 2.7), but had minor shifts in retention times (Figure 2.8). When injection volumes of 7 and 10 µL were used, the resolution between proline and alanine was 2.11. Only a small decrease in resolution (2.04) was noted when the sample injection volume was increased to 15 µL. This shows that 15 µL is a suitable injection volume for subsequent experiments as the resolution between the two key peaks was still above the 1.5 threshold, which is required to achieve complete peak separation (Esmaeilzadeh *et al.* 2016).

**Table 2.7** - Effect of injection volume on the resolution between alanine and proline and their respective peak areas.

| Injection volume (µL) | Alanine | | | Proline | | | Peak resolution |
|---|---|---|---|---|---|---|---|
| | Peak Area (mAU x $10^4$) | Time (min) | Peak Width | Peak Area (mAU x $10^4$) | Time (min) | Peak Width | |
| 7 | 1.16 | 10.7 | 0.312 | 1.14 | 11.4 | 0.328 | 2.11 |
| 10 | 1.67 | 10.6 | 0.334 | 1.99 | 11.3 | 0.348 | 2.11 |
| 15 | 2.43 | 11.3 | 0.291 | 3.03 | 11.9 | 0.306 | 2.04 |

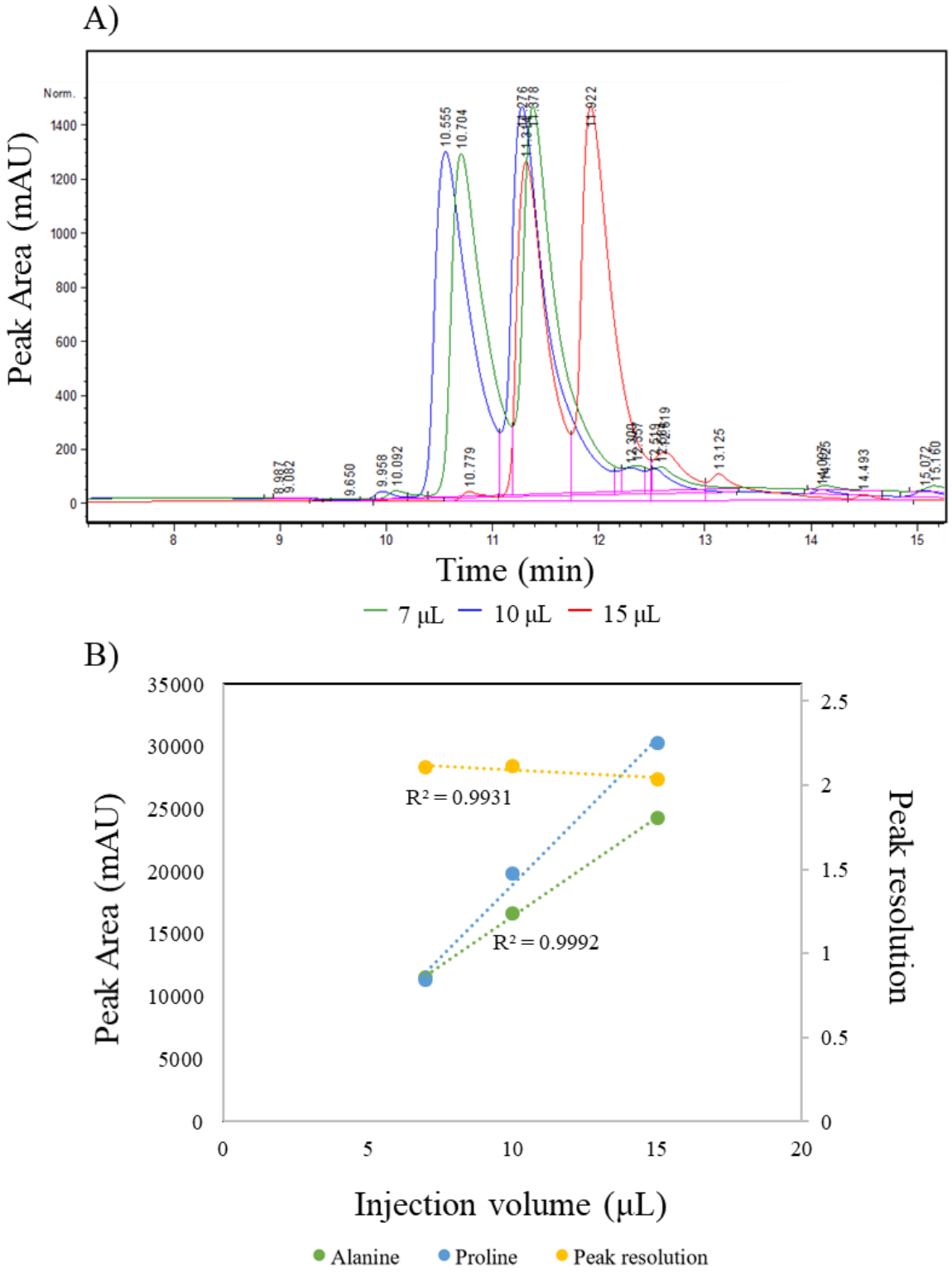


**Figure 2.8** – Impact of increasing injection volume on peak resolution between alanine and proline. (A) Overlaid alanine and proline chromatograms as a function of increasing injection volumes of 7, 10 and 15 µL. Alanine always elutes to the left of proline. (B) Graphs depicting the linear effect of injection volume on peak resolution between alanine and proline and their respective peak areas. Values reflect data from a single experiment.

### 2.3.5.2 Impact of PITC ratio on the resolution between proline and alanine and their respective peak areas

Alanine and proline peaks elute closely to each other as the guard column prolongs the run-time and causes band broadening (Carr *et al.* 2011; Stankovich *et al.* 2013). Previous testing (data not shown) using 300 µL of PITC derivatization mixture (X15 ratio) severely affected the sharpness of the eluted amino acid peaks. Hence, lower concentrations were used in this experimental series. PITC had an unusual peak area-reducing effect in alanine but not proline. Apart from the sudden decline at the X2 PITC ratio (40 µL) dataset, the proline peak area was relatively constant (2.77 to 3.03 x $10^3$) across the tested PITC ratios (Figure 2.9A,Table 2.8). In contrast, the alanine peak declined linearly ($R^2$: 0.9363) as the PITC ratio increased (Figure 2.9B). Additionally, PITC concentrations did not affect peak resolution between proline and alanine as it remained constant (~2) throughout the tested concentrations. Given these results, the original PITC ratio (1X, 20 µL of PITC derivatization mixture) was chosen for the subsequent analysis for three reasons. Firstly, increasing PITC concentrations did not improve peak resolution between proline and alanine. Secondly, the alanine peak area degrades linearly in a PITC dose-dependent manner. Finally, higher PITC concentrations substantially lengthens the mixture drying time as PITC has a high boiling point (221 °C); using lower PITC concentrations shortens the time needed to complete the sample preparation process.

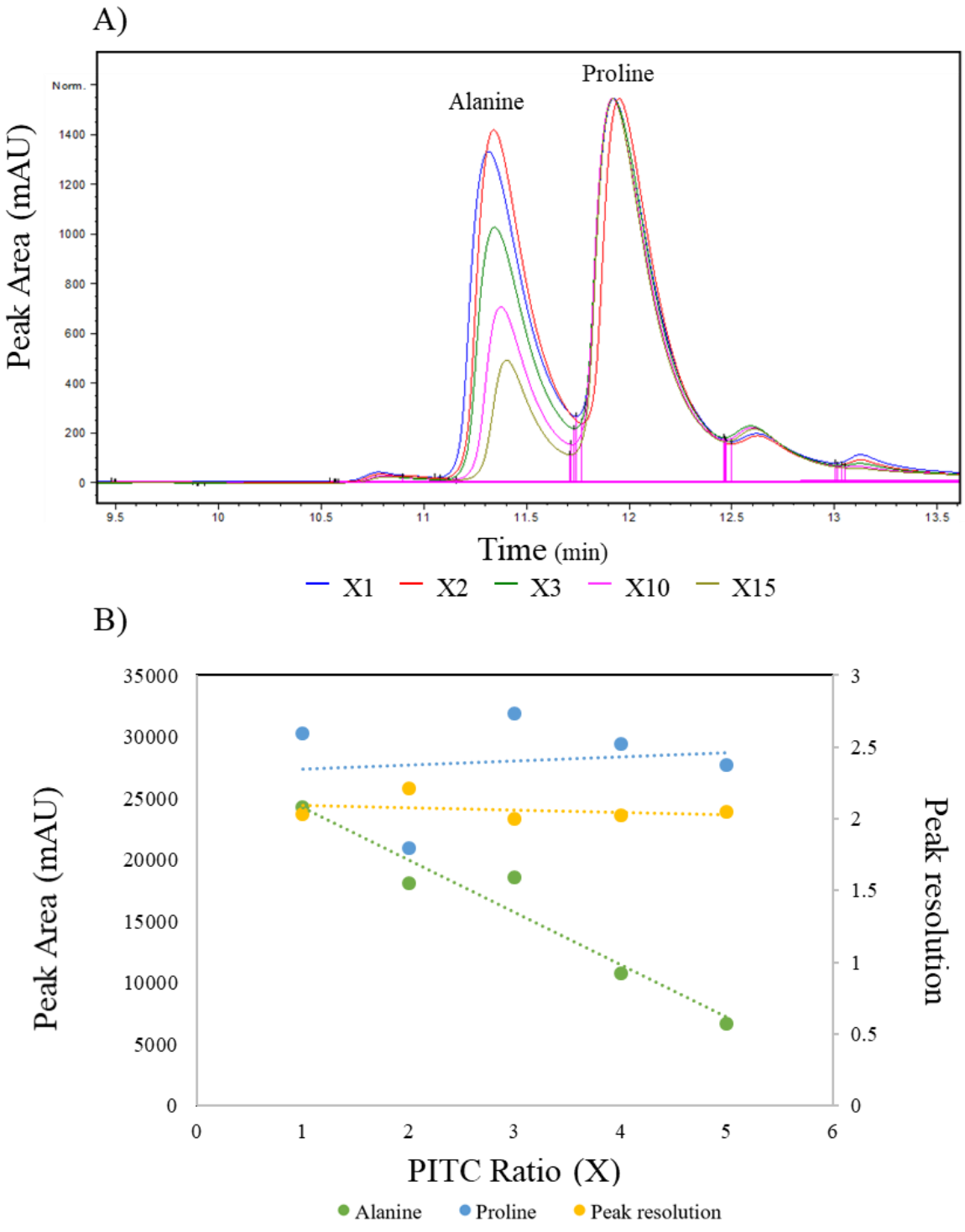


**Figure 2.9** – Effect of increasing PITC ratio on alanine and proline peak. (A) Overlaid alanine (11.3 min) and proline (11.9 min) chromatograms as a function of increasing PITC ratios. (B) Graphs depicting how the PITC ratio impacts the resolution between alanine and proline, and their respective peak areas. Note the linear degradation of alanine ($R^2$ = 0.9363) with an increase in the PITC ratio. Values reflect data from a single experiment.

**Table 2.8**- Impact of increasing PITC ratio on the resolution between alanine and proline peaks and their respective peak areas.

| | Alanine | | | Proline | | | Peak Resolution |
|---|---|---|---|---|---|---|---|
| **PITC Ratio** | **Peak Area (mAU x $10^4$)** | **Time (min)** | **Peak Width** | **Peak Area (mAU x $10^4$)** | **Time (min)** | **Peak Width** | |
| X1 | 2.43 | 11.3 | 0.291 | 3.03 | 11.9 | 0.306 | 2.04 |
| X2 | 1.81 | 11.3 | 0.270 | 2.09 | 12.0 | 0.282 | 2.21 |
| X5 | 1.86 | 11.3 | 0.269 | 3.19 | 11.9 | 0.307 | 2.00 |
| X10 | 1.08 | 11.4 | 0.238 | 2.94 | 11.9 | 0.298 | 2.03 |
| X12 | 0.667 | 11.4 | 0.216 | 2.77 | 11.9 | 0.289 | 2.05 |

### 2.3.5.3 Impact of *N. muscorum* CM sample volume on proline resolution

Proline was successfully detected in a 200 µL *N. muscorum* CM sample, with a 170.7 mAU peak area that eluted at 11.8-minutes. The identity of the 11.8-minute peak as proline was confirmed as the rest of the proline-spiked *N. muscorum* samples (80, 100, 150 and 200 µL) displayed an identical retention time (Figure 2.10, Table 2.9). Proline achieved complete peak separation from its neighbouring peaks (LHS: left-hand side, RHS: right-hand side), apart from the proline-spiked 80 µL CM dataset, which had a peak resolution of 1.37 with its LHS peak. As this was still part of the method development process, it was deemed unnecessary to identify the RHS and LHS peaks at that point of time. By varying *N. muscorum* CM volumes, the proline peak area was expected to increase in a linear manner as all four samples were spiked with identical proline concentrations. However, the proline peak area did not rise linearly ($R^2 = 0.0659$) across increasing *N. muscorum* CM sample volumes, most likely due to competing reaction mechanisms in a complex biological matrix composed of exoproteins (Oliveira *et al.* 2015), EPS (Mehta and Vaidya 1978), auxin (Mirsa and Kaushik 1989; Karthikeyan *et al.* 2009), ABA (Maršálek *et al.* 1992), phenolics and alkaloids (Abdel-Hafez *et al.* 2015), fatty acid derivatives (Abdel-Hafez *et al.* 2015) and sphingolipids (Daly 2013).

To further corroborate this theory, a smaller peak area (3.00 x $10^4$ mAU) was seen in proline-spiked 100 µL CM compared against the proline control (3.26 x $10^4$ mAU), reflecting incomplete spike recoveries. If proline was fully derivatised, the former would have a larger peak area than the latter, as cyanobacteria-derived proline would supplement the internally spiked levels. As this was not the case, it was highly likely that competing reactions in the CM biological matrix was interfering with the derivatization process.

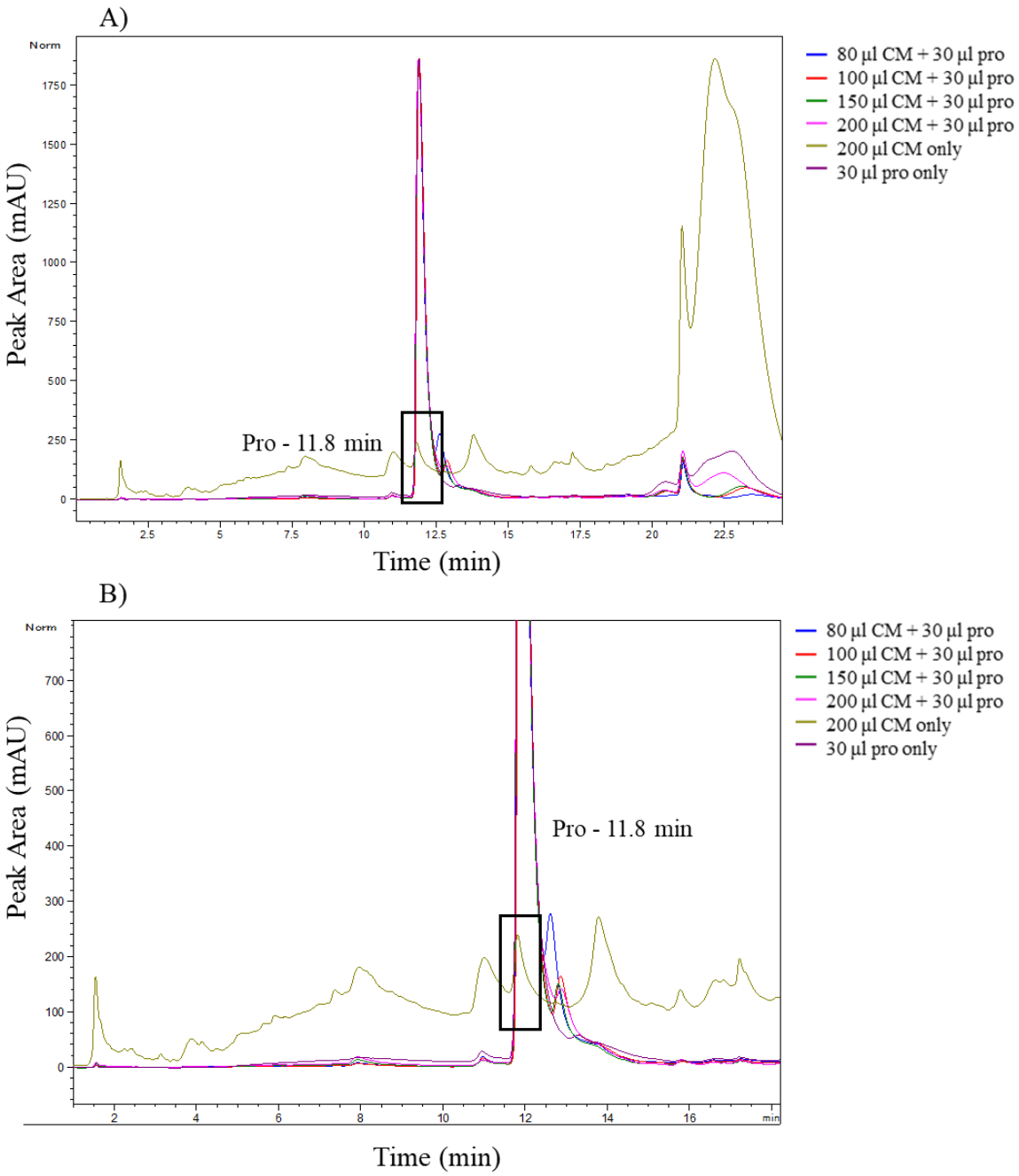


**Figure 2.10 -** Impact of *N. muscorum* CM sample volume on proline (pro) recovery. (A) Overlaid chromatogram of 30 µL proline-spiked *N. muscorum* CM samples (80, 100, 150, 200 µL) and their respective controls (30 µL proline and 200 µL CM). Note how proline elutes at 11.8 minutes in spiked and non-spiked *N. muscorum* samples. (B) Close-up view of the proline peak eluting at 11.8 min as highlighted in the black box. Values reflect data from a single experiment.

**Table 2.9** - Detection of proline in *N. muscorum* CM. Impact of *N. muscorum* CM sample volume on proline resolution.

**Key:** LHS = left-hand side, RHS = right-hand side.

| Sample | Proline | | | LHS peak | | | RHS peak | | |
|---|---|---|---|---|---|---|---|---|---|
| | Time (min) | Peak Area (mAU) | Peak Width | Time (min) | Peak Width | Resolution | Time (min) | Peak Width | Resolution |
| 200 µL CM | 11.8 | 171 | 0.270 | 11.01 | 0.479 | 2.15 | 13.8 | 0.441 | 5.53 |
| 30 µL Pro | 11.9 | $3.26 \times 10^4$ | 0.341 | 10.94 | 0.323 | 2.86 | 13.3 | 0.781 | 2.49 |
| 80 µL CM + 30 µL Pro | 11.9 | $3.81 \times 10^4$ | 0.309 | 11.45 | 0.309 | 1.39 | 12.6 | 0.436 | 1.96 |
| 100 µL CM + 30 µL Pro | 11.9 | $3.00 \times 10^4$ | 0.314 | 10.96 | 0.312 | 2.99 | 12.9 | 0.527 | 2.28 |
| 150 µL CM + 30 µL Pro | 11.9 | $3.41 \times 10^4$ | 0.319 | 10.96 | 0.365 | 2.7 | 12.8 | 0.489 | 2.27 |
| 200 µL CM + 30 µL Pro | 11.9 | $3.58 \times 10^4$ | 0.337 | 11.42 | 0.188 | 1.75 | 12.9 | 0.557 | 2.24 |

### 2.3.5.4 Impact of the guard column on amino acid separation mixture

Results from Section 2.3.5.3 confirmed that proline was present in *N. muscorum* CM but the original stepwise gradient (G1 - Table 2.3) had to be revised for the qualitative assessment of the other amino acids. The amino acid standard mix was formerly separated under low injection volumes (7 µL) but they lost peak sharpness and resolution because higher injection volumes were adopted in later run configurations. The best separation was obtained by lengthening the run-time with a new gradient (G2 - Table 2.3) and Figure 2.11A illustrates the improved separation of the amino acid standard mix under this new gradient. However, many amino acid peaks, including the key peaks of alanine and proline (resolution 3.71) did not resolve to the solvent baseline (see vertical pink lines in Figure 2.11A depicting baseline drifts), impairing the accuracy of proline quantification. Experience informed that if the amino acid standard mixture already had sub-optimum peak separation, actual *N. muscorum* CM samples would have considerably more inferior results. Therefore, a test-run was conducted to assess if elimination of the guard column would improve peak sharpness under elevated 14 µL injection volumes. Following removal of the guard column, the mobile phase was once again modified (G3 - Table 2.3) and a markedly improved chromatogram was obtained, as shortening the run-time reduced peak-broadening and resulted in shaper peaks (Figure 2.11B).

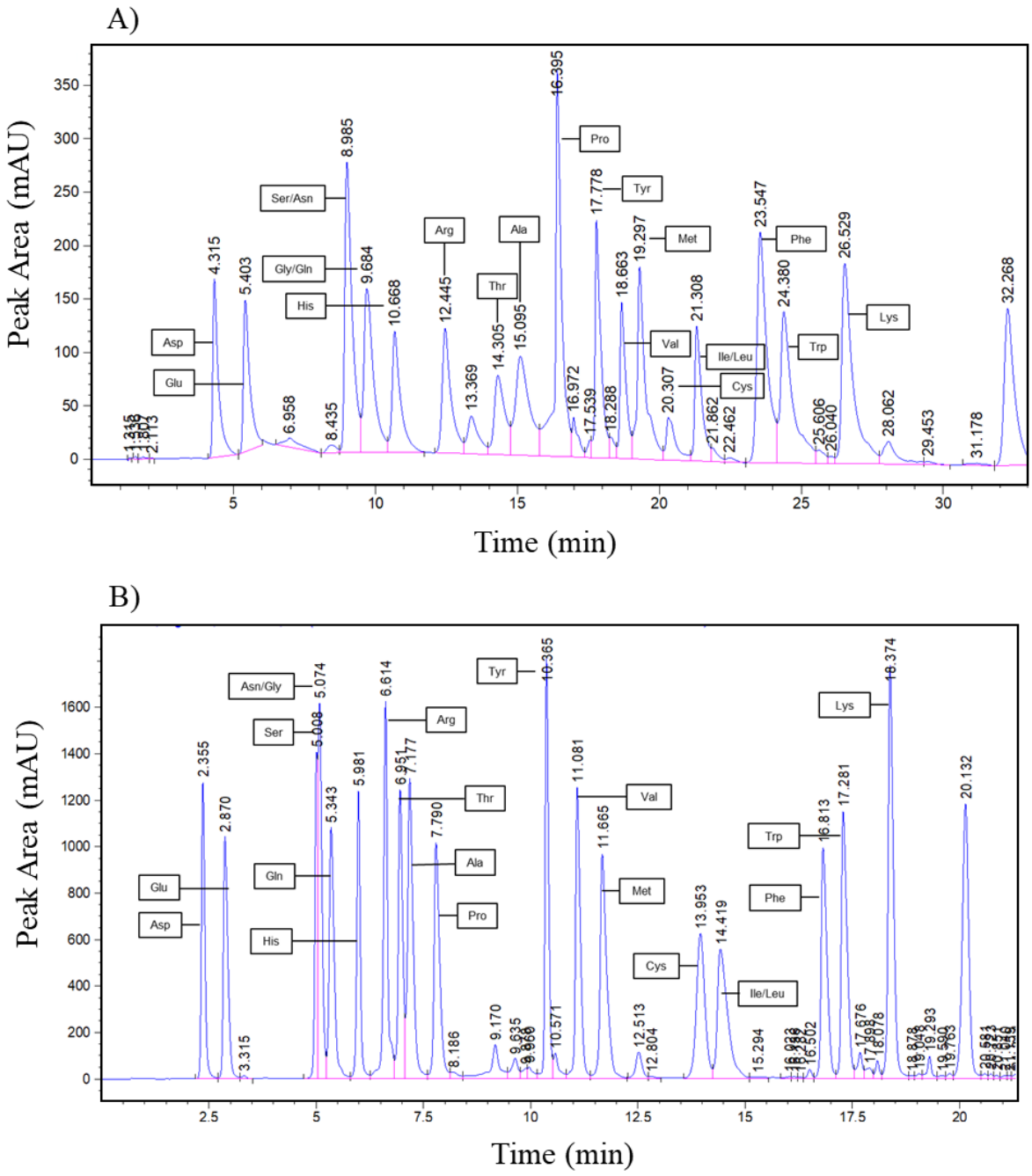


**Figure 2.11** – Separation of the amino acid standard mix with (A) the guard column under G2 gradient and (B) without guard column under G3.

**Key:** Asp - Aspartic acid, Glu - Glutamic acid, Ser - Serine, Asn - Asparagine, Gly - Glycine, Gln - Glutamine, His - Histidine, Arg - Arginine, Thr - Threonine, Ala - Alanine, Pro - Proline, Tyr - Tyrosine, Val - Valine, Met - Methionine, Cys - Cysteine, Ile - Isoleucine, Leu - Leucine, Trp - Tryptophan, Phe – Phenylalanine and Lys – Lysine. Values reflect data from a single experiment.

With the new G3 mobile phase gradient, proline eluted at 7.8 minutes, but more importantly, the peak achieved baseline resolution and had better resolution with alanine (4.61). Some peaks could not be successfully resolved (e.g. Asn/Gly and Ile/Leu) but this was not of great concern. The qualitative assessment of the other amino acids was only of secondary importance, as the primary aim was to quantify proline and the latest protocol modifications enabled this as the proline peak had achieved baseline resolution.

### 2.3.6 Proline quantification and qualitative assessment of the other amino acids in *N. muscorum* CM

A 200 µL volume of *N. muscorum* CM (a 5-fold concentration factor) was analysed for its amino acid composition. However, an unforeseen effect of eliminating the guard column was the loss of column efficiency and lower detection sensitivity of the amino acids. Thus, the injection volumes were increased to even higher levels (70 µL), to make the amino acid peaks more distinguishable from the baseline. Using the G3 mobile phase gradient, proline eluted around the 7.8-minute mark (Figure 2.12A, highlighted in black) and its presence was verified by spiking *N. muscorum* CM with an internal 100 µM proline standard (Figure 2.12B).

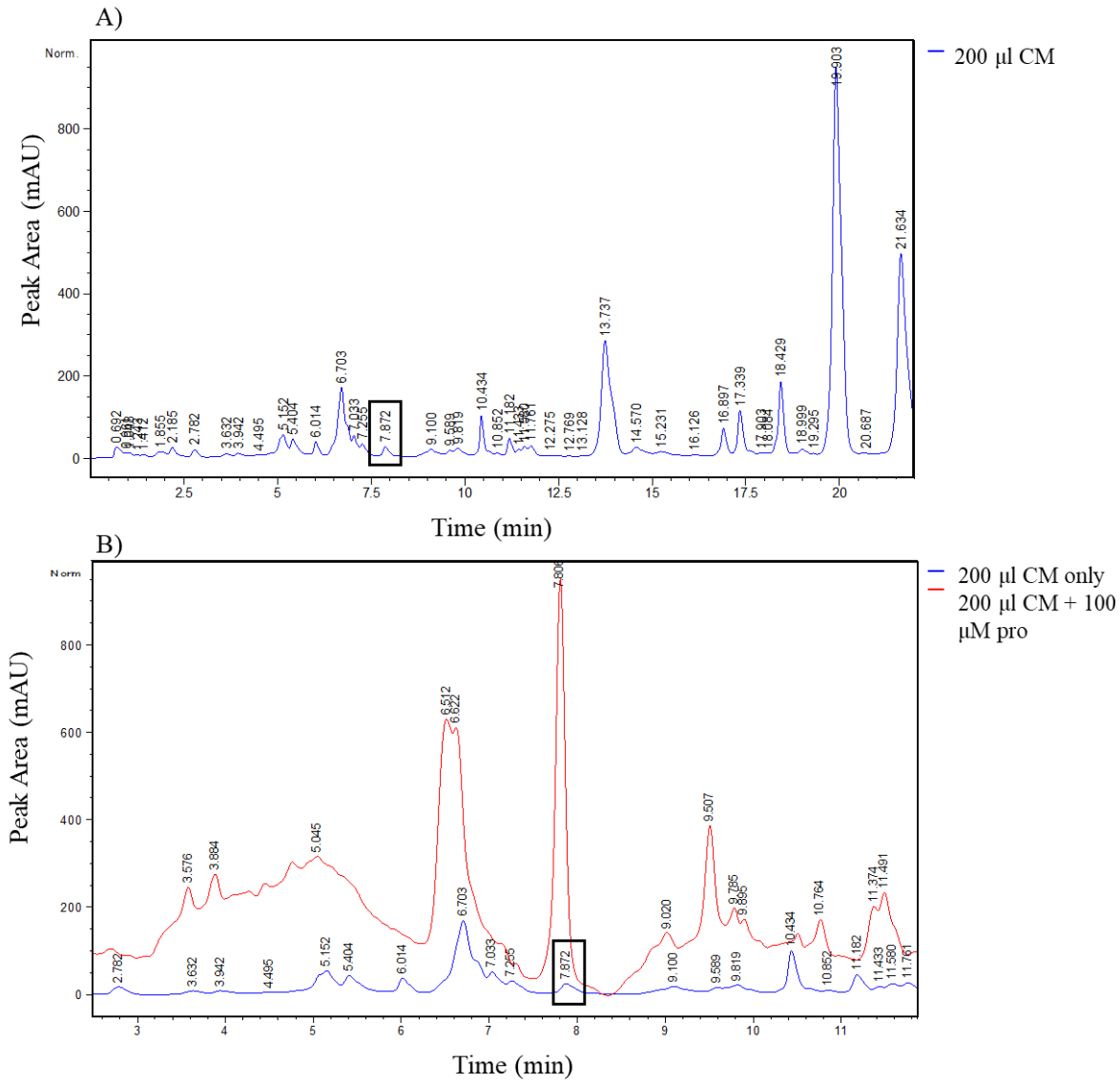


**Figure 2.12** – (A) Detection of proline in 200 µL *N. muscorum* CM sample when no guard column was used. (B) Internally proline-spiked *N. muscorum* CM sample. Confirmation of proline (7.8 min, hightailed in black) obtained by overlaying *N. muscorum* CM and proline-spiked *N. muscorum* CM chromatograms. Values reflect data from a single experiment.

Following this, a proline standard curve was generated (Figure 2.13) using the latest modifications (see Table 2.3, 70 µL injection volume, no guard column, G3 mobile-phase gradient), which had a linearity value of $R^2 = 0.9869$. After accounting for the 5-fold concentration factor of *N. muscorum* sample, the final proline concentration was 11.15 µM.

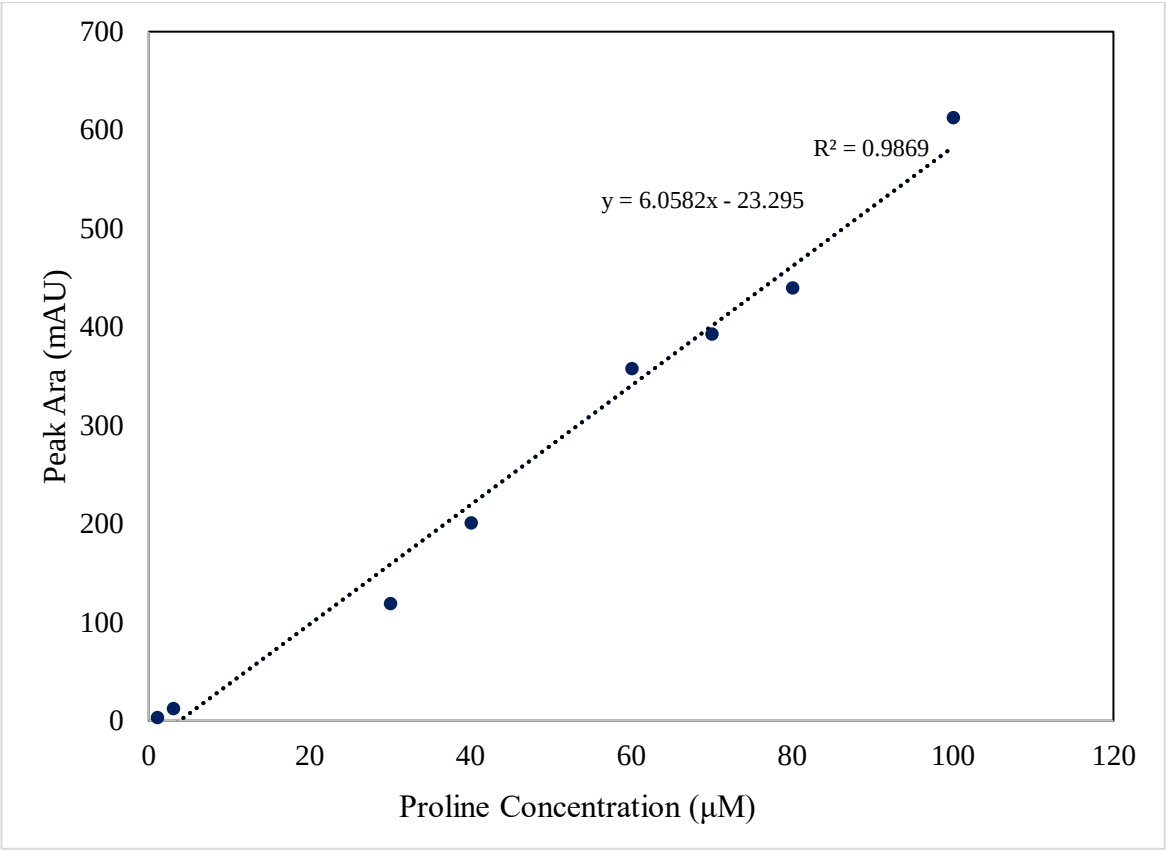


**Figure 2.13 -** Proline standard curve generated using the final protocol (70 µL injection volumes, no guard column and G3 gradient). Final proline concentration detected in *N. muscorum* CM was 11.2 µM. Readings are from a single replicate.

In addition to proline, the following amino acids were detected in *N. muscorum* CM by superimposing the *N. muscorum* CM and amino acid standard mix chromatograms: glutamic acid, serine, asparagine/glycine, glutamine, histidine, arginine, threonine, alanine, tyrosine, valine, methionine, isoleucine/leucine, phenylalanine, tryptophan and lysine (Figure 2.14). Peaks resembling aspartic acid and cysteine were noted, but further work would be required to verify their presence, as their retention times differed slightly from the corresponding peaks in the amino acid standard mix.

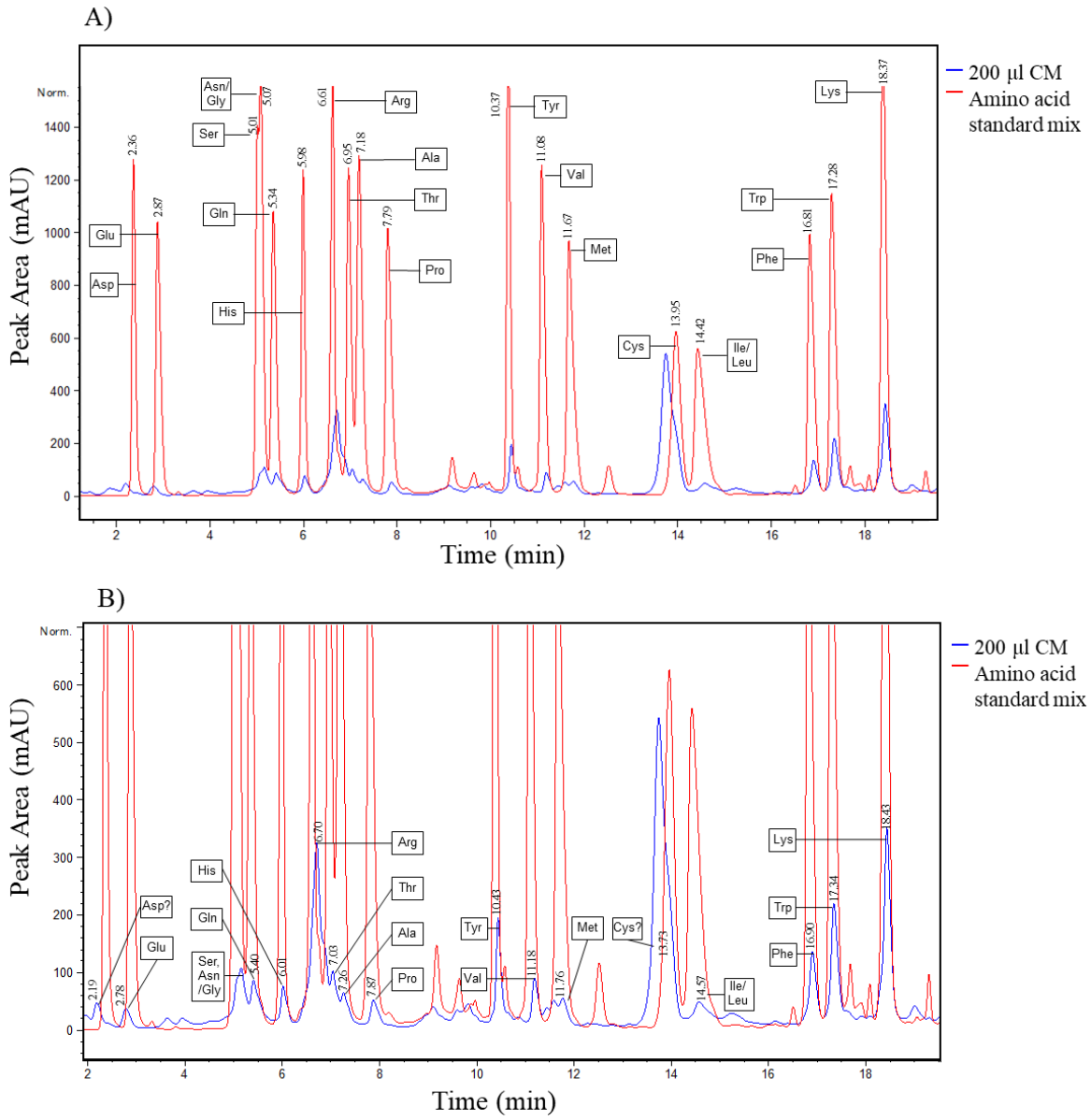


**Figure 2.14** – Detection of proline and other amino acids in *N. muscorum* CM sample. (A) Overlaid chromatogram of *N. muscorum* CM and amino acid standard mix and (B) its close-up view of the individual amino acid peaks. Values reflect data from a single experiment.

## 2.3.7 Confirming the bioactive PCD-suppressing effect of proline

### 2.3.7.1 Exogenous proline suppressed PCD in wild-type (Col-0) *Arabidopsis* seedlings

Two proline solutions were established in BG11 at identical concentrations measured using the ninhydrin assay in autoclaved CM (1.94 µM) and non-autoclaved CM (1.83 µM). The former solution was autoclaved at 121 °C for 15 minutes to determine if proline was the main thermostable bioactive compound in *N. muscorum* CM. Both proline

solutions were diluted across a similar concentration gradient (20-100%) to assess if proline elicits a dose-dependent response. The SDW control was omitted for this series of experiments as past results and statistical analysis (Table 2.4) show that BG11 and SDW treatment results in similar PCD levels, with no bioactive effect noted in treated wild-type *Arabidopsis* seedlings. Proline pre-treated seedlings exhibited a similar stress-response profile as *N. muscorum* CM treatment; treated seedlings had lower stress-induced PCD levels, but negligible changes to necrosis levels (Figure 2.15), demonstrating the bioactive PCD-suppressing ability of proline.

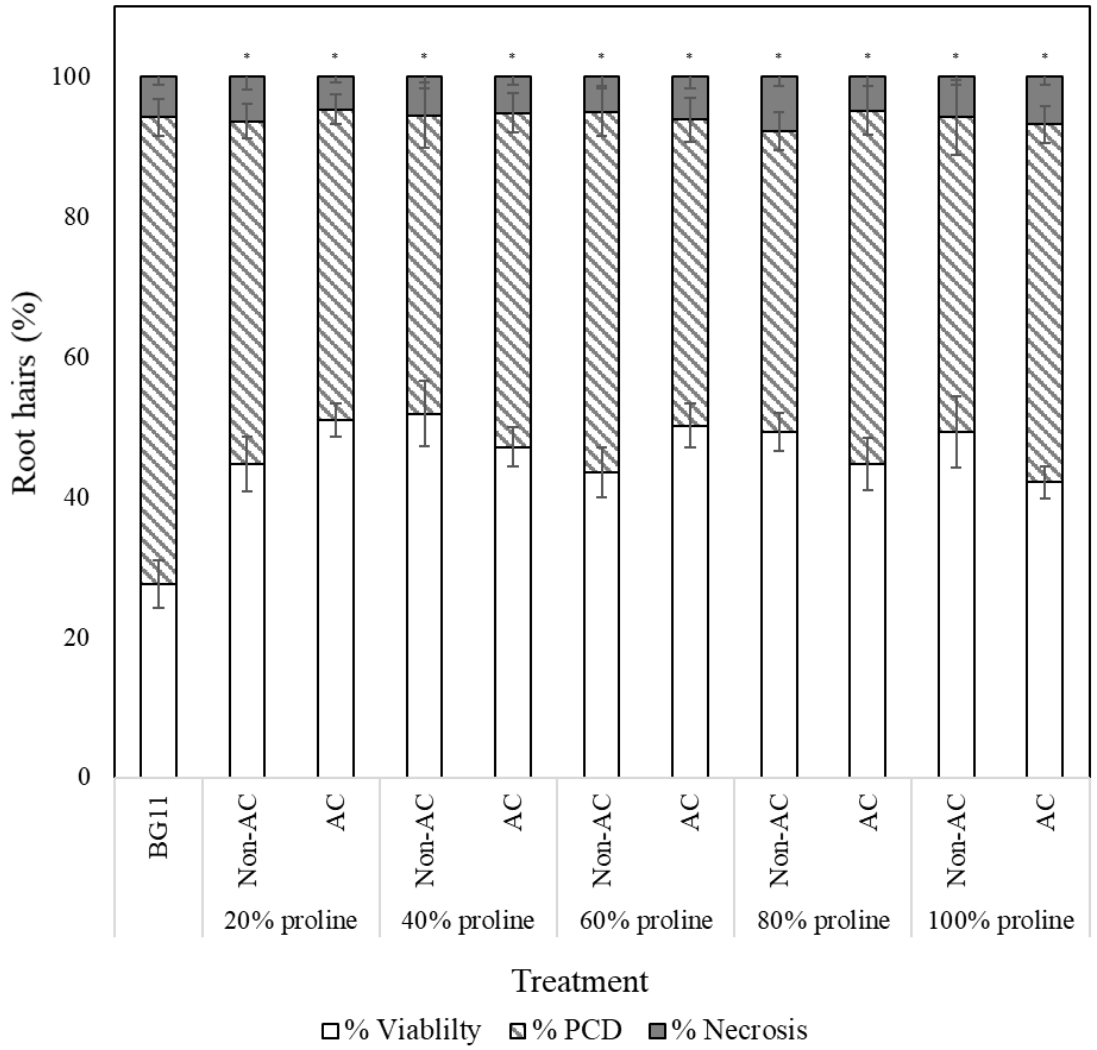


**Figure 2.15** - Effect of autoclaved (AC) and non-autoclaved exogenous proline on root hair viability of *Arabidopsis* at 50 °C. (*) indicates PCD results significantly ($p$<0.05) different from the BG11 control. Values are the average of n ≥12 (± SE) and represent the merged results of 3 experiments. Each cell mode is represented as the percentage of cell mode over total number of root hairs, where viability% + PCD% + necrosis% = 100%.

Linear regression analysis was used to assess if autoclaving attenuated proline bioactivity and if exogenous proline treatment exerted a dose-dependent effect (Table 2.10). Both variables had negligible effects on PCD levels; the R-squared value of the regression model was 0.003, indicating they merely accounted for 0.3% of the variability in PCD levels, a substantial 99 fold-decrease from the original *N. muscorum* CM regression model (R-squared value = 0.297). Therefore, the model showed two key details: (1) proline does not inhibit PCD in a dose-dependent manner as treatment with *N. muscorum* CM did and (2) proline is thermostable as autoclaving did not abrogate its bioactive PCD-suppressing properties.

**Table 2.10** - Exogenous proline linear regression model predicting the dependent variable (% PCD) from two independent variables (% proline fractions and autoclave treatment). (A) Model summary reporting the overall model fit and (B) Parameter estimates of coefficients of the dependent variables.

**(A) Model Summary**

| Model | R | R Square | Adjusted R Square | Std. Error of the Estimate |
|---|---|---|---|---|
| 1 | .053[a] | 0.003 | -0.014 | 12.0 |

a. Predictors: (Constant), Autoclave treatment, % Proline fraction

**(B) Coefficients[a]**

| Model | Unstandardized Coefficients | Std. Error | t | Sig. |
|---|---|---|---|---|
| (Constant) | 47.3 | 4.03 | 11.7 | 0.000 |
| Autoclave treatment | -0.998 | 2.16 | -0.462 | 0.645 |
| % Proline fraction | 0.016 | 0.040 | 0.395 | 0.693 |

a. Dependent Variable: Stress-induced PCD levels

To further corroborate these results, one-way ANOVA analysis showed that all tested proline fractions (autoclaved and non-autoclaved) significantly reduced ($p$<0.05) stress-induced PCD levels of treated *Arabidopsis* seedlings, with up to a 24% mean difference from the BG11 control (Table 2.11). Collectively, the results show that proline was thermostable and also priming the *Arabidopsis* stress response by suppressing PCD as necrosis had an imperceptible impact across the entire range of treatments.

**Table 2.11**- Effect of autoclaved and non-autoclaved exogenous proline on *Arabidopsis* root hair viability at 50 °C heat stress. Values are the average of n ≥ 12 (± SE) and represent the merged results of 3 experiments. A Dunnett *t*-test was used for statistical analysis which treated the BG11 dataset as a control and compared all other group datasets against it. (*) The mean difference is significant at the 0.05 level.

| **Proline Treatments** | | **PCD (%)** | **Mean difference from BG11 control (%)** | ***p*-value** |
|---|---|---|---|---|
| Controls | BG11 | 66.5 ± 2.61 | N/A | N/A |
| 20% | Non-autoclaved | 48.9 ± 2.43 | -17.6* | 0.002 |
| | Autoclaved | 44.3 ± 2.12 | -22.2* | 0.000 |
| 40% | Non-autoclaved | 42.6 ± 4.62 | -24.0* | 0.000 |
| | Autoclaved | 47.7 ± 2.75 | -18.9* | 0.000 |
| 60% | Non-autoclaved | 51.3 ± 3.35 | -15.2* | 0.006 |
| | Autoclaved | 43.6 ± 3.12 | -22.9* | 0.000 |
| 80% | Non-autoclaved | 42.9 ± 2.75 | -23.6* | 0.000 |
| | Autoclaved | 50.4 ± 3.51 | -16.1* | 0.005 |
| 100% | Non-autoclaved | 44.9 ± 5.36 | -21.6* | 0.000 |
| | Autoclaved | 51.0 ± 2.63 | -15.6* | 0.027 |

### 2.3.7.2 Concentrated *N. muscorum* CM and exogenous proline suppressed PCD at similar rates

To examine the differences in bioactivity between *N. muscorum* CM and exogenous proline pre-treated seedlings, each treatment was controlled for their respective proline concentrations (Figure 2.16). One-way ANOVA analysis (Supplementary Table S1) at each % of CM/proline fraction revealed two key trends: (1) the greatest variations primarily involved autoclaved *N. muscorum* CM treated seedlings as they had higher PCD levels compared to the other treatments and (2) significant differences ($p$<0.05) between *N. muscorum* CM and exogenous proline datasets predominantly occurred at the lower concentrations, but largely disappeared at the more concentrated doses. For example, at the 20-40% dilution range, autoclaved *N. muscorum* CM-treated seedlings were more susceptible to heat stress, with 14-23% higher PCD levels compared to seedlings treated with autoclaved and non-autoclaved proline treatments. At concentrated doses though, no significant differences ($p$>0.05) in PCD levels were noted between *N. muscorum* CM and exogenous proline datasets across the 60% and 100% dilution range. On the whole, the results showed that similar PCD-suppression rates took

place at concentrated doses between proline-treated root hairs and their corresponding CM fractions, offering preliminary evidence that proline was the bioactive compound of interest.

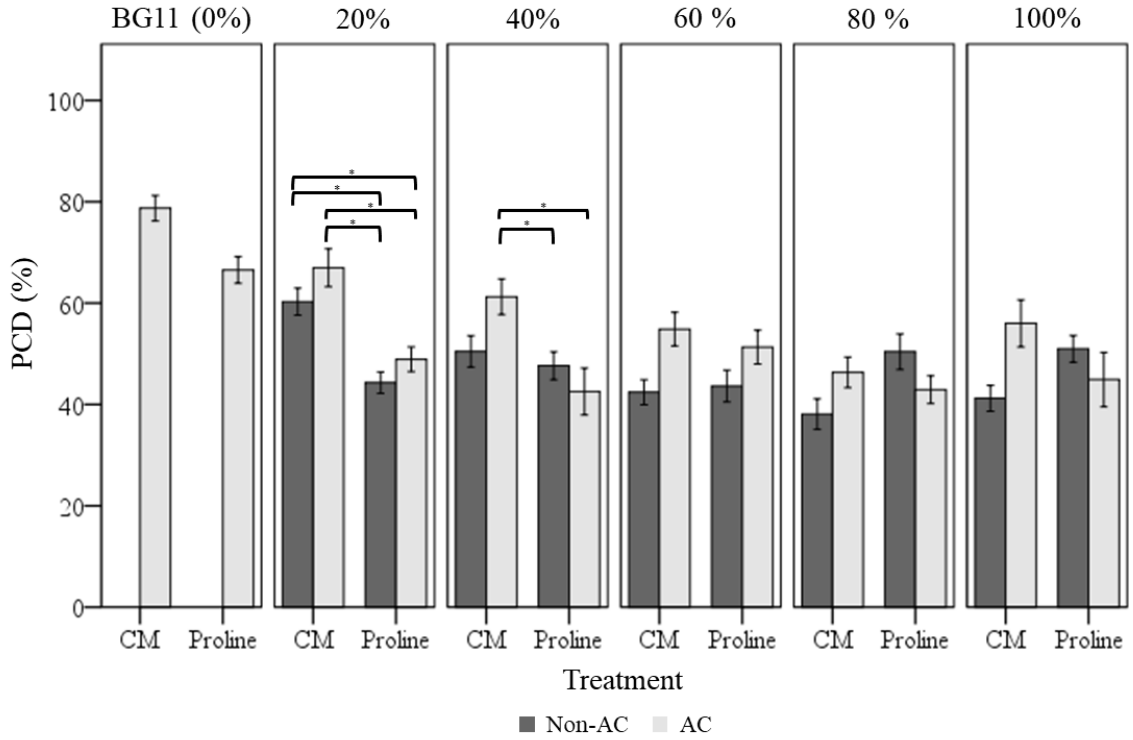


**Figure 2.16** - Comparing stress-induced PCD levels between autoclaved (AC) and non-autoclaved *N. muscorum* CM and exogenous proline in heat shocked *Arabidopsis* seedlings. (*) indicates PCD levels statistically different ($p$<0.05) to each other (Supplementary Table S1), while (0) denotes the BG11 control. Values for each dataset represent the average of n ≥ 8 (± SE) and represent the merged results of 3 experiments.

### 2.3.7.3 Weaker PCD-suppression in exogenous proline and *N. muscorum* CM-treated mutant *Arabidopsis* seedlings

The stress response profile of three impaired proline transporter mutants to *N. muscorum* CM and exogenous proline treatment was compared against wild-type seedlings. All four *Arabidopsis* lines (wild-type, *lht1*, *aap1* and *atprot1-1::atprot2-3::atprot3-2* mutants) were treated with undiluted *N. muscorum* CM (100% CM), low (1 µM), medium (2-5 µM) or high (100 µM) proline levels and two controls (SDW and BG11). For clarity, the SDW dataset is omitted from Figure 2.16 as it has no significant ($p$>0.05) differences with the BG11 control however it is displayed in Table 2.12. In line with past observations, wild-type seedlings treated with *N. muscorum* CM (Section 2.3.3) and exogenous proline (Section 2.3.7.1) had lower PCD rates compared to untreated BG11 controls. Wild-type seedlings benefited the most out of the four tested *Arabidopsis* lines, whether they were treated with exogenous proline or *N. muscorum* CM fractions. For example, treating wild-type plants with 1 or 5 µM proline significantly ($p$<0.05) decreased PCD rates compared to the BG11 control (Table 2.12). Similarly, *N. muscorum* CM-treated wild-type plants had the lowest PCD levels (26.7%) of all four *Arabidopsis* lines, approximately 21% lower than its untreated control. An interesting cytotoxic effect was noted at high proline (100 µM) doses as PCD levels rose to 44.5% and were not statistically ($p$ = 0.894) different from the BG11 control seedlings.

There were a number of interesting observations from the mutant supplementation study as summarised hereafter: (1) the PCD-suppressing effects of proline was attenuated in proline-impaired mutants, (2) the *atprot* triple knockout mutant displayed a stress phenotype more similar to wild-type seedlings, (3) the intra-specific differences between *atprot* triple knockout mutant with *aap1* and *lht1*mutants only becomes apparent at different proline doses, and (4) priming mutants with *N. muscorum* CM eliminated the intra-specific differences between mutants. First, proline-impaired mutants responded differently to exogenous proline treatment (Figure 2.17A). Statistical analysis confirmed that all three mutant lines had no significant differences ($p$>0.05) across the entire 1-100 µM proline treatment compared to their respective BG11 controls (Table 2.12). This was reflected in the stability of their PCD levels as the largest mean differences from their respective BG11 controls were mostly inconsequential, e.g. the *atprot* triple knockout mutant (4.6%), *lht1* (4.8%), and to a lesser extent *aap1* (11.1%). Thus, the beneficial

PCD-suppressing effects observed in proline treated wild-type seedlings were largely lost in the proline-impaired transporter mutants.

**Table 2.12** - Effect of exogenous proline and *N. muscorum* CM on *Arabidopsis* root hair viability at 50°C heat stress between wild-type and impaired proline transporter mutants (*atprot* triple knockout, *aap1* and *lht1*). Values are the average of n ≥ 12 (± SE) and represent the merged results of 3 experiments. A Dunnett *t*-test was used for statistical analysis which treated their respective BG11 dataset as a control and compared all other group datasets against it. (*) The mean difference is significant at the 0.05 level.

| **Treatment** | | **PCD (%)** | **Mean difference from BG11 control (%)** | ***p*-value** |
|---|---|---|---|---|
| Wild-type | BG11 | 48.1 ± 2.92 | N/A | N/A |
| | SDW | 52.7 ± 2.30 | 4.57 | 0.572 |
| | 1 µM proline | 37.6 ± 2.77 | -10.5* | 0.041 |
| | 2 µM proline | 44.2 ± 3.08 | -3.94 | 0.862 |
| | 5 µM proline | 35.7 ± 2.54 | -12.4* | 0.010 |
| | 100 µM proline | 44.5 ± 3.15 | -3.58 | 0.894 |
| | 100% CM proline | 26.7 ± 1.67 | -21.4* | 0.000 |
| *atprot1-1::atprot2-3::atprot3-2* mutant | BG11 | 47.3 ± 3.73 | N/A | N/A |
| | SDW | 46.4 ± 4.63 | -0.97 | 1.000 |
| | 1 µM proline | 43.5 ± 3.47 | -4.49 | 0.972 |
| | 2 µM proline | 43.4 ± 5.22 | -4.64 | 0.967 |
| | 5 µM proline | 45.2 ± 4.64 | -2.77 | 0.999 |
| | 100 µM proline | 48.7 ± 3.78 | 0.65 | 1.000 |
| | 100% CM proline | 38.1 ± 3.87 | -9.91 | 0.408 |
| *aap1* mutant | BG11 | 48.4 ± 2.54 | N/A | N/A |
| | SDW | 55.1 ± 5.81 | 6.72 | 0.623 |
| | 1 µM proline | 41.6 ± 2.43 | -6.85 | 0.585 |
| | 2 µM proline | 57.4 ± 2.98 | 9.02 | 0.329 |
| | 5 µM proline | 55.4 ± 3.35 | 6.96 | 0.570 |
| | 100 µM proline | 59.5 ± 3.59 | 11.12 | 0.153 |
| | 100% CM proline | 39.0 ± 4.33 | -9.37 | 0.293 |
| *lht1* mutant | BG11 | 53.1 ± 2.82 | N/A | N/A |
| | SDW | 55.5 ± 3.30 | 2.37 | 0.994 |
| | 1 µM proline | 50.0 ± 4.32 | -3.11 | 0.975 |
| | 2 µM proline | 51.0 ± 2.92 | -2.11 | 0.997 |
| | 5 µM proline | 55.0 ± 3.41 | 1.83 | 0.999 |
| | 100 µM proline | 58.0 ± 4.22 | 4.83 | 0.849 |
| | 100% CM proline | 37.6 ± 3.71 | -15.6* | 0.014 |

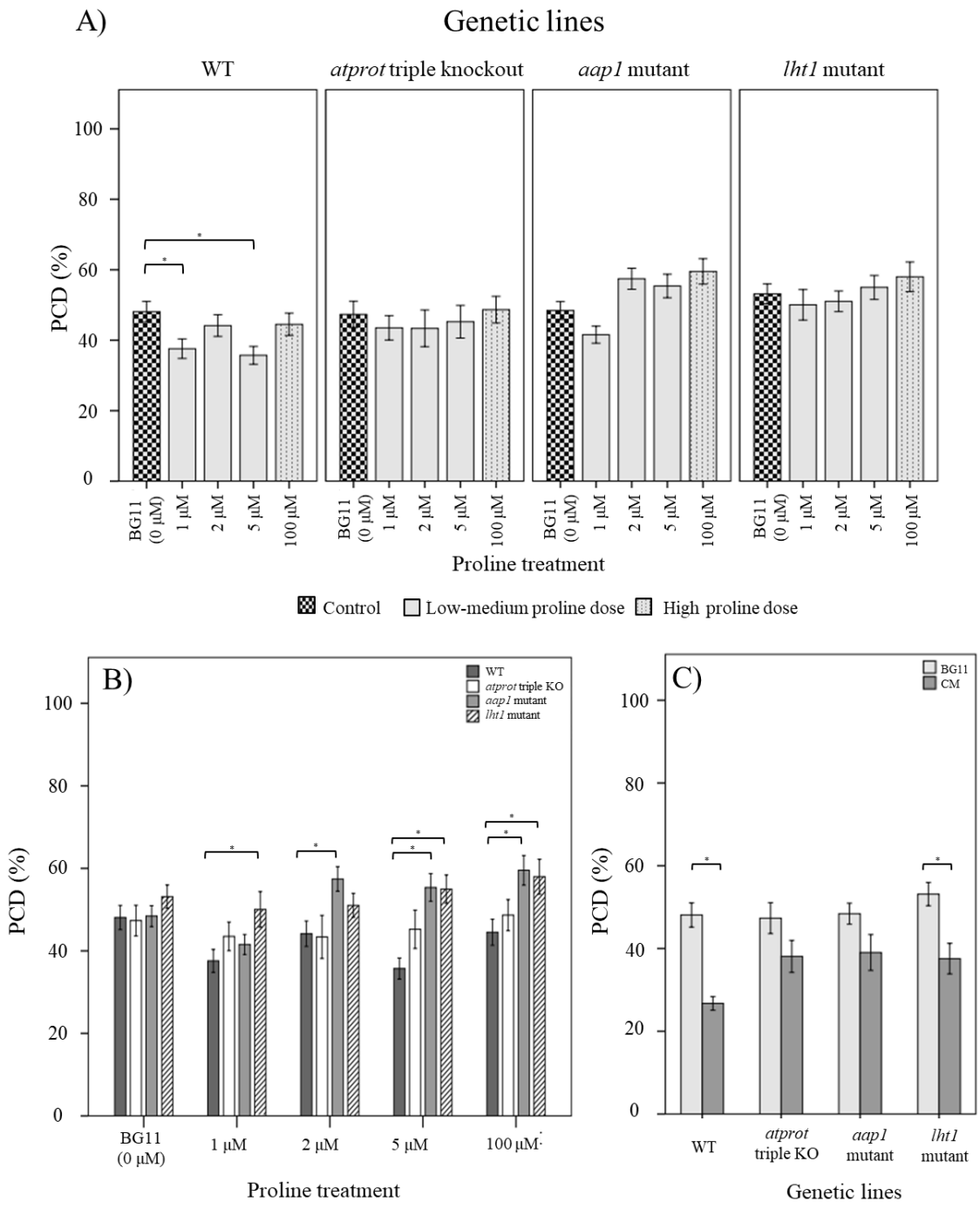


**Figure 2.17** - Examining how proline bioactivity differs between wild-type and impaired proline transporter mutants (*atprot1-1::atprot2-3::atprot3-2*, *aap1* and *lht1*) upon (A-B) proline or (C) *N. muscorum* CM treatment. Figure A and B are the same data collated into different groupings. Datasets marked with an (*) are statistically different ($p$<0.05) to each other (Supplementary Table S2). Values are the average of n ≥ 12 (± SE) and represent the merged results of 3 experiments.

Nevertheless, there was a marked difference between the stress-response profile of proline-specific (*atprot1-1::atprot2-3::atprot3-2*) and the general amino acid transporter (*lht1* and *aap1*) mutants. The *atprot* triple knockout mutant displayed a stress phenotype more akin to wild-type seedlings, unlike the *lht1* and *aap1*knockout mutants (Figure 2.17B). Although PCD levels of the *atprot* triple knockout mutant were generally higher than wild-type seedlings, they were not statistically different ($p>0.05$) from the wild-type seedlings at identical proline doses (Supplementary Table S2). The *atprot* triple knockout mutant also had negligible changes to PCD (43-48%) levels across all proline treatments, even under cytotoxic proline levels. In contrast, *aap1*and *lht1* mutants shared a similar stress phenotype, with higher PCD levels than wild-type and the *atprot* triple knockout mutant.

Next, the intra-specific variances between the *atprot* triple knockout and both general amino acid transporter mutants were especially apparent when they were supplied with low, medium and high proline doses (Figure 2.17B). At low proline levels, all three mutants had similar PCD levels (41-50%) to each other but a different pattern emerged when they were supplied with medium and high proline doses. The *atprot* triple knockout mutant only had slightly higher PCD levels (up to 9.5% increase) at medium and high doses, unlike both general amino acid transporter mutants which had up to an 19% increase in PCD levels compared to wild-type seedlings. This was reflected in statistical analysis showing that *aap1*and *lht1* mutants were significantly different ($p<0.05$) from wild-type seedlings at 5 μM proline doses.

Finally, the phenotypic difference between the *atprot* triple knockout mutant and the general amino acid transporters were eliminated when primed with *N. muscorum* CM (Figure 2.17C). Out of all treatments, all three mutant lines had the lowest PCD (37-39%) levels when treated with *N. muscorum* CM, although the PCD-suppressing effect was still weaker in the mutant lines compared to treated wild-type seedlings. It appears that accompanying bioactive compounds in *N. muscorum* CM were acting synergistically to exert a stronger PCD-suppressing effect, compared to proline acting individually, even in the mutant lines.

# 2.4 Discussion

## 2.4.1 Rationalization for *N. muscorum* CM screening parameters

Survival signals such as platelet-derived growth factors and insulin-like growth factors can inhibit PCD in animal cells (Barres *et al.* 1992) and similar observations have been noted in plants as McCabe *et al.* (1997) showed that carrot cell CM inhibits stress-induced PCD at low cell densities. Previous work by Daly (2013) suggests that *N. muscorum* CM contains pro-survival signals that exert a similar bioactive effect in *Arabidopsis* root hairs but attempts to identify the compound is difficult as *N. muscorum* exudes a broad range of exometabolites. In this chapter, the RHA was used as a rapid screening tool to characterise *N. muscorum* CM bioactivity on *Arabidopsis* heat stress tolerance in terms of viability, PCD and necrosis. Using the workflow summarised in Figure 2.18, proline was successfully identified as the major bioactive compound in *N. muscorum* CM that inhibits stress-induced PCD levels.

The first step of the workflow was to conduct a literature view on all known *N. muscorum* CM exometabolites (summarised in Table 1.1). Next, the baseline heat stress-response was established in wild-type *Arabidopsis* seedlings. As the stress dosage was raised from 25-85 °C, the RHA identified three stress-response phases: stress-tolerant phase, the PCD zone and the necrotic zone. When the stress dosage crosses the threshold to enter a new phase, e.g. from PCD to necrosis, significant changes arise in the overall cell mode composition. For example, PCD is the prevailing mode when root hairs are heat-shocked at temperatures within the PCD zone (50-65 °C). At this phase, root hairs either maintain viability if the cellular protective mechanisms can compensate for the heat-induced damage but will activate PCD if the response is insufficient (Hogg *et al.* 2011). However, in the necrotic zone (75-85 °C), the severe oxidative damage causes most root hairs to die by necrosis, i.e. uncontrolled cell death, although a small portion of root hairs can still trigger PCD. This biphasic cell death motif concurs with heat-shocked *Arabidopsis* seedlings (Hogg *et al.* 2011), *Daucus carota* subsp. *sativus* suspension cultures (McCabe *et al.* 1997), *Nicotiana tabacum* cell cultures (Burbridge *et al.* 2007), UVB-irradiated human keratinocytes cells (Mammone *et al.* 2000) and human tumour HL-60 cells under exposure to methanol, dimethyl sulphoxide, UV radiation, calcium ionophore, and sodium azide (Lennon *et al.* 1991). Following this, 50 °C was chosen as the set-point for

screening *N. muscorum* CM fractions at it represents the inflection point where the largest differences in PCD levels can arise upon elicitor treatment.

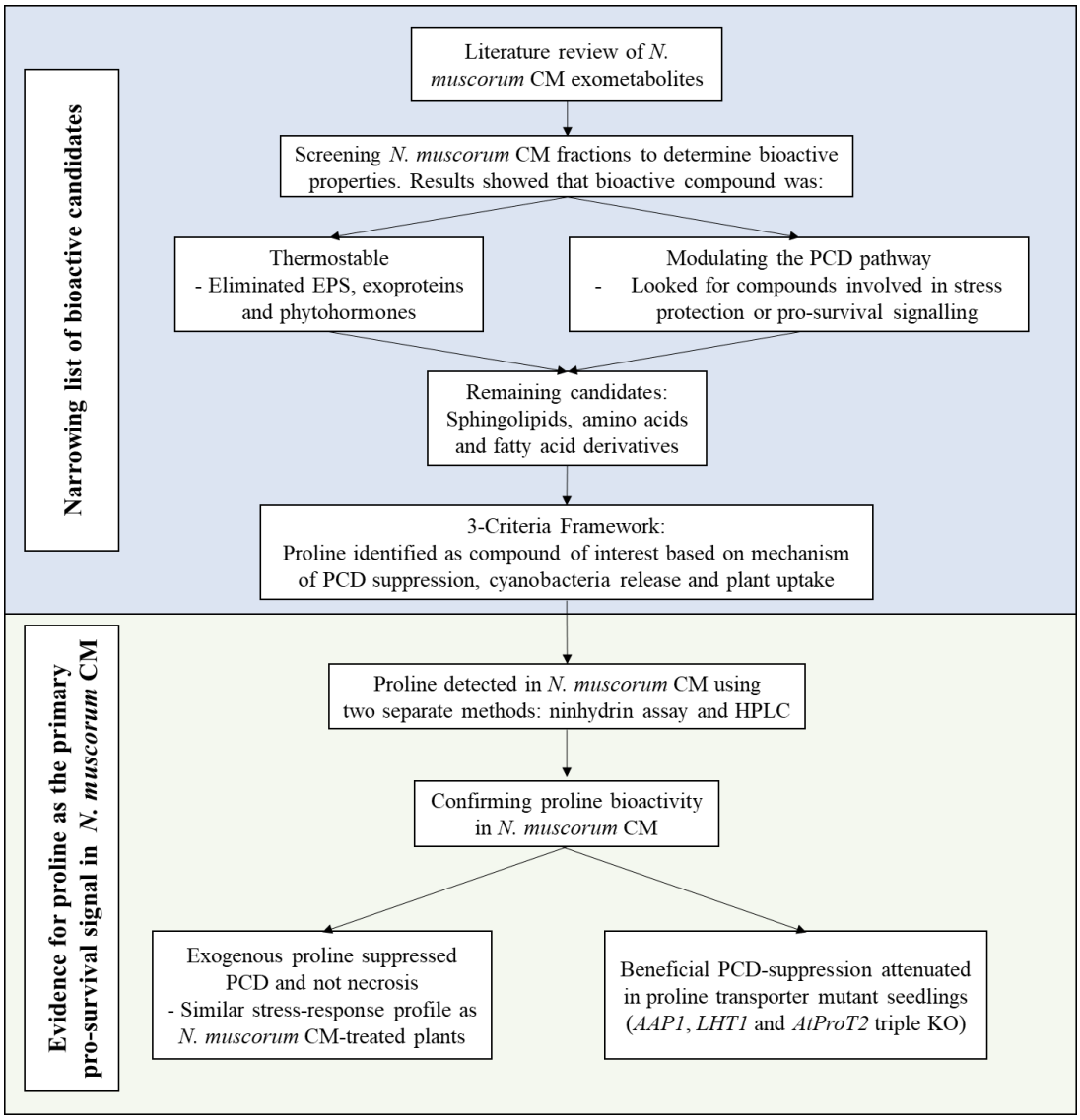


**Figure 2.18** – Workflow for identifying the pro-survival signal in *N. muscorum* CM.

## 2.4.2 Screening *N. muscorum* CM bioactivity

Statistical analysis and linear regression models from the *N. muscorum* CM screening experiment yielded three key takeaways. Firstly, both autoclaved and non-autoclaved *N. muscorum* CM-treated seedlings increased plant stress tolerance by suppressing PCD, showing the main bioactive compound was highly thermostable. Secondly, there was a significant difference ($p$-value of 0.00) between non- and autoclaved fraction treatments, with a 10.3% average difference in PCD levels between all non- and autoclaved treatments (Table 2.5). Autoclaved CM-treated seedlings had consistently higher stress-

induced PCD levels than their non-autoclaved treated counterparts; this trend was consistent across all tested dilutions from 20-100%. The discrepancy in bioactivity strength is likely because of the thermal degradation of thermolabile bioactives as the autoclaving process (121 °C for 15 minutes) attenuates the biological activity of any non-thermostable metabolites. In addition, *N. muscorum* secretes EPS into their growth medium (Mehta and Vaidya 1978) and autoclaving sugars with phosphate (BG11 medium contains high $K_2HPO_4$ concentrations) generates cytotoxic products (Finkelstein and Lankford 1957; Wang and Hsiao 1995). Therefore, the diminished ability of autoclaved *N. muscorum* CM to suppress PCD is likely a combination of two factors: the destruction of additional thermolabile bioactives and leftover cytotoxic byproduct formation from the autoclaving process. Finally, *N. muscorum* CM fractions reduced stress-induced PCD levels in a dose-dependent manner, with negligible changes to necrosis levels across all treatments.

By shifting the viable/PCD threshold and not necrosis, this provided an important clue on how *N. muscorum* CM was enhancing plant stress tolerance. Reape *et al.* (2008) state that modulation of a general stress response alters necrosis levels, while treatments that target the PCD pathway will decrease PCD levels, without affecting necrosis. For example, compared to wild-type lines, peroxidase-overexpressing tobacco lines had greater PCD rates below 55 °C (within the PCD zone) but lower PCD levels above 55 °C (necrotic zone) (Burbridge *et al.* 2007). While this appears contradictory, the results can be understood when viewed from the perspective of the different stress-response phases: stress tolerant, PCD, and necrosis. The peroxidase-overexpressing lines were more sensitive to oxidative damage and thus more prone to PCD at medium stresses. However, their enhanced ROS sensitivity made them more susceptible to high heat stress (> 55 °C) and a larger cell population died by necrosis, causing PCD levels to seemingly fall in proportion (Burbridge *et al.* 2007). This highlights the value of adopting techniques like the RHA that can score multiple cell modes, over single endpoint assays (e.g. TTC, NBT and Evans blue) that only measure cell viability, to generate a more accurate representation of the plant stress response.

To summarise the findings of the screening process, the main PCD-suppressing bioactive compound in *N. muscorum* CM was thermostable and was acting in a dose-dependent manner. It is also likely that additional thermolabile bioactives were acting in synergy

with the main bioactive to suppress PCD; stress-induced PCD levels were constantly lower in non-autoclaved CM treated seedlings than their autoclaved CM-treated counterparts. Lastly, the bioactive compound appeared to be directly affecting the PCD pathway instead of modulating a general stress response that would also affect necrosis levels. These observations were then used as input for the framework to narrow the list of bioactive candidates in *N. muscorum* CM.

### 2.4.3 Building the framework for narrowing the list of bioactive candidates in *N. muscorum* CM

*N. muscorum* secretes a broad assortment of exometabolites into their growth medium that can be grouped into the following categories: exoproteins (Oliveira *et al.* 2015), EPS (Mehta and Vaidya 1978), amino acids (Picossi *et al.* 2005; Pernil *et al.* 2008), phytohormones (Mirsa and Kaushik 1989; Maršálek *et al.* 1992; Karthikeyan *et al.* 2009), phenolics and alkaloids (Abdel-Hafez *et al.* 2015), fatty acids (Abdel-Hafez *et al.* 2015), and sphingolipids (Daly 2013). Table 1.1 provides a brief summary of the different groups and the corresponding studies which they were documented in. Based on the results from the initial *N. muscorum* CM screening, compounds were grouped into orders of importance based on their ability to withstand thermal degradation. This eliminated thermolabile groups such as EPS and exoproteins as primary candidates, while phytohormones were only considered of secondary importance as they undergo significant loss of biological activity upon autoclaving (Sigma-Aldrich 2019).

Alkaloids and phenolics were interesting candidates as they are ROS-scavengers. However, it is challenging to determine if autoclaving would attenuate their bioactive effects as three outcomes (positive, neutral or negative antioxidant activity) can arise from thermal processing (Irina and Mohamed 2012). Diminished antioxidant activity is the most likely outcome because of thermal degradation of the phenolic compounds (Igual *et al.* 2011; Sharma and Gujral 2011). However, studies have also reported instances of elevated phenolic content (Zhang *et al.* 2010; Chandrasekara and Shahidi 2011) and maillard reaction product formation under high temperatures, both leading to stronger antioxidant activity (Kim 2013; Vhangani and Van Wyk 2013). Lastly, autoclaving might not alter overall antioxidant activity because of negligible phenolic turnover and net antioxidant activity (Irina and Mohamed 2012). The *N. muscorum* CM biological matrix is a complex mixture of phenolic compounds that includes *β*-Ionone,

norharman, α-iso-methyl ionone, hexadecane, piperazine, azaperone and isocyclocitral (Abdel-Hafez *et al.* 2015). It is unclear how the unpredictable interactions between the phenolic compounds, e.g. synergistic, neutral or antagonistic, changes when this heterogeneous biological matrix is autoclaved. Further work is needed to characterise how autoclaving influences the ROS-scavenging capacity of *N. muscorum* CM, which is beyond the scope of the thesis.

By filtering candidates based on their thermostability, the remaining candidate groups were amino acids, fatty acid derivatives and LCB sphingolipids. Following this, a simple framework was devised to identify candidates based on three factors: (i) mechanism of PCD suppression, (ii) method of release by cyanobacteria and (iii) method of uptake by plants. Based on the first criterion, proline (Hossain *et al.* 2014a; Rejeb *et al.* 2014a) and sphingolipids (Shi *et al.* 2007; Alden *et al.* 2011) held potential as their bioactive effects have been documented in literature. Nevertheless, existing literature regarding the other two factors made the candidacy for sphingolipids as the pro-survival signal doubtful when contrasted with proline which is a stress-responsive amino acid that accumulates in plants under abiotic and biotic stress (Abrahám *et al.* 2010).

Unlike the common bacterial membrane lipids, sphingolipids are rare and are only found in limited bacterial groups, primarily in the *Sphingomonadales* order and selected members of the *Cytophaga-Flavobacterium-Bacteroidetes* α-proteobacteria group, and δ-, β- and γ -proteobacteria species (Sohlenkamp and Geiger 2016). Nevertheless, Daly (2013) reported the presence of two LCB sphingolipids (sphingosine$^{\Delta 4}$ and phytosphingosine) in *N. muscorum* CM. Both LCBs are pro-apoptotic signals whose exogenous application induced ROS production and PCD in *Arabidopsis* (Shi *et al.* 2007; Alden *et al.* 2011), which contradicts the PCD-suppressing effects noted in *N. muscorum* CM treated plants (Section 2.3.3). Moreover, it is hard to discern the underlying reasons and mechanisms for sphingolipid release by cyanobacteria. Passive diffusion is unlikely as sphingolipids have high molecular weights and are part of the bacteria membrane lipid layer (Sohlenkamp and Geiger 2016).

It is also doubtful that cyanobacteria actively secrete sphingolipids into the extracellular medium; sphingolipids are important secondary messengers in signal transduction and form lipid rafts in eukaryotic cell membranes (Kacprzyk *et al.* 2011). While not much is known about the sphingolipid role in bacterial membranes, the PCD mechanism is highly conserved across plant and animal kingdoms (Watanabe and Lam 2008, 2009). If

cyanobacteria sphingolipids share comparable functions to their eukaryotic counterparts, it is hard to discern reasons for their extracellular secretion, considering the metabolic resources expended on its biosynthesis. Given these points, cell lysis is likely the primary cause for the existence of sphingolipids in *N. muscorum* CM. If this were the case, this would pose an added problem for their role as an extracellular survival signal as sphingolipids inhibit PCD in a dose-dependent manner (Shi *et al.* 2007; Alden *et al.* 2011). A substantial portion of *N. muscorum* cells would have to undergone lysis for the CM to contain the sphingolipid levels needed to induce the dose-dependent PCD-suppressing effects, noted in Section 2.3.3.1. This was evidently not the case as the *N. muscorum* growth curve (Figure 2.4) showed that optical density and chl-*a* concentration increased over the course of nearly four weeks. Moreover, *N. muscorum* cultures could grow continually for at least three months (data not shown) without fresh BG11 supplementation before entering the senescence phase, where mass cell death ensues. Given these points, it was unlikely that sphingolipids were the main bioactive compound of interest in *N. muscorum* CM. Therefore, the analysis henceforth will be restricted to proline and its mechanism of PCD suppression, cyanobacteria release and plant uptake.

#### 2.4.3.1 Criterion One – Mechanism of PCD suppression

Proline is engaged in multiple stress protection roles, ranging from direct intervention to indirect modulation of metabolic routes (Hossain *et al.* 2014a, 2016). Consequently, many studies have described the bioactive effect of exogenous proline in enhancing plant stress resistance. Proline functions as a molecular chaperone and osmolyte, but only has a moderate stabilising effect and protects against denaturing conditions by maintaining osmotic balance and intracellular protein solubility (Auton *et al.* 2011; Liang *et al.* 2013). Proline was also suggested to act as a metal chelator during heavy metal stress (Farago and Mullen 1981; Sharma *et al.* 1998). However, recent work shows that proline is not directly involved in metal chelation but confers protection because of metal-induced water stress (Mishra and Dubey 2006; Sharma and Dietz 2006; Anjum *et al.* 2015). The role of proline in protection against oxidative damage is well documented, and this effect was initially credited to proline's capacity to directly scavenge ROS. This carries significant ramifications for the work in this chapter as ROS signalling is complicit in triggering PCD in animals and plants (Breusegem and Dat 2006; Doyle *et al.* 2010; Wang *et al.* 2013a; Gutiérrez *et al.* 2014). Initial work showed that free proline could scavenge

hydroxyl radicals ($OH^{\cdot}$) (Smirnoff and Cumbes 1989) and singlet oxygen ($^1O_2$) (Alia *et al.* 2001; Matysik *et al.* 2002).

However, recent studies indicate otherwise as the inability of exogenous proline to significantly reduce levels of $^1O_2$ (Signorelli *et al.* 2013), $OH^{\cdot}$ (Natarajan *et al.* 2012), hydrogen peroxide ($H_2O_2$) (Hoque *et al.* 2007; Natarajan *et al.* 2012), and superoxide ($O_2^{-}$) (Hoque *et al.* 2007) indicates that proline does not directly scavenge ROS as originally expected. Instead, a large body of evidence shows that proline functions as an indirect ROS scavenger that upregulates pathway flux through antioxidant and glyoxalase systems (Hoque *et al.* 2008; Kumar and Yadav 2009; Hossain and Fujita 2010; Hossain *et al.* 2010, 2011). Both ROS-detoxification pathways are linked by proline, a central signalling compound that mediates cross-talk between both pathways to defend against oxidative stress (Figure 2.19).

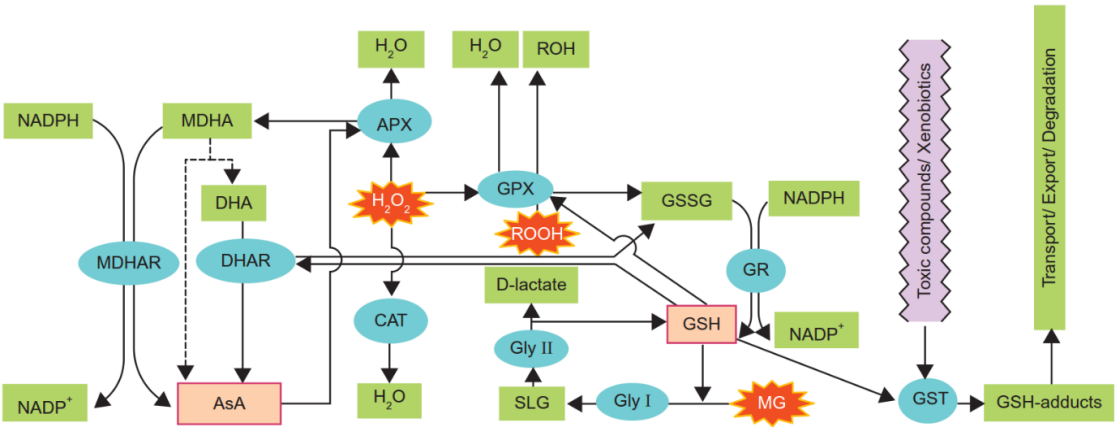


**Figure 2.19** - Cross-talk between the AsA-GSH antioxidative cycle and GSH- based glyoxalase system in plant cells. Dotted lines show non-enzymatic reactions. Image and caption from Hossain *et al.* (2014a).

Stress-induced PCD is triggered by excessive ROS levels and plants rely on several ROS detoxification mechanisms to regulate intracellular ROS levels. ROS are secondary messengers that activate stress-response pathways at low concentrations, but oxidatively damages DNA, proteins, chlorophyll and membranes at excessive levels (Martínez and Araya 2010). Therefore, strict regulation of ROS levels is critical for preserving cell viability; fine-tuning the balance between ROS production and scavenging is carried out by the plant antioxidant defence system comprising an integrated enzymatic and non-enzymatic network (Hasanuzzaman *et al.* 2017). Non-enzymatic antioxidants include

ascorbate (AsA), glutathione (GSH), carotenoids, tocopherols and phenolics, while enzymatic antioxidants include monodehydroascorbate reductase (MDHAR), ascorbate peroxidase (APX), dehydroascorbate reductase (DHAR) and glutathione reductase (GR), which are all units of the influential $H_2O_2$-detoxifying ascorbate-glutathione (Asa-GSH) cycle (Hasanuzzaman *et al.* 2017).

The Asa-GSH cycle works in concert with other antioxidant enzymes such as superoxide dismutase (SOD), catalase (CAT), glutathione peroxidase (GPX), glutathione S-transferase (GST), peroxidase (POX) and guaiacol peroxidase (GPOX) to reduce oxidative damage during stress conditions (Hossain *et al.* 2014a)**.** Exogenous proline strengthens plant stress tolerance by modulating activity of the antioxidant enzymatic network; for example, proline pre-treated mung bean plants under cadmium (Hossain *et al.* 2010) and salt (Hossain *et al.* 2011) stress had upregulated APX, DHAR, GR, GST, GPX, and CAT activity and less oxidative damage compared to untreated controls. Exogenous proline can also regulate levels of non-enzymatic antioxidants such as AsA, GSH, phenolics and tocopherol (Ali *et al.* 2013; Rasheed *et al.* 2014; Shahid *et al.* 2014). Evidence also suggests that the proline-linked pentose phosphate pathway stimulates stress-induced phenolic biosynthesis by driving flux through shikimate and phenylpropanoid pathways (Shetty 1997; Shetty and Wahlqvist 2004).

Apart from upregulation of the plant antioxidant system, ROS detoxification is also closely associated with the glyoxalase system, the methylglyoxal (MG) detoxification pathway (Kaur *et al.* 2015; Hoque *et al.* 2016). The plant glyoxalase pathway was initially presumed to be composed of glyoxalase I (Gly I) and II (Gly II). Gly I catalyses the reaction between MG and GSH to form S-D-lactoylglutathione, which Gly II converts into D-lactate, regenerating GSH in the process (Hossain *et al.* 2014a) as illustrated in Figure 2.19. However, a unique glyoxalase III (Gly III) was recently identified in monocots, dicots, lycopods, gymnosperm and bryophytes, which converts MG directly into D-lactate in a single step without GSH (Ghosh *et al.* 2016). Like ROS, MG is an important signalling molecule at low concentrations, but is cytotoxic at high concentrations (Hoque *et al.* 2016). At basal levels, MG is a secondary messenger that regulates stomata conductance and $K^+$ channels, ROS production, cytosolic $Ca^{2+}$ levels, and expression of ABA-dependent stress-responsive genes (Hoque *et al.* 2016). However, stress exposure induces MG overaccumulation and disrupts metabolic systems by

inhibiting cell division and growth, reacting with proteins and nucleic acids to form advanced glycation end products (AGEs) and inactivating the antioxidant defence system (Hoque *et al.* 2010, 2012, 2016). Stress-induced MG accumulation elevates ROS levels either directly by the cytotoxic presence of MG itself, which causes dicarbonyl stress, or indirectly by AGEs formation which disrupts protein and genomic integrity, causing genotoxicity (Hoque *et al.* 2016).

Substantial cross-talk exist between the glyoxalase and antioxidant defence system and many studies have demonstrated the direct effect of exogenous proline supplementation in ROS detoxification by the glyoxalase system. For example, pre-treatment with exogenous proline increased the stress tolerance of mung beans to salt (Hossain and Fujita 2010; Hossain *et al.* 2011) and cadmium (Hossain *et al.* 2010), tobacco Bright Yellow-2 suspension cells against salt stress (Hoque *et al.* 2008) and *Camellia sinensis* (L.) O. Kuntze plants under chilling stress (Kumar and Yadav 2009). Despite the broad spectrum of plant species and stress types, proline supplementation exerted a global effect across all the studies by stimulating flux through the antioxidant defence and MG detoxification systems; treated plants displayed enhanced stress resistance against oxidative damage in the form of diminished intracellular $H_2O_2$, lipid peroxidation and protein carbonylation levels (Hoque *et al.* 2008; Kumar and Yadav 2009; Hossain and Fujita 2010; Hossain *et al.* 2010, 2011). In addition, exogenous proline directly protects GSH-associated enzyme activities, such as antioxidants (GST and GR) and glyoxalase (Gly II) by inhibiting oxidation of protein thiol groups and maintaining optimal thiol/disulfide redox ratios (Kumar and Yadav 2009). Both ROS and MG detoxification pathways are linked by GSH, a redox buffer that modulates the stress acclimation response (Hossain *et al.* 2016). GSH is one of the most abundant non-protein thiols in plants and it plays a key role in ROS detoxification, either as a direct ROS scavenger or indirectly by being a key substrate or reducing agent to enzymes in the AsA-GSH cycle (GPX, GST and DHAR) and glyoxalase pathways (Hossain and Fujita 2010; Hossain *et al.* 2011). By increasing Gly I and II activities, proline treatment enhances GSH regeneration through the glyoxalase system to lessen the stress-induced oxidative load in plant cells (Hossain and Fujita 2010).

Given these points, there is compelling evidence that proline can lessen stress-induced PCD levels by modulating ROS levels through cross-talk between the antioxidant AsA-GSH cycle and GSH-based glyoxalase system. This is relevant to the framework as ROS

is an early trigger for activating the PCD pathway in plants; a PCD-inducing stress signal generates an intracellular $Ca^{2+}$ spike and induces mitochondrial PTP formation (Yang *et al.* 1997). The subsequent cyt *c* release into the cytoplasm disrupts the mitochondrial ETC and generates a ROS-generating feedback loop that augments the initial PCD-inducing stress signal (Jabs 1999). To summarise, proline plays an integral dual role in reducing MG and stimulating GSH-based ROS detoxification, offering a promising mechanism of action on how proline can reduce stress-induced PCD levels in treated *Arabidopsis* seedlings. This has significance as the major bioactive compound in *N. muscorum* CM was suppressing PCD and not necrosis, strongly indicating that it was directly modulating the PCD pathway, instead of regulating a general stress response that would affect necrosis levels (Reape *et al.* 2008).

#### 2.4.3.2 Criterion Two - Mechanism of cyanobacteria release

The route of amino acid release has not been fully elucidated in cyanobacteria but a strong body of evidence indicates that spontaneous diffusion is the primary mechanism (Montesinos *et al.* 1995; Picossi *et al.* 2005; Pernil *et al.* 2008). Gram-negative soil bacteria, of which cyanobacteria belong to, are known to release compatible solutes (amino acids and low molecular carbohydrates) into the extracellular environment in proportion to the magnitude of dilution (Halverson *et al.* 2000). For example, diluted *Pseudomonas fluorescens* cultures release 22-26% of their amino acid pool into the CM to avoid cell lysis as the sudden water potential increase affects membrane integrity (Halverson *et al.* 2000). Conversely, Gram-positive bacteria have stronger cell walls and can therefore withstand higher turgor pressure and dilution stress (Harris 1981; Halverson *et al.* 2000).

A solute has to be sufficiently hydrophobic to cross the bacteria lipid bilayer (Krämer 1994) and studies with *Streptococcus cremoris* show a linear correlation between the rate constants of passive diffusion against the hydrophobicity of the amino acid side chain (Driessen *et al.* 1987). Proline is considered a neutral amino acid but its hydrophobic side-chain enables it to spontaneously diffuse through the cell membrane (Picossi *et al.* 2005; Pernil *et al.* 2008). To recapture passively leaked amino acids, *N. muscorum* can import a wide range of extracellular amino acids by its family of ABC-type transporters: N-I, N-II, N-III and Bgt (Pernil *et al.* 2015). The transporters have varying affinities and substrate specificity; for example, N-I and N-III transports hydrophobic amino acids, but also

imports glutamine and glutamate (Pernil *et al.* 2015). Despite their overlapping functions, N-III has a preference for importing glycine, while N-I has a strong affinity for proline (Pernil *et al.* 2015). In contrast, N-II is an ABC-type uptake transporter for acidic and neutral polar amino acids (Montesinos *et al.* 1995), while Bgt imports basic amino acids into the cell (Pernil *et al.* 2008).

The combined activity of N-I, N-II and Bgt transporters accounts for more than 98% activity of amino acid uptake in *N. muscorum* (Pernil *et al.* 2008). Thus, mutant *N. muscorum* strains with impaired neutral amino acid transport systems are unable to recapture passively leaked hydrophobic amino acids; consequently, high concentrations of proline, alanine, glycine, isoleucine, leucine, phenylalanine, tyrosine, and valine were present in the growth medium of these mutant strains (Montesinos *et al.* 1995; Picossi *et al.* 2005; Pernil *et al.* 2008). This was reflected in CSX60-R10, the double *natA bgtA* mutant strain with impaired N-1, N-II and Bgt transporters, which released 105.2 μM of alanine in the extracellualr medium after just 48 hours of incubation time in BG11 (Pernil *et al.* 2008). Cell lysis was not the primary mechanism of release as extracellular amino acid concentrations did not correlate with the most abundant intracellular amino acid *(*5-20 mM glutamate) (Picossi *et al.* 2005). In summary, the hydrophobicity of proline enables spontaneous membrane diffusion into the extracellular medium, and cellular lysis is not the primary method of amino acid release. Thus, the evidence strongly points towards passive leakage as the source of extracellular proline in *N. muscorum* CM.

#### 2.4.3.3 Criterion Three - Mechanism of uptake by plants

Plants import amino acids from their surroundings as a source of nitrogen either by passive or active transport. Passive transport relies on diffusion across carriers and channel pores while active transport occurs against the concentration gradient using proton-coupled transporters (Lee *et al.* 2007). Plant transporters involved in proline uptake belong to the amino acid transporter (ATF) or amino acid/auxin permease (AAAP) family. From this ATF/AAAP family, three subfamilies are involved in transporting proline with varying substrate selectivity and affinity (Lehmann *et al.* 2010). The first subfamily is amino acid permease (AAP), which are expressed in the *Arabidopsis* root epidermis, root hairs, and root tips of primary and lateral roots (Lee *et al.* 2007). AAP1 mediates proton-coupled uptake of uncharged amino acids such as glutamate, histidine and neutral amino acids (proline, alanine, glycine, isoleucine, leucine, serine, threonine

and valine) into *Arabidopsis* roots (Lee *et al.* 2007; Lehmann *et al.* 2010). The strong AAP1 expression throughout the root cap and epidermis layer facilitates the transfer of external amino acids into the vascular system for long-distance transport (Lee *et al.* 2007). AAP1 was initially characterised as a low-affinity transport system but was recently shown to be capable of importing amino acids at typical soil levels of 30 μM (Perchlik *et al.* 2014). The second subfamily involved in proline transport is lysine-histidine transporter (*LHT*). In *Arabidopsis*, LHT1 is a high-affinity transporter, i.e. imports solutes even at low concentrations, and transports histidine, acidic and neutral amino acids (including proline) (Hirner *et al.* 2006). The LHT1 expression pattern indicates its two key roles in plant growth; during the early developmental stage, LHT1 is expressed in the rhizodermis of emerging and lateral roots, in agreement with its role in amino acids uptake from soil (Hirner *et al.* 2006). In later stages, LHT1 is expressed throughout the root epidermis and tips, leaf mesophyll, stem, petals and sepals. This is consistent with its second function which is supplying leaf mesophyll with xylem-derived amino acids (Hirner *et al.* 2006).

In contrast to the other two subfamilies with broad substrate specificity, the third proline transporter (ProT) subfamily only imports proline and no other proteinogenic amino acids (Lehmann *et al.* 2010). ProTs from different plant species also transport stress-induced compounds; for example, ProTs from *Arabidopsis* (Breitkreuz *et al.* 1999), *Solanum lycopersicum* (Schwacke *et al.* 1999) and *Avicennia marina* (Waditee *et al.* 2002) import glycine betaine, an osmolyte involved in mitigating water stress (Lehmann *et al.* 2010). Moreover, ProTs from *Arabidopsis* (Grallath *et al.* 2005) and *S. lycopersicum* (Schwacke *et al.* 1999) also transport $\gamma$-Aminobutyric acid, albeit at lower affinities compared to proline uptake. On the whole, the involvement of these amino acid transporter subfamilies (two general and one proline-specific) present a viable mechanism on how proline uptake from *N. muscorum* CM into *Arabidopsis* root hairs can occur.

#### 2.4.3.4 Framework summary

The framework indicated that out of the remaining thermostable compounds (amino acids, fatty acid derivatives and sphingolipids), proline was most likely the candidate of interest. By examining the three variables of the framework, a working paradigm emerged on how cyanobacteria-derived proline can prime the stress response in heat-stressed *Arabidopsis* seedlings (Table 2.13). Firstly, proline can indirectly increase ROS

scavenging and suppress downstream PCD-inducing signals through stimulation of the closely intertwined glyoxalase and antioxidant defence systems (Hossain *et al.* 2014a; Rejeb *et al.* 2014a; Hossain *et al.* 2016). This would account for the lowered PCD levels observed in *N. muscorum* CM treated root hairs as proline is specifically affecting the PCD signalling pathway instead of mounting a general stress response that would also shift necrosis levels (Reape *et al.* 2008). Moreover, the hydrophobicity of the proline amino acid side-chain enables the spontaneous diffusion through the cyanobacteria membrane and into the growth medium (Picossi *et al.* 2005; Pernil *et al.* 2008). Finally, plants have three amino acid transporter sub-families (two general and one proline-specific) that can import proline from their surroundings into plant roots (Lehmann *et al.* 2010). On balance, these findings combine to form a viable hypothesis of how *Arabidopsis* seedlings can assimilate proline from *N. muscorum* CM as a priming step before stress onset.

**Table 2.13** – Framework summary for identification of the bioactive compound(s) in *N. muscorum* CM.

| Criteria | Possible mechanisms | Documented roles of proline in literature |
|---|---|---|
| **1 -** Mechanism of PCD suppression | Targets the PCD pathway | Reducing ROS levels through cross-talk between the antioxidant AsA-GSH cycle and GSH-based glyoxalase system |
| **2 -** Method of cyanobacteria release | Accidental (cell lysis or passive diffusion) or active secretion | Spontaneous membrane diffusion due to hydrophobicity of proline |
| **3 -** Method of plant uptake | Active transport or membrane diffusion | Active transport by 3 amino acid transporter subfamilies: two general (AAP and LHT) and one proline-specific (ProT) |

## 2.4.4 Proline detection in *N. muscorum CM*

Proline was identified in *N. muscorum* CM using two methods: the ninhydrin assay and reverse-phase HPLC. Using the ninhydrin assay, proline was measured in autoclaved and non-autoclaved CM at concentrations of 1.94 µM and 1.83 µM, respectively. The ninhydrin assay is a colorimetric method for quantifying proline as ninhydrin produces a distinctive yellow chromophore when reacting with proline, unlike the other proteinogenic amino acids that generates a purple anion known as the Ruhemann's complex (Friedman 2004). Proline, and its derivative hydroxyproline, do not produce the

Ruhemann's complex, as their imino group (-NH) is bound to the five-membered ring and are not free to react with ninhydrin, like the other free $\alpha$-amino (-$NH_2$) groups present in the other amino acids (Friedman 2004). For additional evidence, a HPLC method was developed for detecting proline and the other amino acids based on protocols by Heinrikson and Meredith (1984) and Kwanyuen and Burton (2010). Nineteen amino acids, including proline, were reported in the *N. muscorum* extracellular filtrates but the published method by Pernil *et al.* (2008) lacked key details that limited its use for reproducibility. Firstly, the authors did not disclose the mobile phase gradient used for peak separation, and chromatograms of the identified amino acids in *N. muscorum* CM were absent from the paper. Moreover, the study did not specify the sample injection volumes, nor the concentration factor of the lyophilized *N. muscorum* CM samples; this can produce significant downstream problems as it would be easy to overload the column or cause broadened peaks. Lastly, the *N. muscorum* CM and amino acid standards were directly added to the derivatizing solution containing ethanol, $H_2O$, triethanolamine and PITC. This diverges from other protocols (Heinrikson and Meredith 1984; Kwanyuen and Burton 2010) as PITC reacts with amino acids to form PTC-amino acid under alkaline conditions and samples need to be neutralised and dried before derivatization to ensure that all the HCl is evaporated (Walker and Mills 1995). Elimination of all HCl also has an added benefit of eliminating an unidentified peak that elutes after histidine (Heinrikson and Meredith 1984).

To resolve these issues, a series of chromatographic parameters (injection volume, PITC derivatization mixture ratio, *N. muscorum* CM sample volume and impact of guard column) were examined to develop a method for identifying the amino acids in *N. muscorum* CM. Larger injection volumes, up to 15 µL, were suited for downstream analysis as a higher signal-to-noise ratio was achieved, without loss of peak resolution between proline and alanine, which remained above the 1.5 threshold. However, minor shifts in the retention times of both peaks in line with increasing injection volumes were observed, perhaps because of an insufficient equilibration period for the column to return to its initial gradient composition. Alternatively, increasing sample volumes can affect retention times; sample molecules need to be present in a tight, concentrated band at the column head for identical elution times and are affected when large injection volumes are utilised (Ren *et al.* 2013). Next, the impact of increasing the ratio of the PITC derivatization mixture was examined. PITC reacts in a 1:1 ratio with amino acids to form

PTC-amino acids but PITC can also form side-reactions with the $\alpha$-amino group of proteins (Jacobs and Niall 1975). This poses a problem as *N. muscorum* already secretes 139 exoproteins into the extracellular filtrate (Oliveira *et al.* 2015), which is further aggravated if the release of intracellular proteins from cell lysis is taken into account.

As Pernil *et al.* (2008) did not divulge the original concentration factor of the *N. muscorum* CM samples, the impact of PITC on peak resolution had to be assessed to ensure that sufficient PITC was being used to drive the derivatization reaction to completion as amino acids have to contend with all other amine group-containing exometabolites. However, raising the PITC concentration severely alters the sample drying times as PITC has a high boiling point of 221 °C. Samples incubated with a 1X PITC derivatization ratio dry under 2 hours, while a 12X sample mix takes around three days, which substantially affects peak resolution. Therefore, a balance had to be struck between the PITC derivatization mixture ratio and drying times to ensure sufficient peak separation and resolution. Previously, Heinrikson and Meredith (1984) reported that higher PITC concentration usage did not significantly influence downstream analysis. The results in this chapter agree with the original findings but only to a certain extent; proline peak areas remained stable even up to a 12-fold increase in the PITC derivatization mixture, apart from the sudden decline in the 2-fold increase dataset. However, alanine peak areas degraded linearly ($R^2$: 0.9363) in a dose-dependent manner as PITC concentrations were raised. It is unclear why this effect takes place and if it extends to the other amino acids. For these reasons, the PITC derivatization mixture was maintained at its original concentrations as it appears sufficient to drive the derivatization reaction to completion, without compromising on drying times.

Using these chromatographic parameters, proline was detected in a 5-fold concentrated *N. muscorum* CM sample (200 µL *N. muscorum* CM, dried and resuspended in 40 µL 0.1 M HCl) and its identity confirmed by spiking *N. muscorum* CM of varying volume (80, 100, 150 and 200 µL) with equal amounts of proline. Proline eluted at the 11.8-minute mark across all the non-spiked and spiked *N. muscorum* CM samples, thus verifying its presence in *N. muscorum* extracellular filtrate. By varying *N. muscorum* CM sample volume, the proline peak area was hypothesised to increase linearly as all samples were spiked with identical proline concentrations. However, a clear effect was not observed because of severe interferences from the sample matrix; *N. muscorum* CM contains a vast array of exometabolites that was interfering with the precision of the method as the peak

area of proline did not increase linearly ($R^2 = 0.0659$) across increasing *N. muscorum* CM sample volumes. This was also reflected in the incomplete spike recoveries noted in the proline-spiked 100 µL CM dataset which had a smaller peak area than the proline control, despite receiving no additional *N. muscorum* CM to supplement the proline levels.

Lastly, the guard column was removed to improve peak sharpness and the separation of the amino acid standard mix. All the results reported so far were performed with a guard column to avoid overloading the main column and to prolong the shelf-life of its $C_{18}$ stationary phase as rapid column deterioration tends to occur with PITC procedures (Walker and Mills 1995). However, the guard column that was being used had significantly different configurations from the original method employed by Pernil *et al.* (2008) owing to the lack of resources to purchase one. The guard column used in this study had a different particle size (3.5 µm) from the main column (5 µm) and a longer length (75 mm) than the original guard column (40 mm) operated by Pernil *et al.* (2008). By removing the guard column, an improved chromatogram was achieved as reducing the run-time culminated in less peak-broadening and shaper peaks, as represented in Figure 2.11. While some peaks could still not be fully resolved (e.g. Asn/Gly and Ile/Leu), this study was primarily interested with proline quantification and only the qualitative assessment of the other amino acids. However, elimination of the guard column had an unexpected effect of decreasing the column efficiency; this affected *N. muscorum* CM peak separation which was already poor in the first place as the resolution for some amino acid peaks were barely above the 1.5 threshold. An efficient column can separate more individual analytes with better resolution and by shortening the overall column length, the amino acid peaks were scarcely distinguishable from the noisy baseline as a result of the analyte complexity in *N. muscorum* CM. Therefore, the injection volume was temporarily raised to 70 µL to enhance the signal-to-noise ratio, i.e. to make the amino acid peaks more prominent from the baseline. With this final method, the following amino acids were detected in *N. muscorum* CM: proline, glutamic acid, serine, asparagine/glycine, glutamine, histidine, arginine, threonine, alanine, tyrosine, valine, methionine, isoleucine/leucine, phenylalanine, tryptophan, lysine, and likely, aspartic acid and cysteine.

Quantification of proline using a proline standard curve as a reference found it to be 11.2 µM, which was higher than the original values measured in the ninhydrin assay, but this was largely a result of different *N. muscorum* CM samples being analysed. The original

*N. muscorum* CM properties used in the ninhydrin assay were $OD_{730}$ (1.17), chl-*a* (14.14 µg/mL), carotenoid (3 µg/mL), while the properties of the *N. muscorum* CM batch in the HPLC analysis were $OD_{730}$ (1.67), chl-*a* (33.19 µg/mL) and carotenoid (9.77 µg/mL). Thus, the elevated proline levels in HPLC analysis were primarily a result of using older cultures, which had an approximate 2 to 3-fold increase in chl-*a* and carotenoid levels, respectively. The original *N. muscorum* batch was no longer at hand as there was a time-gap of 1.5 years between the experiments, and older cultures in the deceleration phase were specifically chosen for better amino acid detection sensitivity as culture age significantly influences the composition of cyanobacteria exometabolites (Volk 2007).

### 2.4.5 Confirmation of proline as the main bioactive compound of interest in *N. muscorum* CM

By supplementing seedlings with exogenous proline at concentrations measured in *N. muscorum* CM, further evidence was obtained for proline as the pro-survival signal. Exogenous proline elicited a remarkably similar stress response profile to *N. muscorum* CM treatment by increasing viability levels by suppressing PCD, but not necrosis. Autoclaving proline did not attenuate its PCD suppressing effects and statistical analysis revealed no significant difference in PCD levels between *Arabidopsis* seedlings treated with exogenous non-autoclaved proline, confirming that proline was thermostable and responsible for the stress-priming effect in treated seedlings. Nevertheless, exogenous proline did not suppress PCD in a dose-dependent manner as *N. muscorum* CM fractions did, at least not in the current tested range. It is likely that proline acts in synergy with the accompanying bioactive exometabolites in *N. muscorum* CM to exert a stronger PCD-suppressing effect than individual proline treatments alone.

The ability of exogenous proline to inhibit stress-induced PCD levels in wild-type seedlings offered preliminary evidence for its role as a pro-survival signal, but further investigations using proline impaired transporter mutants were required. A previous study determined that wild-type *Arabidopsis* roots could import amino acid levels as low as 2 µM (Svennerstam *et al.* 2011). In this experimental set-up, the stress response of three mutants was evaluated across exogenous proline treatment at low (1 µM), medium (2-5 µM) and high (100 µM) proline levels and 100% *N. muscorum* CM, compared to wild-type seedlings. The performance of the mutants was assessed over a proline gradient as all three transporter families have varying proline affinities. AAP1 was first characterised

as a low-affinity transporter (Svennerstam *et al.* 2011) but Perchlik *et al.* (2014) showed that AAP1 could import amino acids at typical soil levels of 30 µM and was not merely limited to uptake at high concentrations; 2-week-old *aap1* mutants had significantly ($p$<0.05) reduced uptake of proline, alanine, glutamine, serine and glutamate compared to wild-type plants, ranging from 10-43% depending on the amino acid in question (Perchlik *et al.* 2014). In comparison, LHT1 is a broad-specificity, high-affinity transporter that imports histidine, acidic and neutral amino acids (Lehmann *et al.* 2010).

Lastly, ProT are proline-specific transporters and three members of this family have been characterised in *Arabidopsis* (AtProT1, AtProT2 and AtProT3) (Lehmann *et al.* 2011). All three AtProTs members are localised on the plasma membrane but are expressed differently throughout the plant. AtProT1 is expressed in the phloem throughout the whole plants, and is present in the vascular tissue of leaves, petioles, roots, flowers, siliques, and stems (Rentsch *et al.* 1996). However, AtProT1 expression is very weak in root tissues as it was not present in root tips and was barely detected in emerging lateral roots (Rentsch *et al.* 1996). On the other hand, AtProT2 expression is predominantly found in the root cortex and epidermis (root hairs, root tip and root cap), while AtProT3 expression is only found in the epidermal leaf cells (Grallath *et al.* 2005). Heterologous expression in *Saccharomyces cerevisiae* showed that ProT transporters had the highest proline affinity out of the three family groups, e.g. AtProT1 (427 µM), AtProT2 (500 µM), AtProT3 (999 µM), AAP1 (60 µM) and LHT1 (0.5 µM) (Lehmann *et al.* 2010). Nevertheless, the uptake studies were done in heterologous expression systems, which might not necessarily reflect the same kinetic properties of actual *in planta* transporters. By comparing the mutant lines against wild-type seedlings across the proline gradient, we can determine if proline is the major bioactive candidate in *N. muscorum* CM, while simultaneously discerning the individual roles of each transporters in proline uptake during stress application.

#### 2.4.5.1 Proline impaired mutants had higher PCD levels compared to wild-type seedlings

All three mutants exhibited a distinctive stress response profile from wild-type seedlings under identical proline doses. Under low-to-medium proline doses, wild-type seedlings had lower stress-induced PCD levels, but this priming effect was lost in the mutant lines, notably in *aap1* and *lht1* mutants. This was supported by statistical analysis as all mutant lines had no significant variations ($p$>0.05) in PCD levels compared to their respective

BG11 controls. Considering the diminished capacity of mutant seedlings to import proline and their subsequently higher PCD levels, this offered further evidence for proline as the pro-survival signal. Nevertheless, it must be acknowledged that stressed plants can raise internal proline levels by upregulating proline biosynthesis instead of relying on external proline uptake. However, prokaryotic studies show that proline uptake is favoured over biosynthesis if the osmolyte is already available (Roesser and Müller 2001). Similar discoveries have been hinted in plants; osmotic stressed maize (Verslues and Sharp 1999) and salt stressed barley roots (Ueda *et al.* 2007) have elevated proline levels, despite low proline biosynthetic activity in root tips. Elevated HvProT expression and minimal pyrroline-5-carboxylate synthetase (P5CS1) activity in salt-stressed barley root cap cells further underscore this phenomenon (Ueda *et al.* 2001). P5CS1 is the key enzyme of the proline biosynthetic cycle that converts glutamine into glutamic semialdehyde; this intermediate cyclizes into Δ1-pyrroline-5-carboxlyate (P5C), the precursor to proline. Furthermore, plant growth is suspended during stress onset and is only resumed when stress is lifted (Kavi Kishor and Sreenivasulu 2014) as the stress-acclimation response consumes significant energetic resources to achieve a new metabolic steady state, e.g. osmolyte biosynthesis, ROS and methylglyoxal detoxification systems (Tausz *et al.* 2004). If stressed plants can freely import exogenous proline from its surroundings, they can channel more resources towards other stress-responsive pathways for improved survival rates. Collectively, this evidence implies that plants also prefer importing proline, if readily available, instead of biosynthesis during stress onset (Verslues and Sharma 2010). Hence, the results here offer further evidence for proline as the main bioactive compound as its beneficial PCD-suppressing effects was noted in wild-type seedlings but lost in the proline impaired transporter mutant lines.

#### 2.4.5.2 No strong phenotype for *atprot* triple (*atprot1-1::atprot2-3::atprot3-2*) knockout mutant

Although all three mutants did not respond to the PCD-suppressing effects of proline, a distinct stress-response profile was observed between the general amino acid transporter (*lht1* and *aap1*) and *atprot* triple knockout mutants. The *atprot* triple knockout mutant displayed a stress phenotype more reminiscent of wild-type seedlings than their fellow mutant lines. On the surface, this may appear surprising as the AtProT family has the highest proline affinity for proline and does not transport other proteinogenic amino acids, i.e. it does not suffer from substrate competition as the other general amino acid

transporters do (Lehmann *et al.* 2011). Moreover, ProT expression is correlated with osmotic stress and elevated ProT expression has been detected across multiple species such as *Arabidopsis* (ProT2), mangrove (AmT1, 2 and 3) and barley (HvProT) plants, in response to proline accumulation during salt stress (Lehmann *et al.* 2011). Taken together, the *atprot* triple knockout mutant was initially presumed to be the most stress-susceptible line out of all the mutants, considering how three genes were being knocked out. However, the results proved contrary as the *atprot* triple knockout mutant had highest resistance to heat shock out of the examined mutant lines. While this appears confounding, the results coincide with the past study by Lehmann *et al.* (2011) who showed that single, double and triple *atprot* knockout mutants did not express strong phenotypical differences and proline levels compared to wild-type seedlings under stress exposure. No appreciable changes were identified between the shoot size, root length and flowering times of the mutants compared to their wild-type counterparts, prompting the authors to suggest that compensation by other root-localised proline transporters was responsible for the phenotype overlap between wild-type and *atprot* knockout mutants (Lehmann *et al.* 2011). The results here also reflect this phenomenon as significant deviations in PCD levels compared to wild-type seedlings only arose when either LHT1 or AAP1 was inactivated. Phloem-localised AtProT1 is responsible for long-distance proline translocation and can be replaced by the AAP1 transporter, while AtProT2 is found in root epidermis (including root hairs) and imports extracellular proline into the root cortex, and AtProT2 can be substituted by both LHT1 and AAP1 transporters. Consequently, the results shown here reinforce past findings of the functional overlap shared between ProT and other proline transporters (as summarised in Table 2.14).

**Table 2.14** – Summary of *Arabidopsis* amino acid transporters that transport proline. Information adapted from Rentsch *et al.* (1996), Grallath *et al.* (2005); Hirner *et al.* (2006), Lee *et al.* (2007), Lehmann *et al.* (2011) and Perchlik *et al.* (2014).

**Key:** '+' indicates functionality confirmed in the literature. '-' indicates no functionality confirmed.

| Transporter | Localisation | Transports | Function | | |
|---|---|---|---|---|---|
| | | | Importing extracellular amino acids | Long-distance amino acid phloem transport | Supplying leaf epidermal or mesophyll cells with amino acids |
| AAP1 | Strong expression in phloem, root epidermis, root hairs, and primary and lateral root tips | Glutamate, histidine and neutral amino acids | + | + | - |
| LHT1 | Rhizodermis of emerging and lateral roots, root epidermis and tips, leaf mesophyll, stem, petals and sepals. | Histidine, acidic and neutral amino acids | + | - | + |
| AtProT1 | Expressed in the phloem. Also present in the vascular tissue of leaves, petioles, roots, flowers, siliques, and stems. Weak expression in root tissues | Proline | - | + | - |
| AtProT2 | Root cortex and epidermis (root hairs, root tip and root cap) | Proline | + | - | - |
| AtProT3 | Epidermal leaf cells | Proline | - | - | + |

### 2.4.5.3 Similar stress phenotype shared by general amino acid mutant transporters

It is unclear why *lht1* and *aap1* mutants had a greater susceptibility to heat shock, considering how they share overlapping functions with members of the *atprot* family (Table 2.14). Without further long-term studies, it would be difficult to identify the mechanisms underlying their differences, but existing literature suggest three causes: the impaired capacity to import proline into root cells (*aap1* and *lht1* mutants) (Lee *et al.* 2007; Perchlik *et al.* 2014), ineffectiveness in cycling amino acids across plant tissue (*lht1* mutant) (Hirner *et al.* 2006), and the inability to transport proline over long-distances to leaves and other organs (*aap1* mutant) (Lee *et al.* 2007; Perchlik *et al.* 2014). For in-depth reviews on each subject, the reader is encouraged to refer to the cited studies above. The following sections offer a brief summary of each scenario and commentary on how they might relate to the trends noted here.

#### *2.4.5.3.1 aap1 and lht1 mutants have an impaired ability to import proline into root cells*

A potential cause for the comparable stress phenotype exhibited by *lht1* and *aap1* mutants is their severely impaired ability to import proline into roots. As mentioned in Section 2.4.5.1, stressed plants favour importing proline instead of utilising the biosynthetic route (Verslues and Sharma 2010). This might account for the higher stress-induced PCD levels noted in the *lht1* and *aap1* mutants, but not in the *atprot* triple knockout mutant. AAP1 and LHT1 transporters are localised to the plasma membrane of root tissues; AAP1 is preferentially expressed in vascular tissue, and LHT1 in non-vascular tissue (Hirner *et al.* 2006). AAP1 is strongly expressed in the root epidermis (hairless and hair-bearing epidermal cells) and throughout the primary and secondary root tips (Lee *et al.* 2007). Conversely, LHT1 is expressed across a broader tissue range such as roots, leaves, stems, flowers, and siliques, reflecting its more diverse roles: expression in root tips (rhizodermis of emerging and lateral roots) imports extracellular amino acid, while localisation in leaf mesophyll and epidermis cells retrieves amino acids from the apoplasm into leaf cells (Hirner *et al.* 2006). Amino acid uptake studies have highlighted the influence of both transporters; for example, *aap1* mutants experienced up to a 43% reduction in uptake rates, depending on the investigated amino acid (Perchlik *et al.* 2014). This reflects AAP1 expression within the root epidermis as the wide surface area of root hairs enables the efficient import of extracellular amino acids into roots (Lee *et al.* 2007; Perchlik *et al.*

2014). A comparable situation is seen in LHT1 transporters as *lht1* mutants displayed up to an 80% decline in neutral and acidic amino acid uptake (Hirner *et al.* 2006). In contrast, Lehmann *et al.* (2011) found similar proline levels between the salt stressed leaves of the *atprot* triple knockout mutant and wild-type seedlings as proline uptake was compensated by other root-localised transporters (LHT1 and AAP1). Collectively, these results suggest that root-mediated amino acid uptake may play a bigger role in stress tolerance than initially thought.

#### *2.4.5.3.2 lht1 mutant - impaired ability to partition amino acids across plant tissue*

Apart from importing extracellular amino acids, LHT1 transporters play a crucial role in partitioning amino acid across plant tissues. Hirner *et al.* (2006) demonstrated that *lht1* mutant plants accumulated high amino acids levels in the apoplast and displayed retarded growth even in stress absence. They attributed the retarded growth phenotype to the diminished capacity to import amino acids from the apoplasm into leaf mesophyll cells; a 10-fold reduction in uptake of proline was noted in *lht1* mutant mesophyll protoplasts compared to their wild-type counterparts. Subsequent LHT1 re-expression in vegetative tissues successfully reversed its growth defects, emphasising the relevance of LHT1-mediated amino acid partitioning across plant tissues for efficient N use and plant growth. Building on this work, the results here suggest that the importance of LHT1-mediated amino acid cycling might extend to stress tolerance. Proline cycling is an essential aspect in the stress recovery response as the failure to partition amino acids efficiently throughout plant tissues disrupts proline homeostasis. Proline accumulates during stress onset for protection, but is degraded in meristematic tissues (root tips, shoot apex, lateral buds and inflorescence) as an energy source after stress is lifted (Kavi Kishor and Sreenivasulu 2014). For example, oxidation of a single proline molecule generates 30 ATP molecules and aids the maintenance of redox balance ($NADP^+$/NADPH ratio) through the oxidative pentose phosphate pathway (Servet *et al.* 2012). This is echoed in the upregulation of proline catabolic enzymes (P5CS2, P5CR and ProDH1) in meristematic tissues during the stress recovery phase (Kavi Kishor and Sreenivasulu 2014). However, stress can disrupt proline homeostasis and coupled with the defective amino acid cycling in *lht1* mutants, the resultant incomplete proline catabolysis generates lethal P5C levels, which triggers PCD, rather than increasing stress resistance (Servet *et al.* 2012).

#### *2.4.5.3.3 aap1 mutant – impaired ability for long distance proline translocation via the phloem*

Long-distance transport of amino acids between roots, shoot and other plant organs occurs through the vascular bundle and strong AAP1 expression in the phloem implies a vital role for importing extracellular amino acids into the vascular bundle for subsequent long-distance transport to organ sinks (Hirner *et al.* 2006; Lee *et al.* 2007). However, the inability of *aap1* mutants to translocate proline into N-sinks like the shoot might account for its greater susceptibility to heat stress compared to wild-type seedlings. Hirner *et al.* (2006) demonstrated that *lht1* mutants could not retrieve proline efficiently from the apoplast into leaf mesophyll cells and displayed a retarded growth phenotype even in the absence of stress. If the stress-susceptibility of *lht1* mutants can be partly attributed to the inability to retrieve amino acids from the vascular system into leaves, perhaps the failure of *aap1* mutants to translocate proline to the aerial plant tissue shares the same end-issue: the inability of photosynthetic leaves to access proline for efficient proline cycling across plant organs. Failure to cycle proline effectively throughout plant tissue is further exacerbated once the signalling role of proline is factored in. There is growing evidence that proline translocation to different plant organs acts as a metabolic signal for inducing proline dehydrogenase (ProDH) transcription, the catabolic enzyme that breaks down proline into P5C (Verslues and Sharma 2010). As high proline levels induces ProDH transcription, ProDH expression is downregulated during stress but upregulated upon stress relief or exogenous proline supplementation (Satoh *et al.* 2002; Sharma and Verslues 2010). ProDH maintains proline homeostasis by catabolizing proline, yielding energy and maintaining redox potential between sub-cellular compartments (Kavi Kishor and Sreenivasulu 2014).

During the stress recovery stage, root-localised proline is oxidised to generate ATP and NADPH which plant cells use as building blocks to restart growth after stress is lifted. Proline oxidation takes place in the mitochondria as ProDH is bound to the mitochondrial inner membrane and cells must maintain optimal ProDH activity or risk ROS formation and disruption of redox balance (Kavi Kishor and Sreenivasulu 2014). If *aap1* mutants have upregulated ProDH activity because of failure to translocate proline to organ sinks, the accumulation of cytotoxic proline levels in certain plant tissues can prove lethal as incomplete proline catabolysis leads to concentrated P5C levels, activating PCD in plant cells (Verslues and Sharma 2010). Hare *et al.* (2002) demonstrated that cytotoxic proline

levels causes oxidative damage in mitochondrial cristae by elevating flux through the mitochondria electron transport (MET) chain in ATP generation. This increased ROS formation, leading the MET chain to become increasingly leaky, which further amplified ROS levels and oxidative damage. Hence, the limited capacity of *aap1* mutants to transport proline over long distances to other proline sinks might lead to elevated ProDH activity and MET flux, generating lethal ROS levels.

#### *2.4.5.3.4 Summary of shared stress phenotypes by lht1 and aap1 mutants*

Proline homeostasis plays just as a prominent role in the stress recovery phase as proline accumulation does in the stress response (Kavi Kishor *et al.* 2005; Kavi Kishor and Sreenivasulu 2014). This offers a potential explanation for the similar PCD levels exhibited by *aap1* and *lht1* mutant seedlings; both mutants have a diminished ability to import extracellular proline and must rely primarily on the biosynthetic route upon stress onset. In addition, the failure to cycle proline efficiently throughout the plant, e.g. inability to import proline from apoplast into leaf mesophyll cells (*lht1* mutant) or long-distance proline translocation to organ sinks (*aap1* mutant), disrupts proline homeostasis, which can prove fatal as excessive P5C (a byproduct of ProDH) triggers PCD (Servet *et al.* 2012). Hence, the reduced ability to accumulate proline and maintain proline homeostasis might account for the similar stress-response profile shared by here by *lht1* and *aap1* mutants.

### 2.4.5.4 Cytotoxic Proline levels - Difference between wild-type and mutant lines

Cytotoxic proline supplementation raised stress-induced PCD levels in wild-type seedlings as excessive proline doses are detrimental to plant survival (Rodriguez and Heyser 1988; Hare *et al.* 2001, 2002). However, cytotoxic proline levels did not affect *lht1* and *aap1* mutants because of their limited capacity to assimilate proline. Similar investigations have reported this phenomenon. For instance, *aap1* mutants were not as vulnerable as wild-type seedlings to toxic amino acid analogues for proline (azetidine-2-carboxylate), glutamate (N-methylsulphoximine), isoleucine (o-menthylthreonine), and glutamine (2-amino-6-diazo-5-oxo-l-norleucine); the mutant line grew better and had higher fresh weights than wild-type seedlings as they assimilated lower rates of the toxic analogues (Perchlik *et al.* 2014). In addition, *aap1* mutants were also resistant to cytotoxic concentrations of neutral amino acids, including proline (Lee *et al.* 2007). The researchers attributed the higher *aap1* mutant survival rates to the lower accumulation of these amino

acids: 10 mM amino acid uptake studies revealed that *aap1* mutants experienced a 30-50% decrease in neutral amino acid uptake rates, compared to wild-type seedlings (Lee *et al.* 2007). Therefore, the ability of amino acid transporter mutant lines to withstand cytotoxic amino acid levels concurs with past studies reporting similar phenomena.

#### 2.4.5.5 Mutant lines benefitted from *N. muscorum* CM treatment, but to a lesser extent than wild-type seedlings

*N. muscorum* CM treatment produced the lowest stress-induced PCD levels across wild-type and mutant lines, although the PCD-inhibiting effect was still weaker in the latter. This reinforces previous findings (Section 2.4.2) that additional pro-survival signals in the biological matrix are acting synergistically with proline to exert a stronger PCD-inhibiting effect than individual proline treatments alone. The identity of these additional compounds has not been substantiated as it lies outside the scope of this thesis, but candidates include EPS, ROS-detoxifying exoproteins, phenolics and phytohormones. EPS such as arabinose, glucose, galactose, rhamnose, xylose and ribose have been detected in *N. muscorum* CM (Mehta and Vaidya 1978). As sugars, EPS are organic osmolytes that protect macromolecular structure under denaturing stress conditions (Judy and Kishore 2016). Sugars have attributes that fulfil the osmolyte compatibility hypothesis: high solubility, zwitterionic and non-toxic at high concentrations (Yancey 2001, 2005). Moreover, Lehman and Long (2013) showed that EPS production of succinoglycan and galactoglucan in *S. meliloti* protected against oxidative damage by reducing $H_2O_2$ levels.

Exoproteins have long half-lives that allow them to remain stable and functional in spite of unfavourable extracellular conditions (Christie-Oleza *et al.* 2015). When the exoproteome of *N. muscorum* was profiled, a considerable subset of the identified exoproteins was associated with ROS detoxification, indicating that it is important to maintain redox homeostasis, even outside the cell (Oliveira *et al.* 2015). Moreover, the high concentrations of phenolics and alkaloids in *N. muscorum* CM may buffer against oxidative damage (El-Sheekh *et al.* 2006; Abdel-Hafez *et al.* 2015). By reducing ROS levels and subsequent oxidative damage, these antioxidants may suppress the triggering of PCD-signals.

Phytohormones are plant development regulators and the extracellular presence of auxin (Mirsa and Kaushik 1989; Karthikeyan *et al.* 2009) and ABA (Maršálek *et al.* 1992) have been documented in *N. muscorum* and both are known to enhance plant stress tolerance.

This likely occurs through cross-talk between ABA and proline homeostasis as exogenous ABA application increases AtP5CS1 and AtP5CS2 transcription, which are proline biosynthetic enzymes (Kavi Kishor *et al.* 2005). Transgenic ABA-overexpressing lines were more stress tolerant as overexpression of AtEDT1/HDG1 in *Brassica oleracea* var. *alboglabra* plants exhibited a unique phenotype (upregulated auxin production and ABA hypersensitivity) and was more resistant to drought and osmotic stress (Zhu *et al.* 2016). Auxin also modulates proline homeostasis by upregulating transcription of P5Cs and ornithine ι-aminotransferase (OsOAT); the latter is involved in proline metabolism and OsOAT transcription is induced by exogenous phytohormone (auxin and ABA) treatment (You *et al.* 2012). OsOAT-overexpressing rice plants were cross-tolerant against drought and osmotic stress, with lower lipid peroxidation levels because of upregulated antioxidant (GSH, GPX and POD) activity (You *et al.* 2012). The transgenic plant also accumulated significantly higher proline levels under non-stressed conditions, providing further stress protection by acting as an osmoprotectant, indirect modulator of ROS levels, and redox-buffering agent (You *et al.* 2012).

# 2.5 Conclusions:

This chapter provides evidence that cyanobacteria-derived proline increases *Arabidopsis* stress tolerance by suppressing PCD. Using the RHA as a high-throughput screening tool for characterising *N. muscorum* CM bioactivity, the main bioactive compound was found to be thermostable and directly affecting PCD levels but not necrosis. Using a literature review-derived framework to narrow the list of candidate bioactive compounds, proline was identified as a compound of interest. The presence of proline in *N. muscorum* CM was confirmed using the ninhydrin assay and HPLC. Subsequent testing with exogenous proline treatment showed similar stress-response profiles with *N. muscorum* CM treatment (higher viability, lower PCD and unaffected necrosis levels), although the higher viability rates observed in *N. muscorum* CM treatment are likely due to synergistic interactions between additional thermolabile bioactive compounds. Further evidence for proline as the compound of interest was provided using three impaired proline-transporter mutants (*aap1*, *lht1* and *atprot1-1::atprot2-3::atprot3-2*). Unlike the *atprot* triple knockout mutant, both general amino acid transporter (*lht1* and *aap1*) mutants displayed similar stress phenotypes to each other, with consistently higher PCD levels than wild-type seedlings at medium-to-high proline doses. All three mutant lines had lower viability and higher PCD levels when treated with *N. muscorum* CM compared to wild-type

seedlings, providing additional evidence for proline as the main bioactive compound present in *N. muscorum* CM. Both *N. muscorum* CM and exogenous proline altered the PCD sensitivity threshold and primed the stress-acclimation response. This offers preliminary evidence of a novel biofertiliser mechanism which enhances plant stress tolerance independent of the existing mechanisms documented in the literature. Agriculture must continually evolve in a sustainable manner to meet the rising food demands and biofertilisers provide a novel supplementary role along with conventional fertilisation and pest management strategies. Screening potential PGPR inoculants for elevated proline biosynthesis can potentially aid efforts to improve crop yield security despite rapidly changing meteorological conditions.

# Chapter 3 - Programmed cell death as a marker of plant stress tolerance: a high-throughput method of screening for cereal varieties exhibiting stress tolerance

## 3.1 Introduction

The world population is advancing at steady rates and is predicted to reach 9.7 billion by the year 2050 (United Nations 2017). Nearly half of the food calories consumed by the world are composed of cereals, with the predominant cereals being wheat, rice, maize, millet and sorghum; these five staple crops make up almost 44% of the calories ingested per capita worldwide (Reynolds *et al.* 2016). As the world population swells, so does the food demand; Thomson (2003) estimates that cereal yields need to increase by 70-100% to arrive at the global demand target of 3 billion tonnes in 2050. Consequently, agriculture systems rooted solidly in practices that sustain and enhance the natural environments must evolve to meet this rising food demand. Until recently, a relatively predictable climate has allowed commercial farmers to prioritise high-yielding cereals over stress tolerant varieties. However, the potential payoffs of high-yielding varieties are redundant if plants are liable to succumb to stress as climate abnormalities causes crops to have increasing encounters with unique abiotic and biotic stress combinations, which negatively impact growth rates and yield (Pandey *et al.* 2017).

Climate change affects cereal yields primarily by heat and osmotic stress because of rising temperatures, but also triggers downstream stresses in the form of flooding, frost, and bacterial and viral infections (Porter *et al.* 2015). An increase in greenhouse gas emissions has been the underlying factor driving the ascent of global temperatures, and this has negative ramifications on cereal yields (Wang *et al.* 2018). For example, southern European countries that experience more severe environmental fluctuations have lower wheat yield gains than more climate-stable northern counterparts (Porter and Semenov 2005) and Asseng *et al.* (2013) predicts that for every 1 °C rise in average global temperature, grain yields will depreciate by 6%. Global temperatures are rising incrementally at 0.2 °C per decade (Wang *et al.* 2018) and the escalating climate variability has led to short periods of acutely high temperatures, causing heatwaves to become increasingly common (Reynolds *et al.* 2016). By occurring more frequently, these cycles of acute heat shock can have a negative impact on crop yields by affecting pollen viability, kernel numbers and seed weight, especially if plants are stressed during the

heading and flowering stages (Stratonovitch and Semenov 2015). Under rising temperatures, crop yields are even more affected if exposed to stress combinations as modifications to plant physiology and the weakening of the defence system makes plants more susceptible to pathogens and reduces competitive ability against weeds (Pandey *et al.* 2017). High temperature has the unfortunate effect of increasing the occurrences of vector-borne diseases and encouraging pathogen growth such as *Ralstonia solanacearum*, *Acidovorax avenae* and *Burkholderia glumae* (Kůdela 2010). Coupled with a swiftly expanding global population, rising temperatures that impact crop yields have driven the expansion of farmlands to meet the rising food demands. However, intensive agriculture practices themselves play a substantial role in the emission of greenhouse gases, leading to an ever-amplified loop between rising temperatures and food insecurity (Wang *et al.* 2018).

Under such climate uncertainty, breeders are tasked with prioritising yield safety over yield gains because without adjustments, the present generation of cereals cannot resist the increasingly frequent and harsh environmental fluctuations (Reynolds *et al.* 2016). Thus, the challenge to prioritise crop yield security demands a concerted effort to screen and characterise the germplasm of wild crop relatives to utilise genetic variability for producing nutritionally dense crop varieties with enhanced stress resilience. Traditionally, enhancing plant stress tolerance relied on crop breeding programmes, application of environment-damaging fungicides, pesticide and fertilisers, or genetic modification. The intensive use of fungicides is not sustainable in the long run and while breeding programmes are effective, it takes time to produce new varieties with the desired characteristics. In addition, the advancement of climate change and new pathogen strains may overtake breeders' ability to introduce new varieties rapidly enough to meet increasing demands. Direct genetic modification is more efficient, but such crops must contend with the stigma attached to genetic modified organisms and prolonged safety testing trials are needed before they are released commercially. Regardless of the methods used to increase plant stress tolerance, there is a growing consensus to broaden the focus from production of high-yielding crops, to producing more stress-tolerant varieties as yield improvements must not come at the expense of the environment (Coleman-Derr and Tringe 2014; Meena *et al.* 2017; Pandey *et al.* 2017). Consequently, many methods have been developed to study the intricate molecular, biochemical and physiological processes underlying plant stress tolerance.

During stress onset, plants reprogram their metabolic networks by modulating stress-response genes transcription, mRNA post-transcription and protein post-translational mechanisms. Over the years, researchers have developed a diverse range of molecular biology techniques to investigate the different stress-response phases, such as transcriptomics (mRNA transcriptional and post-transcriptional analysis, e.g. micro-RNA and small interfering RNAs (Chinnusamy *et al.* 2010), proteomics (2-dimensional liquid chromatography, polyacrylamide gel electrophoresis, difference gel electrophoresis (Ahmad *et al.* 2016), metabolomics (gas/liquid chromatography-mass spectrometry, capillary electrophoresis and nuclear magnetic resonance spectroscopy (Obata and Fernie 2012) and phenomics (high-throughput phenotyping) (Singh *et al.* 2018). These methods integrate enormous amounts of information to generate a high-resolution picture of the plant stress response but they are laborious processes that involves significant technical expertise. In contrast, biochemical and physiological techniques are simpler techniques that offer useful information in the form of stress biomarkers. Oxidative damage is a common measure of plant stress tolerance as excessive ROS levels damage subcellular components (mitochondria, chloroplast and plasma membrane) and trigger PCD under lethal ROS levels (Petrov *et al.* 2015). There are many methods for quantifying oxidative damage, such as total antioxidant capacity, lipid peroxidation, ion leakage as an indicator of membrane damage, measurement of non-enzymatic (e.g. phenols, ascorbate and glutathione), and enzymatic antioxidant levels (e.g. GPX, SOD and POD) (Elavarthi and Martin 2010; Jambunathan 2010). Osmolyte (e.g. proline, sugars and glycine betaine) levels are another important biochemical parameter that regulate cell volume and maintain osmotic balance during stress onset (Maness 2010; Verslues 2010). In addition, ion quantification ($Na^+$, $K^+$, and $Cl^-$) is used to screen plants for salt tolerance as the ability to partition and cycle ions through the different tissues is vital for surviving salt stress (Munns *et al.* 2010).

PCD plays an important role in plants, both in the developmental process of tissue and organs, and in response to environmental stress. Developmentally-induced PCD is a genetically controlled process activated at specific time-points of plant growth for vegetative and reproductive tissue development (Kacprzyk *et al.* 2011). In contrast, plants activate environmentally-induced PCD as a protective mechanism during abiotic (drought, salt, osmotic, high temperatures and light, heavy metal exposure, flooding) and biotic (pathogen infection) stress onset (Petrov *et al.* 2015). This has broad implications

for global agricultural practices as stress-induced PCD affects crop yield and productivity (Mittler and Blumwald 2010). With the advance of climate change and an increasing global population, there is a growing interest in development of strategies for inhibiting stress-induced PCD to minimise crop yield losses.

Plants are sessile organisms and have evolved a range of protective mechanisms to ensure continued survival when faced with unfavourable conditions. There are instances when stress-induced PCD activation is beneficial such as aerenchyma formation during hypoxia stress (Lenochová *et al.* 2009). For example, hypoxic maize root and stem cells undergo PCD to form aerenchyma as it generates longitudinal air channels; this enables gaseous diffusion from shoots to water-logged roots for survival under $O_2$-limiting conditions (Lenochová *et al.* 2009). PCD also plays an import role during the HR against pathogen infection (Lam *et al.* 2001). Unlike animal systems, plants lack an immune system and rely on PCD activation as a pathogen containment strategy; invaded cells undergoing PCD transmit signals to surrounding healthy cells to activate defence mechanisms to prevent the spread of pathogens (Hoang *et al.* 2016). By erecting a barrier of PCD cells, plants limit biotrophic pathogens only to the infection site as they require living host cells for colonisation and spreading (Lam *et al.* 2001).

Nevertheless, PCD activation in response to most abiotic stresses usually signifies that damaged cells are unable to cope with prolonged redox imbalance; PCD is activated as the cells' last act of preservation because of stress-induced oxidative damage to organelles and macromolecules (Wituszynska and Karpinski 2013). Unlike necrotic death, selective PCD activation improves the overall chances of plant survival as it maintains tissue and organ integrity by eliminating damaged cells that accumulate during stress (Wituszynska and Karpinski 2013). By eliminating cells in a controlled manner, the surviving plant cells can recycle the metabolic precursors from dying cells to increase survival chances (Hoang *et al.* 2016). Thus, stress-induced PCD can either be beneficial or detrimental depending on the context: PCD can either trigger adaptations to environmental stress (hypoxia and HR response) or is the last act of preservation by damaged cells unable to cope with prolonged stress exposure. Consequently, there is growing interest by the research community in the manipulation of PCD pathways with the aim of generating more robust, stress tolerant plant varieties. For example, the introduction of anti-apoptotic genes *AtBAG4* (*Arabidopsis*), *Hsp70* (*Citrus tristeza* virus) and *p35* (*Baculovirus*) into rice

plants reduced salt-induced PCD and ROS levels in transgenic lines compared to wild-type plants (Hoang *et al.* 2015). All three transgenic lines had better growth parameters (photosynthetic efficiency, growth rate and crop yield) and a stronger ROS-scavenging ability, compared to wild-type plants. Expression of *p35* increases the antioxidant capacity of host cells by direct $H_2O_2$ scavenging, while *Hsp70* and *AtBAG4* expression reduced ROS levels in transgenic lines by indirectly modulating ROS-scavenging pathways and ion homeostasis. Hoang *et al.* (2015) also showed that all three anti-apoptotic expressing lines maintained functional ion transporters under salt stress and lines could extrude excess $Na^+$ and sustain optimal cytoplasmic $Na^+/K^+$ levels for continual cellular activity. Kim *et al.* (2014) observed similar favourable effects when they introduced the anti-apoptotic mammalian *Bcl-2* gene into rice plants; *Bcl-2*-overexpressing rice plants had lower salt stress-induced PCD levels than wild-type plants as *Bcl-2* inhibited $K^+$ efflux across the plasma membrane, reduced cytoplasmic $Ca^{2+}$ levels and repressed *OsVPE2* and *OsVPE3* transcription. The ability of mammalian *Bcl-2* to inhibit plant VPEs transcription was interesting as VPEs are cysteine proteinases involved in vacuole-mediated PCD; *OsVPE3* suppression in salt stressed-rice plants diminished vacuole rupture incidences by preserving the structural integrity of the vacuole membrane (Lu *et al.* 2016). These transgenic plant studies show that biological kingdoms share a highly conserved PCD mechanism and offer encouraging evidence for the modulation of PCD pathways to generate plants with broad-spectrum stress tolerance (Hoang *et al.* 2015).

For these reasons, it is important for researchers to have a wide variety of methods for quantifying PCD levels. Current methods rely on either the direct scoring of PCD based on its distinctive cell morphology (retracted cytoplasm) or indirectly by tracking PCD-triggering molecular signals such as levels of ROS, reactive nitrogen species, intracellular $Ca^{2+}$, glutathione redox signature and cyclic guanosine monophosphate (Chen *et al.* 2018; Doccula *et al.* 2018; Terrón-Camero *et al.* 2018) and various mitochondrial markers (Xiao *et al.* 2018). Other indirect methods for quantifying PCD include the measurement of molecular markers generated under oxidative damage (reactive carbonyl species, DNA and lipid damage) (Mano and Biswas 2018), or PCD executors such as mitogen-activated protein kinase (MAPK) (Wu and Jackson 2018) signalling cascades and VPEs activity (Hatsugai and Hara-Nishimura 2018). These methods cover a wide range of context for investigating the different phases of the stress response, but it is important to stress that

cells are integrating multiple PCD-inducing signals across the different subcellular compartments, and not just a lone signal as measured by the aforementioned methods (Petrov *et al.* 2015). The perception of stress cues generates PCD-inducing signals at the ER, chloroplast, and mitochondria, but each organelle has distinctive mechanisms for processing the signal (Petrov *et al.* 2015). This was illustrated in work by Kacprzyk *et al.* (2017) who showed that chemical modulators that alter mitochondrial permeability transition, ATP synthesis and $Ca^{2+}$ signalling also inhibit protoplast retraction in stressed cells, proving that multiple signalling pathways are acting collectively to modulate PCD.

These intricate signalling networks emphasise the serious consequences held by the cellular decision to trigger PCD for survival of the whole organism. Cells regulate PCD by balancing pro- and anti-apoptotic signals, and the decision to live or die depends on where the balance shifts. This highlights the biggest difference found between indirect and direct PCD quantification methods; indirect methods track the progression of molecular markers, signalling networks, or metabolic changes that stressed cells undergo, while direct PCD scoring shows the outcome of the decision-making procedure: whether cells stay alive or undergo PCD. For these reasons, this chapter provides evidence that direct PCD scoring is a useful marker of stress tolerance as it integrates multiple input-streams to provide a cohesive picture of the stress response. However, only a few *in vivo* studies have used direct PCD scoring as it is difficult to access and section PCD cells embedded around viable tissue (Balk and Leaver 2001). Instead, *in vitro* plant cell cultures are a popular model system for PCD research as cell suspensions are homogenous and their synchronised responses to potential PCD modulators makes it easy to monitor their effects on the cell status using live-imaging (Reape *et al.* 2008).

However, plant cell cultures can be labour intensive to establish as not all pluripotent cells across different plant species will display the dispersed phenotype needed for microscopy work (Cimini *et al.* 2018). Because of divergent mitotic patterns, plant cells from different species may differentiate into calli or cell chains, causing cells to clump together and disrupt the uniformity of the suspension cultures (Cimini *et al.* 2018). Therefore, not all plant cell cultures have the right morphologies for direct PCD scoring and therefore must be tested on a species-to-species basis. As plants are complex organisms and have many signalling pathways acting in concert to regulate the PCD network, the reduced complexity of cell cultures makes it easy to assess how single cells respond to PCD

modulators. However, it is also important to assess the effects of these modulators in the whole plant context, as tissue-specific cells will likely not respond in a synchronised manner as homogenous plant cell culture cells do (Reape *et al.* 2015).

Therefore, there is a growing interest in using *in vivo* plants as model systems for investigating plant PCD and an analysis of the different models (e.g. root cap cells, lace plant, trichomes, leaf epidermal cells and seed embryos) can be found in the review by Kacprzyk *et al.* (2011). Each *in vivo* model system has its own specific niche offer a more accurate representation than artificially controlled reconstructions using *in vitro* methods. Besides these models, Hogg *et al.* (2011) proposed using root hairs as a model system for directly scoring PCD cells. Root hairs are lateral single-celled extensions from root epidermal cells, present in quantities large enough for sample enumeration, and are easily accessible for pharmacological treatment. The protocol developed in root hairs was termed the RHA and used to establish heat stress-response curves in *Arabidopsis* seedlings, but Hogg *et al.* (2011) also successfully extrapolated the assay to *Medicago truncatula*, *Zea mays* and *Quercus robur* seedlings.

Using a combination of FDA staining and corpse morphology, the RHA can quantify cell viability, PCD, and necrosis levels simultaneously and holds an important advantage over alternative assays that only measure a single variable. Viability assays that only measure cell viability do not distinguish between PCD and necrotic death. This has important significance as van Doorn *et al.* (2011) has called for the reclassification of plant PCD as necrotic death. Van Doorn *et al.* (2011) asserts that cytoplasm retraction, a hallmark PCD feature, is merely a post-mortem effect caused by the rupture of the plasma membrane. Under his proposed nomenclature, necrotic death is caused by the early rupture of the plasma membrane and subsequent collapse of the cell on itself. However, this proposal does not account for the distinctive cell death morphology displayed in highly stressed cells which do not have retracted protoplasts (Reape and McCabe 2013). Therefore, his proposed necrosis reclassification does not distinguish between cells that die with and without cytoplasm retraction, conventionally scored as PCD and necrosis, respectively, under classical definitions.

However, recent work has shown that cytoplasm retraction is a valid plant PCD marker as it is an active and interruptible process driven by cellular $Ca^{2+}$ influx; inhibition of $Ca^{2+}$

influx modulated PCD and cytoplasmic retraction but not necrotic death (Kacprzyk *et al.* 2017). Contrary to the proposals by van Doorn *et al.* (2011), cytoplasm retraction preceded the loss of the plasma membrane integrity, showing that cytoplasmic retraction was not caused by protoplast collapse but a driver of downstream PCD signalling events, as PCD could be disrupted even after cytoplasm retraction had occurred (Kacprzyk *et al.* 2017). This was reflected in the treatment of *Arabidopsis* with fumonisin $B_1$ and spectinomycin (modulators of sphingolipid signalling, mitochondrial function and chloroplast protein biosynthesis) which inhibited PCD even after cells had initiated cytoplasm retraction. Both treatments delayed the full advancement of PCD by uncoupling cytoplasm retraction from loss of plasma membrane integrity, resulting in a stalled death morphology (viable cells with retracted cytoplasm) (Kacprzyk *et al.* 2017). Given the considerable differences between PCD and necrosis in terms of signalling, morphology and regulation, it is essential to distinguish between both cell death modes to generate an accurate picture of plant cell death studies across different research groups (Reape *et al.* 2008; Reape and McCabe 2013). Thus, if a stress response is only assessed using viability levels, it loses context whether cells are dying by activated PCD or uncontrolled necrotic death.

Previously, Hogg *et al.* (2011) showed that the RHA was transferable between plant species, while Kacprzyk *et al.* (2014) demonstrated its use with genetic and pharmacological tools to assess the signalling networks regulating the PCD response in *Arabidopsis* seedlings. This chapter builds on these past works to show that stress-induced PCD levels can be a novel marker for stress tolerance. An experimental workflow was developed using the RHA as a rapid, early screening tool for identifying stress tolerant and susceptible varieties: 1-2-day-old *Triticum aestivum* (wheat) and *Hordeum vulgare* (barley) seedlings had a (salt and/or heat) stress applied, and the stress response quantified in terms of viability, PCD and necrosis.

By examining the dose-dependent stress response, the inflection point for each species and stress treatment was identified. The inflection points indicate the stress dose which exhibited the largest variances in stress-induced PCD levels. Once identified, the inflections points were used to assess the basal, induced and cross-stress tolerance of eight wheat varieties. This was done by applying heat and salt stress in a time-course experiment to assess how wheat varieties differed in their response to single, combined

and multiple individual stress exposure. Single stress exposure involves the application of a single stress-factor, multiple individual stresses are non-overlapping repetitive stresses occurring at different time-points, while combined stress are two or more stresses applied simultaneously or that overlap to a certain degree (Pandey *et al.* 2017).

Basal tolerance was assessed using single and combined stress exposure as both treatments highlight the intrinsic ability of plants to survive stress by its baseline physiological state without prior stress exposure or acclimation (Arbona *et al.* 2017). Combined stress exposure are distinct from single stress-factor treatments as the former generates a unique stress phenotype, one highly distinct from individually applied stresses (Mittler 2006; Rasmussen *et al.* 2013; Rivero *et al.* 2014). Rasmussen *et al.* (2013) divided the unique stress phenotype into five categories, but for simplicity's sake, this chapter examines the stress-response in terms of a positive, netural or negative net interaction based on their stress-induced PCD levels. These interactions are based on the original stress phenotypes devised by Mittler (2006) who divided the response into synergistic, antagonistic or neutral interactions, of which all five stress modes fall into (Figure 3.1A). Lastly, multiple individual stresses were used to investigate induced and cross-stress tolerance, the phenomenon where the initial stress exposure makes plants more resistant to other stress types (Walter *et al.* 2013; Rejeb *et al.* 2014b; Pandey *et al.* 2017). As Figure 3.1B illustrates, the first stress cue can either prime (positive and neutral) or predispose (negative) plants to recurrent stress exposure (Pandey *et al.* 2017).

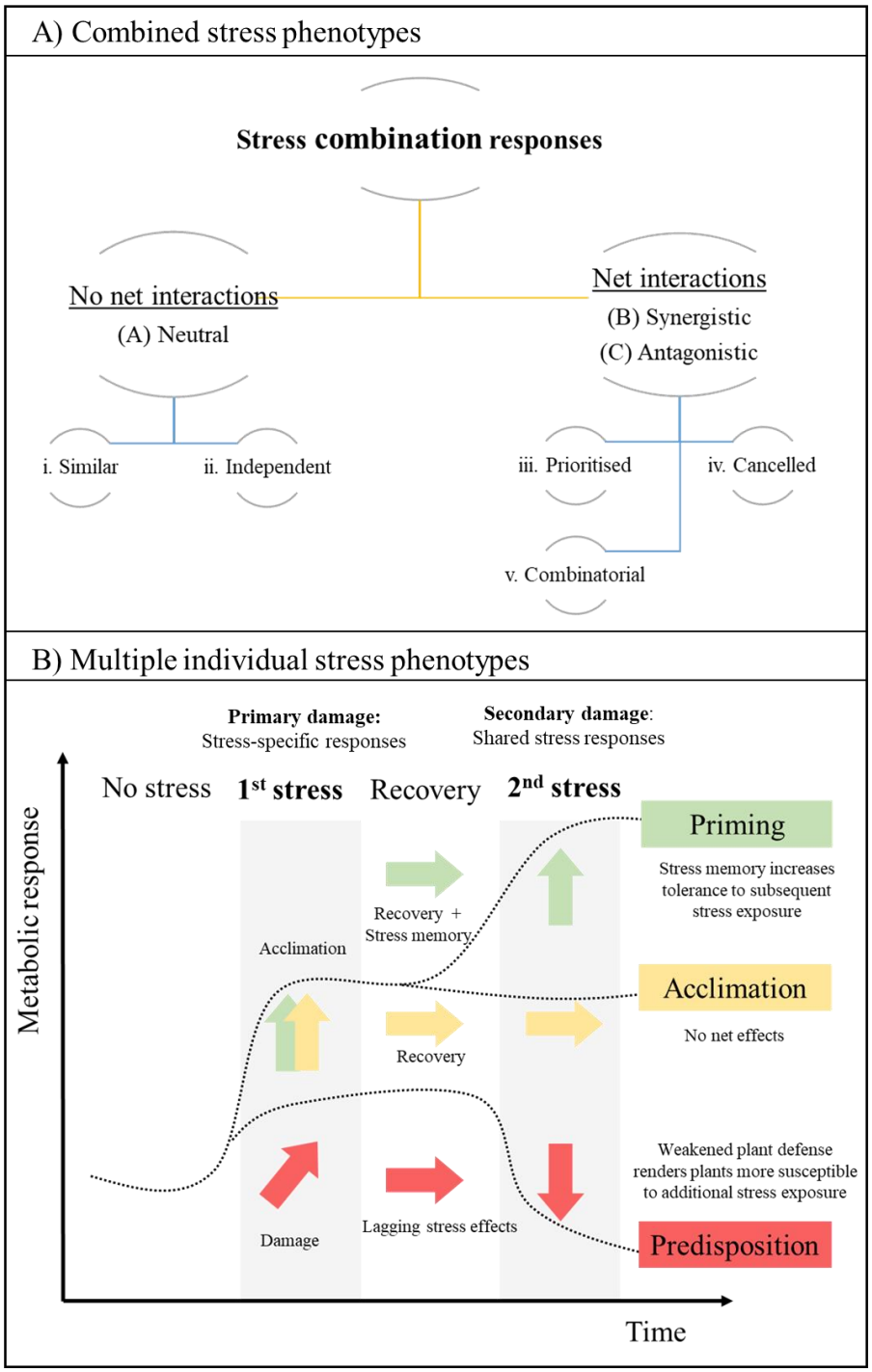


**Figure 3.1** - (A) The stress response phenotype after combined stress can be grouped into three categories: neutral, synergistic and antagonistic (Mittler, 2006), which can be further sub-divided into five sub-categories: similar, independent, prioritised, cancelled and combinatorial (Rasmussen *et al.* 2013). (B) The putative positive, neutral and negative stress response phenotype of plants under multiple individual stress applications. The first non-lethal stress cue either primes (positive and neutral) or predisposes (negative) plants to subsequent stress encounters. Image and information adapted from Tausz *et al.* (2004), Walter *et al.* (2013.) and Pandey *et al.* (2017).

Priming enables plants to reach a new metabolic steady-state higher than its pre-stress levels by reprogramming the metabolome and making epigenetic changes; primed plants either become resistant to the second stress encounter without additive damage (neutral – maintains same steady state), or have improved tolerance (positive – higher metabolic steady state) (Tausz *et al.* 2004; Walter *et al.* 2013; Pandey *et al.* 2017). Conversely if the cell protective mechanisms are insufficient, predisposition makes plants more vulnerable to repetitive stresses because of lagging stress effects (e.g. excessive oxidative damage) that leads to degradation of the metabolic steady state and higher cell death rates (Tausz *et al.* 2004; Walter *et al.* 2013). By examining how individual wheat varieties respond to the different stress exposures, this chapter demonstrates how stress-induced PCD levels can be used to rapidly screen the formation of unique stress phenotypes under combined stress, while examining how basal, induced and cross-stress tolerance affects cereal survival.

### 3.1.1 Aims and Objectives

Conventional screening methods to identify stress-tolerant cereal varieties relies on expensive, labour-intensive field testing and molecular biology techniques. In this chapter, the RHA, originally established in *Arabidopsis*, was adapted to wheat and barley seedlings. By scoring stress-induced PCD levels, the RHA was used as a rapid screening tool to identify stress-tolerant and susceptible varieties against transient heat (wheat and barley) and salt (wheat) exposure. Stress-induced PCD levels also facilitated the assessment of the basal, induced and cross-stress tolerance of wheat varieties using single, combined and multiple individual stress exposures by applying concurrent heat and salt stress in a time-course experiment.

**Chapter aims:**

- Investigate heat (25-55 °C) tolerance in barley and wheat seedlings.
- Investigate salt (50-250 mM NaCl) tolerance in wheat seedlings.
- Establish stress matrices to identify stress-tolerant and susceptible cereal varieties.
- Investigate basal, induced and cross-stress tolerance of wheat varieties to heat and salt stress at the viable/PCD inflection point (35 °C for heat, 150 mM NaCl for salt stress).

## 3.2 Materials and Methods

### 3.2.1 Growth and sterilisation procedures for seedlings

Three spring barley varieties were provided by Seedtech®, while four spring wheat, four winter wheat and four winter barley varieties were supplied by KWS UK®. Spring and winter varieties differ in the season they are sown; the latter require vernalisation in the cold to flower, while the former does not. In barley, the vernalisation response is controlled by two major loci at *VRN-H1* and *VRN-H2*; spring alleles have deletions in both loci that enable flowering without vernalization (Cockram *et al.* 2007). A similar scenario occurs in wheat, but five vernalization-responsive genes (*Vrn1–5*) have been identified (Cattivelli *et al.* 2002). The respective identities of the individual varieties cannot be revealed per the signed Material Transfer Agreement with the companies in question. Therefore, their properties will be discussed without disclosure of their official identities and referenced materials, and they will be referred to in this thesis as their cereal identifiers as listed in Table 3.1. These varieties were primarily developed for cultivation under a temperate climate, although not all varieties are available on the market. For example, SW4 was tested as a candidate variety for breadmaking in 2013/2014 and performed relatively well in terms of yield (102-106 t/ha as % mean of controls across two UK test sites). However, this variety is not available in the market and appears not to have passed the final stages of testing. Regardless of their status on the commercial market, the companies have stated that the lines provided here were selected based on final yield, growth habitat, ear emergence, maturity and disease profile, but not against tolerance to specific abiotic stresses. Hence, the RHA was used as an early-screening method for pinpointing stress-tolerant or susceptible lines to guide additional characterisation work in the future.

**Table 3.1** – Cereal variety Identifier, Corresponding Species, Season and Provider.

**Key**: 'SB' = spring barley, 'WB' = winter barley, 'SB' = spring wheat, 'WW' = winter wheat.

| Seed Identifier | Species | Season | Provider |
|---|---|---|---|
| SB1 | *H. vulgare* (Barley) | Spring | Seedtech ® |
| SB2 | | | |
| SB3 | | | |
| WB1 | *H. vulgare* (Barley) | Winter | KWS UK® |
| WB2 | | | |
| WB3 | | | |
| WB4 | | | |
| SW1 | *T. aestivum* (Wheat) | Spring | KWS UK® |
| SW2 | | | |
| SW3 | | | |
| SW4 | | | |
| WW1 | *T. aestivum* (Wheat) | Winter | KWS UK® |
| WW2 | | | |
| WW3 | | | |
| WW4 | | | |

#### 3.2.1.1 *T. aestivum* (wheat) seedling preparation and germination

Wheat seeds were soaked in SDW at room temperature for 3 hours. In a sterile flow cabinet, water was drained from seeds, a 20% bleach solution (Domestos® disinfectant: sodium hypochlorite 4.5g per 100g) was added, and the mixture was shaken for 4 minutes and rinsed 5 times with SDW. Using sterile forceps, 10 sterile seeds were placed in between two layers of sterile 10 mm Whatman® filter paper (pre-soaked with 3 mL SDW) in a sterile Thermo Scientific® Petri dish. Seeds were arranged far apart from one another to prevent roots from tangling after germination to minimise root hair damage. Plates were sealed with Parafilm, wrapped in foil and stratified at 4 °C for at least two days to synchronise germination. To germinate seeds, plates were placed in a 21 °C growth chamber (light regime: 33 µmol/$m^2$/s, 16-hour light: 8-hour darkness) and used for stress assays after 1 day of growth.

#### 3.2.1.2 *H. vulgare* (barley) seedlings preparation and germination

To prepare barley seeds for testing, a similar protocol for wheat seedlings was used. However, barley seeds were left to grow for 2 days as initial testing (data not shown) showed that germination levels were inadequate after 1 day of growth. During the initial round of testing, examination of the seedlings under the microscope revealed a swollen

root meristem and that root hairs were clustered too densely for accurate scoring. An additional day of growth negated these problems, hence 2-day-old barley seedlings were used for subsequent assays.

## 3.2.2 Evaluating heat and salt tolerance

### 3.2.2.1 Establishing heat stress response curves in *H. vulgare* and *T. aestivum* seedlings

A similar protocol to *Arabidopsis* seedlings (Section 2.2.2) were used, but with several amendments as the cereal seedlings were too large to fit into the 24-well plates. Barley and wheat seedlings were transferred into Petri dishes under aseptic conditions with care to prevent mechanical damage, which would inflate the root hair background death levels. 2 mL SDW was pipetted into the germination plates and swirled to dislodge the roots from the filter paper. Seedlings were transferred to Petri dishes (filled with 25 mL SDW), heated for 10 minutes in a water bath at specific temperatures (25, 35, 45, 50 or 55 °C) and returned to the 21 °C growth chamber. Viability and cell death (PCD and necrosis) were scored 14-16 hours after stress application to allow PCD morphology to develop fully (Hogg *et al.* 2011). At least 100 root hairs were scored per seedling across both sides of the primary root to provide an accurate representation of viable, PCD and necrosis levels. At least 4 seedlings were scored per treatment ($n \geq 4$) and when possible, the data from three experiment replicas merged to yield a final sample size of $n \geq 12$.

Each cell mode is depicted as the percentage of cell mode over total number of root hairs. Only the longer root in 1-day-old wheat seedlings were counted as shorter roots lacked enough root hair density for accurate scoring. In contrast, 2-day-old barley seedlings have multiple roots (3-5) of relatively equal length. Unstressed barley roots were scored using the RHA to evaluate if roots had intra- or inter-level variations. The results from Section 3.3.1.2 show that barley roots had minimal deviations in viability levels between roots of the same seedlings. Thus, only one root per barley seedling was scored in the subsequent heat stress curves.

### 3.2.2.2 Establishing salt stress response curves in *T. aestivum* seedlings

Due to time constraints, only one species was investigated for salt tolerance. Wheat was chosen over barley as it is one of the most economically important staple crops that provide nearly half of the of the global food calories, alongside with rice, maize, peal

millet and sorghum (Reynolds *et al.* 2016). 1-day-old wheat seedlings were placed into Petri dishes filled with 25 mL NaCl (50, 100, 150, 200 or 250 mM) for 5 minutes, before being transferred into new Petri dishes containing 25 mL SDW. Seedlings were returned to the 21 °C growth chamber and scored 14-16 hours after stress application. On occasion, salt-stressed wheat seedlings displayed mixed markers (retracted cytoplasm and FDA positive) because of plasmolysis. Under these circumstances, root hairs displaying mixed markers were rinsed with SDW and remounted on microscope slides without additional FDA staining. This removes excessive background FDA staining and makes it easier to distinguish between viable (strong fluorescence) and PCD (weak, almost imperceptible fluorescence) root hairs.

#### 3.2.2.3 Evaluating single, combined and multiple stress response of *T. aestivum* seedlings to heat and salt stress

Eight wheat varieties were examined for their response to single, combined and multiple stress. As result of identifying the 35 °C heat and 150 mM NaCl inflection points, 1-day-old wheat seedlings were subjected to heat (35 °C) and/or salt (150 mM NaCl) stress at specific time-intervals, as depicted in Figure 3.2. In the first data-set, samples were subjected to 35 °C stress for 10 minutes as the 0-minute mark, followed by 150 mM NaCl stress for 5 minutes at the 30, 60, 120 and 120-minute mark, followed by transfer into 25ml SDW. In the second data-set, samples were subjected to 150 mM NaCl stress for 5 minutes at the 0-minute mark, transferred into SDW-containing plates, and followed by 35 °C heat stress for 10 minutes at the 30, 60, 120 and 120-minute mark. Controls included single-stress (35 °C only, or 150 mM NaCl only) and double-stressed (heat and then salt (H+S) or, salt and then heat (S+H) at the 0-minute mark). Figure 3.2 illustrates the process for examining basal and induced tolerance using single, combined and multiple individual stresses.

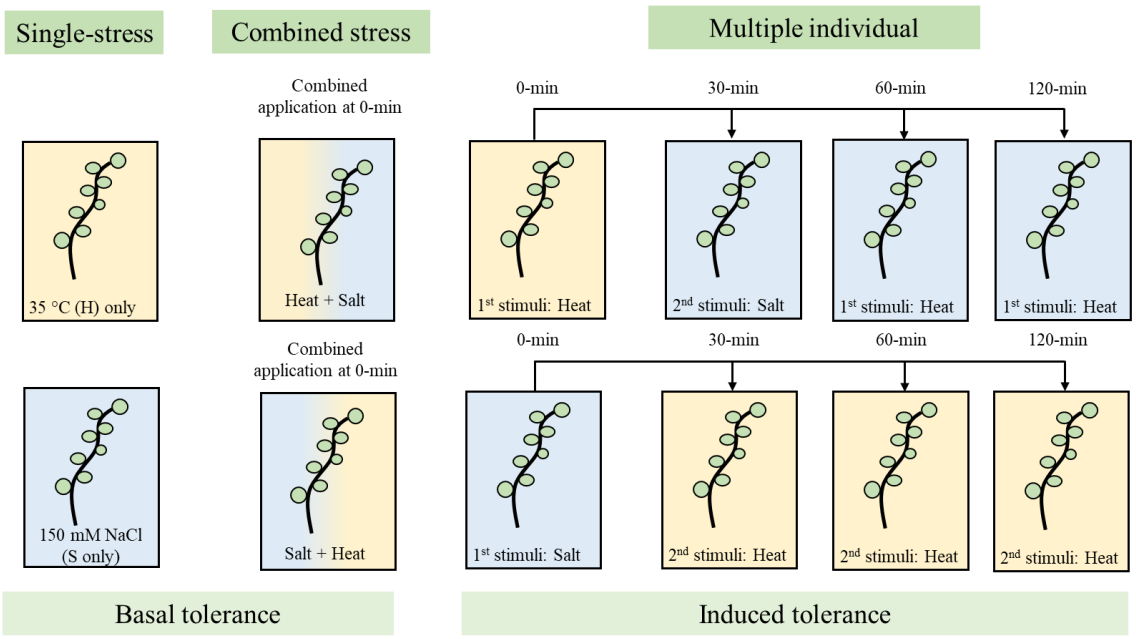


**Figure 3.2** – Experimental workflow used to assess basal stress tolerance (single and combined), and induced stress tolerance (multiple individual) in wheat seedlings in response to 35 °C heat (H) and/or 150 mM NaCl salt (S) stress. Single-stress involves the application of a single stress-factor (H only, or S only), combined stress involved the overlapping application of 35 °C heat followed by salt stress (H+S; 0-min) and vice versa (S+H; 0-min), and multiple individual testing involves the application of the first stress stimuli (0-min), followed by application of the second stress stimuli at 30- , 60- and 120-mins.

## 3.3 Results

### 3.3.1 Evaluating potential differences in root hair viability in seedlings with more than one root.

The RHA was originally validated in *Arabidopsis* seedlings which have a single primary root 5-days post germination (Hogg *et al.* 2011). Barley, wheat and other cereal crops have at least three roots emerging from the seed. Therefore, it was necessary to determine if background viability and death levels were similar in all roots of the same age, before establishing stress-response curves in both cereals.

#### 3.3.1.1 *T. aestivum* seedlings

Germinated 1-day-old wheat seedlings typically have a long main root that is flanked by two shorter roots (see Figure 3.3A). Only the longer root was scored because the shorter roots lack sufficient root hair density to reach the 100-root hair threshold for an accurate representation of the overall viable and total cell death levels (Hogg *et al.* 2011).

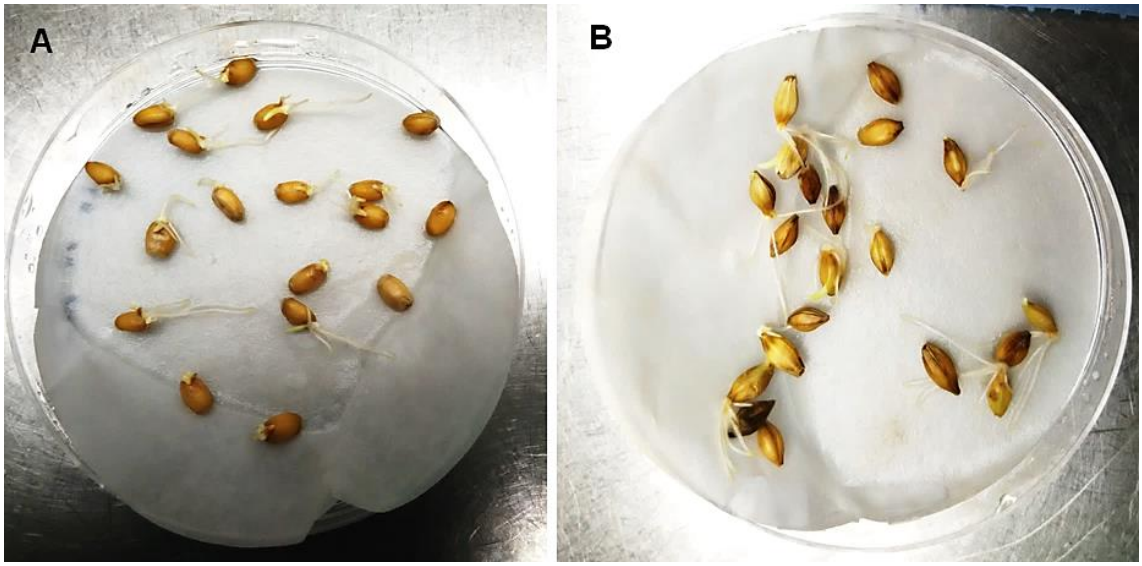


**Figure 3.3** - A) Germinated 1-day-old wheat seedlings typically have a long main root that is flanked by two shorter roots. B) Germinated 2-day-old barley seedlings have around 3-5 roots, all roughly equal length.

#### 3.3.1.2 *H. vulgare* seedlings

Unlike wheat seedlings, 2-day-old barley seedlings have multiple roots (3-5) of approximately equal length (Figure 3.3B) and had to be assessed if unstressed barley roots had similar viability levels within the same seedling (intra-level variations) and across other samples (inter-level variations). Two spring barley varieties (SB1 and SB3) were examined for these potential differences and the results showed that each individual variety had similar intra-viability levels, i.e. roots of the same sample, between seedlings. This can be seen in their respective charts depicting their scatter-plots (Figure 3.4A, C) and average viability from all roots of the same seedling (Figure 3.4B, D). Apart from the outlier at SB3 Seedling 3 (Root 2 had 39% viability, remaining roots had 65-83% viability), there was insignificant intra-variation between viability levels of roots of the same seedling. Statistical analysis supported this as no significant differences ($p>0.05$) was detected between the average root viability levels across seedlings in both SB1 and SB3 varieties, respectively (Table 3.2). As roots from the same seedling had insignificant variability between each other, only 1 root from each barley seedling was scored in heat stress experiments (Section 3.3.2).

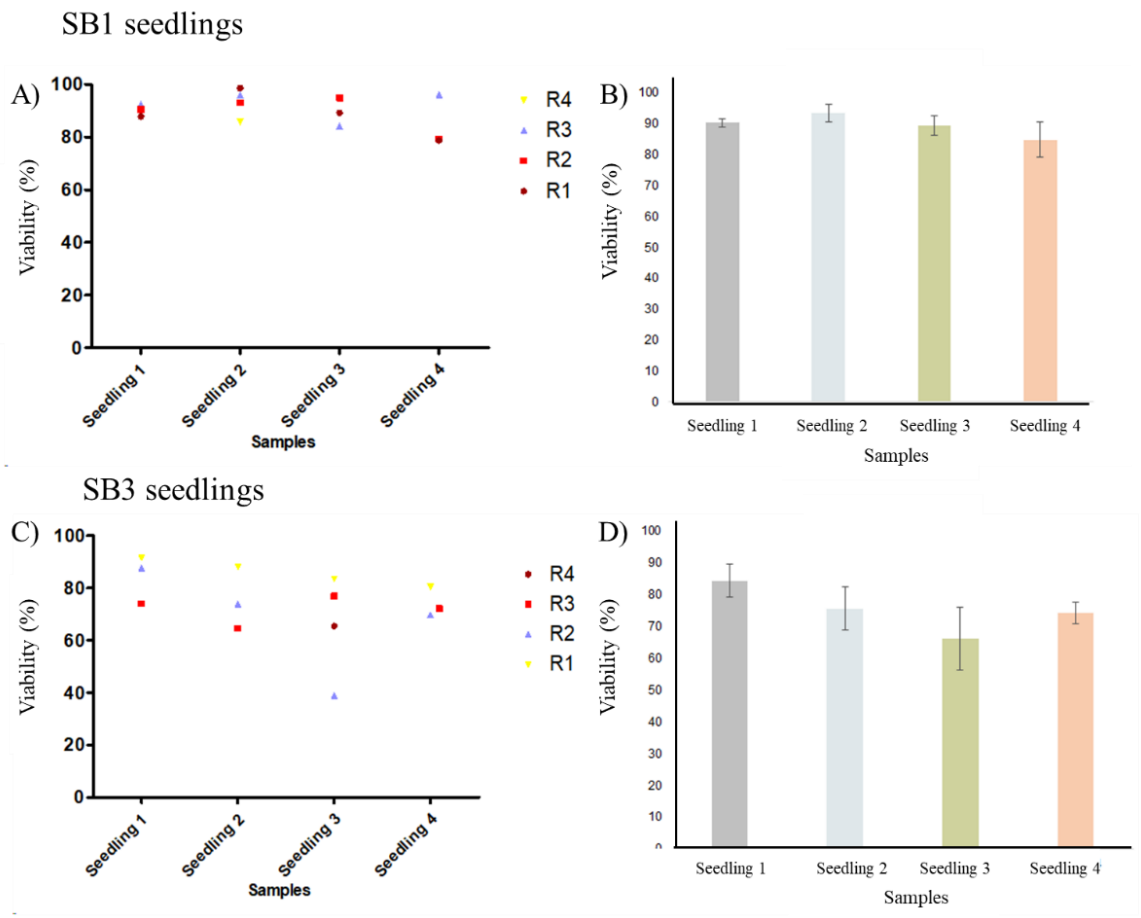


**Figure 3.4** – Evaluating root hair viability in spring barley SB1(A-B) and SB3 (C-D) varieties. Scatter-plots (A, C) reflect differences between (intra-) roots of the same seedlings, while bar-charts (B, D) reflect the average viability of all the roots of the same seedling to compared (inter-) differences between samples. Values represent n ≥3 (± SE).

**Key:** R1= Root 1, R2 = Root 2, R3 = Root 3, R4 = Root 4.

**Table 3.2** - Statistical analysis of the differences in average viability levels between (A) SB1 and (B) SB3 seedlings. A one-way ANOVA Tukey post-hoc test showed no significant differences ($p$>0.05) between all four seedlings. The average value for each seedling was represented by n ≥3.

| (A) SB1 seedlings | | PCD Mean Difference (%) | Std. Error | Sig. |
|---|---|---|---|---|
| 1 | 2 | -3.13 | 4.8 | 0.912 |
| | 3 | 0.83 | 5.13 | 0.998 |
| | 4 | 5.6 | 5.13 | 0.703 |
| 2 | 1 | 3.13 | 4.8 | 0.912 |
| | 3 | 3.97 | 4.8 | 0.840 |
| | 4 | 8.73 | 4.8 | 0.324 |
| 3 | 1 | -0.83 | 5.13 | 0.998 |
| | 2 | -3.97 | 4.8 | 0.840 |
| | 4 | 4.77 | 5.13 | 0.790 |
| 4 | 1 | -5.6 | 5.13 | 0.703 |
| | 2 | -8.73 | 4.8 | 0.324 |
| | 3 | -4.77 | 5.13 | 0.790 |

| (B) SB3 seedlings | | PCD Mean Difference (%) | Std. Error | Sig. |
|---|---|---|---|---|
| 1 | 2 | 8.9 | 11.14 | 0.853 |
| | 3 | 18.27 | 10.42 | 0.353 |
| | 4 | 10.23 | 11.14 | 0.796 |
| 2 | 1 | -8.9 | 11.14 | 0.853 |
| | 3 | 9.37 | 10.42 | 0.806 |
| | 4 | 1.33 | 11.14 | 0.999 |
| 3 | 1 | -18.27 | 10.42 | 0.353 |
| | 2 | -9.37 | 10.42 | 0.806 |
| | 4 | -8.03 | 10.42 | 0.866 |
| 4 | 1 | -10.23 | 11.14 | 0.796 |
| | 2 | -1.33 | 11.14 | 0.999 |
| | 3 | 8.03 | 10.42 | 0.866 |

## 3.3.2 Evaluating the stress response in *H. vulgare* seedlings

### 3.3.2.1 Evaluating *H. vulgare* varieties for thermotolerance

Four winter barley (WB) and three spring barley (SB) varieties were tested for their thermotolerance by stressing 1-day-old seedlings for 10 minutes at temperatures ranging from 25 to 55 °C. Based on the changing cell mode ratios across the temperature gradient, three stress-response phases were noted: 1) stress-tolerant (25 °C) where PCD levels were at their lowest and necrosis levels were negligible, 2) the viable/PCD inflection point (35 °C), and 3) the PCD zone (45-55 °C) where the majority of root hairs died by PCD. A clear distinction was observed between the seasonal varieties as all three spring varieties had consistently lower PCD levels at low heat stress (25-35 °C) compared to their four winter counterparts (Figure 3.5). The PCD levels of the spring barley varieties remained stable (10-17%) across 25 °C and 35°C heat stress, unlike the winter varieties which increased when heat stress was increased from 25 °C (35% to 40%) to 35 °C (43% to 63%). Statistical analysis confirmed these observations: PCD levels only changed significantly ($p$<0.05) in WB1, WB2 and WB4 seedlings when heat stress was increased from 25 °C to 35 °C but remained stable in the remaining varieties (Supplementary Table S3).

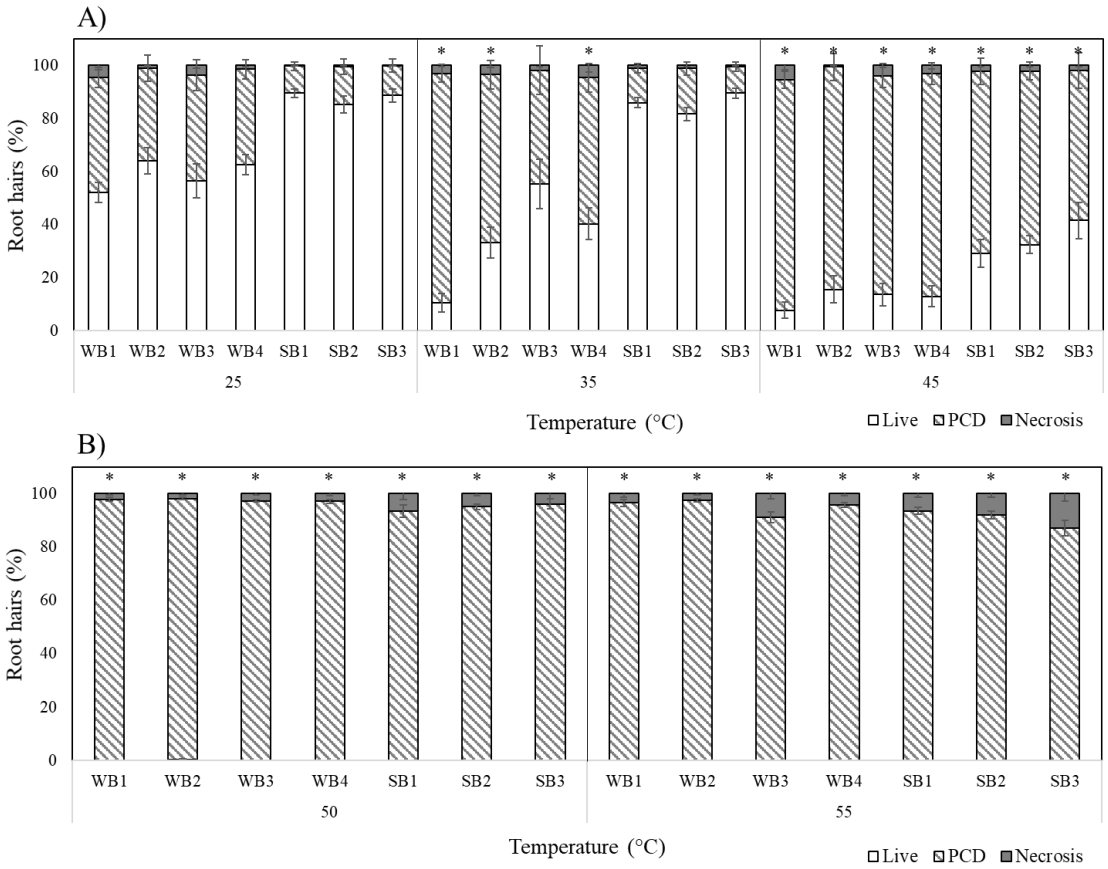


**Figure 3.5** - Effect of (A) low-to-medium or (B) high heat stress on root hair viability and cell death (PCD and necrosis) levels in varieties of winter (WB1-4) and spring (SB1-3) barley. (*) indicates PCD results significantly ($p$<0.05) different from the 25 °C dataset (Supplementary Table S3). Values are the average of n ≥ 8 (± SE) and represent the merged results of at least 2 experiments. Each cell mode is represented as the percentage of cell mode over total number of root hairs, where viability% + PCD% + necrosis% = 100%.

A similar trend was noted at medium heat stress (45 °C) where spring varieties remained more resistant to heat shock, with average PCD levels of 63%. In contrast, PCD levels of all four winter barley varieties was significantly higher (83-87%) at 45 °C. At high stress (50-55 °C), no difference was observed between winter and spring varieties as viability levels declined to ~0%, with PCD being the predominant cell death mode across all varieties. Figure 3.5A illustrates the clear thermotolerance differences between seasonal varieties: at low-to-medium heat shock, spring varieties maintained low PCD levels, unlike heat-susceptible winter barley varieties. Stress-induced PCD was the predominant cell mode across all varieties at 45 °C, while necrosis levels were generally unchanged at temperatures up to 50 °C, but started to increase at 55 °C in WB3 and SB3 (Figure 3.5B).

### 3.3.3 Evaluating the stress response in *T. aestivum* seedlings

#### 3.3.3.1 Evaluating *T. aestivum* varieties for thermotolerance

Four spring wheat (SW) and four winter wheat (WW) varieties were tested for their resilience to transient heat stress (Figure 3.6). Like barley seedlings, wheat seedlings had three stress-response phases: stress tolerant (25 °C), viable/PCD inflection point (35 °C) and the PCD zone (45-55 °C). Mixed tolerance was seen across both spring and winter varieties. At low heat stress (25 °C), WW1 had the highest PCD levels (53.2%), followed by SW4 (36.8%) and SW3 (23.9%). A comparable trend was observed at 35 °C as SW4, WW1 and WW4 had the highest PCD (46-47%) of all the varieties, with limited changes in viability and necrotic levels. Interestingly, distinctions between the thermotolerance of wheat varieties was detected as early as 35 °C which was determined as the viable/PCD inflection point. Apart from WW2, WW3 and WW4 whose PCD levels rose significantly ($p<0.05$) as heat shock increased from 25 °C to 35 °C, the remaining varieties maintained similar PCD levels despite the increase in stress intensity (Supplementary Table S4). At higher heat stress (45 °C), the variations in PCD levels receded as most wheat varieties had ~80% PCD, although SW1, SW2 and WW4 lines still exhibited remarkable heat resistance, with stress-induced PCD levels ranging from 63 to 71%. Beyond this point, viability levels declined to ~0%, with PCD remaining the primary death mode from 50-55 °C. Even at 55 °C heat shock, necrotic levels remained remarkably stable across the wheat varieties and temperature gradient, apart from WW1 and WW2 seedlings which had a 2- to 3-fold increase in necrotic levels, compared to their nearest 50 °C data-point.

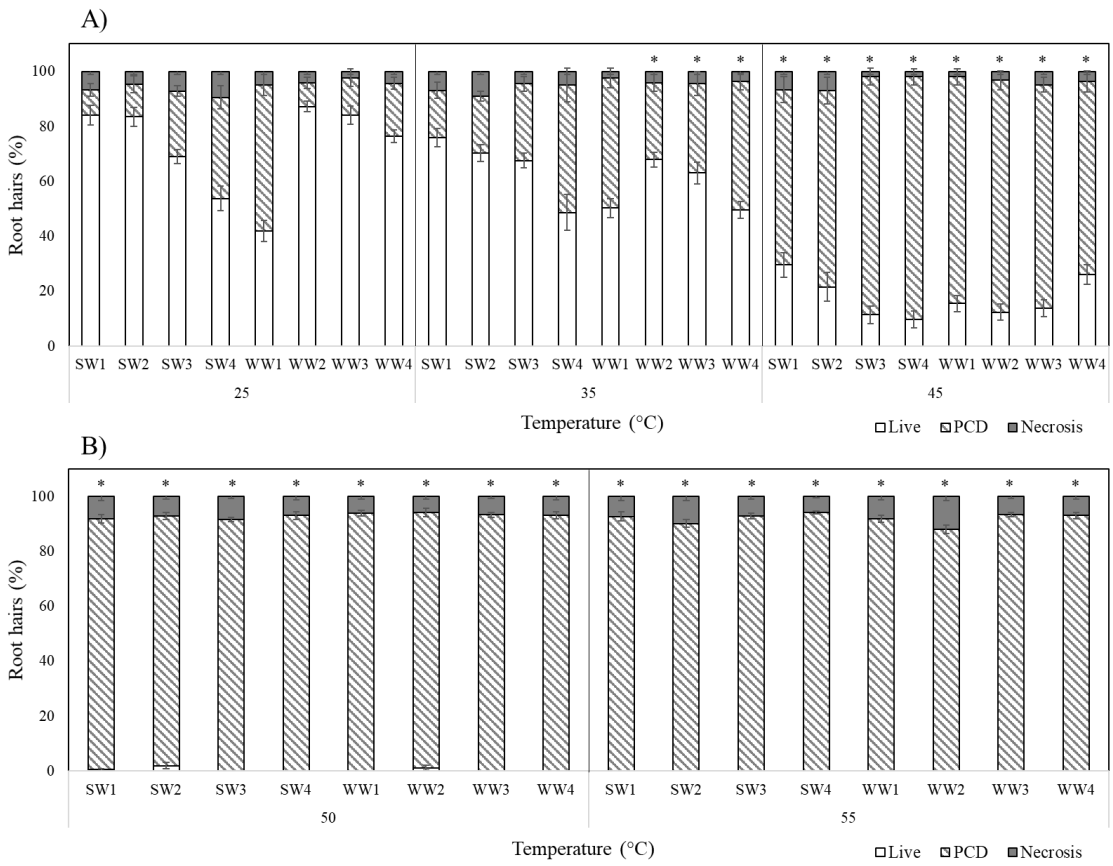


**Figure 3.6** - Effect of (A) low-to-medium or (B) high heat stress on root hair viability and cell death (PCD and necrosis) levels of four spring wheat (SW1-4) and four winter wheat varieties (WW1-4). (*) indicates PCD results significantly ($p<0.05$) different from the 25 °C dataset (Supplementary Table S4). Values are the average of $n \geq 12$ (± SE) and represent the merged results of 3 experiments. Each cell mode is represented as the percentage of cell mode over total number of root hairs, where viability% + PCD% + necrosis% = 100%.

### 3.3.3.2 Evaluating *T. aestivum* varieties for salt tolerance

Four spring wheat (SW1-4) and four winter wheat (WW1-4) varieties were tested for their tolerance to transient salt stress, ranging from 50-200 mM NaCl. Distinguishing between viable and PCD root hairs in salt-stressed wheat seedlings was more challenging compared to heat-shocked seedlings, owing to cell plasmolysis. Figure 3.7 demonstrates the mixed markers (retracted cytoplasm but fluorescent) exhibited by some root hairs under salt-stress. This was reminiscent of the 'stalled death' morphology first reported by Kacprzyk *et al.* (2017), where PCD has been initiated but not fully progressed to completion. When root hairs with mixed markers were encountered, they were rinsed with SDW and remounted without additional FDA staining to remove excessive background florescence. This made it easier to distinguish between viable (strong florescence) and PCD (weaker fluorescence, coupled with granular and partially retracted cytoplasm under white light) root hairs. Figure 3.7A illustrates the differences between viable (white arrow) and PCD root hairs (black arrow) under fluorescent light, Figure 3.7B is the same visualisation but visualised under white light, whereas Figure 3.8C shows the microscopic view when both images are super-imposed over each other.

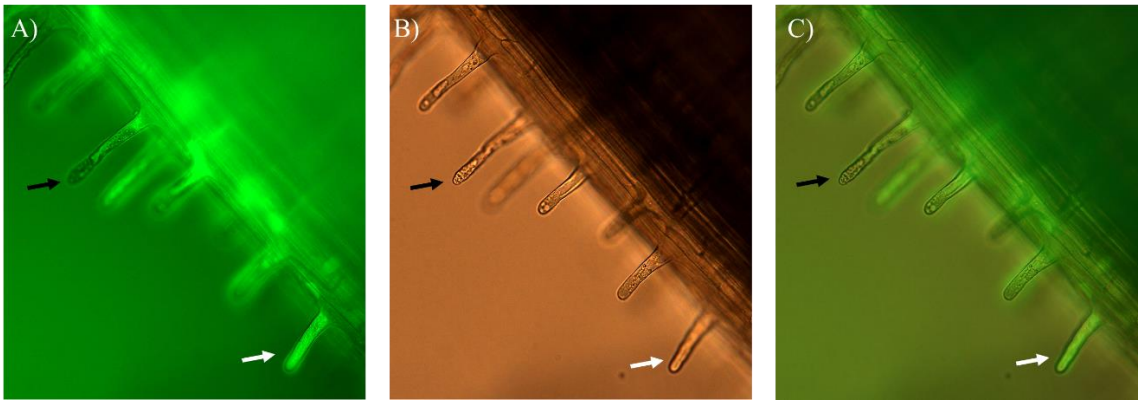


**Figure 3.7** - Mixed markers (FDA positive but retracted cytoplasm) of salt-shocked wheat (*T. aestivum*) root hairs under (A) fluorescent light, (B) full spectrum white light, and (C) when both images are superimposed. Note the difference in fluorescence magnitude between viable root hairs (white arrow), and PCD root hairs (black arrow). Images authors own and captured using an Olympus BX61 microscope under 400X magnification.

Following the optimisation of the scoring procedure, the wheat varieties were tested for their tolerance to transient salt stress (Figure 3.8) and three stress-response phases were detected: stress-tolerant (50-100 mM NaCl), viable/PCD inflection point (150 mM NaCl), and the PCD zone (200-250 mM NaCl). Even at low salt stress (50-100 mM),

distinctions between the salt tolerant varieties were seen as SW4 consistently had the highest PCD levels (~35%) out of all the varieties, followed by WW1 and WW2 (27-33%). In contrast, SW1, SW2, WW3, WW4 were identified as the salt-tolerant lines as they had the lowest stress-induced PCD (15-20%) out of all the varieties.

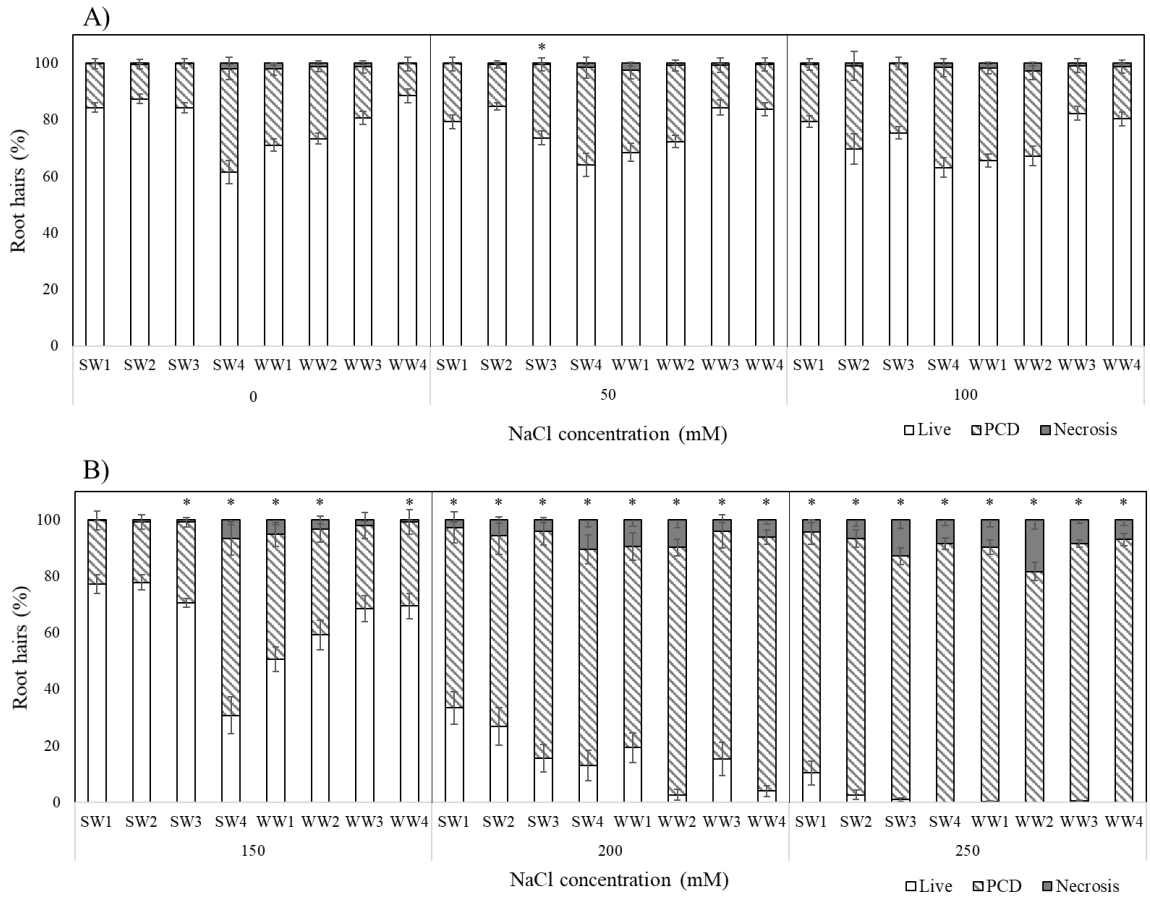


**Figure 3.8** –Effect of (A) low or (B) medium-to-high salt stress on root hair viability and cell death (PCD and necrosis) levels of four spring wheat varieties (SW1-4) and four winter wheat varieties (WW1-4). (*) indicates PCD results significantly ($p<0.05$) different from the 0 NaCl (i.e. SDW control) dataset (Supplementary Table S5). Values are the average of $n \geq 12$ (± SE) and represent the merged results of 3 experiments. Each cell mode is represented as the percentage of cell mode over total number of root hairs, where viability% + PCD% + necrosis% = 100%.

The discrepancies became even larger when effects were examined at 150 mM NaCl (viability/PCD inflection point); PCD levels predictably increased across all varieties but the same three varieties (SW4, WW1 and WW2) had elevated PCD levels compared to other varieties tested. WW1 and WW2 had PCD levels ranging from 37-44%, while SW4 had almost double PCD levels (62.6%), an 27.2% increase from its nearest 100 mM data-point. The remaining five varieties had similar PCD levels ranging from 21-

30%. Beyond this point, medium salt stress (200-250 mM) caused PCD to become the predominant cell mode over viable and necrosis levels. Interestingly, SW1 and SW2 still had the lowest PCD levels at 200 mM NaCl (64-68%), indicative of their salt tolerance, since the average PCD levels across the other varieties was 80.9%. Nevertheless, this discrepancy disappeared at higher NaCl doses (250 mM) as PCD (85-93%) became similar across all eight varieties Necrosis levels did not change significantly across the salt treatments, except WW2 whose necrosis levels doubled when NaCl treatment was increased from 200 mM (9.8%) to 250 mM (18.3%).

### 3.3.3.3 Screening wheat varieties for dual stress tolerance to heat and salt

As explained in the preceding sections, three stress-response phases were noted across the heat and salt stress gradients: stress-tolerant, viable/PCD inflection point, and the PCD zone. The discovery of the three distinct stress-response phases across all the heat and salt stress gradients prompted the preparation of a tolerance matrix (Table 3.3) to determine if wheat varieties displayed dual tolerance to both heat and salt stress.

**Table 3.3** - Tolerance matrix examining the tolerance and susceptibility of wheat seedlings to salt and heat stress at different stress-response phases (stress-tolerant, viable/PCD inflection point and PCD zone) highlights SW1 and SW2 as stress tolerant varieties.

**Key**: '**X**' = Stress-susceptible, '++' = stress-tolerant, '+' = moderately stress-tolerant

| | | **Variety** | | | | | | | |
|---|---|---|---|---|---|---|---|---|---|
| **Stress-response Phase** | **Stress Applied** | **SW1** | **SW2** | **SW3** | **SW4** | **WW1** | **WW2** | **WW3** | **WW4** |
| **Stress-tolerant** | **25 °C** | ++ | ++ | **x** | **x** | **x** | ++ | + | + |
| | **PCD (%)** | 9.1 | 11.9 | 23.9 | 36.8 | 53.2 | 8.66 | 13.7 | 19.2 |
| | **50 mM NaCl** | + | ++ | **x** | **x** | **x** | **x** | ++ | ++ |
| | **PCD (%)** | 20.4 | 15.0 | 26.0 | 34.4 | 29.0 | 26.9 | 15.0 | 15.9 |
| **Viable/PCD inflection point** | **35 °C** | ++ | ++ | + | **x** | **x** | + | + | **x** |
| | **PCD (%)** | 17.3 | 20.7 | 28.0 | 46.5 | 47.4 | 28.0 | 32.7 | 46.7 |
| | **150 mM NaCl** | ++ | ++ | + | **x** | **x** | **x** | + | + |
| | **PCD (%)** | 22.5 | 21.5 | 28.5 | 62.6 | 44.3 | 37.3 | 29.4 | 29.7 |
| **PCD zone** | **45 °C** | ++ | + | **x** | **x** | **x** | **x** | **x** | + |
| | **PCD (%)** | 63.8 | 71.5 | 86.9 | 88.3 | 82.6 | 84.5 | 81.3 | 70.3 |
| | **200 mM NaCl** | ++ | ++ | **x** | + | + | **x** | **x** | **x** |
| | **PCD (%)** | 63.8 | 67.6 | 80.1 | 76.5 | 71.1 | 87.4 | 80.5 | 89.7 |

As previously stated, the largest deviations in stress-induced PCD levels arise at the inflection point, making it easier to compare differences in the tolerance strength of the varieties. While fluctuations do occur at the other phases, stress-induced PCD levels tend to cluster too closely to pick out subtle variations between the investigated varieties. For example, PCD is generally low in the stress-tolerant zone, but predominantly high in the PCD zone. Consequently, emphasis was placed on the performance at the viable/PCD inflection point to identify stress-tolerant or susceptible varieties.

The first stress-tolerant phase (25 °C; 50 mM NaCl) denotes the phase where cell protective mechanisms can repair oxidative damage, thereby maintaining high viability and low PCD levels. As illustrated in Figure 3.9 and Table 3.3, low salt tolerance was observed in SW3, SW4, WW1 and WW2 seedlings, with PCD levels ranging from 26-34%, compared to the remaining seedlings exhibiting PCD of 15-20%. Similar varieties were also found to be susceptible to minimal (25 °C) heat stress, as elevated PCD levels were found in SW3 (23.9%), SW4 (36.8%) and WW1 (53.2%), and to a certain extent, WW4 (19.2%). This was substantially different from the four remaining varieties which averaged 10.8% PCD. Lines tolerant to heat stress include SW1, SW2 and WW2 which had PCD levels between 9-12%, while NaCl-tolerant lines include SW2, WW3 and WW4 which had ~15% PCD.

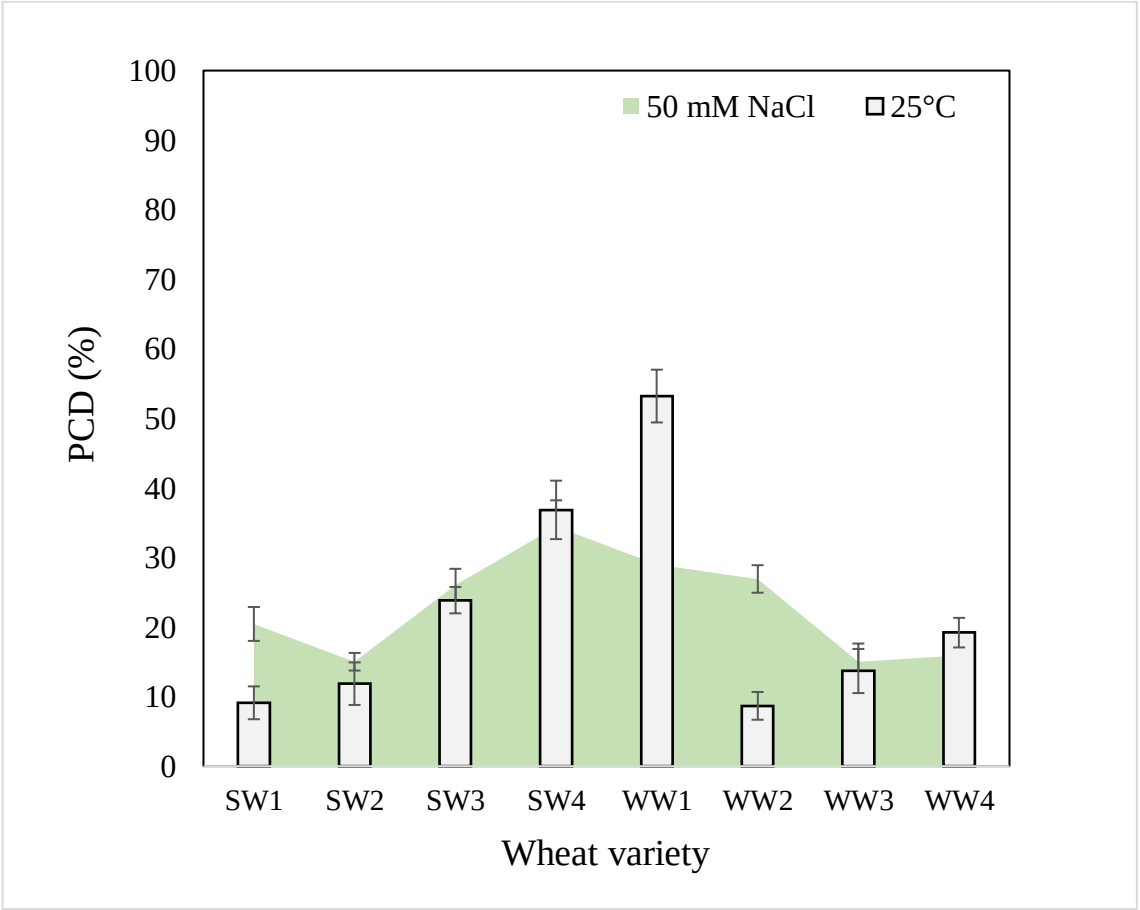


**Figure 3.9** - Evaluating PCD levels at the stress-tolerant phase in wheat seedlings by overlaying heat (25 °C) and salt (50 mM) stress datasets.

A similar trend was observed at the viable/PCD inflection point (35°C; 150 mM NaCl) as shown in Figure 3.10 and Table 3.3. At 150 mM NaCl, the highest PCD values were seen in SW4 (62.6%), WW1 (44.3%) and WW2 (37.3%), while the PCD levels in the other lines only ranged between 21-30%. The lowest PCD levels at 150 mM NaCl were seen in SW1 and SW2 which had ~22% PCD. Under 35°C heat stress, elevated PCD (~47%) was seen in SW4, WW1 and WW4, whereas the lowest PCD levels were seen in SW1 (17.3%) and SW2 (20.7%), and the remaining varieties ranged from 28-33% PCD. Collectively, these results show that similar wheat varieties displayed dual tolerance (SW1 and SW2) or susceptibility (SW4 and WW1) to independent heat and salt stress.

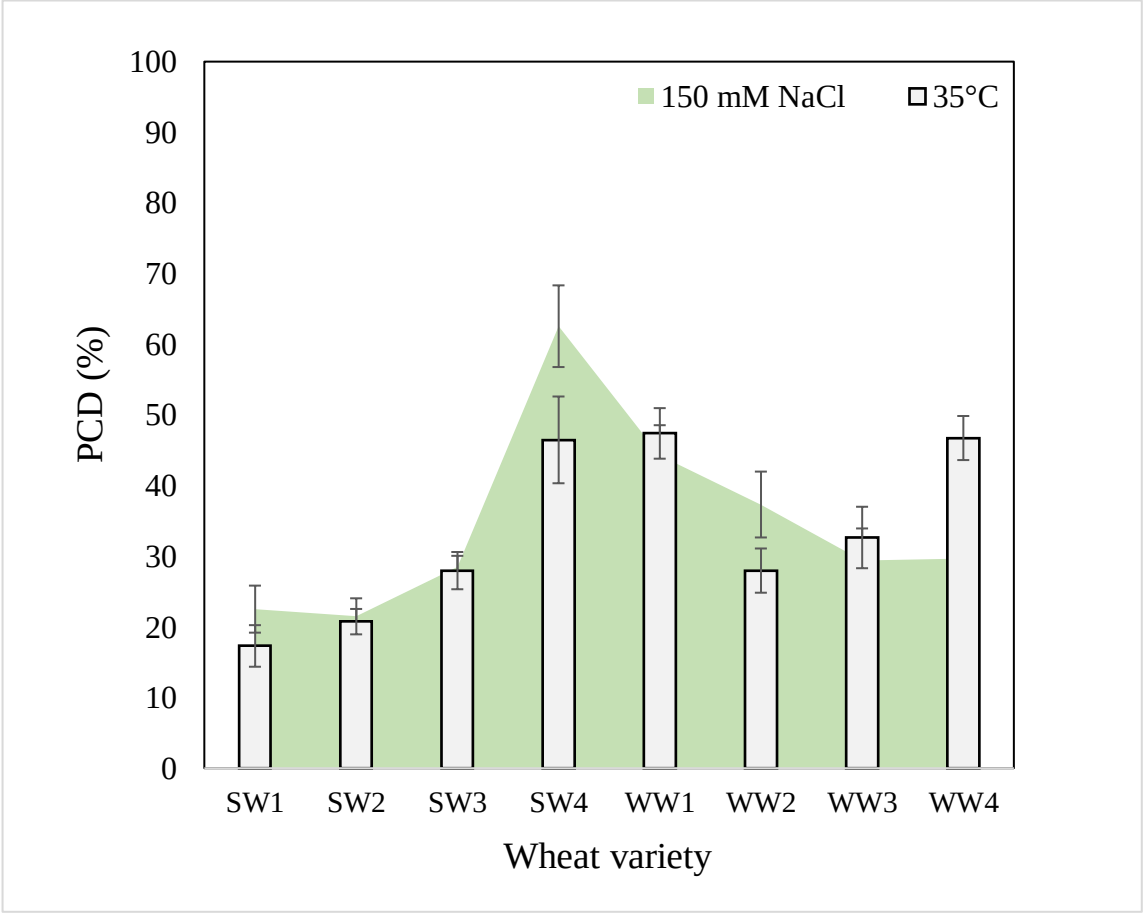


**Figure 3.10** - Evaluating PCD levels at the viable/PCD inflection point in wheat seedlings by overlaying heat (35°C) and salt (150 mM) stress datasets.

Finally at the PCD zone (45°C; 200 mM NaCl), SW1 and SW2 were the only varieties that maintained PCD levels lower than 70% at 200 mM NaCl (Figure 3.11). The rest of the varieties had elevated PCD values, with the highest PCD levels (80-90%) being observed in SW3, WW2, WW3 and WW4. At 45°C, SW1, SW2 and WW4 had the lowest PCD levels (64-71%), while all the remaining lines had PCD levels >81%.

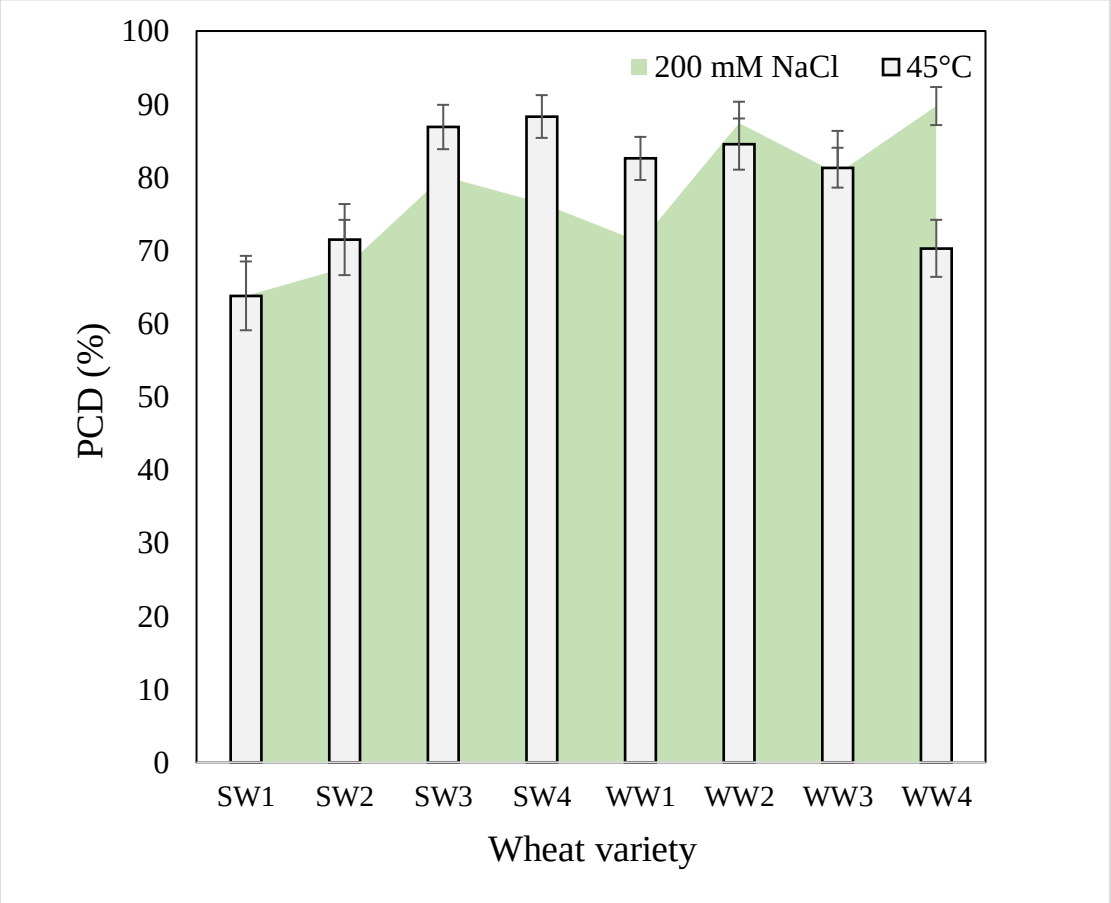


**Figure 3.11** - Evaluating PCD levels at the PCD zone in wheat seedlings by overlaying heat (45°C) and salt (200 mM) stress datasets.

### 3.3.4 Evaluation of *T. aestivum* varieties for basal, induced and cross-stress tolerance to heat and salt stress

Three types of stress exposure were investigated in this study: single, combined and multiple individual stresses. Basal tolerance of the seedlings was examined at the viable/PCD inflection point by applying single (35 °C or 150 mM NaCl) or combined stress (simultaneous heat and salt stress exposure a the 0-min timepoint). The adaptive tolerance was evaluated by administering the first stress trigger (heat or salt) at the 0-min mark, followed by the second stress across three time-points (30, 60 and 120 minutes).

Figure 3.12 depicts how each individual wheat variety responds to unique stress exposures as a function of their stress-induced PCD levels. Given that basal tolerance reflects the genetically pre-determined ability to withstand stress without prior exposure (Arbona *et al.* 2017), SW1 and SW2 were identified as varieties with high basal tolerance, while SW4 and WW2 were singled out as varieties with low basal tolerance, based on their performance against single and combined stress treatments (Section 3.3.4.2). Interestingly, varieties with high basal tolerance (SW1 and SW2) had a slow induced tolerance response, unlike stress-susceptible SW4 and WW1 which adapted faster (Section 3.3.4.3).

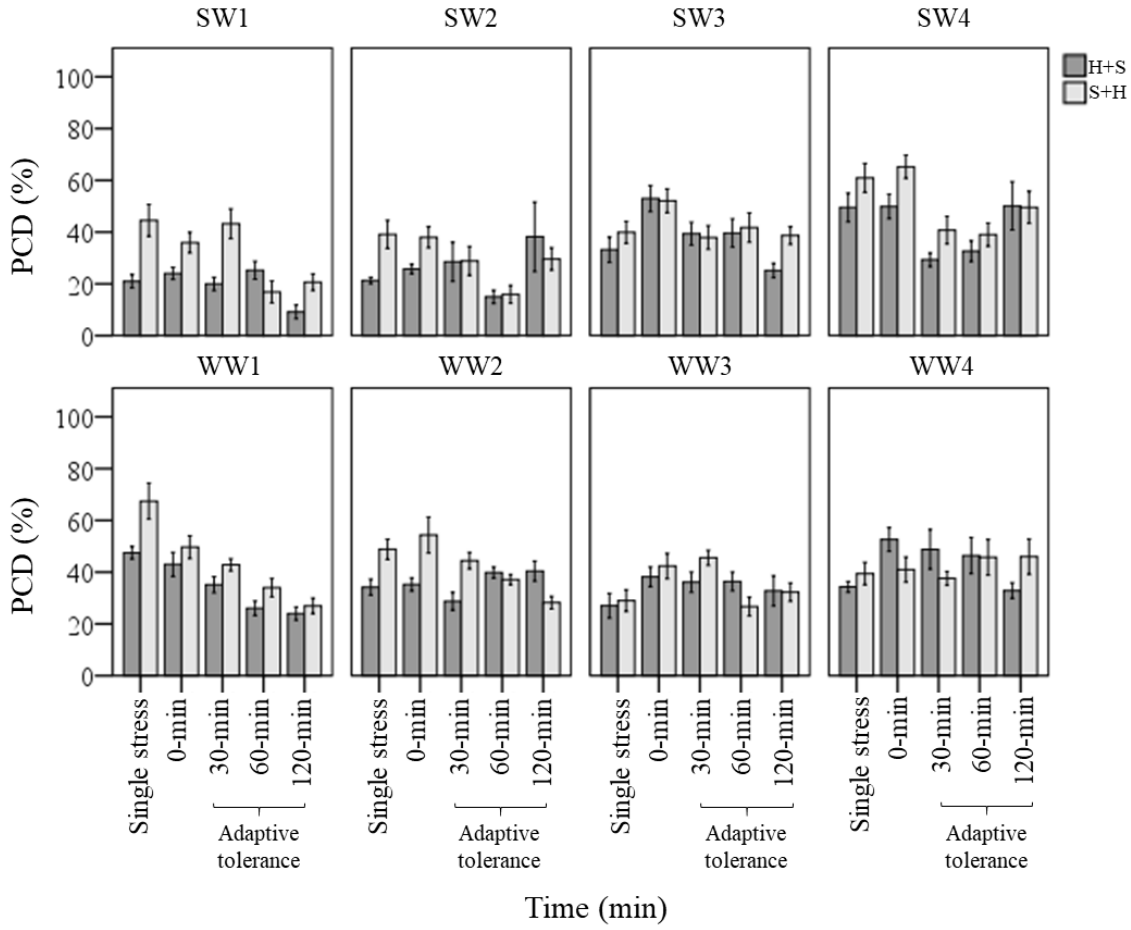


**Figure 3.12** - Examining how single, combined and multiple individual stress exposures affects stress-induced PCD in wheat varieties. The initial stress cue (35 °C heat or 150 mM NaCl) is applied at the 0-min mark, followed by the second stress application at different time-points (30, 60 and 120-min). (H+S) refers to heat stress as the initial cue, followed by salt stress, while (S+H) refers to salt stress as the first cue, followed by heat stress at the relevant time-points. Values are the average of $n \geq 4$ (± SE) and represent the merged results of ≤3 experiments.

By varying the initial stress cue, a few interesting overall trends were noted, which were not immediately apparent from the data presented in Figure 3.12. For that reason, the average stress-induced PCD levels of all eight varieties were merged (Figure 3.13). After controlling for the H+S, and S+H datasets, the following trends were revealed. Firstly, cross-stress tolerance experiments showed that stress acclimation and priming were the predominant responses when seedlings were either first heat or salt-shocked, respectively (Section 3.3.4.1). Secondly under combined stress, seedlings that were first salt shocked had similar PCD levels (47.8%) as the single stress-factor control (46.3%), but initially heat shocked seedlings had greater stress-induced PCD (40.8%) compared to the heat stressed only dataset (34.1%) (Section 3.3.4.2). Next, varieties with high basal tolerance (SW1 and SW2) had a slower induced tolerance response, unlike stress-susceptible SW4 and WW1 which responded faster to the second stress cue (Section 3.3.4.3). Finally, salt stress had a dominating effect over heat stress, and that initial salt shock had a lagging PCD-suppressing effect (Section 3.3.4.4).

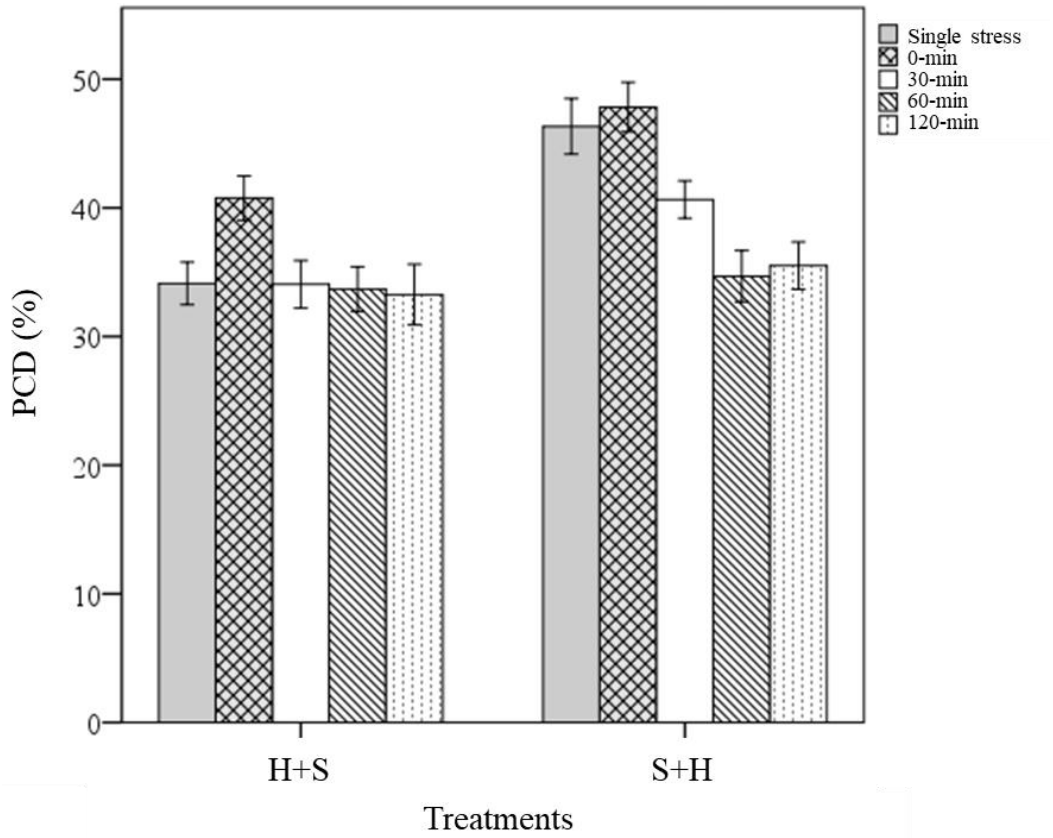


**Figure 3.13** – Overall trends noted in stressed wheat seedlings by varying the initial stress cue. Values represent the average PCD levels across the eight varieties, where n ≥ 4 (± SE) and represent the merged results of ≤3 experiments.

### *3.3.4.1 T. aestivum* cross-stress tolerance depends on the initial stress cue

Cross-stress tolerance was evaluated in terms of priming (lower PCD levels), acclimation (neutral PCD levels) and predisposition (higher PCD levels) to the second applied stress type, compared to their respective single stress-factor datasets (Figure 3.14). When heat was applied as the first stimulus and followed by subsequent NaCl shock, only SW4 and WW1 were grouped under the primed category, while the remaining varieties fell under the acclimation category. However, wheat varieties responded differently when they were first subjected to NaCl shock, followed by later heat stress. Despite maintaining identical stress doses, the varieties were re-shuffled into different categories: primed (SW1, SW2, SW4, WW1 and WW2) and acclimation (SW3, WW3 and WW4). Predisposition was not observed across both datasets, regardless of the initial stress cue. Thus, stress acclimation was the primary response (75%) when heat-shocked wheat varieties were assessed for their cross-stress tolerance to subsequent salt stress, Conversely, priming (62.5%) was the dominant mode in varieties first treated with salt stress, even though identical stress doses were maintained.

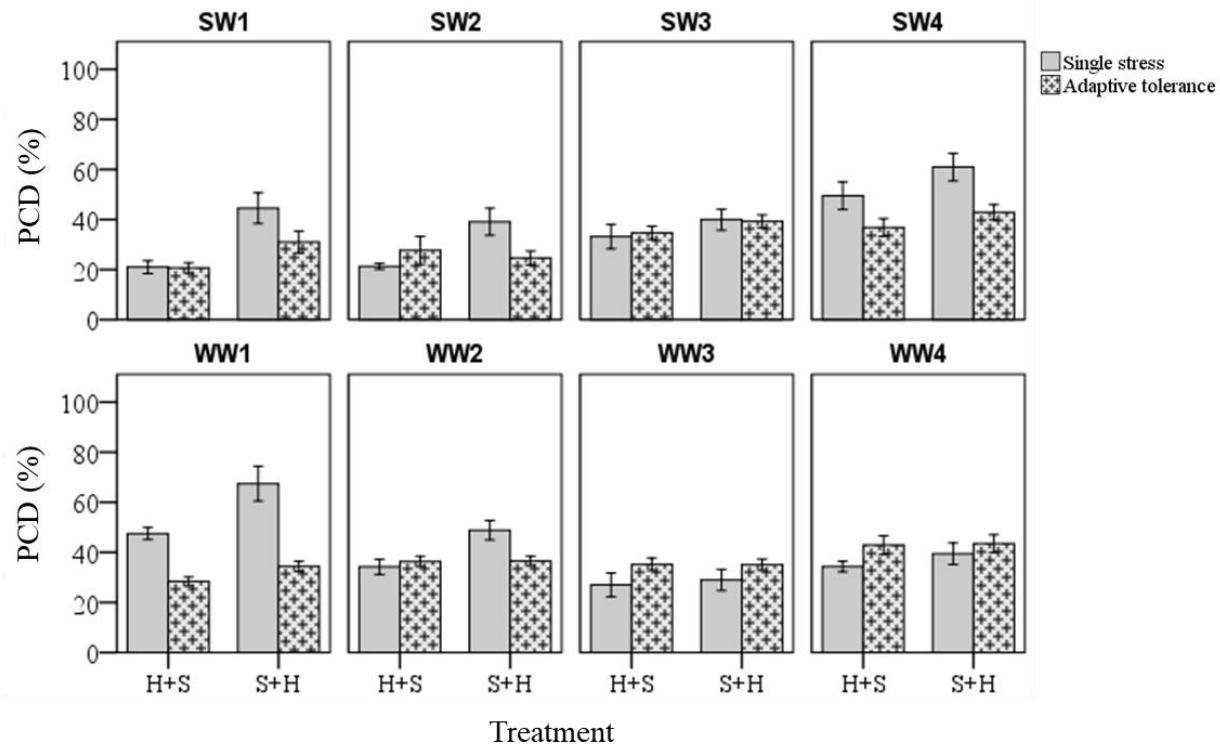


**Figure 3.14** – Induced tolerance changes across individual wheat varieties and different initial stress cues. Values represent the average PCD levels across 30, 60 and 120-min datasets, where n ≥ 4 (± SE) and represent the merged results of ≤3 experiments.

The tendency for specific stress responses based on the initial stress cue (e.g. stress acclimation in H+S; priming in S +H) is illustrated in Figure 3.13, which depicts the average PCD levels of all the varieties across both H+S and S+H datasets. When heat shock was the initial stress-cue, similar PCD levels (33-34%) were noted between the single heat stress-factor and the multiple stress (30, 60 and 120 mins) dataset. This shows that additional salt shock did not negatively affect previously heat stressed seedlings, i.e. seedlings were stress-acclimatised to recurrent exposure. However, a different stress response pattern emerged when salt stress was the initial stress cue; exposure to NaCl successfully primed seedlings to subsequent heat damage as lower PCD levels were recorded at the 30, 60 and 120-min datasets compared to the single NaCl stress-factor dataset. Despite maintaining identical stress doses, these results demonstrate that initial exposure to different stress cues can result in divergent stress-responses. To further corroborate these results, Table 3.4 highlights how the individual wheat varieties respond differently across the H+S and S+H treatments, in terms of repetitive (cross-stress tolerance) and combined (basal tolerance) stress exposure.

**Table 3.4** - Stress matrix summarizing the effect of (A) cross-stress tolerance and (B) the combined stress in response to heat and salt shock in wheat varieties.

**Key:** '+' denotes a reduction in stress-induced PCD levels, '=' denotes no substantial PCD changes and '-'indicates a net rise in PCD levels from their respective single stress-factor controls.

A) Cross-stress tolerance

| Treatment | SW1 | SW2 | SW3 | SW4 | WW1 | WW2 | WW3 | WW4 |
|---|---|---|---|---|---|---|---|---|
| H+S | = | = | = | + | + | = | = | = |
| | 0% | 7% | 2% | -13% | -19% | 2% | 8% | 9% |
| S+H | + | + | = | + | + | + | = | = |
| | -14% | -14% | -1% | -18% | -33% | -12% | 6% | 4% |

Key for (A): '+' priming, '=' stress acclimation and '-' predisposition.

(B) Combined stress interactions

| Treatment | SW1 | SW2 | SW3 | SW4 | WW1 | WW2 | WW3 | WW4 |
|---|---|---|---|---|---|---|---|---|
| H+S | = | = | - | = | = | = | - | - |
| | 3% | 5% | 20% | 0% | -4% | 1% | 11% | 19% |
| S+H | = | = | - | = | + | = | - | = |
| | -9% | -1% | 12% | 4% | -17% | 5% | 13% | 2% |

Key for (B): '+' synergistic, '=' neutral and '-' antagonistic interactions.

### 3.3.4.2 Individual wheat varieties under combined stress exposure exhibit varying stress responses

Basal tolerance to combined stress was assessed by examining the interactions between heat and salt stress in terms of synergistic (lower PCD levels), antagonistic (higher PCD levels), or neutral (no net changes in PCD levels) compared to their respective single stress-factor datasets. The unique stress phenotypes displayed by the individual varieties were organised into a stress matrix (Table 3.4), where most of the stress combination results fell under the neutral (62.5%) category. It was noteworthy to see that varieties previously identified as heat and salt tolerant (SW1 and SW2) by their performance at the viability/PCD inflection point at single stress-factors (Table 3.3) exhibited similar basal tolerance under combined stress exposure. The inverse situation also held true; individual heat and salt-susceptible varieties (SW4 and WW1) also demonstrated higher susceptibility to combined stress exposure. Figure 3.15 depicts the role of basal tolerance in the correlation between single stress-factor and combined stress exposure; for example in the S+H dataset, salt-tolerant varieties (SW1 and SW2) varieties had the lowest PCD levels (36-38%), while salt-susceptible SW4 line had the highest PCD levels (65%). The remaining varieties displayed varying degrees of tolerance: moderately tolerant (WW3 and WW4: 41-42%) and semi-susceptible (SW3, WW1, WW2: 50-54%). A similar scenario was observed in the H+S dataset; thermotolerant SW1 and SW2 varieties had the lowest PCD (24-26%), while the highest PCD levels were seen in SW3, SW4 and WW4 (50-53%). The remaining varieties (WW1, WW2 and WW4) showed varying degrees of tolerance, with PCD ranging from 35 to 43%.

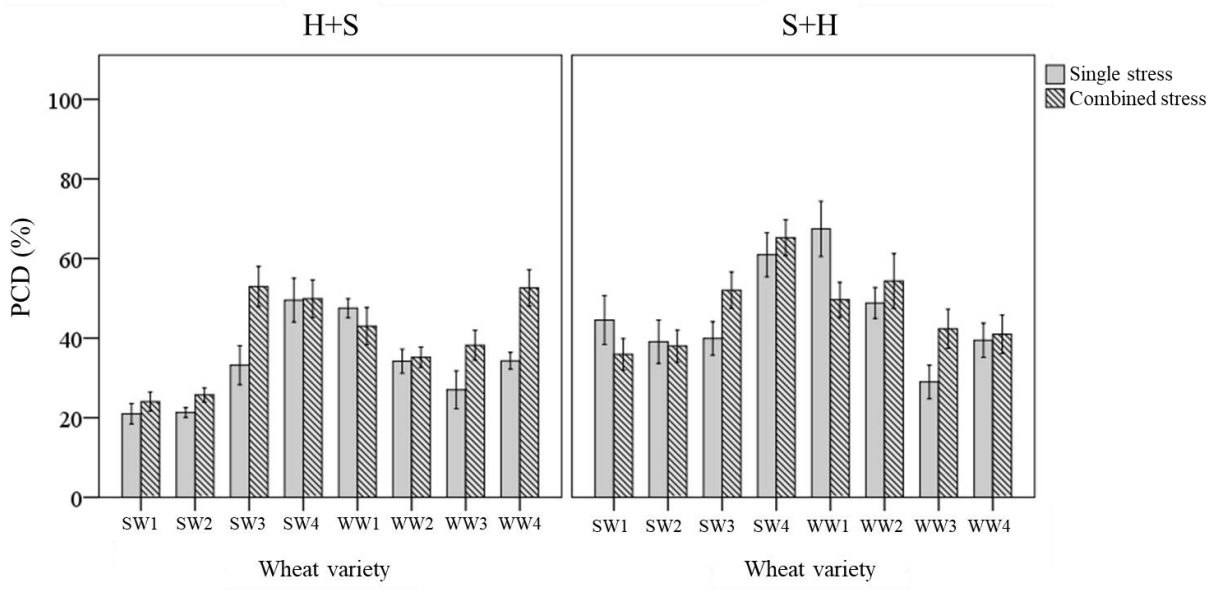


**Figure 3.15** – Basal tolerance varies across wheat varieties and after different initial stress cues. Combined stress PCD data reflect the PCD levels recorded at simultaneous stress exposure (H+S or S+H) at the 0-min mark. Values are the average of n ≥ 4 (± SE) and represent the merged results of ≤3 experiments.

### 3.3.4.3 Stress-tolerant varieties responded slower to priming compared to stress-susceptible varieties

Stress-tolerant varieties were predicted to mount a faster counteracting response than stress-susceptible varieties, but this was not evident here. SW1 and SW2 retained similar PCD levels in the 30 min H+S dataset with their respective single (H only) stress-factor datasets (Figure 3.16). However, cross-stress tolerance to salt stress was only noted at the later stages as PCD levels only decreased significantly at the 60-min (SW2) and 120-min (SW1) timepoints. In contrast, stress-susceptible SW4 reacted faster as PCD levels declined by 21% at the 30-min H+S dataset compared to its single heat stress-factor dataset. A similar pattern, although to a lesser extent, appeared in heat primed WW1 seedlings, whose PCD levels declined by 12% at the 30-min dataset compared to its H-only control. In view of the slower adaptive response in stress-tolerant varieties, heat priming enabled the stress susceptible SW4 line to maintain similar PCD levels (28%) in line with the tolerant SW2 variety, despite additional salt stress exposure at the 30-min timepoint. Considering how the plant stress response is a combination of both basal and induced tolerance, this suggests that a rapid induced response can partially make up for low basal tolerance, given successful priming and sufficient time-lag between repeated stresses.

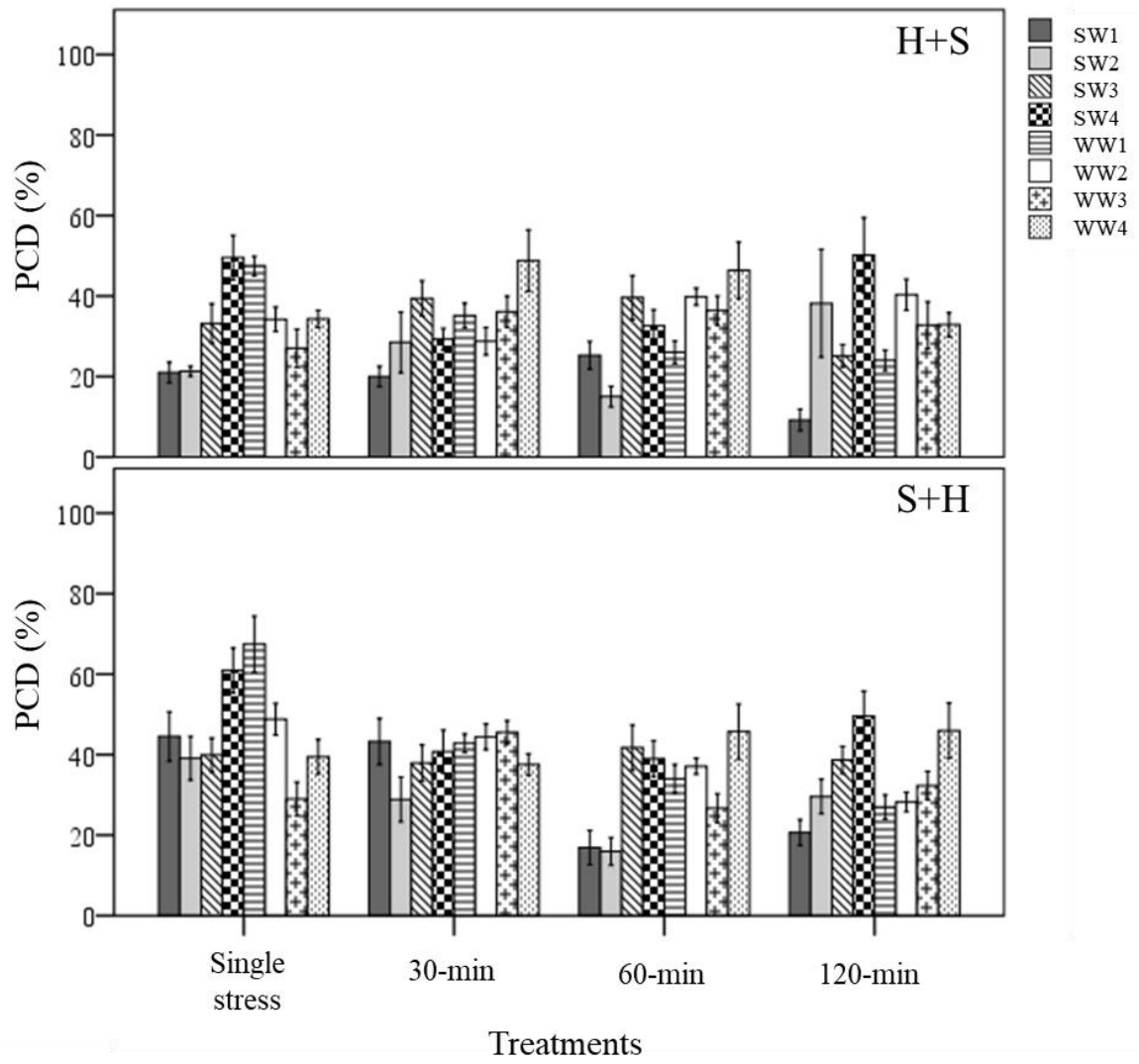


**Figure 3.16** – Examining induced tolerance changes across eight individual wheat varieties after different initial stress cues. The initial stress cue (35 °C heat or 150 mM NaCl) cue is applied at the 0-min mark, followed by the second stress application at different time-points (30, 60 and 120-min). (H+S) refers to heat stress as the initial cue, followed by salt stress, while (S+H) refers to salt stress as the first cue, followed by heat stress at the relevant time-points. Values are the average of $n \geq 4$ (± SE) and represent the merged results of ≤ 3 experiments.

A similar temporal pattern was noted when salt stress was the initial cue; cross-stress tolerance to heat stress only took place at the later stages (60-min) for both stress-tolerant SW1 and SW2 varieties. Like heat priming treatment, salt priming rapidly suppressed PCD levels in varieties with low basal tolerance (SW4 and WW1), to the extent of both lines sharing similar PCD levels (41-43%) as the tolerant SW1 (43%) variety at their respective 30-min S+H datasets. Despite their slower adaptive response, SW1 and SW2 varieties still retained the lowest PCD levels out of all the varieties when the cross-stress tolerant effect finally took place. Regardless of the initial stress, cue, PCD levels at the

60-min dataset for SW1 and SW2, initially primed with heat (15 to 24%) and salt (16 to 17%), were substantively lower than the average PCD values for the remaining varieties across heat (36.8%) and salt stress (37.5%) priming treatments. On balance, this shows that stress-susceptible varieties responded quicker than stress-tolerant varieties as illustrated in Figure 3.16.

### 3.3.4.4 Statistical analysis of the effect of using different initial stress cues on subsequent PCD levels

Results showed that applying salt stress as the initial cue followed with heat stress, exerted a stronger cytotoxic effect on PCD levels ($p$-value = 0.02) compared to the inverse scenario when heat was the first stress cue, despite maintaining identical stress dosages (Table 3.5). Only a small mean difference of 4.3% was observed between the overall (S+H) and (H+S) datasets. However, this only represents the average values across the eight varieties. When controlling for the individual varieties, larger drifts between the H+S and S+H datasets were seen. For example, statistically higher ($p$<0.05) PCD levels in S+H datasets, compared to H+S datasets were seen in SW1 (11.4%), SW4 (8.5%) and WW1 (5.9%), (Supplementary Table S6).

**Table 3.5** – Independent samples $t$-test examining the effects of applying different stress cues as the initial cue on PCD levels. Inputted data consisted of PCD levels scored across 0, 30, 60 and 120-mins.

| | **Group Statistics** | | | ***t*-test for Equality of Means** | | |
|---|---|---|---|---|---|---|
| Initial Stress cue | N | Mean | Std. Error Mean | Sig. (2-tailed) | Mean Difference | Std. Error Difference |
| Heat and Salt (H+S) | 395 | 35.5 | 0.964 | 0.002 | -4.31 | 1.35 |
| Salt and Heat (S+H) | 376 | 39.9 | 0.947 | | | |

It is also worth noting that the stronger PCD-inducing signal in salt-shocked seedlings (S+H) largely disappearing at later stages. When controlling for PCD levels across the different stress-treatment time-points, the S+H datasets had higher PCD levels than their H+S counterparts at 0-min (S+H: 47.8%; H+S: 40.8%) and 30-min (S+H: 40.6%, H+S: 34.1%), but were similar at the later stages at 60-min (33-34%) and 120-min (33-35%). Hence, the longer the lag between stress applications, the better the priming effect as PCD levels decreased concurrently. Statistical analysis confirmed this as both the later datasets (60-and 120-min) were significantly lower ($p$<0.05) than the single salt stress-factor dataset. The results show that given enough time, the salt priming effect resulted in similar

PCD-suppression rates with seedlings first subjected to heat shock. Figure 3.13 depicts the lagging PCD-supressing effect of the initial salt shock cue, while Figure 3.12 shows the how this general behaviour differs from variety to variety.

## 3.4 Discussion

Here, three case studies are used to illustrate how stress-induced PCD levels can be used to investigate cereal stress tolerance. In the first instance, the RHA was used to directly score *in vivo* PCD levels in heat-stressed barley and wheat seedlings. Mixed thermotolerance across the seasonal wheat varieties was observed but a sharp distinction between heat resistant spring and heat susceptible winter barley varieties was also noted.

### 3.4.1 *H. vulgare* and *T. aestivum* thermotolerance

Expansion of cereal yields to satisfy the demands of a rising population is challenging as the rapidly changing meteorological conditions is a damage multiplier that aggravates effects of the ongoing and normal stress conditions that cereals are already subjected to (Reynolds *et al.* 2016). Therefore, yield safety is a growing concern that breeders are focused on when developing new high-yielding crop generations that can resist harsh meteorological events and elevated temperature and $CO_2$ levels. Ideally, this new crop generation should possess high basal and adaptive stress tolerance as climate change exposes plants to both transient and acute heat cycles, and gradual rises in global temperatures (Reynolds *et al.* 2016). This calls for extensive phenotyping work and the work in this chapter seeks to contribute to this endeavour by presenting a workflow for screening cereal seedlings for high basal and adaptive tolerance to multiple stress types.
This chapter outlines the usage of the RHA as a PCD quantification tool for investigating stress-tolerance in cereals by capturing the subtle variations between inter-species (barley and wheat) and intra-species (spring and winter varieties). For example, barley (SB1, SB2 and SB3) and wheat (SW1, SW2 and WW3) varieties tolerant at low 25 °C heat stress had similar PCD levels (8-14%), but PCD levels varied greatly between both species when heat stress was increased to 35 °C. All three spring barley varieties maintained similar PCD levels, with an average value of 13.4%, while the wheat varieties had considerably higher average PCD levels at 23.6%. This is in line with past findings regarding the differences in basal thermotolerance between heat-shocked barley and wheat seedlings (Abernethy *et al*. 1989; Kruse *et al.* 1993).

Upon imbibition, barley seeds express constitutive, developmentally regulated heat shock proteins (HSPs) during the early germination stages to protect against sudden heat shock, before seedling establishment (Kruse *et al.* 1993). HSPs could be detected as early as in

2-day-old barley seedlings, with a unique HSP profile that varied according to the developmental stage. For example, Kruse *et al.* (1993) found that HSP70 was constitutively expressed throughout the growth stages, while HSP26 was found in 2-day-old seedlings, but not at the latter development stages. In addition, transcriptomic analysis showed older seedlings had substantially higher levels of heat shock mRNA compared to younger seedlings (Kruse *et al.* 1993).

In contrast to barley, wheat seeds possessed the highest thermotolerance 9-12 hours after imbibition but lost this protective effect over time; Abernethy *et al.* (1989) detected four (58 to 60, 46, 40, and 14 kDa) developmentally-regulated HSPs following 1.5 hours of imbibition, but these HSPs were largely absent after 12 hours. Similarly, the constitutive expression of 70 and 90 kDa HSP groups were higher at 1.5 hours, than 12 hours of imbibition. The authors attributed the rapid decline of the initially high thermotolerance of germinating wheat seeds to the loss of developmentally-regulated HSPs (Abernethy *et al.* 1989). These studies show that developing barley and wheat seedlings have different temporal regulation patterns of thermotolerance, which might account for the PCD level variances observed in this chapter, particularly at 35 °C.

Besides the inter-species differences, it is interesting to note how quantification of PCD levels captured the intra-species variances between spring and winter varieties. A clear distinction was seen between heat tolerant spring and heat susceptible barley varieties. In contrast, mixed heat tolerance was seen across the wheat spring and winter varieties. Without further investigations, it would difficult to determine why these differences exist as thermotolerance is a polygenic trait controlled by multiple stress-response genes (Hasanuzzaman *et al.* 2013). It is difficult to pinpoint a single gene to establish a cause-and-effect relationship as the plant response to heat stress is spatially and temporally regulated, which differs across tissues and the development stage (Rejeb *et al.* 2014b). The response of plants to heat stress varies from genotype and heat treatment (intensity and duration) but can be divided into stimulus perception, signal transduction and upregulation of heat stress-responsive genes to initiate physiological and biochemical alterations (Hasanuzzaman *et al.* 2013). For example, Qin *et al.* (2008) used transcriptome analysis to evaluate the differences in the gene expression of heat tolerant (TAM107) and heat susceptible (Chinese Spring) wheat varieties. They found that 11% of total heat responsive probe sets responded to short and prolonged heat stress treatments, with 313

probe sets differentially expressed between both wheat genotypes. The thermotolerant variety had stronger expression of heat-responsive genes encoding for HSPs, proteins and transcription factors involved in signalling pathways (phytohormone, $Ca^{2+}$ and sugar), transcription and translation (RNA and ribosomal protein biosynthesis) processes, primary and secondary metabolisms, and proteins related to other abiotic stresses (Qin *et al.* 2008).

Therefore, a multitude of stress-responsive genes are acting in concert to repair heat-induced damage. However, protein denaturation is a primary symptom of heat stress (Wang *et al.* 2004) and evidence suggests that HSP expression might account for the varying thermotolerance exhibited by the seasonal varieties of barley and wheat, as elaborated in Section 3.4.1.1. Plant HSPs can be classified into high (70-110 kDa) and low MW (< 40 kDa) groups and are divided into five different families: Hsp100, Hsp90, Hsp70, Hsp60 and small Hsps (sHsp) (Liu *et al.* 2015). All HSPs classes are molecular chaperones that protect proteins under denaturing conditions, but some have overlapping functions. For example, Hsp70 and Hsp90 regulates the transcription of other HSPs, chaperone, and stress-response proteins via heat-shock factors (HSFs), while sHsp and Hsp70 maintains protein conformation to prevent aggregation (Wang *et al.* 2004).

### 3.4.1.1 Polymorphism around HSP locus

The genetic diversity of HSPs play an important role in conferring heat tolerance; Marmiroli *et al*. (1994) discovered that HSP expression pattern varied across five barley varieties of varying thermotolerance. The 70 kDa HSP was induced in all five genotypes, but low-MW HSP expression varied greatly across the five varieties and exhibited the largest variance at 35 °C and 40 °C (Marmiroli *et al.* 1994). In a later study, Marmiroli *et al.* (1998) found a high degree of polymorphisms at the *Hvhsp17* gene locus that encoded for a low-MW HSP across winter and spring barley varieties. Restriction fragment length polymorphism (RFLP) analysis of two HSPs genes (*TaHSP16.9* and *Hvhsp17*) in 27 barley varieties showed that spring and winter barley varieties could be successfully partitioned into two dendrogram clusters, showing that polymorphisms around the HSP genes accurately predicted winter and spring barley varieties (Marmiroli *et al.* 1998).

Given these points, Marmiroli *et al.* (1998) and Maestri *et al.* (2002) have proposed that HSP molecular diversity is an important predictor for thermotolerance. Apart from

predicting the divergent thermotolerance between spring and winter barley varieties, HSP molecular diversity might also account for the mixed tolerance exhibited in the seasonal wheat varieties. Barley plants are diploid organisms, but wheat plants can either have diploid, tetraploid or hexaploid genomes; polyploid cereals have a higher HSP diversity than diploid cereals because of the additive effect from the subgenomes (Maestri *et al.* 2002). Perhaps this accounts for why mixed tolerance was seen across spring and winter wheat varieties, but not in barley as polyploidy affects HSP diversity and other stress-response genes, culminating in significantly divergent stress phenotypes from their original diploid parents (Arbona *et al.* 2017).

#### 3.4.1.2 Polymorphism around *Vrn1* locus

Besides HSP polymorphisms, two polymorphic vernalization-responsive (*VRN*) loci differentiates winter and spring barley varieties; winter varieties need prolonged exposure to low temperatures to flower, while spring varieties do not require vernalization (Cockram *et al.* 2007). Vernalization in European barley is controlled predominantly by two major loci at *VRN-H1* (also termed *Sh2*/*Sgh2*, located on chromosome 5H), and *VRN-H2* (also termed *Sh*/*Sgh*, located on chromosome 4H), whereas spring barley alleles have deletions in both loci that enables flowering without vernalization (Cockram *et al.* 2007). Conversely, wheat has five *VRN* loci predominantly localised on the long arms of chromosome 5A, 5B and 5D, containing the *Vrn1*, *Vrn2*, *Vrn3* and *Vrn4* loci (Cattivelli *et al.* 2002). Due to the homoeologous relationship between barley and wheat chromosomes, RFLP analysis showed that this region corresponds to the *VRN-H1* locus of barley (Laurie 1997), i.e. barley chromosome 7 is homoeologous to the wheat chromosome 5 (Linde-Laursen *et al.* 2004).

The region near the *VRN-H1* locus has many stress-response genes, which might explain the differences observed here between cereal spring and winter varieties. Dubcovsky *et al.* (1995) investigated the linkage relationships among genes responding to drought, salt and heat stress in diploid *Triticum monococcum* L. and found that the long arm of chromosome 5 had the highest concentration of stress-induced genes, such as dormins, early-salt-induced (*ESI*) genes, dehydrins and HSPs. In another study, Van Zee *et al.* (1995) identified two dehydrin genes (*Dhn1* and *Dhn2*) involved in cold, drought and salt acclimatisation, localised near the region controlling for the winter hardiness quantitative trait loci (QTL) effect on the long arm of barley chromosome 7. Similarly, Quarrie *et al.*

(1994) identified a QTL that regulated ABA biosynthesis in response to drought on wheat chromosome 5. Interestingly, a similar QTL controlling for leaf ABA content under drought was also identified in barley chromosome 7, homoeologous to the chromosome 5 region containing the ABA-associated QTL in wheat (Quarrie *et al.* 1994). The exact function of the QTL was not confirmed but the authors speculate that it might regulate cell membrane fluidity as genetic variation in ABA accumulation correlates to changes in membrane fluidity and ion leakage in salt stressed plants. If this hypothesis were correct, this QTL might also be involved in other responses to counter stress-induced damages to the cell membrane integrity (Quarrie *et al.* 1994). Therefore, the genetic linkage between the *VRN*-H1 loci and other locus modulating the stress-response, might account for the differences observed in stress resistance between winter and spring barley varieties.

### 3.4.2 Salt tolerance in *T. aestivum*

The RHA was also used to investigate the difference in salt tolerance across eight wheat varieties by subjecting seedlings to transient NaCl doses. Mixed salt tolerance was seen across the wheat varieties, which was assessed based on fluctuations in their stress-induced PCD levels, as necrosis was negligible under the tested NaCl gradient. This was especially apparent when seedlings were subjected to salt stress at the viable/PCD inflection point. At this inflection point, SW1 and SW2 were identified as salt tolerant varieties, SW3, WW3 and WW4 as moderately salt-tolerant and SW4, WW1 and WW2 as susceptible lines. However, distinctions between their salt tolerance could already be seen at low salt concentrations; for example, at 50 mM (stress-tolerant phase), the salt-sensitive lines already had an average PCD value of 30.1% unlike the remaining varieties which had an average value of 18.5%. These results highlight the usefulness of stress-induced PCD levels as a rapid high-throughput method for screening varieties. Like heat tolerance, it is difficult to pinpoint salt tolerance to a single gene as it is a polygenic trait controlled by multiple genes and signalling pathways (Zuther *et al.* 2007). Thus, quantification of stress-induced PCD levels integrates all these interacting networks to provide a single end-point measurement of the stress treatments.

Collectively, the results here demonstrate the utility of the RHA as a quick and useful screening tool to identify varieties of interest exhibiting enhanced or poor stress resistance. Once identified, further experimental testing using transcriptomics, proteomics and metabolomics can be performed to determine why different lines possess

varying degrees of salt tolerance. For example, Wang *et al.* (2008) performed a detailed proteomic study comparing the stress response of salt-sensitive common wheat (*T. aestivum*; variety: Jinan 177) compared to its salt-tolerant hybrid (*T. aestivum* × *Thinopyrum ponticum*; variety: Shanrong No.3) and found 110 differentially expressed proteins, of which 34 were variety-specific and 49 salt-responsive. The differences in protein expression were seen across all stress response stages, from the earliest stage at signal perception to the latter stages involving metabolome reprogramming. For example, the authors found five differentially expressed proteins involved in the signal transduction pathway, including the heterotrimeric G protein subunit, ethylene receptor and DWARF3. These proteins play important roles for translating the original stress stimuli into a specific cellular response; for example, compared to Jinan 177, the salt-tolerant variety Shanrong No.3 had a 7-fold lower expression of the ethylene receptor than its salt-susceptible counterpart, but had higher DWARF3 levels, which regulates gibberellin biosynthesis. Wang *et al.* (2008) also found variations in the transcription and translational machinery between both salt-stressed wheat varieties; compared to Jinan 177, Shanrong No.3 had significantly higher levels of DNA/RNA helicase, but lower eukaryotic translation initiation factor 5A3, which shuttles mRNA from nucleus to cytoplasm. Differences were also seen between a variety of transporters: Shanrong No.3 had higher levels of vacuolar proton ATPase (V-ATPase) which powers the $Na^+/H^+$ tonoplast antiporter to maintain optimal $Na^+/K^+$ levels to prevent ion toxicity. Finally, the authors also observed different expression patterns of various defence-associated proteins, such as chaperones, proteolytic proteins, and ROS-detoxifying enzymes. These proteins were involved in maintaining protein conformation, reducing oxidative damage, and removing abnormal proteins to prevent additional cellular damage (Wang *et al.* 2008).

The detailed work presented by Wang *et al.* (2008) shows that wheat salt tolerance occurs at many levels, e.g. signal transduction, transcription, translation, proteins, metabolites, and further characterisation work will be needed to discern why the different varieties examined here possess varying degrees of salt tolerance. Nevertheless, evidence suggests that it might be related to stress-responsive genes connected to osmotic shock. By examining stress-induced PCD levels, the variation in salt tolerance across the wheat varieties could be detected, even with a transient 5-min exposure to NaCl. Munns (2010) showed that the plant response to salt stress can be divided into different time-scales: minutes (transient phase), hours (recovery phase), days (adjustment phase), weeks

(vegetative development phase) and months (reproductive phase). A detailed explanation of the various phases can be found in the review by Munns, (2010) but are briefly summarised as follows: when plants are first exposed to salt stress, cells lose their turgor and experience an instant cessation in cell expansion in leaves and roots. Cells gradually regain their turgor after 30 minutes and reach a new steady state through osmotic adjustment (Frensch and Hsiao 1995; Passioura and Munns 2000). Leaf and root growth rates partially recover after a few hours, but alterations to the cell wall rheology causes the growth rate to settle at a new steady rate substantially lower than what was observed at pre-stress conditions (Munns *et al.* 2000). Prolonged stress exposure over days reduces meristematic activity and alters plant physiology by decreasing leaf emergence rates and lateral bud formation, causing a higher root to shoot ratio (Munns 2010). Modifications to plant physiology becomes even clearer after weeks of salt exposure in the form of severely reduced lateral root, branch and tiller formation (Nicolas *et al.* 1993). Months of salt exposure results in modified reproductive development, with altered flowering times and severely reduced seed production (Munns *et al.* 1995).

Given these points, salt-stressed plants are experiencing a combination of osmotic shock and ion toxicity; at the early stages (minutes-to-hours), salt exposure induces cellular dehydration and inhibit cell elongation, causing drought-like symptoms in plants, i.e. osmotic stress (Munns 2010). At later stages though (days-to-months), growth retardation is caused by excessive ion accumulation which leads to leaf senescence. Depending on the salt tolerance of the plant, the reduced photosynthetic capacity either retards plant growth rates or causes premature death (Munns 2010). In this chapter, seedlings were only subjected to transient NaCl shock for 5-minutes, so cells were presumably suffering the effects of osmotic stress, instead of excessive ion accumulation that develops at latter stages of protracted salt exposure. Therefore, the varying salt tolerance of the individual wheat varieties is most likely a function of their ability to tolerate osmotic shock, instead of excessive ion accumulation.

### 3.4.3 Screening wheat varieties for dual stress tolerance

It was interesting to draw parallels between the heat and salt stress experiments as varieties previously identified as heat susceptible also displayed similar vulnerabilities to salt stress. For example, heat susceptible SW4 and WW1 seedlings had elevated PCD levels compared to their counterparts treated with 50-150 mM NaCl. This might offer

hints why SW4, a relatively high-yielding breadmaking variety, is not available commercially as it did not appear to pass the final stages of testing. Likewise, thermotolerant varieties (SW1 and SW2) identified in Section 3.3.3.3 were similarly tolerant to salt stress under low-to-medium salt stress. To decipher why wheat varieties were displaying dual tolerance levels to both salt and heat stress, it helps to first understand the downstream damage caused by both stresses, and the subsequent stress-response phases. When plants encounter stress, they follow a sequential response pattern: alarm, acclimation, resistance, followed either by an exhaustion (overwhelmed plants die prematurely), or recovery (establishment of a new metabolic state after stress is lifted). An extended analysis of the different phases can be found in the review by Kosová *et al.* (2015) but are summarised as follows: the alarm phase involves perception of the stress stimuli by various plasma membrane-localised protein complexes, which is amplified and propagated to the nucleus by the MAPK cascade and secondary messengers ($Ca^{2+}$, $H_2O_2$ and nitric oxide). In the acclimation phase, the amplified signal induces changes to gene expression by modulating transcription factors and regulatory proteins; activation of stress-responsive transcription factors leads to the genome-wide reprogramming of the metabolome (Meena *et al.* 2017). Following this, upregulation of stress-protective and structural proteins occurs at the resistance phase. Some stress-protective proteins are unique for the encountered stress, while others are induced in response to a multitude of stresses as they cause overlapping downstream secondary damage (Wang *et al.* 2003).

The elevated risk of protein misfolding is the most prominent characteristic of heat stress and in response, plants accumulate HSPs (Wang *et al.* 2004). Nevertheless, heat stress also affects cellular ion homeostasis by disrupting cell membrane fluidity and plasma membrane- and tonoplast-localised ion pumps (Rivero *et al.* 2014). The ensuing downstream damage induces a combination of osmotic and oxidative stress, leading to retarded growth and photosynthetic rates (Hasanuzzaman *et al.* 2013). Conversely, salt stress decreases soil water potential, causing $Na^+$ overaccumulation and disruption of $K^+$ uptake by root cells. By interrupting cytosolic $Na^+$: $K^+$ balance, salt stress inflicts secondary damage by affecting cell osmotic potential, ion homeostasis and oxidative damage (Munns 2010). If left unchecked, the progressively cytotoxic conditions damage key macromolecules and the plasma membrane, leading to cellular dehydration, bleaching and eventually senescence (Munns 2010). To mitigate salt stress effects, plants up-regulate the SOS stress signalling pathway and accumulate osmolytes and Late

Embryogenesis Abundant (LEA) proteins, for osmotic adjustment and to inhibit protein aggregation and enzyme degradation (Wang *et al.* 2003). Salt-stressed plants also display elevated ATP-dependent $Na^+/H^+$ transporter levels for $Na^+$ exclusion or intracellular vacuole compartmentation (Kosová *et al.* 2015).

These mechanisms describe primary stress-specific responses but plants also have 'downstream housekeeping genes' for dealing with the secondary damage caused by these primary stresses (Munns 2010). When plants encounter stress, they first experience primary, stress-specific (salt or heat) damage, followed by downstream secondary damage (e.g. oxidative damage, protein denaturation and aggregation, and cellular dehydration) (Wang *et al.* 2003). Therefore, plants have divergent stress-specific pathways that protect against the initial primary damage (e.g. heat: protein denaturation; drought: cellular dehydration; salt stress: ion toxicity), but also upregulate similar downstream 'housekeeping' pathways for counteracting the overlapping secondary damage effects (Munns 2010). This was reflected in the similar secondary damage symptoms displayed by plants under heat or salt stress, e.g. elevated ROS levels, inhibition of key metabolic enzymes and macromolecular deterioration of proteins, cell membranes, nucleic acids and the cell cytoskeleton (Rivero *et al.* 2014). For these reasons, plants adopt similar protective mechanisms against heat and salt stress in response to overlapping secondary damages; examples of shared responses include cell volume regulation (through osmolyte and hydrophilic protein accumulation), ion homeostasis, maintenance of cell membrane potential and upregulation of ROS and MG-detoxifying pathways (Hoque *et al.* 2012b; Rivero *et al.* 2014; Hossain *et al.* 2016). It is also interesting to note that sHsps are also upregulated in response to heat and salt stress as cellular dehydration, being a shared symptom between both stresses, increases the risk of protein unfolding and aggregation (Wang *et al.* 2004; Hossain *et al.* 2016). In addition, sHsps are correlated with abiotic stress tolerance as they protect the mitochondrial Complex I electron transport chain from oxidative damage in salt-stressed *Z. mays* plants (Hamilton and Heckathorn 2001), and inhibit PCD by regulating the intracellular redox state in mammalian cells (Arrigo 1998). Collectively, the dual tolerance exhibited by varieties to heat and salt stress is most likely because of the higher expression of these conserved response pathways.

### 3.4.4 Basal, induced and cross-stress tolerance to heat and salt stress

In this section, stress-induced PCD levels were used to assess the basal, induced and cross-stress tolerance using a combination of single, combined and multiple individual stresses. Basal tolerance was assessed using single and combined stress exposure, while induced and cross-stress tolerance was examined using repetitive, i.e. multiple individual, stress exposure. Individual stress conditions have been intensely researched over the years but plants are constantly experiencing unique stress combinations under field conditions (Mittler 2006). For example, farmlands in the semi-arid regions of the world tend to face a combination of salt, heat and drought stress (Rivero *et al.* 2014), and increasing evidence suggest that plants under combined stress display a unique 'stress phenotype' that has little overlap with the phenotypes displayed under individual stresses (Mittler 2006). Hence, there have been increasing calls to study the response of plants under conditions that mimic field conditions as the stress response under two combined stresses is novel and cannot be merely extrapolated from studies where stresses were applied individually (Rasmussen *et al.* 2013; Rivero *et al.* 2014). When plants are exposed to a single stress, plants specifically tailor their transcriptomic, metabolomic and physiological state to combat the stress cue, and the response will be tuned differently to counteract the unique effects of combined stress exposure (Mittler 2006). This was demonstrated in a landmark study by Rasmussen *et al.* (2013) who studied the effect of five individual (cold, heat, high-light, salt, and flagellin) and six double-stress combinations in 10 *Arabidopsis* ecotypes; 61% of the transcriptome changes to combined stress could not be predicted from their individual stress treatments alone.

#### 3.4.4.1 Stress-tolerant varieties had high basal tolerance but a slow induced response

The survival of plants to stress depends on basal and adaptive tolerance and a few interesting observations were noted when screening varieties for these attributes. Given that basal tolerance reflects the inherent ability to resist stress without previous exposure (Arbona *et al.* 2017), SW1 and SW2 were identified as varieties with high basal tolerance as PCD levels did not change significantly between combined stress exposure and their respective single (heat or salt) stress-factor control. Similarly, SW4 and WW1 were classified as varieties with low basal tolerance, based on their elevated stress-induced PCD levels to single and combined stress treatments (Section 3.3.4.2). Conversely, induced tolerance reflects the adaptive capacity to mount a counteracting stress response

to the initial stress stimulus (Arbona *et al.* 2017) as exposure to non-lethal stress can form an ecological stress memory for cross-stress tolerance (Walter *et al.* 2013). Intriguingly, SW1 and SW2 had an unexpectedly slower cross-stress tolerance response compared to their stress-susceptible counterparts. Both varieties were initially hypothesised to have a fast induced tolerance response as Kawasaki *et al.* (2001) previously showed that salt-tolerant rice (Pokkali) responded faster than a salt-sensitive (IR29) variety to salt stress. Transcription upregulation in Pokkali started a mere 15 mins after the shock, while IR29 had a four-fold delayed response, suggesting that its slow ability to process stress cues was the underlying reason for its ineffective stress response (Kawasaki *et al.* 2001). However, no significant PCD changes were observed when stress was applied at the 1$^{st}$ time point (30-mins) in SW1 and SW2. Instead, the benneficial PCD-suppressing effects were only noted when the second stress cue was applied at the later stages. This stands in contrast to stress-susceptible varieties with low basal tolerance, like SW4 and WW1, that adapted faster to recurrent stresses. Both SW4 and WW1 had substantially lower PCD levels, even when the second stress cue was applied at the 30-min time-point, showing that the first stress-imprint successfully primed them against additive damage from recurrent stress exposure. Collectively, the results show that stress-susceptible varieties responded faster than stress-tolerant varieties and evidence suggest that signalling components play a prominent role in this process as they control the reprogramming of cellular molecular machinery (Rejeb *et al.* 2014b).

For example, mechanical wounding increased the salt tolerance of tomato plants because of cross-talk between sigalling pathways involving calmodulin-like activities, the signalling peptide system, and jasmonic acid biosynthesis (Capiati *et al.* 2006). Similarly, Hossain *et al.* (2016) found that ROS and MG were involved in cross-stress tolerance to salt and drought stress; ROS and MG have important signalling roles at low levels but are cytotoxic under high levels (Hoque *et al.* 2016; Hossain *et al.* 2016). Cross-stress tolerance to drought and salt stress was successfully imprinted in *Brassica campestris* L. by transient exposure to heat (Hossain *et al.* 2013) and cold shock (Hossain *et al.* 2016) by modulation of ROS and MG-detoxification systems. Both pathways are linked by GSH which is an important redox-regulating compound involved in the acclimation response to multiple stress types (Hossain *et al.* 2016). Transcription factors also play an important role in cross-stress tolerance as the reprogramming of the cells molecular machinery is controlled by stress-responsive transcription factors; for example, rice *Spl7* encodes a

class-A HSF that protects against high UV radiation and heat stress by inhibiting cell death (Yamanouchi *et al.* 2002). Spontaneous lesions, reminiscent of the PCD hypersensitive response, formed on the leaves of *spl7* mutants but not in wild-type plants, even though plants were subjected to abiotic and not biotic stresses. The lesion-mimic phenotype of *spl7* mutants was successfully reversed with the introduction of wild-type *Spl7* genes and displayed no lesion development throughout the growth period, unlike the *spl7* mutants (Yamanouchi *et al.* 2002). Likewise, the dehydration-responsive transcription factor (DREB1A) is involved in osmotic stress, but transgenic DREB1A-overexpressing *Arabidopsis* lines exhibited enhanced tolerance to salt, drought and freezing stress compared to wild type plants (Kasuga *et al.* 1999).

Perhaps similar signalling components are at play for the identified cross-stress tolerant varieties, accounting for the differences observed in their high basal tolerance, but slow induced tolerance. For example, the transcriptional regulator MBF1c modulates basal thermotolerance but not induced tolerance (Ahammed *et al.* 2016); MBF1c regulates stress-responsive gene elements (HSFs and DREB transcription factors), ethylene, salicylic acid and trehalaose in response to heat damage (Ahammed *et al.* 2016). Phytohormones also play an important role in both tolerance responses: salicyclic acid-dependent signalling increases basal thermotolerance, but is not required for adaptive tolerance (Clarke *et al.* 2004), while ABA-deficient *Arabidopsis* mutants demonstrated substantial losses of basal and acquired thermotolerance (Larkindale *et al.* 2005). Similarly, jasmonate acts concertedly with salicylic acid to stimulate basal tolerance in heat stressed *Arabidopsis* (Clarke *et al.* 2009), unlike ethylene which negatively impacts it (Kazan 2015). Futher work will be needed to deduce the impact of these signalling molecules in the identified varieties of interest, but the results here demonstrate that stress-induced PCD levels can be a useful marker of ecological stress memory. The identified stress-susceptible varieties had faster induced tolerance and despite the time-lag between the two stress exposure, both lines had not returned to their earlier homeostatic state and mounted a faster counteracting response, making them more tolerant to repeated stress - even that of a different origin (Walter *et al.* 2013).

It is also worth noting that the favoured modes of stress-response employed by stress-tolerant SW1 and SW2 (high basal tolerance, but slow induced response) and stress-susceptible SW4 and WW1 (low basal tolerance, but fast induced response) is remarkably

similar to the strategies employed by two species of poplar tree: salt tolerant *Populus euphratica* and salt susceptible *Populus* × *canescens* (Janz *et al.* 2010). The elevated basal tolerance of *P. euphratica* was reflected in the high constitutive expression of salt sensitive genes but had comparatively low transcriptional responsiveness compared to *P.* x *canescens*. The salt-tolerant *P. euphratica* was slower to react to external changes in salt levels and did not rely on a global defence strategy unlike its salt-susceptible counterpart. Instead, *P. euphratica* was already pre-adapted to osmotic stress by the constitutive activation of cell protective mechanisms. Even in the absence of stress, elevated flux was seen in certain permanently activated pathways involved in ROS detoxification (phenolic compounds), osmolyte biosynthesis (glucose, fructose, raffinose, and myoinositol), ion carriers ($Na^+$, $K^+$) and metabolite transporters. Nevertheless, the permanent activation of these pathways imposed a high energetic and metabolic burden and Janz *et al.* (2010) suggested that the stress-anticipatory preparedness came at the cost of diminished flexibility and a slower transcriptome response against fluctuating salt levels. Perhaps a comparable scenario is at play for SW1 and SW2 as despite their slower induced tolerance, both varieties had the lowest overall PCD levels because of their inherently high basal tolerance.

#### 3.4.4.2 Salt stress dominance over heat stress

An interesting phenomenon was observed when different initial stress cues were used during combined and multiple individual stress treatments. Despite maintaining identical stress doses, salt stress application followed by subsequent heat stress exerted a stronger cytotoxic effect on PCD levels compared to the reversed scenario (Figure 3.13). PCD levels under combined S+H treatment did not deviate from the average PCD levels of the single stress-factor (S-only) treatment, showing that heat stress did not have an additive effect as the secondary stress. However, this was not the case for the reverse scenario as H+S treatment generated higher PCD levels over the single heat (H-only) treatment. This intriguing phenomenon occurs as one stress can exert a stronger primary defence response over others, when plants face multiple stresses. This phenomenon was demonstrated by Rasmussen *et al.* (2013) who subjected *Arabidopsis* to six types of double stress combinations and found that the transciptome responds in five distinct patterns: combinatorial, cancelled, prioritised, independent and similar. The 'prioritised stress phenotype' refers to the preference of one stress response over the other, while the 'similar mode' describes the stress phenotype where the transcription pattern is similar for both

single stress-factors and the combined stress treatment. Under 'combinatorial mode', the transcription pattern at individual stresses are similar to each other but are highly distinct when both stresses are combined and are predominantly associated with the intersection between the biotic (pathogen induced HR, systemic acquired resistance) and abiotic (response to high light, cold and oxidative stress) cross-talk pathways. In contrast, the 'cancelled stress phenotype' displays a unique transcription pattern under combined stress that returns to baseline control values and are associated with secondary metabolite biosynthesis and growth regulation. The last stress phenotype is the 'independent mode' (associated with photosynthetic machinery), where the transcription pattern is only similar between the combined stress with only one of the single stress-factor treatments, but not the other.

Of the six stress combinations examined by Rasmussen *et al.* (2013), heat and salt-stressed *Arabidopsis* seedlings had the highest level (73.8%) of unpredictable responses (combinatorial, cancelled, or prioritised). The transcription expression of these three modes were highly distinct and could not be predicted by simply overlapping gene expressions from single-stress experiments. The prioritised mode was of particular interest to the work here as it refers to instances where plants prioritise one stress response over the other when exposed to combined stresses. When *Arabidopsis* was exposed to combined salt and heat stress, it had the highest prioritised transcripts level (12.1%) out of the six examined stress combinations and Rasmussen *et al.* (2013) found a greater response of salt transcripts compared to heat transcripts, showing that salt stress dominated the heat stress response. The results here align with transcriptomic data by Rasmussen *et al.* (2013) as stress-induced PCD levels obtaining using the RHA also accurately portrayed the dominance of salt stress over heat stress.

#### 3.4.4.3 Varying stress phenotypes displaced under combined heat and salt stress

Under combined stress, plants can display a unique stress phenotype which Rasmussen *et al.* (2013) divided into five categories. However for ease of analysis, this chapter refers to the original stress phenotypes by Mittler (2006) who divided the response into synergistic, antagonistic, or neutral interactions, which all five stress modes of Rasmussen *et al.* can be traced from (Figure 3.1A). Sometimes, combined stress can result in better

plant robustness (e.g. mechanical injury increased salt tolerance of tomato plants) (Capiati *et al.* 2006) or elevated vulnerability to the second stress (e.g. heavy metal exposure aggravated the effects of drought stress) (Barceló and Poschenrieder 1990). The individual stress response can differ between varieties, as illustrated in the stress matrix (Table 3.4). Most varieties responded neutrally to combined stress, apart from SW3 and WW3, which were outliers for antagonistic activity, i.e. higher PCD values for both H+S and S+H interactions. These results concur with past observations that plants display a unique stress phenotype when subjected to overlapping stress that is not necessarily additive, and that combined stress should be regarded as a new state of abiotic stress that requires a novel adaptive stress response (Mittler 2006; Rasmussen *et al.* 2013; Rivero *et al.* 2014). However, an important caveat should be added to the original hypothesis as the results here demonstrate that stress phenotypes can vary even amongst different varieties of the same species and that caution should be exercised when extrapolating findings across different research groups. This intra-species diversity can be advantageous as the RHA enables agronomists to identify stress-tolerant varieties early in the screening process, without relying on exhaustive large-scale field trials or costly analytical chemistry and molecular biology techniques.

# 3.5 Conclusions

This chapter demonstrates the use of root hairs as a model system for studying plant stress tolerance as direct scoring of stress-induced PCD levels integrates multiple stress-response pathways for a simple outcome, i.e. do plant cells stay alive or undergo PCD. The RHA was originally developed in *Arabidopsis* and in this chapter, the method was successfully exported to cereals to evaluate the heat and/or salt tolerance of barley and wheat varieties. By examining heat stress-induced PCD levels, a clear distinction between thermotolerant spring and thermo-susceptible winter barley varieties was highlighted. Further studies are needed to elucidate the mechanisms behind this difference, but existing literature suggest that polymorphisms around the HSP and *Vrn1* locus may be involved in the clear partitioning of spring and winter barley varieties into two separate groups (Marmiroli *et al.* 1998). In addition, eight wheat varieties were examined for their tolerance to heat and salt stress; comparison of their individual viability/PCD inflection point identified stress tolerant (SW1 and SW2) and stress susceptible (SW4 and WW1) varieties. Following this, stress-induced PCD levels were used to assess the basal, induced and cross-stress tolerance of the eight wheat varieties

to heat and salt stress using single, multiple individual and combined stress exposures, respectively. Interesting parallels could be drawn from the earlier single-stress experiments as the same varieties demonstrated similar cross-stress tolerance (SW1 and SW2) and susceptibility (SW4 and WW1) towards to heat and salt stress.

Results also show that stress-tolerant varieties (SW1 and SW2) had high basal tolerance but a slower induced response compared to stress-susceptible varieties (SW4 and WW1), which was remarkably similar to the defensive strategy employed by salt tolerant *P. euphratica* (Janz *et al.* 2010). In addition, the dominant and more damaging effect of salt over heat stress was demonstrated; application of salt stress as the first stress cue induced a stronger cytotoxic effect than heat stress even though identical stress doses were maintained. This was in line with the past study by Rasmussen *et al.* (2013) who found a greater response in salt transcripts compared to heat transcripts, showing that the salt stress response was prioritised over heat stress. The RHA was also successfully used to detect intra-species variations of the unique stress phenotype displayed under combined heat and salt stress. Collectively, the work in this chapter shows that the strength of the RHA lies in its simplicity and scalability as it can be easily adapted across various plant species and stress protocols in a simple 'plug-and-play' fashion. The RHA can be used for identifying varieties with traits of interest for downstream work, investigating the unique stress-phenotypes exhibited under combined stress and can detect intra-species variations, all in a fast and economical manner.

# Chapter 4 - Evaluating the PCD-suppressing effect of exogenous proline in plant stress tolerance

## 4.1 Introduction

Conventional agricultural practices have raised crop yields, but this has developed at the expense of long-term soil fertility and native microbial communities (Choudhury *et al.* 2014). Existing literature (see Chapter 1) has established that PGPR biofertilisers offer a novel, supplementary solution for conventional chemical fertilisation and pesticide management practices . Nevertheless, PGPR biofertilisers have not been widely adopted because of the difficulty in obtaining reliable effects under field applications (Schoebitz *et al.* 2013). The irregularity of crop response to inoculants is due to environmental fluctuations (soil moisture, temperature, pH and salt levels), protozoa predation, and competition with local soil microbiota community (Wu *et al.* 2012). This inconsistency is predominantly due to the quality of formulation, which is an integral feature in successfully establishing and commercializing PGPR inoculants (John *et al.* 2011).

Two critical areas that hinder the performance of PGPR inoculant strains have been identified: bacterial survival in the rhizosphere and colonization of plant tissue (Wood *et al.* 2001). For PGPR strains to be effective, the newly introduced strains must compete with the indigenous microbiota population for nutrients and colonisation sites to establish biofilm networks around plant roots (Santi *et al.* 2013). Biofertiliser formulation plays an important role in determining the success or failure of the PGPR inoculant, and conventional formulations are either in the form of powder, granulated or liquid suspensions (John *et al.* 2011). Carrier materials for powder and granulated formulations are often peat or clay based, but have significant chemical variability and PGPR cells have low survival rates when stored for prolonged periods (Cassidy *et al.* 1996). Liquid formulations are easier to apply but require storage under low temperatures to maintain cell viability and performance; the lack of carrier protection also results in low cell survival rates, uneven cell distribution around the seed coat and contamination during storage and transport (Bashan *et al.* 2002; Schoebitz *et al.* 2013).

Despite these constraints, the latest industry report by Mordor Intelligence (2019) estimates the global biofertiliser market to be worth USD 1.57 billion in 2018 and is predicted to rise in the upcoming years because of the growing demand for organic food.

The global farmland area used for organic farming has risen from 43.7 million hectares (2014) to 64.2 million hectares (2017), driving the usage of biofertilisers to sustainably boost soil fertility and enhance plant stress tolerance (Mordor Intelligence, 2019). The global biofertiliser market is highly fragmented but is predominantly segmented into four key corporations: Monsanto BioAg®, Kiwa Bio-Tech®, Lallemand Plant Care® and Agrino® (Mordor Intelligence, 2019). Table 4.1 summarises a selection of their existing products, formulation, method of incorporation and trial data. Information regarding constraints during use, e.g. inoculant survival rates, diffusion rates or efficacy during rainfall, is scarce as companies do not list such proprietary details on their product pages. In addition, Bayer® acquired Monsanto BioAg® in June 2018 and it is unclear if they will continue the existing biofertiliser products.

**Table 4.1** - List of biofertilisers on the market, their formulation, mechanism of action and trial data. Products shown here are four key corporations in the global biofertiliser market according to Mordor Intelligence (2019).

| | | | | Trial Data | |
|---|---|---|---|---|---|
| **Company** | **Product name, formulation, incorporation method and country of use.** | **PGPR strains** | **Properties** | **Crop** | **Data** |
| **Lallemand Plant Care®** | **Rise™ P**[1] **:** A wettable powder applied as a soil spray (150 g/ha) trialled in France. | *Bacillus amyloliquefaciens strain IT45* | Increases bio-available P and increases root growth | Silage Maize[2] | 20% increase in yield and 6% increase of energy value produced per hectare |
| | | | | Sugar beet[3] | - A 95% chance of achieving 4 tonnes/ha<br>- A 4% yield grain (significant test at 5% threshold)<br>- Earlier row coverage at beginning of growth cycle |
| | **Rise™ P DualTech**[4]**:** A wettable powder applied as a soil spray (1 kg g/ha) trialled in France. | *Bacillus amyloliquefaciens strain IT45 and LYCC* yeast fractions | Yeast fractions acts as a nutrient source to the P-solubilizing *Bacillus* IT45 | Oilseed Rape[5] | Increase in crown diameter<br>20% increase in root biomass |

[1] https://lallemandplantcare.co.uk/products/details/rise-p/
[2] https://lallemandplantcare.co.uk/wp-content/uploads/2018/02/PSH-RISE-P-Silage-Maize-ENG.pdf
[3] https://lallemandplantcare.co.uk/wp-content/uploads/2018/02/PSH-RISE-P-Sugar-Beet-ENG.pdf
[4] https://lallemandplantcare.co.uk/products/details/greenstim/
[5] https://lallemandplantcare.co.uk/wp-content/uploads/2018/02/PSH-RISE-P-Oilseed-Rape-ENG.pdf

| | | | | Trial Data | |
|---|---|---|---|---|---|
| **Company** | **Product name, formulation, incorporation method and country of use.** | **PGPR strains** | **Properties** | **Crop** | **Data** |
| **Lallemand Plant Care®** | **Rise™ P DualTech**[4]**:** A wettable powder applied as a soil spray (1 kg g/ha) trialled in France. | *Bacillus amyloliquefaciens strain IT45 and LYCC* yeast fractions | Yeast fractions acts as a nutrient source to the P-solubilizing *Bacillus* IT45 inoculant, enabling rapid colonization of plant roots | Oilseed Rape[5] | Increase in crown diameter<br>20% increase in root biomass |
| | **Prestop®**[6]**:** A wettable powder applied using foliar spray and root application on edible crops (500 g/m3 compost or soil). Trialled in France | *Gliocladium catenulatum* strain *J1446* | Protects against fungal pathogens (*Pythium, Phytophthora, Rhizoctonia, Fusarium, Didymella sp* and *Botrytis cinerea*) by secreting fungal cell wall degrading enzymes | Proprietary trail data not published publicly | |
| **Agrino®** | **iNvigorate®**[7]**:** Liquid inoculant applied using drip irrigation (0.76 L/ha). Trialled in USA | *Clostridium pasteurianum* and *Azotobacter vinelandii* | Increases bio-availability of soil macronutrients, and promotes growth of a robust soil microbiome around the rhizosphere | Almond trees[8] | Increased almond yield by 11% over a 2-year study |
| **Monsanto BioAg®** | **Biodoz™**[9]**:** Formulated in peat. Used in seed application (140 g/ha) | *Rhizobium meliloti* | Nitrogen-fixing inoculant for alfalfa | Proprietary trail data not published publicly | |

[4] https://lallemandplantcare.co.uk/products/details/greenstim/
[5] https://lallemandplantcare.co.uk/wp-content/uploads/2018/02/PSH-RISE-P-Oilseed-Rape-ENG.pdf
[6] https://lallemandplantcare.co.uk/products/details/prestop-roots-application/
[7] http://agrinos.com/products/invigorate
[8] http://agrinos.com/sites/default/files/Agrinos_Almonds_TrialData_Pacific.pdf
[9] http://www.monsantobioag.com/global/emea/Products/Pages/Biodoz-Alfalfa.aspx

| | | | | Trial Data | |
|---|---|---|---|---|---|
| **Company** | **Product name, formulation, incorporation method and country of use.** | **PGPR strains** | **Properties** | **Crop** | **Data** |
| **Monsanto BioAg®** | **JumpStart®[11]:** Applied as wettable powder for seed application (0.25 g/kg of seed) or as granules in-furrow application (8.25 kg/ha) | *Penicillium bilaii* | Increases bio-available P and increases root growth | Proprietary trail data not published publicly | |
| | **Met52® BIO1020®[12]:** Applied as granules in potting compost (0.5 kg/m³) or for open ground usage (50-150 kg/ha) | *Metarhizium anisopliae strain F52* | Bioinsecticide against black vine weevil larvae in fruit and ornamental plants | | |
| | **Optimize™ Pulse[13]:** Liquid inoculant for seed application (160 ml/50 kg) | Combination of *Rhizobium leguminosarum* and LCO (lipo-chitooligosaccharide) technology | Improved nodule formation and BNF of pea plants. LCOs strengthen the symbiotic relationship between the plant and PGPR inoculant, leading to greater plant nutrient uptake | | |
| | **TagTeam™ LCO[14]:** Applied as liquid inoculants for seed application (90ml/50 kg seeds) or as granules in-furrow application (4 kg/ha) | Rhizobium inoculant, *Pencillium bilaii and* LCO | Enhanced BNF of soybean plants and higher nodule numbers. Higher phosphate bio-availability and plant nutrient uptake | | |

[11] http://www.monsantobioag.com/global/emea/Products/Documents/4JumpStart/JumpStart_flyer_EN1015.pdf
[12] http://www.monsantobioag.com/global/emea/Products/Pages/Met52-Bio1020granular.aspx
[13] http://www.monsantobioag.com/global/emea/Products/Pages/OptimizePulse-PeaLentil.aspx
[14] http://www.monsantobioag.com/global/emea/Products/Pages/TagTeam-LCO-soybean.aspx

| Company | Product name, formulation, incorporation method and country of use. | PGPR strains | Properties | Crop | Data |
|---|---|---|---|---|---|
| **Monsanto BioAg®** | **Cell-Tech® Soybean[15]:** Applied as liquid inoculants for seed application (75ml/27 kg of seeds) or as granules in-furrow application (5.55 kg/ha) | *Bradyrhizobium japonicum* and *Bradyrhizobium elkanii* | Improved nodulation for soybeans in cool soils | Proprietary trail data not published publicly | |
| **Kiwa Bio-Tech® Products Group Corporation** | **Microorganism Bacterium Agent®[16]:** Wettable powder applied by spreading or banding method (2.67 kg/ha) | *Bacillus subtilis, Paenibacillus Kribbensis* and *Bacillus megaterium* | Soil phytoremediation, enhances soil water-holding capacity and improves crop yield and pathogen resistance | | |

[15] http://www.monsantobioag.com/global/emea/Products/Pages/Cell-Tech-Soybean.aspx
[16] http://kiwabiotech.com/kiwa/microorganism-bacterium-agent-series/#1532504198159-d89b133d-7464

Bioencapsulation offers an interesting alternative to conventional formulation and free cell dispersal techniques as it immobilises cells within polymeric microspheres (size range of 1-1000 µm) for controlled release into the environment (Rathore *et al.* 2013). Microspheres are usually composed of water-soluble polymers that are permeable to nutrients, gas and metabolites; the semi-permeable polymeric matrix provides optimum conditions for bacterial growth for extended periods and temporary protection against a harsh external environment (Rathore *et al.* 2013). Unlike conventional formulations, whose immediate PGPR release impacts only the early stage of plant growth, the gradual release from microbeads confers long-term effects by minimising the rain wash-off problem and helping to maintain a high cell population around host roots for colonization (John *et al.* 2011; Schoebitz *et al.* 2013) as illustrated in Figure 4.1.

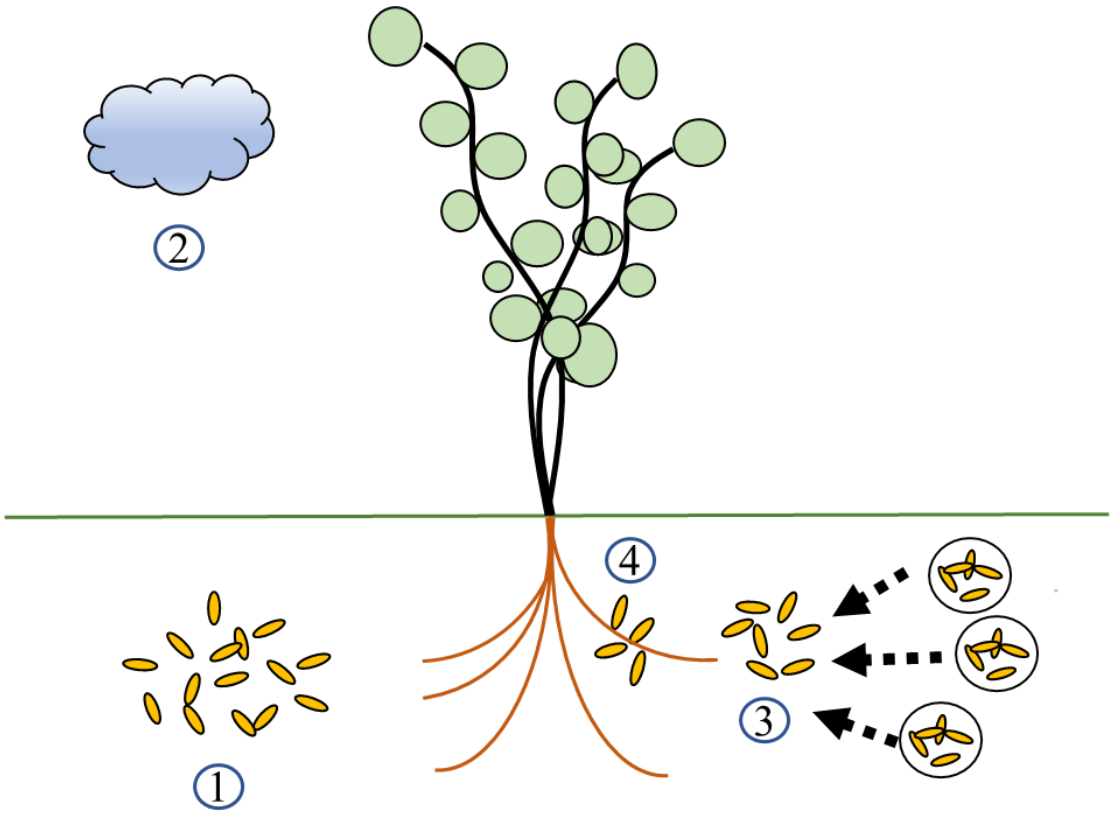


**Figure 4.1** – Differences between conventional biofertiliser formulation and encapsulated cells. Conventional formulation (1) only impact the early inoculation stage and have low survival rates due to predation and rain wash-off (2). Encapsulated cells are released gradually (3) for long-term biofertilising effects and (4) maintain a high cell population around roots for colonization. Image author's own.

Nevertheless, PGPR encapsulation is not a straightforward process as many factors must be considered during the formulation process. Firstly, a balance must be achieved between maintaining high cell survival rates during the manufacturing process, while ensuring a uniform loading of cells into the microbeads (Schoebitz *et al.* 2013). A significant portion of encapsulated cells do not survive the bead dehydration process; for example, the survival yield of encapsulated *Azospirillum brasilense* and *Raoultella terrigena* was less than 1% of the original cell count (Schoebitz *et al.* 2012). Secondly, the efficiency of nutrient and oxygen diffusion greatly drops after travelling short distances of 300-500 µm, culminating in lower cell viability in larger beads (Christenson *et al.* 1993). Smaller microspheres (< 300 µm) have better oxygen penetration depth but have poor settling properties (McLoughlin 1994). Moreover, if the encapsulated cells are used as a seed coating and the formulation contains a high water content, there is the added risk of undesirable seed germination during storage as cells require water for survival, but seeds need to avoid to inhibit germination (John *et al.* 2011). In Section 2.3.7.1, proline was shown to be remarkably thermostable as it could withstand autoclaving with no loss of PCD-suppressing bioactivity. Hence, compared to live cells, proline is likely to be able to withstand the intensive manufacturing conditions, e.g. high temperatures, extreme pH levels, sonication and bead dehydration, involved in the encapsulation process.

Agrochemical encapsulation is an expanding research field as it extends several advantages over conventional formulation techniques. The principal benefit rests with the controlled and gradual release of the bioactive ingredient, instead of an abrupt burst, which bears important downstream implications (Wang *et al.* 2016). The immediate discharge of agrochemicals reduces its efficacy and to compensate for the losses, higher agrochemical concentrations must be loaded to attain similar efficacy rates (Kashyap *et al.* 2015). In addition to the economic costs, this can pose serious environmental problems, as the immediate release of heavily concentrated doses can prove cytotoxic to soil microbiota and is at further risk of runoff into watercourses (Kashyap *et al.* 2015). Microspheres avoid these problems as they provide a protective shell for the bioactive compound that controls the rate of release into the environment, depending on the physiochemical properties of the polymer matrix (McLoughlin 1994). The controlled and sustained release of the bioactive compounds prolongs the bioactive effect, reduces the dosage effect required for efficacy, and is less hazardous to the surrounding environment

(Zhang *et al.* 2015). Moreover, encapsulated agrochemical particles should have a better shelf life than immobilised live cells as the latter are limited by nutrient and oxygen diffusion and require storage at specific temperatures for extended cell survival (Bashan *et al.* 2014).

The polymer matrix of the biocapsules can be based on synthetic or natural materials, and each have different strengths and weaknesses. Compared to natural polymers, synthetic polymers are more chemically stable and less prone to microbial degradation, but often require harsher processing conditions that would affect cell survival rates (De-Bashan and Bashan 2010; Rathore *et al.* 2013). Chitosan is synthetically derived from chitin and is a versatile polymer suitable for agriculture as it has excellent biocompatibility, is non-toxic and bio-degradable; it has been used as a slow-release system for delivering pesticides, fertiliser, herbicides and micronutrients to plants (Kashyap *et al.* 2015). Moreover, chitosan is classified as a biostimulant and its application is known to increase abiotic and biotic stress tolerance (du Jardin 2015). For example, chitosan treatment partially alleviated drought symptoms in *Thymus daenensis* plants by stimulating proline accumulation and decreasing lipid peroxidation damage (Bistgani *et al.* 2017). Similarly, chitosan oligosaccharides induced SAR against *tobacco mosaic virus* in *Arabidopsis* treated plants (Jia *et al.* 2016), while chitosan derivatives demonstrated broad-spectrum insecticidal and fungicidal activity against *Spodoptera littoralis*, *Botrytis cinerea* and *Pyricularia grisea* (Rabea *et al.* 2005).

Cyanobacteria-based microspheres have also been used to encapsulate the fungicide tebuconazole (TEB) (Zhang *et al.* 2015). Researchers generated double-walled microspheres by using *Synechocystis* sp. strain PCC 6803 cells to encapsulate TEB and the resultant TEB-loaded cyanobacteria shell coated with an urea–formaldehyde (UF) layer. Zhang *et al.* (2015) found that the additional UF coating acted as an efficient diffusion barrier as the double-walled spheres dampened the initial burst release and had improved controlled release properties over single-walled microspheres. Consequently, the sustained TEB release by double-walled spheres significantly prolonged antifungal activity; its control efficacy against wheat powdery mildew (over 80%) proved remarkably persistent even after 12 days of inoculation, unlike the commercial formulation (containing identical TEB concentrations at 40 mg/L) which declined to 52.3% over the same period (Zhang *et al.* 2015). On the whole, the polymers used to

encapsulate proline may hold specific advantages, in addition to their main function as a protective shell for the bioactive ingredient. For example, chitosan has biostimulant properties, synthetic polymers like poly(lactic-co-glycolic acid) (PLGA) are more mechanically and chemically robust, while cyanobacteria cultures may be an attractive economic option as proline can be harvested from their extracellular filtrate, and the cells used to encapsulate the cyanobacteria-derived proline itself.

However, before these proline microspheres can be generated, it was essential to first appraise the effects of exogenous proline on plants across a concentration range. Many studies have established the beneficial effects of proline supplementation on plant stress tolerance (Hossain and Fujita 2010; Aggarwal *et al.* 2011; Anjum *et al.* 2014), but other studies noted that overly high proline supplementation causes oxidative damage to plants (Hare *et al.* 2001, 2002). Moreover, the work in past chapters has thus far, only tested the effects of proline at the viability/PCD inflection point (50 °C) in *Arabidopsis*, and not at the other phases (stress-tolerant, PCD and necrosis) and in other plant species. Therefore, this chapter seeks to assess the extent of the proline bioactive effect across different proline gradients (1- 1000 μM) and heat stress thresholds (25, 45, 52 and 55 °C) in *Arabidopsis* seedlings. Following work in the model plant organism, exogenous proline (1-1000 μM) was assessed to determine if a similar PCD-suppressing effect could be detected in heat-stressed barley and wheat seedlings at 45 °C. It was especially important to determine if a cytotoxic proline threshold could be detected.

### 4.1.1 Aims and Objectives

The results from this chapter will inform future work concerning the development of a slow-release proline delivery system for enhanced plant stress tolerance. Some important factors to consider for downstream formulation work include the maximum safe proline levels that can be loaded into the microspheres; this is a safety precaution against accidental ruptures, should the proline contents be completely discharged from the microbeads in a sudden, concentrated burst. Another factor to consider is the effectiveness of proline across different stress intensities to determine its optimum application timing. Therefore, the RHA was used to assess two key variables for the encapsulation formulation process: (1) the maximum safety dosage of proline and (2) proline efficacy across varying stress intensities.

**Chapter aims:**

- Evaluate the PCD-suppressing effect of proline across a broad concentration range (1-1000 μM) and across different heat-shock temperatures (25, 35, 45, 52 and 55 °C) in *Arabidopsis* seedlings.
- Evaluate the PCD-suppressing effect of proline (1-1000 μM) in wheat and barley seedlings.

## 4.2 Materials and Methods

### 4.2.1 Growth and sterilisation procedures for *Arabidopsis thaliana*, *H. vulgare* and *T. aestivum* seedlings

*Arabidopsis* (Section 2.2.1), wheat and barley (Section 3.2.1) seeds were sterilised and germinated as described in previous sections.

### 4.2.2 Proline treatment and heat stressing of *Arabidopsis thaliana*, *H. vulgare* and *T. aestivum* seedlings

Similar protocols in past chapters were used to assess the effect of proline treatment on heat-stressed *Arabidopsis* Col-0 (Section 2.2.2), spring barley (SB) (Section 3.2.2.1) and spring wheat (SW) seedlings (Section 3.2.2.1). 5-day-old *Arabidopsis* seedlings were placed individually into 24-well plates (Sarstedt© Tissue Culture Plate) filled with 1 ml of pre-vortexed proline (1, 1.83, 2, 5, 10, 100 and 1000 µM) solutions established in BG11 and incubated for 3 hours at room temperature. Seedlings were than stressed at 50 °C for 10 minutes in a pre-heated Grant SUB Aqua Pro 26 water bath, before being returned to their 21 °C growth chamber. To assess the effect of proline treatment on cereals, 1-day-old wheat and 2-day-old barley seedlings were placed into sterile Petri dishes containing 25 ml of proline solution (1, 2, 5, 100 or 1000 µM) for three hours at room temperature. Seedlings were heat-stressed in Grant SUB Aqua Pro 26 water bath for 10 minutes at 45 °C and returned to the growth chamber. The stress response was enumerated in terms of root hair viability, PCD and necrosis after 14-16 hours of stress application to allow sufficient time for the death morphologies to develop.

### 4.2.3 Chitosan-proline nanoparticles synthesis

Chitosan (50 mg) was dissolved in 50 mL 1% (v/v) acetic acid and stirred for 30 minutes until a clear solution was obtained. Two tripolyphosphate (TPP) solutions were prepared to produce proline-loaded and unloaded (control) nanoparticles. For the control, a TPP solution was prepared by dissolving 10 mg TPP in 5 mL DW, while proline-loaded nanoparticles were generated by adding 1 mM proline into the diluted TPP solutions. Using a Pasteur pipette, both TPP solutions were added drop-wise into two separate chitosan solutions over 30 minutes, while being stirred at 800 rpm. The reaction mixture was left stirring overnight at room temperature, followed by centrifugation (Sigma® 3-

18KS) at 24000 *x* g for 30 minutes at 10 °C. The supernatant was discarded, and the chitosan nanoparticle pellet resuspended in 20 mL DI using a probe sonicator (Sonics® Vibra-Cell™ VCX 130). The mixture was placed on ice and sonicated at full amplitude for 30 seconds, followed by a 30 second break. This cycle was repeated six times until the mixture was fully resuspended. The suspended mixture was placed overnight in a -20 °C freezer and the frozen aqueous nanoparticle solution lyophilized using a freeze dryer (Labconco FreeZone$^{2.5®}$) and stored at -20 °C until further use.

### 4.2.4 PLGA-proline microparticles synthesis

PLGA polymer (200 mg) was dissolved in 2mL dichloromethane. A 50 µL DI volume (for unloaded particles) or 1mM proline volume (for loaded particles, dissolved in DI) was added drop-wise to the PLGA solution over 30 minutes, while stirring at 800 rpm. The mixture was sonicated using a probe sonicator (Sonics® Vibra-Cell™ VCX 130) at full amplitude for 30 seconds, followed with a 30 second intermittent break. The sonication was performed while the mixture was standing on ice and this cycle was repeated six times to form the primary water-in-oil (W/O) emulsion. The emulsion was added to 4 ml 1% polyvinyl alcohol (PVA) solution and subjected to two more cycles of probe sonication on ice, to form the water-in-oil-in-water (W/O/W) emulsion. The double emulsion was transferred to 100 mL of 0.3% w/v PVA solution and left stirring for 3 hours at 800 rpm, to allow the dichloromethane to evaporate and the microparticles to harden. The mixture was centrifuged (Eppendorf Centrifuge 5810®) at 4000 *x* g for 10 minutes and the supernatant discarded. The particles were washed three times with DI to eliminate the PVA and the pellet placed overnight in the -20 °C freezer. The particles were freeze-dried (Labconco FreeZone$^{2.5®}$) for 3 days and stored at -20 °C until further use.

### 4.2.5 Scanning electron microscopy

PLGA-proline microparticles were coated with gold powder using an Emitech® K500X sputter coater. Images of the microparticles were taken using a Hitachi® S-246ON scanning electron microscope, operating at 18 kV.

# 4.3 Results

## 4.3.1 Evaluating the effect of proline at low, medium, and high heat stress in *Arabidopsis* seedlings

### 4.3.1.1 Effect at low and high heat stress

Previous testing in *A. thaliana* established that exogenous proline treatment was effective at the specific concentrations measured in *N. muscorum* CM (1.83 µM proline, Section 2.3.7.1) and at 1 and 5 µM proline (Section 2.3.7.3) at 50 °C, the viability/PCD inflection point. Therefore, additional testing was performed to evaluate the dose-dependent effect of exogenous proline across a broader concentration range (1-1000 µM) and across different stress intensities. To that end, the stress response, in terms of viability, PCD and necrosis, was evaluated after exposure to low stress intensities between 25 and 45 °C, medium stress intensities between 50 and 52 °C and high stress intensity of 55 °C. Results show that under low heat stress, no significant variations in PCD levels occurred between the control treatments (SDW and BG11) and exogenous proline supplied at the concentrations detected in *N. muscorum* CM (Figure 4.2A). For example, PCD levels across the SDW, BG11 and proline-treated seedlings ranged from 22-23% (25 °C), 22-28% (35 °C) and 38-42% (45 °C). This shows that under the concentrations tested in this work, exogenous proline supplementation did not have a beneficial PCD-inhibiting effect at low heat shock, unlike at the 50 °C viable/inflection point (Figure 2.15).

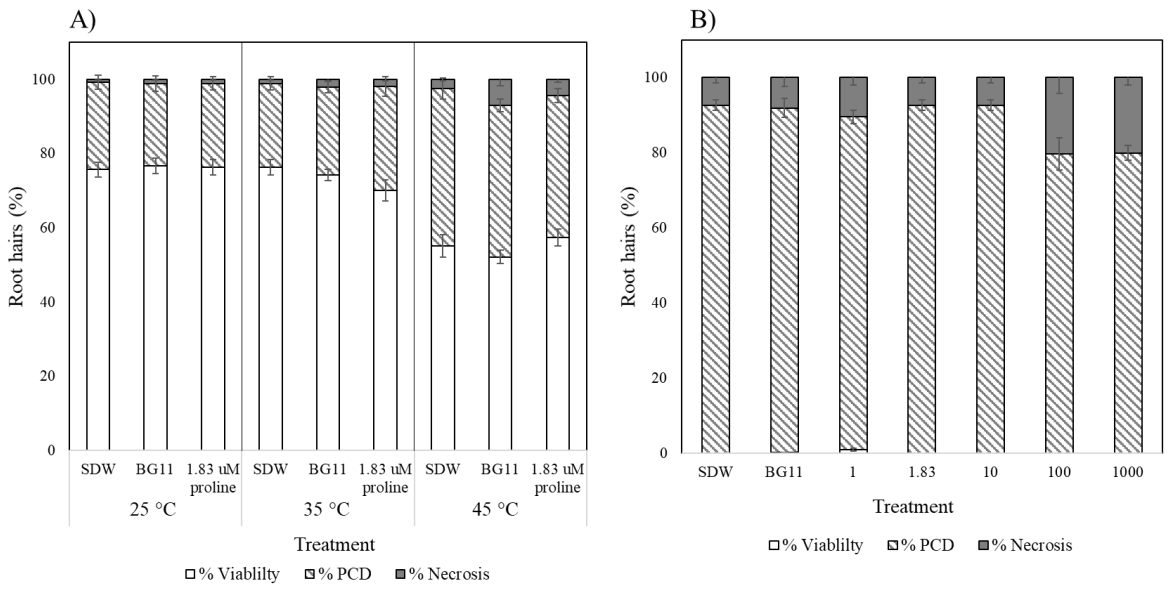


**Figure 4.2** – (A) Effect of exogenous proline treatment at low heat stress (25-45 °C) in wild-type *Arabidopsis* seedlings. Values represent merged results of 4 experiments, n ≥16 (± SE). (B) Effect of exogenous proline treatment at high heat stress (55°C) in wild-type *Arabidopsis* seedlings. Values represent merged results of 2 experiments, n=8 (± SE). Each cell mode is represented as the percentage of cell mode over total number of root hairs, where viability% + PCD% + necrosis% = 100%.

Interestingly, comparable findings were noted when seedlings were subjected to high heat stress (55 °C), even though proline was supplemented across a wider range (1-1000 μM) than the low stress experiments. This was done to assess if proline would have a bioactive effect near the PCD/necrosis threshold, i.e. the point where most cells are undergoing PCD, but can experience a rapid increase in necrosis levels upon elicitor treatment. The earlier regression model analysis predicted that exogenous proline does not suppress PCD in a dose-dependent manner (Table 2.10), but the experiment was conducted using a smaller proline gradient (0.366-1.83 μM proline), and a larger proline gradient was used here to determine if *Arabidopsis* seedlings would respond differently. Proline was initially hypothesised to have a beneficial PCD-suppressing effect at 55 °C; for at this stress magnitude, root hair viability was ~0% in both SDW and BG11 controls, with PCD being the dominant cell death mode. However, the results proved contrary as proline supplementation was unable to inhibit stress-induced PCD even across the full gradient (Figure 4.2B). From 1 to 10 μM proline supplementation, PCD levels remained stable (88.7-92.6%) but declined at higher proline (100-1000 μM) concentrations owing to elevated necrosis levels which were ~20% (compared to the 7-8% baseline in SDW and BG11 controls).

### 4.3.1.2 Effect at medium heat stress

The previous results indicated that proline had low efficacy under low and high heat stress. Further testing revealed that the PCD-suppression effect was only noted at 50 °C and 52 °C heat shock, a substantially narrower bioactive range than expected. In 50 °C heat-shocked seedlings, a clear delineation was noted between beneficial low-to-medium proline treatments and cytotoxic high proline doses (Figure 4.3A). To streamline work, the SDW control was omitted for the 50 °C heat shock experiments as past results and statistical analysis showed that BG11 and SDW-treated seedlings have similar PCD levels at this temperature (Table 2.4). *Arabidopsis* seedlings had consistently lower PCD levels compared to the BG11 control when the proline treatment was between 1 to 8 µM and apart from the 3 µM treatment, all of these proline doses were statistically ($p$<0.05) distinct from the control seedlings (Table 4.2). Beyond 8 µM, PCD levels rose and subsequently peaked at 54% in the 1000 µM proline-treated seedlings, indicative of the cytotoxic effects of excessive proline supplementation. Only one inflection point was observed between 10-100 µM proline treatment (Figure 4.3B), exhibiting the consistency of the stress response at 50 °C, unlike 52 °C heat-shocked seedlings, which had four inflection points across the same proline gradient.

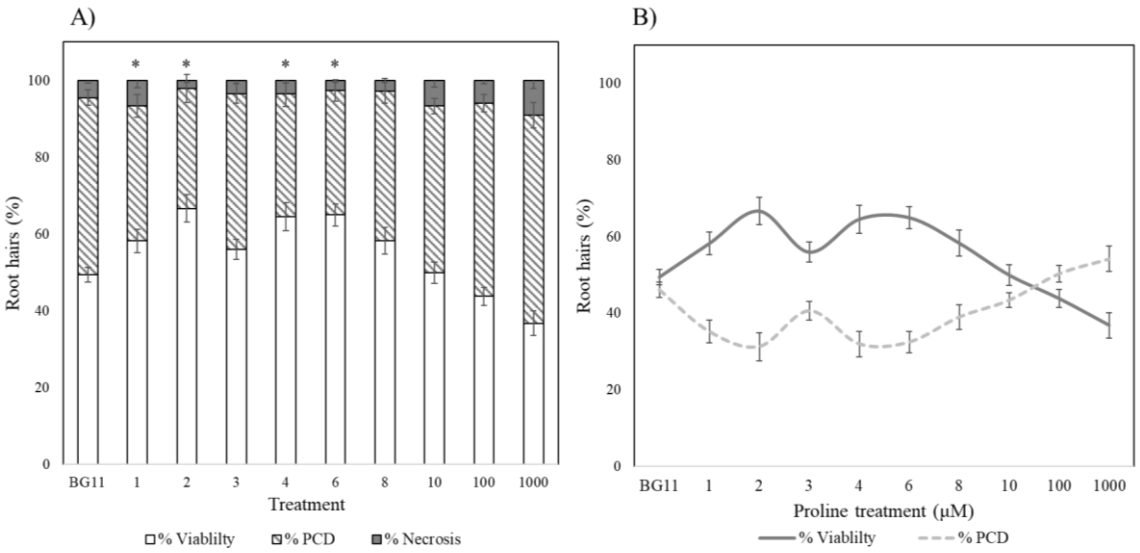


**Figure 4.3** - (A) Effect of proline treatment (1-1000 µM) at 50 °C in wild-type *Arabidopsis* seedlings. (B) Note the single inflection point (where % viability = % PCD) between 10-100 µM. Values represent merged results of 3 experiments, n≥12 (± SE). (*) indicates PCD results significantly ($p$<0.05) different from the BG11 control. Each cell mode is represented as the percentage of cell mode over total number of root hairs, where viability% + PCD% + necrosis% = 100%.

**Table 4.2** - Effect of exogenous proline treatment after 50 °C heat shock on stress-induced PCD levels in *Arabidopsis* seedlings. Values represent merged results of 3 experiments, n≥12 (± SE). A Dunnett *t*-test was used for statistical analysis which treated the BG11 dataset as a control and compared all other group datasets against it. (*) indicates PCD results significantly ($p<0.05$) different from the BG11 control.

| Proline treatment (µM) prior to 50 °C heat stress | % PCD | Mean difference from BG11 (%) | Sig. |
|---|---|---|---|
| 0 (BG11) | 46.1 ± 1.96 | N/A | N/A |
| 1 | 35.2 ± 2.98 | -10.9* | 0.033 |
| 2 | 31.2 ± 3.68 | -14.9* | 0 |
| 3 | 40.6 ± 2.51 | -5.53 | 0.584 |
| 4 | 31.9 ± 3.31 | -14.2* | 0.001 |
| 6 | 32.4 ± 2.83 | -13.7* | 0.002 |
| 8 | 39.0 ± 3.23 | -7.17 | 0.378 |
| 10 | 43.4 ± 1.96 | -2.73 | 0.988 |
| 100 | 50.3 ± 2.23 | 4.19 | 0.877 |
| 1000 | 54.2 ± 3.34 | 8.07 | 0.245 |

Conversely, the PCD-suppression effect of proline at 52 °C heat shock was highly erratic. At low proline doses (1-3 µM), treated seedlings had similar PCD (45-53%) levels to the BG11 (53%) control seedlings. This was followed by unusually high PCD levels in the 4 µM treatment (73%), followed by a sudden drop to 39% in the 6 µM proline-treated seedlings (Figure 4.4A). From treatment concentrations of 8 µM and upwards, PCD levels were persistently higher than that seen in the BG11 control seedlings, with a mean difference ranging from 3-11%. Statistical analysis reflected the inconsistency of the stress response at 52 °C as only 4 and 6 µM proline treatment resulted in significant ($p<0.05$) differences from the BG11 treated control seedlings (Table 4.3). Multiple inflection points (where % viability = % PCD) were observed in 52 °C heat-shocked seedlings at 1-1.83 µM, 1.83-2 µM, 4-5 µM and 6-8 µM (Figure 4.4B). To streamline the presented data, the SDW dataset was omitted from Figure 4.4 as it has no significant ($p>0.05$) differences with the BG11 control but is shown in Table 4.3.

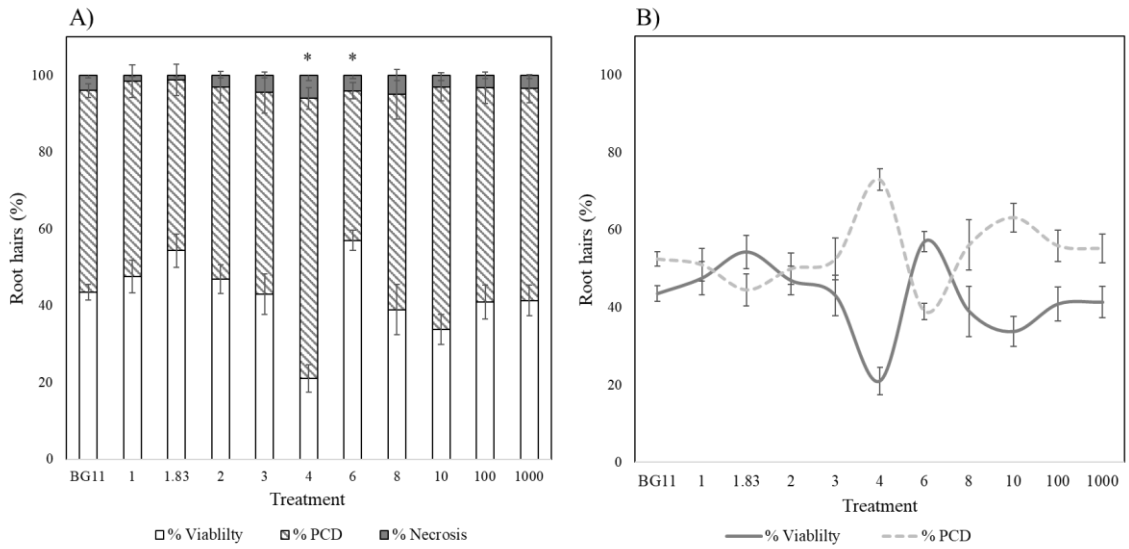


**Figure 4.4** – (A) Effect of proline treatment (1-1000 µM) at 52 °C, (B) Four inflection points (where % viability = % PCD) were seen between 1-1.83 µM, 1.83-2 µM, 4-5 µM and 6-8 µM. Values represent merged results of 3 experiments, n≥12 (± SE). (*) indicates PCD results significantly ($p$<0.05) different from the BG11 control. Each cell mode is represented as the percentage of cell mode over total number of root hairs, where viability% + PCD% + necrosis% = 100%.

**Table 4.3** - Effect of exogenous proline treatment at 52 °C heat shock on stress-induced PCD levels in *Arabidopsis* seedlings. Values represent merged results of 3 experiments, n≥12 (± SE). A Dunnett *t*-test was used for statistical analysis which treated the BG11 dataset as a control and compared all other group datasets against it. (*) indicates PCD results significantly ($p$<0.05) different from the BG11 control.

| Proline treatment (µM) prior to 52 °C heat stress | % PCD | Mean difference from BG11 (%) | Sig |
|---|---|---|---|
| 0 (BG11) | 52.5 ± 1.84 | N/A | N/A |
| 0 (SDW) | 55.4 ± 3.51 | 2.91 | 0.999 |
| 1 | 51.0 ± 4.25 | -1.49 | 1.00 |
| 1.83 | 44.5 ± 4.13 | -7.98 | 0.478 |
| 2 | 50.0 ± 4.10 | -2.51 | 1.00 |
| 3 | 52.5 ± 5.37 | 0.04 | 1.00 |
| 4 | 73.0 ± 2.82 | 20.5* | 0.00 |
| 6 | 39.0 ± 2.10 | -13.5* | 0.034 |
| 8 | 56.1 ± 6.44 | 3.65 | 0.998 |
| 10 | 63.2 ± 3.68 | 10.73 | 0.213 |
| 100 | 55.9 ± 4.02 | 3.41 | 0.995 |
| 1000 | 55.2 ± 3.71 | 2.72 | 0.999 |

### 4.3.2 Effect of exogenous proline in *T. aestivum* and *H. vulgare* seedlings

Previous results identified SW4 wheat (Section 3.3.3.1) and WB1 barley (Section 3.3.2.1) as thermo-susceptible, while SW2 (Section 3.3.3.1) was classified as a thermotolerant wheat variety. All three lines were supplemented with proline before being heat shocked, and a few differences were noted between the cereal species. Firstly, exogenous proline suppressed PCD in both wheat and barley seedlings, but proline efficacy was markedly stronger in WB1 treated seedlings (Figure 4.5). For example, when proline was supplemented across 1-10 µM, the average difference in PCD levels compared to the SDW and BG11 controls were approximately 19% for both SW2 (Figure 4.6A) and SW4 (Figure 4.6B) proline-treated seedlings, but 28.3% for WB1 proline-treated seedlings.

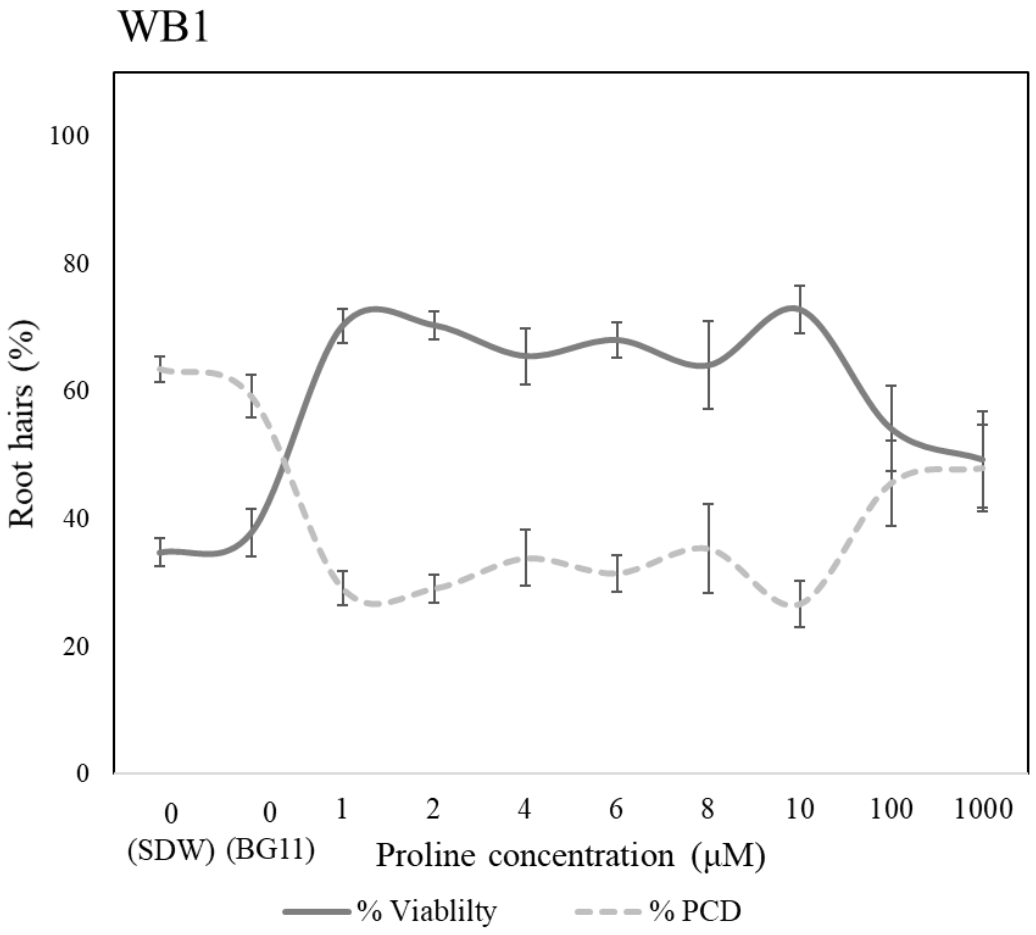


**Figure 4.5** - Effect of exogenous proline treatment at 45 °C in thermo-susceptible WB1 barley. Values represent merged results of 3 experiments, n≥12 (± SE). Each cell mode is represented as the percentage of cell mode over total number of root hairs, where viability% + PCD% + necrosis% = 100%, but the necrotic data is omitted here for clarity.

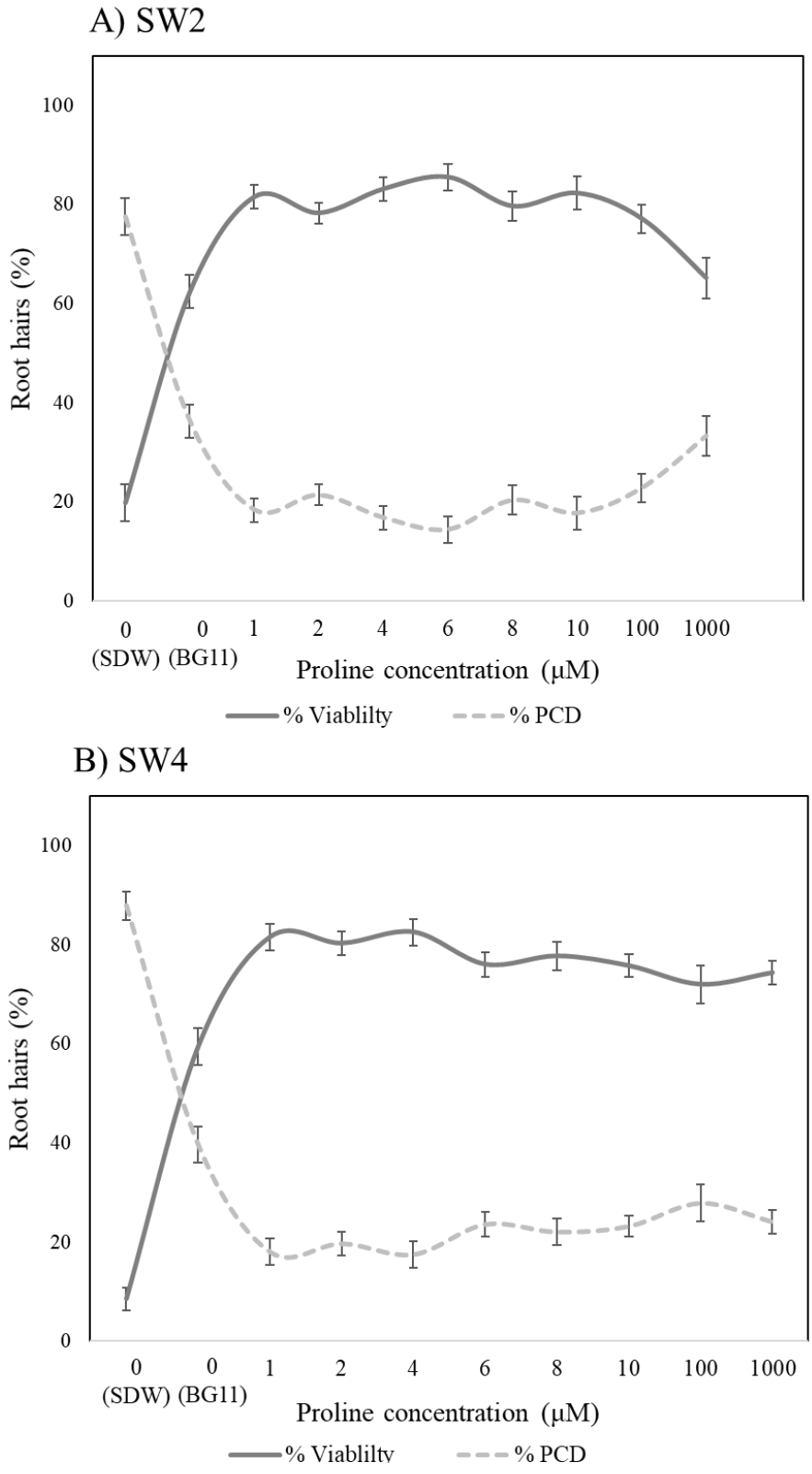


**Figure 4.6** - Effect of exogenous proline treatment at 45 °C in (A) thermotolerant SW2 wheat, (B) thermo-susceptible SW4 wheat. Values represent merged results of 3 experiments, n≥12 (± SE). Each cell mode is represented as the percentage of cell mode over total number of root hairs, where viability% + PCD% + necrosis% = 100%, but the necrotic data is omitted here for clarity.

Secondly, BG11 (59.2%) and SDW (63.5%) had no bioactive effect in treated barley seedlings as their PCD levels were not statistically distinct ($p$>0.05) from each other (Table 4.4). However, BG11 treatment had an unusual PCD-suppressing effect in both wheat varieties that was highly statistically significant ($p$<0.05); SW2 and SW4 experienced an immense 39.5% and 48.2% decline, respectively, in PCD levels relative to the SDW control seedlings. This curious effect was not detected in the BG11 controls of WB1 (Figure 4.5) or *Arabidopsis* seedlings (Figure 4.3), conceivably due to inter-species variances. Finally, all three cereal varieties proved surprisingly tolerant to elevated proline doses (> 100 μM) that would otherwise be cytotoxic in *Arabidopsis*. While no inflection point was noted across the three cereal lines, both wheat varieties were more tolerant to elevated proline doses compared to barley. Significant PCD inhibition ($p$<0.05) still took place when seedlings were pre-treated at 100 μM (SW2 and SW4) and 1000 μM (SW4), but this was not the case for barley. In WB1 seedlings, one-way ANOVA analysis established that PCD levels of WB1 seedlings pre-treated with ≥ 100 μM proline were not significantly ($p$>0.05) different from the BG11-treated control (Table 4.4C).

Additionally, past work identified SW2 and SW4 as heat tolerant and susceptible varieties, respectively; this was reflected by the higher PCD levels exhibited by SW4 (87.9%) compared to SW2 (77.6%) in their SDW-treated controls. However, it was noteworthy to see that BG11 and proline pre-treatment exerted a beneficial pro-survival effect that eliminated the initial discrepancies in basal tolerance. Similar PCD levels were recorded across both varieties in BG11 (SW2: 36.3%, SW4: 39.7%) and proline-treated seedlings; the average PCD levels across 1-100 μM proline treated seedlings was 18.8% (SW2) and 21.7% (SW4), respectively. Like *Arabidopsis*, proline did not exert a dose-dependent effect across barley and wheat seedlings; similar PCD-suppression levels were noted across the proline gradient tested, apart from selected cytotoxic proline doses in WB1 and SW2 seedlings. This shows that proline levels as low as 1 μM was enough to elevate wheat and barley stress tolerance, even at 45 °C heat shock

**Table 4.4** – Effect of exogenous proline treatment at 45 °C heat shocked wheat (A – SW2, B – SW4) and barley (C-WB1) seedlings. Values, n≥12 (± SE). A Dunnett *t*-test was used for statistical analysis which treated the BG11 dataset as a control and compared all other group datasets against it. (*) The mean difference is significant at the 0.05 level.

**A) SW2**

| Proline treatment (µM) prior to 45°C heat stress | % PCD | Mean Difference from BG11 (%) | Sig. |
|---|---|---|---|
| 0 (BG11) | 36.3 ± 3.50 | N/A | N/A |
| 0 (SDW) | 77.6 ± 3.99 | 39.5* | 0.000 |
| 1 | 18.3 ± 2.39 | -19.8* | 0.000 |
| 2 | 21.3 ± 2.14 | -16.7* | 0.003 |
| 4 | 16.7 ± 2.29 | -21.3* | 0.000 |
| 6 | 14.4 ± 2.66 | -23.7* | 0.000 |
| 8 | 20.3 ± 2.92 | -17.8* | 0.002 |
| 10 | 17.7 ± 3.33 | -20.4* | 0.000 |
| 100 | 22.7 ± 2.75 | -15.3* | 0.009 |
| 1000 | 43.0 ± 7.32 | -4.8 | 0.854 |

**B) SW4**

| Proline treatment (µM) prior to 45°C heat stress | % PCD | Mean Difference from BG11 (%) | Sig. |
|---|---|---|---|
| 0 (BG11) | 39.7 ± 2.64 | N/A | N/A |
| 0 (SDW) | 87.9 ± 3.61 | 48.2* | 0.000 |
| 1 | 18.1 ± 2.43 | -21.6* | 0.000 |
| 2 | 19.7 ± 2.71 | -20.0* | 0.000 |
| 4 | 17.5 ± 2.49 | -22.2* | 0.000 |
| 6 | 23.6 ± 2.71 | -16.1* | 0.000 |
| 8 | 22.0 ± 2.12 | -17.6* | 0.000 |
| 10 | 23.2 ± 3.74 | -16.5* | 0.001 |
| 100 | 27.8 ± 4.27 | -11.8* | 0.023 |
| 1000 | 24.1 ± 2.4 | -15.6* | 0.002 |

**C) WB1**

| Proline treatment (µM) prior to 45°C heat stress | % PCD | Mean Difference from BG11 (%) | Sig. |
|---|---|---|---|
| 0 (BG11) | 59.2 ± 3.40 | N/A | N/A |
| 0 (SDW) | 63.5 ± 2.05 | 4.25 | 0.951 |
| 1 | 29.2 ± 2.64 | -30.1* | 0 |
| 2 | 29.1 ± 2.18 | -30.2* | 0 |
| 4 | 33.8 ± 4.40 | -25.4* | 0 |
| 6 | 31.5 ± 2.87 | -27.7* | 0 |
| 8 | 35.4 ± 7.01 | -23.9* | 0.001 |
| 10 | 26.7 ± 3.58 | -32.6* | 0 |
| 100 | 45.6 ± 6.71 | -13.6 | 0.127 |
| 1000 | 48.0 ± 6.79 | -11.3 | 0.473 |

### 4.3.3 Scanning electron microscope image of PLGA-proline microspheres

Preliminary work has already been done to generate proline microspheres using PLGA and chitosan as the polymer matrix. Figure 4.7 depicts the spherical nature of the PLGA-proline microparticles captured using a Hitachi® S-246ON scanning electron microscope. Images of the chitosan nanoparticles could not be captured as the Hitachi® S-246ON instrument lacked the ability to capture images on the nano-scale and the project lacked the resources needed to outsource the imaging work to an external laboratory. These are only preliminary results, but further optimisation of the proline encapsulation process and testing of their efficacy lies further on in the research process, as detailed in Chapter 5.

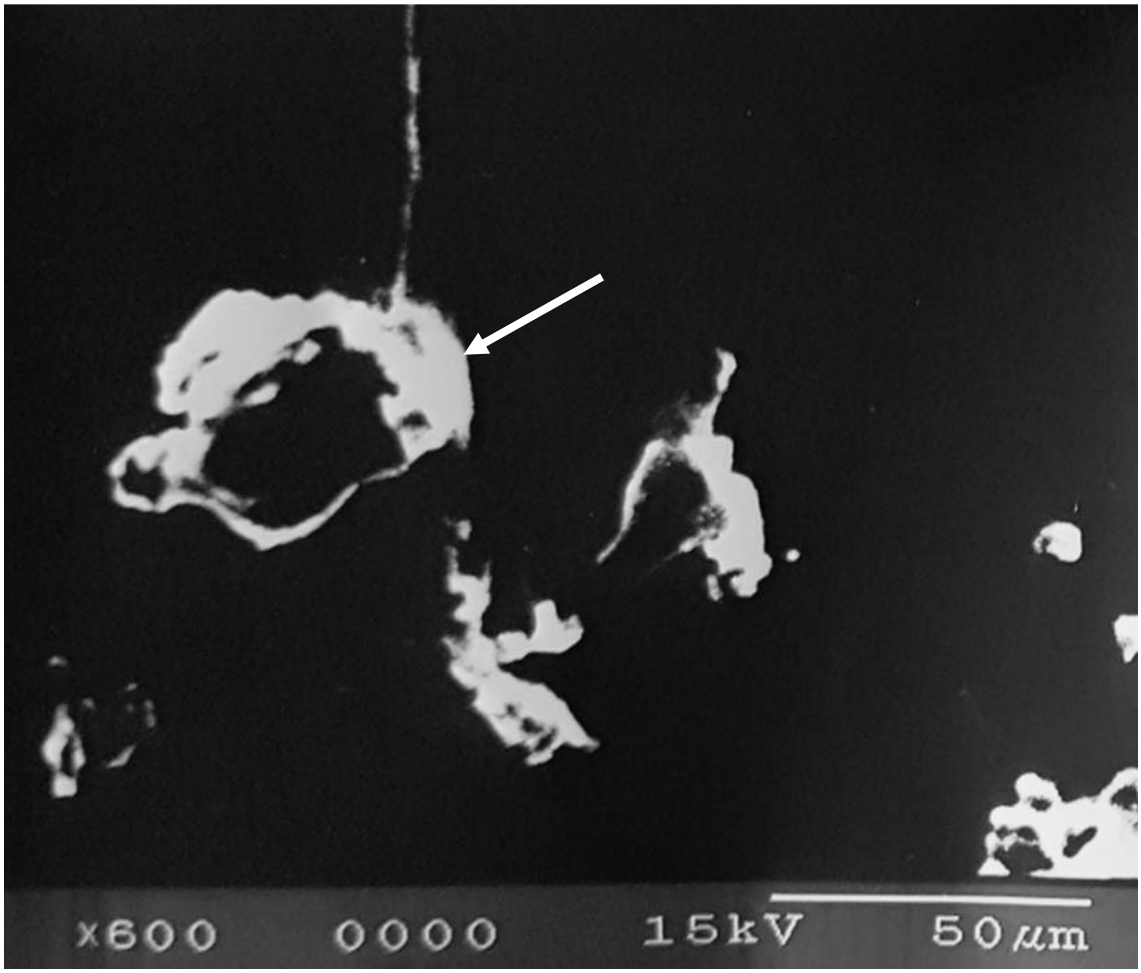


**Figure 4.7** – PLGA-proline microparticles. Note the spherical nature of the PLGA microparticles (white arrow), which are approximately 50 µm in diameter. Image author's own captured using a Hitachi® S-246ON scanning electron microscope.

## 4.4 Discussion

### 4.4.1 Bioactive effect of proline effective only at a narrow range

Encapsulation technology might be the next generation technique for delivering PGPR inoculants or agrochemicals to plants. Currently, the key agricultural companies that produce biofertilisers still rely on conventional formulation methods, e.g. powder, liquid or peat (Table 4.1), presumably owing to the relative newness of encapsulation technology and the cost associated with it. For future applications of this project, this thesis proposes using encapsulation technology to deliver proline gradually to plants. However two key variables must be factored in the formulation process for encapsulation to be successful: (1) the maximum safe dosage of proline that can be administered without having cytotoxic effects, and (2) proline efficacy across different stress intensities for optimum application timing. The two variables are discussed in detail in the following sections.

#### 4.4.1.1 Maximum safe dosage of proline

Encapsulated microspheres enable the continuous release of agrochemicals for prolonged bioactivity, thus reducing the dosage effect needed for efficacy (Kashyap *et al.* 2015). Nevertheless, care must be taken to ensure that microspheres are not loaded with overly high proline levels, as this will safeguard against accidental ruptures if the microspheres have poor mechanical stability. For example, the structural integrity of alginate-based microspheres are disrupted by low pH levels, cation chelating agents, and anti-gelling cations (Rathore *et al.* 2013). Therefore, this chapter sought to assess the extent of the dose-dependent response of proline over a broad concentration range (1-1000 μM). A large gradient was evaluated to strike a balance between prolonging the bioactive effect, while avoiding cytotoxicity; the more proline is loaded, the longer its efficacy as it would take longer for the proline reservoir within microspheres to be gradually emptied, but too much proline would be hazardous to plants. Furthermore, past studies have reported a proline dose-dependent effect and this work sought to assess if a similar phenomenon would occur in heat stressed seedlings. For example, Posmyk and Janas, (2007) reported that exogenous proline stimulated germination rates in cold-stressed (5°C) *Vigna radiata* L. seeds in a dose-dependent manner and protected against chilling injury by membrane stabilisation and reducing lipid peroxidation damage. Similarly in salt-stressed *Saccharum officinarum* L. seedlings, exogenous proline reduced $Na^+$ accumulation

proportionally to the duration of proline exposure and upregulated antioxidant activity (APX, CAT and POD) (Medeiros *et al.* 2015).

However, the results here proved contrary as exogenous proline did not exert a dose-dependent effect in *Arabidopsis*, barley or wheat seedlings. Moreover, the work here found that proline was only effective at low-to-medium doses (1-10 μM) when *Arabidopsis* seedlings were heat shocked near the viability/PCD inflection point. For example, excessive proline supplementation near the PCD/necrosis threshold prompted a three-fold increase in stress-induced necrotic levels. However, the three cereal varieties were more tolerant to elevated proline supplementation (> 100 μM) that would otherwise prove cytotoxic if supplied to *Arabidopsis* seedlings. SW2 was the most tolerant variety, followed by SW4 and WB1, respectively, with both wheat varieties being more tolerant than WB1 to overly high proline doses. While this may appear to be surprising, this concurs with existing literature detailing how plants have a highly dynamic response to heat stress that varies according to plant genotypes (Hasanuzzaman *et al.* 2013).

The cytotoxic proline effect is interesting as Hare *et al.* (2002) demonstrated that excessive proline degradation drives substantial flux through the MET chain, which elevates ROS levels and causes severe oxidative damage to chloroplast and mitochondrial ultrastructure in *Arabidopsis* leaves. If a comparable scenario takes place here, excessive proline supplementation increases the ROS sensitivity and causes treated seedlings to be more susceptible to necrosis, rather than PCD, when exposed to heat shock near the PCD/necrosis threshold. Burbridge *et al.* (2007) reported a similar phenomenon as peroxidase-overexpressing tobacco lines with enhanced ROS sensitivity died predominantly by PCD under medium stresses but were more vulnerable at higher stress intensities and died primarily by necrosis because of overwhelming oxidative damage.

On the whole, the results here concur with past reports as the correlation between proline accumulation and plant stress tolerance applies only to a certain point; low concentrations confer plant stress tolerance in a dose-dependent manner, but excessively high doses induce cell death (Kavi Kishor *et al.* 2005; Hayat *et al.* 2012; Kavi Kishor and Sreenivasulu 2014). Under excessive proline supplementation, the elevated stress-induced PCD and necrosis levels is reminiscent of the reported cytotoxic effects of over-supplying plants with proline. Studies in *Arabidopsis* hypocotyl explants (Hare *et al.*

2001) and *Distichlis spicata* suspension cultures (Rodriguez and Heyser 1988) show that exogenous proline provides beneficial effects at low concentrations but inhibits growth when supplied at excessively high concentrations. Similarly, rice seedlings that were over-supplied with proline exhibited symptoms of cadmium heavy metal stress poisoning, with inhibited root growth and elevated root peroxidase activity (Chen and Kao 1995). This cytotoxic effect is attributed to incomplete proline degradation as proline homeostasis is essential for maintaining cell division for sustainable plant growth under long-term stress (Kavi Kishor *et al.* 2005; Kavi Kishor and Sreenivasulu 2014). Disruption of proline homeostasis leads to P5C overaccumulation, which perturbs redox homeostasis and elevates ROS levels, culminating in cell death (Deuschle *et al.* 2004). Altogether, the results show that proline doses beyond 100 μM exerts a cytotoxic effect in *Arabidopsis* and barley, but not in wheat seedlings. Having determined this dosage threshold, this will be factored into the encapsulation formulation process to ensure that accidental microsphere dissolution will be less hazardous to the surrounding environment.

#### 4.4.1.2 Proline efficacy across different stress intensities

Biofertilisers can be applied at different plant growth stages depending on the formulation and mechanism of action; for example, Biodoz™ and Nitragin™ Gold are $N_2$-fixing *Rhizobium* inoculants applied as a seed coating, while Prestop® is dispersed using a foliar spray as a preventative measure against fungal pathogens (Table 4.1). Similarly, proline microspheres should ideally be administered as a preventative measure to buffer against abiotic stress, especially if irregular meteorological conditions, such as high temperatures or prolonged drought, have been forecasted. Timing is crucial in this context, as optimum applications will result in highest efficacy. In line with this, proline bioactivity was evaluated across different temperatures to ascertain its optimum performance. Unfortunately, the results showed that proline was only effective at a narrow stress range, as demonstrated in *Arabidopsis* seedlings.

At low and high heat shock, proline-treated plants had similar stress-induced PCD levels as their control seedlings. Presumably, root hairs acclimated to low-stress levels by upregulating cell protective mechanisms such as osmolyte biosynthesis and antioxidant defence (Tausz *et al.* 2004), without requiring additional priming from proline supplementation. However, excessive heat exposure at the PCD/necrosis threshold was too much for plant cells to endure and proline treatment was unable to suppress PCD at

55 °C heat shock. This was likely due to excessive protein denaturation and disruption of the cell membrane fluidity, a common characteristic of cells under heat stress (Wang *et al.* 2004). Instead, effective PCD-suppression was only observed when plants were exposed to stress near the viable/PCD inflection point, with substantial variations in the consistency of the stress-response between 50 °C and 52 °C heat-shocked *Arabidopsis* seedlings. The differences in the inflection points between both datasets reflected this. At 50 °C heat shock, a clear delineation could be seen between the BG11 control and proline treated seedlings as high PCD suppression was observed up to 6 μM, followed by a gradual decline until the inflection point was reached near the midpoint between 10 and 100 μM. In contrast, exogenous proline induced a highly variable response in 52 °C heat-shocked seedlings, as the only significant PCD suppression (13.5% reduction from BG11 control) was noted in the 6 μM proline treatment. The inconsistency of the stress response was manifested in the four inflection points observed across the 1-1000 μM proline gradient. Apart from the unusually high PCD levels in 4 μM proline-treated seedlings, similar or higher PCD levels to the BG11 control seedlings were encountered when seedlings were treated to low or elevated proline doses, respectively.

It is unclear why proline exerted a clear PCD-suppression effect at 50 °C but not at 52 °C, considering how both temperatures fall within the PCD zone. A feasible interpretation for this discrepancy is the proximity to the PCD/necrosis threshold; 52°C might be too near this threshold at which stress levels are just too high to recover from. Proline may modulate multiple plant stress responses, but if the severity of the injury is too high, i.e. near the PCD/necrosis threshold, exogenous proline treatment will not suffice to restrict excessive protein denaturation and ROS generation, associated with heat-induced damage (Hasanuzzaman *et al.* 2013). The overwhelming oxidative damage depletes the antioxidant activity and degrades the metabolic system, culminating in lipid peroxidation, electrolyte leakage, and eventual cell death (Tausz *et al.* 2004).

Collectively, the results show the valuable PCD-suppressing effects of proline bears an important caveat; its efficacy was only displayed when *Arabidopsis* seedlings were exposed to stress near the viability/PCD inflection point. No bioactive effect was observed in proline-treated seedlings at the other stress-response thresholds (stress-tolerant and PCD/necrosis), at least in the context of transient heat shock and in *Arabidopsis* seedlings. Perhaps a different outcome will arise under different testing

conditions, e.g. prolonged, but milder stress exposure, or in different plant species and growth stages, as proline efficacy was only evaluated in 5-day-old *Arabidopsis* seedlings. This would be an area of interest for future investigations as the heat stress response in plants constantly shifts across different plant genotypes, stress intensity and duration (Hasanuzzaman *et al.* 2013). For now, the results indicate that optimum application of proline microspheres as a preventative measure against abiotic stress is only effective at limited stress intensities.

### 4.4.2 Bioactive effect of proline and BG11 in cereals

Exogenous proline also increased cereal stress tolerance by suppressing PCD in wheat and barley varieties, as was observed in *Arabidopsis* seedlings. These findings are in line with heat-stress studies that also observed the ability of exogenous proline to confer thermotolerance in chickpea (Kaushal *et al.* 2011) and barley seedlings (Oukarroum *et al.* 2012). External proline supplementation in heat-shocked chickpea seedlings resulted in lower lipid peroxidation levels, higher tissue viability and preservation of chlorophyll and cell membrane integrity (Kaushal *et al.* 2011). The lower oxidative damage by proline-treated seedlings was attributed to the upregulation of various enzymatic (SOD, CAT, APX and GR) and non-enzymatic (AsA and GSH) enzymes (Kaushal *et al.* 2011). At 45 °C heat shock in barley seedlings, exogenous proline increased the thermostability of the oxygen-evolving complex (OEC) in photosystem II (Oukarroum *et al.* 2012). Besides stabilising the OEC's critical $Mn^{2+}$ cluster, exogenous proline also functioned as a supplementary electron donor to PSII to ensure continued NADPH production (Oukarroum *et al.* 2012).

However, BG11 had an unusual PCD-suppression effect in wheat seedlings not observed in *Arabidopsis* and barley seedlings. BG11-treated SW2 and SW4 seedlings had significantly ($p<0.05$) lower stress-induced PCD levels relative to their SDW control, with a decline of 39.5% and 48.2%, respectively. While this effect is unusual, it is not entirely uncommon as the mineral status of plants is highly influential in stress survival (Cakmak 2005; Robertson 2013; Wang *et al.* 2013b). BG11 is the nutrient medium for *N. muscorum*, and it contains a rich mix of macronutrients and micronutrients for cyanobacteria growth. The formulation is compromised of dipotassium phosphate, sodium nitrate, magnesium sulfate, calcium chloride, citric acid, ferric ammonium citrate, EDTA (disodium magnesium salt) and a trace metal solution containing boric acid,

manganese chloride, zinc sulfate, sodium molybdate, copper sulfate and cobalt nitrate (Table 2.1).

Exposure to elevated temperatures causes mass protein misfolding, disruption of the plant-water balance and cell membrane integrity, and inhibition of photosynthesis (Waraich *et al.* 2012). Careful management of plant nutrition can partially alleviate these heat stress symptoms and out of the listed compounds in BG11 medium, nitrogen (N), potassium ($K^+$), calcium ($Ca^{2+}$), magnesium ($Mg^{2+}$), boron (B), and manganese ($Mn^{2+}$) are known to increase plant thermotolerance (Waraich *et al.* 2012). Exogenous application of N and $Mg^{2+}$ are known to reduce ROS levels through stimulation of SOD, CAT and POD antioxidant activity (Waraich *et al.* 2012); both elements also form the critical porphyrin ring in chlorophylls required for photosynthesis to prevent over-reduction of the photosynthetic ETC (Fiedor *et al.* 2008). Micronutrients like B and $Mn^{2+}$ also have key roles in many fundamental physiological processes, while the latter is an essential cofactor in SOD and the OEC in PSII (Millaleo *et al.* 2010; Salomé 2017). In addition, $K^+$ is the most abundant cation in plant cells and acts as an inorganic osmolyte (Wang *et al.* 2013b). Osmoregulation is a regular response feature to many stresses as cellular water imbalance is a common secondary effect of a multitude of primary stress signals (Sharma and Dietz 2006; Zhu 2016). Compatible osmolytes are upregulated to regulate cell volume to protect against water-stress such as fluctuations in temperature and pressure, desiccation, salinity, freezing and metal toxicity (Verslues and Sharma 2010; Lv *et al.* 2011). The roles of inorganic and organic osmolytes depend on the length of the water-stress: inorganic osmolytes like $K^+$ play an essential role under short-term water loss by decreasing intracellular water potential relative to the external environment (Yancey 2001, 2005). The accumulation of inorganic osmolytes ($K^+$, $Cl^-$ and $Na^+$) within cells helps to re-establish cell turgidity, which is partially controlled by voltage-gated $K^+$ transporters localised at the plasma membrane (Wang *et al.* 2013b). If water-stress conditions persist, organic osmolytes replace their inorganic counterparts because excessively high cellular ionic concentrations are cytotoxic (Yancey 2001, 2005). In short, inorganic osmolytes play an important role in maintaining plant-water homeostasis under short-term water stress, but are supplemented by organic osmolytes under long-term conditions (Yancey 2001, 2005).

Nevertheless, if one is to speculate, the presence of $Ca^{2+}$ likely accounts for the primary bioactive effect observed in BG11-treated wheat seedlings. Many studies have shown that exogenous $CaCl_2$ application confers higher thermotolerance in treated plants (Jiang and Huang 2001; Kleinhenz and Palta 2002; Kolupaev *et al.* 2005). While $Ca^{2+}$ is primarily known as an essential signaling molecule, it also has an essential structural role in maintaining cell wall and plasma membrane integrity (Robertson 2013). For example, potato tubers treated with $CaCl_2$ had increased cell membrane stability (Kleinhenz and Palta 2002). By elevating $Ca^{2+}$ concentrations in the root zone, the effects of prolonged heat stress were partially alleviated by enabling continued meristematic activity, notably in secondary shoots (Kleinhenz and Palta 2002). Exogenous $CaCl_2$ treatment also increased the thermotolerance in two cool-season grasses (*Poa pratensis* L. and *Festuca arundinacea* L.) by upregulating enzymatic antioxidant activities of CAT, GR and AP (Jiang and Huang 2001). $CaCl_2$-treated plants also experienced lower oxidative damage in the form of reduced lipid peroxidation damage (Jiang and Huang 2001). Similarly, $CaCl_2$-treated wheat seedlings had upregulated GPOX, SOD and CAT antioxidant activity, and were more tolerant to high heat stress than untreated controls (Kolupaev *et al.* 2005). Additional studies have shown that $Ca^{2+}$ also plays a critical role in the induction of HSPs to gain thermotolerance (Trofimova *et al.* 1999; Saidi *et al.* 2009). Interestingly, exogenous $Ca^{2+}$ supplementation exerts a beneficial priming effect by causing minor oxidative damage (Kolupaev *et al.* 2005). Prior to heating, $Ca^{2+}$ exposure caused short-term oxidative damage by increasing ROS and lipid peroxidation levels, which primed cells to increase the rate of defense responses when seedlings were heat-shocked (Kolupaev *et al.* 2005). This is reminiscent of how exposure to a non-lethal stress cue can leave a stress-imprint that facilitates elevated resistance against recurrent stress encounters (Walter *et al.* 2013).

#### 4.4.2.1 Reconciling the role of $Ca^{2+}$ in PCD initiation and stress tolerance

The ability of exogenous $Ca^{2+}$ treatment in enhancing stress tolerance may appear to be surprising as $Ca^{2+}$ is a secondary messenger common to animal apoptosis and plant PCD (Kacprzyk *et al.* 2011). However, PCD activation is triggered by intracellular $Ca^{2+}$ spikes as demonstrated by Kacprzyk *et al.* (2017) who showed that inhibition of $Ca^{2+}$ flux into the cell using $Ca^{2+}$ channel blockers ($LaCl_3$ and $GdCl_3$) suppressed cytoplasmic retraction and delayed PCD-induced cell death. Other studies have shown that stress exposure generates a customized $Ca^{2+}$ signature (e.g. varying amplitude, duration and frequency)

in the cytoplasm for each stress cue and that an assortment of $Ca^{2+}$ sensors links each custom $Ca^{2+}$ signature to the specific stress-defence response pathway (Laude and Simpson 2009; Stael *et al.* 2012). In the absence of stress though, plant cells carefully regulate cytoplasmic $Ca^{2+}$ levels to maintain substantially lower concentrations (100 nM) than cell walls and organelles (0.1-80 mM) (Robertson 2013). Plant cells rely on autoinhibitory $Ca^{2+}$ ATPase pumps and tonoplast-localised cation exchange proteins to export cytoplasmic $Ca^{2+}$ into the vacuole and ER; both protein groups are safety mechanisms that dampen cytoplasmic $Ca^{2+}$ signals to avoid triggering unintended PCD (Cakmak 2005; Robertson 2013; Wang *et al.* 2013b). Collectively, the careful regulation between extracellular and intracellular $Ca^{2+}$ transport reconciles the seemingly contradictory role of $Ca^{2+}$ in thermotolerance and as a secondary messenger in PCD initiation.

#### 4.4.2.2 Possible role of $Ca^{2+}$ in the BG11 bioactive effect observed in *T. aestivum* seedlings

Nevertheless, $Ca^{2+}$ supplementation does not always confer stress-tolerance across all plant species as it failed to modulate $Na^{+}$ accumulation in salt-stressed maize (Cramer 2002) or rice seedlings (Yeo *et al.* 1987; Yadav *et al.* 1996). This interspecies variability effect is likely at play here too as the PCD-suppressing effects of BG11 was observed only in wheat, but not *Arabidopsis* and barley seedlings. Without additional testing, it is difficult to speculate why the mineral status of BG11 only impacted wheat seedlings. Nonetheless, a potential explanation might lie in the differences between SnRK2 (sucrose non-fermenting 1-related protein kinase 2), a key enzyme in abiotic stress (e.g. drought, salt, cold and osmotic) signal transduction network (Kulik *et al.* 2011). SnRK2 regulates water stress-response (e.g. LEA proteins) genes but is primarily recognised for its key role in ABA signalling pathways (Fujita *et al.* 2009). The key targets for SnRK2 phosphorylation are the ABRE-binding factors (ABFs) and ABA-response-element-binding proteins (AREBPs), which trigger a large-scale transcriptional response of ABA-regulated genes to reprogram the plant metabolome for increased stress resistance (Kulik *et al.* 2011). Interestingly, the SnRK2 protein in barley (Barker *et al.* 1996) and *Arabidopsis* (Zhang *et al.* 2008) are calcium-independent as exogenous $Ca^{2+}$ supplementation did not increase enzyme activity. However, Coello *et al.* (2012) showed that the 42 kDa SnRK2 in wheat roots are calcium-dependent as exogenous $CaCl_2$ supplementation resulted in an impressive eight-fold rise in AREBP1 and AREBP2

peptide phosphorylation activity. ABA is well known for its integral role in the osmotic stress response, but also plays a significant function in heat tolerance (Sah *et al.* 2016; Huang *et al.* 2016; Wang *et al.* 2017). For example, the heat shock factor HSFA6b acts as a central regulator that links ABA-signalling pathways to heat stress responses, including HSPs expression (Huang *et al.* 2016). This $Ca^{2+}$-dependent response in wheat seedlings might account for the BG11 bioactive effect in wheat, but not in *Arabidopsis* and barley seedlings, and further testing would be required to substantiate this hypothesis.

# 4.5 Conclusions

In this chapter, the results show that the bioactive effect of proline was only effective across a narrow stress range. PCD-suppression was only displayed when seedlings were heat-shocked at the viability/PCD inflection point (50 °C and to a lesser degree, 52 °C). No PCD-suppression was observed when *Arabidopsis* seedlings were subjected to heat shock across the stress-tolerant (25-45 °C) and PCD/necrosis (55 °C) threshold, at least with regards to transient and acute stress exposure. Treatment of *Arabidopsis*, wheat and barley seedlings with varying proline levels established that PCD-suppression occurred under low concentrations, but were cytotoxic under higher concentrations, in line with past studies reporting the cytotoxic effects of excessive proline supplementation. In addition, proline supplementation elicited comparable stress-induced PCD levels across the thermotolerant SW2 and thermo-susceptible SW4 varieties, illustrating the effectiveness of priming to compensate for poor basal stress tolerance. Finally, BG11-treated wheat seedlings had unusually low PCD levels, showing that the plant mineral status must not be overlooked in the stress survival and recovery process. The $Ca^{2+}$-dependent SnRK2 in wheat seedlings might account for why the PCD-suppression effect of BG11 treatment was not detected in *Arabidopsis* and barley seedlings.

# Chapter 5 - Conclusions and Future Perspectives

This project aimed to investigate the hypothesis that bioactive compound(s) in *N. muscorum* CM could be identified and used for increasing plant stress tolerance. To investigate this hypothesis, a workflow was developed using *Arabidopsis* root hairs as a model system to screen *N. muscorum* CM fractions for bioactive properties. Initial screening experiments showed that *N. muscorum* CM fractions reduced stress-induced PCD levels in a dose-dependent manner, with inconsequential changes to necrosis levels. Autoclaving did not attenuate the efficacy of CM fractions, establishing the thermostability of the main bioactive. However, autoclaved fractions had consistently lower PCD-suppression rates, demonstrating that *N. muscorum* CM contains additional thermolabile bioactives.

The main outcome from the screening process was that the main bioactive compound was thermostable and influencing the PCD pathway; this information was applied to narrow the list of bioactive candidates from a literature review of known *N. muscorum* exometabolites. Thermolabile groups such as EPS and exoproteins were disqualified as prime candidates, while phytohormones, alkaloids and phenolics were regarded with secondary importance as thermal processing usually culminates in the loss of bioactivity. The remaining thermostable candidate groups were amino acids, fatty acid derivatives and LCB sphingolipids. A framework was developed to identify candidates of importance based on three variables: 1) mechanism of PCD suppression, 2) cyanobacteria release and 3) plant uptake. Out of the compounds considered, proline had the properties that best satisfied the three variables.

Firstly, exogenous proline reduces ROS levels by upregulating the antioxidant AsA-GSH cycle and GSH-based glyoxalase system (Kumar and Yadav 2009; Hossain and Fujita 2010; Hossain *et al.* 2011, 2014b), which carries significance, as elevated ROS levels trigger PCD activation (Breusegem and Dat 2006; Doyle *et al.* 2010; Wang *et al.* 2013a; Gutiérrez *et al.* 2014). Next, cyanobacteria are Gram-negative soil bacteria with weaker cell walls than their Gram-positive counterparts (Harris 1981; Halverson *et al.* 2000) and the hydrophobic nature of proline enables its spontaneous membrane diffusion into the extracellular environment (Picossi *et al.* 2005; Pernil *et al.* 2008). Lastly, plants have three amino acid transporter subfamilies that can import proline: two general (AAP1 and

LHT1) and one proline-specific (ProT) (Lehmann *et al.* 2010). Collectively, proline was the strongest candidate out of the remaining thermostable compounds as it best fulfilled the framework and offered a feasible proposition of how cyanobacteria-derived proline can be assimilated by plants to decrease vulnerability against stress.

The existence of proline in *N. muscorum* CM was verified using two independent methods: the ninhydrin assay and reverse-phase HPLC. The original HPLC method by Pernil *et al.* (2008) lacked key details that limited its reproducibility. Therefore, an improved protocol was required to detect the amino acids in the complex matrix that is *N. muscorum* CM. Apart from proline, the following amino acids were also detected: glutamic acid, serine, asparagine/glycine, glutamine, histidine, arginine, threonine, alanine, tyrosine, valine, methionine, isoleucine/leucine, phenylalanine, tryptophan and lysine. Amino acid peaks resembling aspartic acid and cysteine were likewise noted, but further work in modifying the mobile phase gradient will be needed to confirm their presence.

Confirmation of proline as the main bioactive compound in *N. muscorum* CM was performed using two experimental series. In the first set of experiments, autoclaved and non-autoclaved exogenous proline was supplied to *Arabidopsis* seedlings at the exact concentrations measured in *N. muscorum* CM. Exogenous proline elicited a remarkably similar stress-response profile as *N. muscorum* CM fractions by modulating the PCD sensitivity threshold of treated seedlings. This offered more evidence for proline as the candidate of interest as proline efficacy was not lost with autoclaving, confirming its thermostable nature. However, exogenous proline did not suppress PCD in a dose-dependent manner as *N. muscorum* CM fractions had done; it is likely that proline acts synergistically with accompanying thermolabile bioactives in *N. muscorum* CM to wield a stronger PCD-suppressing effect, compared to individual proline treatments. For the second set of RHA experiments, proline impaired transporter mutants were treated with exogenous proline or *N. muscorum* CM and their stress response compared against wild-type seedlings. Mutant lines exhibited a diminished ability to import proline when they were supplied with cytotoxic proline levels; excessive proline doses elevated stress-induced PCD levels in wild-type seedlings, but mutant lines remained unaffected because of their limited capacity to assimilate proline. In heat shock experiments, all three mutants had higher PCD levels than wild-type *Arabidopsis* seedlings under similar proline

treatments. This provided additional evidence for proline as the major bioactive compound as the PCD-suppressing effects noted in wild-type seedlings were lost in the mutant lines.

While all three mutants did not respond to the priming effects of proline, there appeared a clear delineation between the stress-response profile between the general (*lht1* and *aap1*) and proline-specific (*atprot1-1::atprot2-3::atprot3-2*) mutant transporters. The *atprot* triple knockout did not have a strong phenotype because of the overlapping functions shared with the other transporters. *lht1* and *aap1* mutants were more vulnerable to heat shock because of the weakened capacity to import proline into root cells (both mutants), the inability to import proline into leaf mesophyll cells (*lht1* mutant), and impaired capacity for long-distance proline translocation (*aap1* mutant). This shows that proline homeostasis plays just as important a role as proline accumulation for survival against stress. Both *lht1* and *aap1* mutants have a limited capacity to import proline into root cells and rely primarily on proline biosynthesis to mitigate stress symptoms. This is aggravated by the failure to cycle proline efficiently throughout plant tissue as disruption of proline homeostasis increases lethality rates as P5C overaccumulation triggers PCD. Finally, *N. muscorum* CM treatment had the strongest PCD-suppression levels across wild-type and mutant lines, although this effect was weaker in the mutant lines. This supports previous findings in the initial screening experiments that CM contains bioactives that operate synergistically to suppress PCD compared to individual proline treatments alone. Future work to identify these synergistic bioactives will be needed and candidates include EPS, ROS-detoxifying exoproteins, phenolics, phytohormones and sphingolipids.

Purification and analysis of these potential pro-survival compounds will require significant work. For example, the method outlined by Richert *et al.* (2005) can be applied to fractionate the *N. muscorum* EPS into three groups (sheath, capsulated and released polysaccharides). Identification of the individual sugars can be achieved using Fourier transform infrared (FTIR) spectroscopy and gas chromatography (Richert *et al.* 2005). The oxygen radical absorbance capacity (ORAC) assay can be used to assess the total antioxidant capacity of *N. muscorum* CM (Gillespie *et al.* 2007). The ORAC assay measures the rate of free radical quenching by hydrogen donation and can be used alongside the Folin–Ciocalteu colorimetric assay to measure the phenolic content in *N.*

*muscorum* CM (Ainsworth and Gillespie 2007). Using both assays to investigate the strength of ROS-detoxification will help estimate how much phenolic compounds contribute towards the general antioxidant capacity of *N. muscorum* CM and if other non-enzymatic antioxidants (e.g. ascorbate) are involved. Following that, identification of these phenolic compounds can be carried out using GC-MS analysis, per the methods reported by Abdel-Hafez *et al.* (2015).

An excellent paper by Karadeniz *et al.* (2006) describes the extraction, purification and quantitative detection of microbial phytohormones, such as auxin, gibberellin, cytokinin and ABA. Lastly, quantitative and unbiased recovery of lipids from cell-free supernatant can be achieved using methyl-*tert*-butyl ether extraction (Matyash *et al.* 2008). Using aminopropyl solid-phase extraction, sphingolipids can be fractionated into their respective classes: free ceramides, neutral glycosphingolipids, neutral phospholipids, acidic phospholipids, phosphorylated sphingoid bases, phosphoceramides and sulfatides (Bodennec *et al.* 2000). GC analysis can be used to profile the lipid content in each fraction. These potential bioactive compounds will be evaluated in wild-type and similar mutant (*aap1*, *lht1* and triple *atprot* knockout) lines, unless new proline transporter mutants are discovered. While single knockout *atprot* mutants could be investigated, e.g. *atprot1*, *atprot* 2 or *atprot3*, the benefits of investigating them are limited as the work done in this project and Lehmann *et al.* (2011) have shown they do not exhibit a strong phenotype, as other root-localised transporters are compensating for their loss-of-functions.

In Chapter 3, root hairs were again used as a model system for scoring *in vivo* PCD levels. The RHA was originally developed for *Arabidopsis* seedlings, and here the assay was extended for use in the agriculturally-important crops, barley and wheat. A protocol was developed for sterilising and germinating cereal seeds under axenic conditions, and experiments were performed to determine if potential variations existed in seedlings of the same species. Unlike *Arabidopsis* seedlings which have a single primary root, 1-day-old wheat seedlings have one long main root, surrounded by two shorter roots. However, only the main root in wheat seedlings were scored as the shorter, flanking roots lacked the root hair density needed to obtain an accurate portrayal of the overall viable, PCD and necrosis levels. In comparison, 2-day-old barley seedlings have around 3-5 roots of roughly equal length and a series of experiments was carried out to gauge their suitability

for the RHA. Testing revealed that barley roots from the same seedling had insignificant variability with each other. Thus, only a single root was scored per barley seedling for the subsequent heat shock experiments. Altogether, the RHA was successfully developed as a high-throughput method (~4 days from germination to data collection) for screening multiple cereal varieties and stress treatments together. Subsequently, by examining heat stress-induced PCD levels, a sharp delineation was observed between thermotolerant spring and thermo-susceptible winter barley varieties. Existing literature suggest that polymorphisms around the HSP and *VRN-H1* locus may account for the divergences in heat stress resistance between the seasonal barley varieties (Marmiroli *et al.* 1998; Maestri *et al.* 2002) and further investigations using stress-responsive probes and RFLP analysis can help to elucidate the mechanisms behind these differences.

In addition, eight wheat varieties were examined for their tolerance against heat and salt stress, independently. First, the inflection point for each stress was identified, and by analysing their stress-induced PCD levels at this inflection point, these reference markers were used to compare the different stress effects. Interestingly, thermotolerant wheat varieties (SW1 and SW2) were found to be similarly tolerant against salt stress. Likewise, heat-sensitive varieties (SW4 and WW1) exhibited similar vulnerabilities against salt shock. Heat and salt exposure induces primary stress-specific damage in the form of elevated protein misfolding (Wang *et al.* 2004) and disruption of cytosolic $Na^+$: $K^+$ balance (Munns 2010), respectively. However, the similar tolerance levels exhibited against heat and salt, two seemingly distinct stresses, is possible because of shared 'downstream housekeeping genes' that mitigate the overlapping secondary damage (e.g. oxidative damage and disruption of cellular osmotic potential) induced by these primary stresses (Munns 2010). Thus, the ability of SW1 and SW2 to resist two seemingly different stresses is likely because of a higher innate flux through these secondary damage-mitigating pathways, resulting in elevated basal tolerance in both varieties.

In the latter sections of Chapter 3, stress-induced PCD levels were used to evaluate basal, induced and cross-stress tolerance of the wheat varieties against heat and salt stress. Basal tolerance refers to the inherent capacity of plants to resist stress without previous exposure (Arbona *et al.* 2017) and was investigated here using a combination of single and combined stress exposures. Induced and cross-stress tolerance reflects the flexible ability of plants to mount a counteracting stress response against the initial stress cue (Walter *et*

*al.* 2013; Pandey *et al.* 2017), which were assessed by applying repetitive stresses of a different origin. Interestingly, stress-susceptible SW4 and WW1 lines had low basal tolerance against single and combined stress application, but a faster induced response against repetitive stress exposure. Low basal tolerance was partially compensated by a rapid induced response and the stress memory likely led to enhanced resistance against repetitive stress (Walter *et al.* 2013). An inverse scenario was noted in SW1 and SW2, as the stress-tolerant varieties had higher basal resistance, but a slower induced response compared to stress-susceptible lines. This was a similar strategy adopted by salt tolerant *P. euphratica* which had elevated basal expression of salt sensitive genes, but lower transcriptional responsiveness compared to *Populus* × *canescens*, its salt-susceptible counterpart (Janz *et al.* 2010). *P. euphratica* is pre-adapted to salt stress by constitutive expression of stress-responsive genes (ROS detoxification, osmolyte biosynthesis, ion carriers and metabolite transporters), but this elevated metabolic state came at the price of lower flexibility and a slower transcriptional response against salt stress (Janz *et al.* 2010). Evidence indicates that heat and salt tolerant SW1 and SW2 varieties used a comparable stress-anticipatory approach. Thus, the method outlined by Janz *et al.* (2010), e.g. examination of their transcriptomic (microarray analysis) and metabolomic data (Fourier Transform-Ion Cyclotron Mass Spectrometry), can be used to confirm this hypothesis. Additionally, signalling compounds (ROS, MG, $Ca^{2+}$, and phytohormones) (Clarke *et al.* 2004, 2009; Capiati *et al.* 2006; Hossain *et al.* 2016) and transcription factors (DREB1A, HSFs and MBF1C) (Kasuga *et al.* 1999; Ahammed *et al.* 2016) play a critical role in cross-stress tolerance and is another potential area of interest for future investigations. Collectively, the RHA can identify wheat varieties with unusual properties for further downstream tests using high-resolution molecular biology techniques, e.g. transcriptomics, proteomics and metabolomics, to determine how these differences arise.

Moreover, the RHA also successfully captured the dominance of salt stress over heat stress, matching the transcriptomics data presented by Rasmussen *et al.* (2013) who noted that plants prioritise the stress response against salt over heat stress, once again highlighting the versatility of the RHA. Compared to molecular biology techniques that are highly informative, but are expensive and labour intensive, the RHA is a comparatively simple method that integrates multiple input streams to a simple binary response: cell survival or death. By relying on careful experimental design, the RHA can

be scaled and tailored to different stress protocols in a simple ‘plug-and-play’ manner to explore a variety of experimental aims.

The results here also present additional evidence for past work showing that combined stress should be treated as a unique state of abiotic stress, and not one that can be solely discerned from individual stress-factor studies (Mittler 2006; Rasmussen *et al.* 2013; Rivero *et al.* 2014). Multiple wheat varieties were screened simultaneously and their stress response phenotypes recorded in a stress matrix, as first presented by Mittler (2006). However, the work elucidated here offers a cautionary reminder that while stress matrix tables are useful infographic tools, care must be applied if attempts are made to extrapolate results across research groups as stress phenotype can differ even within members of the same species. To summarise, the RHA is an adaptable tool that can be readily modified for different protocols and Chapter 3 presents a case-study for detecting intra-species variations in basal, induced and cross-stress tolerance. By identifying varieties with interesting traits, e.g. SW1 and SW2 (high basal tolerance, but slow adaptive response) or SW4 and WW1 (low basal tolerance, but fast adaptive response), the RHA can guide further experimental testing to elucidate their molecular and biochemical differences.

However, it must be acknowledged that these bookmarked varieties were identified under short-term stress and at early seedling stages. Future work should involve the evaluation of these varieties at later growth stages using conventional stress biomarkers. A few examples of stress-biomarkers that can be measured include total antioxidant capacity (Gillespie *et al.* 2007), biochemical stress markers (proline, ascorbate, glutathione, phenolic compounds, methylglyoxal and lipid peroxidation) (Ainsworth and Gillespie 2007; Queval and Noctor 2007; Abrahám *et al.* 2010; Mustafiz *et al.* 2010) and leaf disc assays (relative water content, cell membrane stability, cell viability and chlorophyll content) (Warren 2008; Jambunathan 2010; Verslues 2010). The resultant data would yield useful information on whether stress-induced PCD levels at the early growth stages correlates with future performance.

In Chapter 4, proline efficacy was tested in *Arabidopsis* and in cereal seedlings (SW2, SW4 and WB1). Proline pre-treatment successfully inhibited PCD in heat-shocked barley and wheat seedlings, with similar stress-induced PCD levels detected in heat tolerant

SW2 and heat susceptible SW4 varieties, showing that proline priming can compensate for low basal tolerance. For these reasons, a potential application for this project is the development of a slow-release proline delivery system. Proline microspheres offer various advantages over conventional PGPR formulation as the controlled release of proline confers long-term effects and it avoids the complications involved with dealing with live microorganism, e.g. high death rates during formulation process, contamination, short-term storage life, risk of predation and competition with soil microbiota (John *et al.* 2011; Schoebitz *et al.* 2013). However, two key variables had to be assessed before the method development process for proline encapsulation could be started. In Chapter 4, two key variables were examined for the proline encapsulation formulation process. The first examined variable was the maximum safety dosage of proline, and this was assessed in *Arabidopsis*, wheat and barley seedlings. A large proline gradient was assessed to ascertain the optimum balance needed to lengthen the bioactive effect, while avoiding the hazardous side-effects brought about by concentrated proline doses. Contrary to past work, the results here showed that exogenous proline efficacy did not act in a dose-dependent manner; treatment of *Arabidopsis* seedlings indicated that PCD-suppression was only active under low-to-medium proline doses but was cytotoxic at concentrations beyond 100 μM. However, the cereal varieties were considerably more tolerant to high proline doses that would otherwise be cytotoxic to *Arabidopsis*, and both wheat varieties were more resistant than WB1 against elevated proline doses. To summarise, proline accumulation did not correlate linearly with stress tolerance and that 8 μM (*Arabidopsis*), 10 μM (barley) and 100 μM (wheat) was the maximum safety proline doses tolerated by plants.

The next variable to be examined was proline efficacy across different stress magnitudes for optimum applications. Proline was only effective at transient stress near the viability/PCD threshold as no PCD-suppression was observed with pre-treated *Arabidopsis* seedlings at the stress-tolerant and PCD/necrosis thresholds. Perhaps different outcomes will arise under prolonged stress regimes, but for now, proline efficacy was only displayed at a limited stress range. Finally, BG11 exerted a curious PCD-suppressing effect only in wheat seedlings but not in *Arabidopsis* and barley, showing that the plant mineral status can play an important role in survival against heat stress. BG11 contains a mixture of macro- and micronutrients, but $Ca^{2+}$ is a strong candidate for the bioactive effect seen only in wheat seedlings. Plant SnRK2 is a key enzyme in the

signal transduction network linking the cross-talk between drought, salt, cold and osmotic stress; SnRK2 regulates ABA- and water stress-responsive genes to reprogram the metabolome for enhanced stress resistance (Fujita *et al.* 2009; Kulik *et al.* 2011). Interestingly, the SnRK2 protein is $Ca^{2+}$ dependent in wheat, but not in barley (Barker *et al.* 1996) and *Arabidopsis* (Zhang *et al.* 2008). The $Ca^{2+}$-dependent SnRK2 in wheat seedlings might be an underlying factor for why BG11 had a bioactive effect in wheat, but not in the other plant species and further investigations would be needed to substantiate this hypothesis. To corroborate this theory, the potential PCD-suppressing effect of $Ca^{2+}$ supplementation would have to be examined using the RHA in *Arabidopsis*, wheat and barley seedlings. If a divergent response, akin to what was noted in BG11-treated seedlings occurs, SnRK2 loss-of-function mutants, which have been generated in *Arabidopsis* (Fujii *et al.* 2011) should be obtained and assessed for their response against $Ca^{2+}$ supplementation.

Thus far, this project has described the beneficial properties of *N. muscorum* CM and exogenous proline for elevating plant stress tolerance under controlled laboratory settings. However, it is pertinent to acknowledge the challenges involved in achieving similar efficacy rates under real-world conditions. If time and resources were permitting, the logical next step of this project would be to develop a sustainable technology which could be applied in agriculture. To that end, I propose a slow-release proline delivery system using encapsulation technology which would buffer plants against stress in the field. Biofertilisers have not been widely adopted by farmers because of logistical constraints and the failure to perform reliably under field conditions. Agrochemical encapsulation overcomes most of the constraints impeding the performance of live inoculants, for several reasons. For example, an extensive variety of manufacturing techniques can be used to generate the microspheres, with no need to consider cell viability as the greatest death rates occurs during the manufacturing process (Schoebitz *et al.* 2012). This enhances the chances of generating microspheres of uniform size and shape, which are essential to achieve high mechanical stability and synchronised release rates of the bioactive compound. Moreover, the controlled release of the agrochemical prolongs the bioactive effect and requires smaller dosages to attain comparable efficacy rates (Kashyap *et al.* 2015). In turn, this poses fewer problems to plants and the surrounding environment in the event of accidental rupture (Zhang *et al.* 2015). Finally,

encapsulated agrochemicals do not suffer from bacterial contamination and have better shelf-life compared to their live biofertiliser counterparts.

Preliminary work to develop proline microspheres has been started using PLGA as the encapsulation matrix. Future work to assess the efficacy of the proline microspheres is required. First, proline microspheres would undergo extensive characterisation work by examining sample morphology (electron scanning microscopy), particle size analysis (laser diffraction or dynamic light scattering) and FTIR spectroscopy to confirm proline encapsulation and structural changes to the microspheres. Bioassay experiments would also be required, first under hydroponic conditions to evaluate the kinetic properties of proline release from microspheres, followed by field testing if optimistic results are obtained in the hydroponic testing. Given the robustness of the HPLC method optimised in this work, this technique could be used to determine the encapsulation efficiency, as well as the kinetics of proline release. Conventional plant stress biomarkers could also be quantified to evaluate the effectiveness of the proline microspheres, such as cell membrane stability, total antioxidant capacity and biochemical markers, as mentioned above.

# Appendix I: Supplementary data for Chapter 2

**Supplementary Table S1** – Comparing stress-induced PCD levels between autoclaved (AC) and non-autoclaved *N. muscorum* CM and exogenous proline in heat shocked *Arabidopsis* seedlings. Values for each dataset represent the average of n ≥ 8 (± SE) and represent the merged results of 3 experiments. A one-way ANOVA Tukey post-hoc test was used for statistical analysis. (*) indicates the mean difference is significant at the 0.05 level.

| Treatment | **20% Non-AC CM** | | | **20% AC CM** | | | **20% Non-AC proline** | | | **20% AC proline** | | |
|---|---|---|---|---|---|---|---|---|---|---|---|---|
| | 20% AC CM | 20% Non-AC proline | 20% AC proline | 20% Non-AC CM | 20% Non-AC proline | 20% AC proline | 20% Non-AC CM | 20% AC CM | 20% AC proline | 20% Non-AC CM | 20% AC CM | 20% Non-AC proline |
| Mean Difference | -6.69 | 11.1* | 16.0* | 6.69 | 18.1* | 22.7* | -11.4* | -18.1* | 4.61 | -16.0* | -22.7* | -4.61 |
| Std. Error | 3.87 | 4.04 | 3.95 | 3.87 | 4.17 | 4.08 | 4.04 | 4.17 | 4.24 | 3.95 | 4.08 | 4.24 |
| Sig. | 0.321 | 0.034 | 0.001 | 0.321 | 0.000 | 0.000 | 0.034 | 0.000 | 0.699 | 0.001 | 0.000 | 0.699 |

| Treatment | **40% Non-AC CM** | | | **40% AC CM** | | | **40% Non-AC proline** | | | **40% AC proline** | | |
|---|---|---|---|---|---|---|---|---|---|---|---|---|
| | 40% AC CM | 40% Non-AC proline | 40% AC proline | 40% Non-AC CM | 40% Non-AC proline | 40% AC proline | 40% Non-AC CM | 40% AC CM | 40% AC proline | 40% Non-AC CM | 40% AC CM | 40% Non-AC proline |
| Mean Difference | -10.78 | 7.89 | 2.80 | 10.78 | 18.7* | 13.6* | -7.89 | -18.7* | -5.09 | -2.80 | -13.6* | 5.09 |
| Std. Error | 4.94 | 5.04 | 4.85 | 4.94 | 5.04 | 4.85 | 5.04 | 5.04 | 4.95 | 4.85 | 4.85 | 4.95 |
| Sig. | 0.143 | 0.407 | 0.938 | 0.143 | 0.003 | 0.036 | 0.407 | 0.003 | 0.734 | 0.938 | 0.036 | 0.734 |

| Treatment | **60% Non-AC CM** | | | **60% AC CM** | | | **60% Non-AC proline** | | | **60% AC proline** | | |
|---|---|---|---|---|---|---|---|---|---|---|---|---|
| | 60% AC CM | 60% Non-AC proline | 60% AC proline | 60% Non-AC CM | 60% Non-AC proline | 60% AC proline | 60% Non-AC CM | 60% AC CM | 60% AC proline | 60% Non-AC CM | 60% AC CM | 60% Non-AC proline |
| Mean Difference | -12.4* | -8.90 | -1.23 | 12.4* | 3.54 | 11.21 | 8.90 | -3.54 | 7.67 | 1.23 | -11.21 | -7.67 |
| Std. Error | 4.33 | 4.33 | 4.58 | 4.33 | 4.25 | 4.51 | 4.33 | 4.25 | 4.51 | 4.58 | 4.51 | 4.51 |
| Sig. | 0.029 | 0.181 | 0.993 | 0.029 | 0.839 | 0.074 | 0.181 | 0.839 | 0.334 | 0.993 | 0.074 | 0.334 |

| Treatment | 80% Non-AC CM | | | 80% AC CM | | | 80% Non-AC proline | | | 80% AC proline | | |
|---|---|---|---|---|---|---|---|---|---|---|---|---|
| | 80% AC CM | 80% Non-AC proline | 80% AC proline | 80% Non-AC CM | 80% Non-AC proline | 80% AC proline | 80% Non-AC CM | 80% AC CM | 80% AC proline | 80% Non-AC CM | 80% AC CM | 80% Non-AC proline |
| Mean Difference | -8.23 | -4.84 | -12.34 | 8.23 | 3.40 | -4.11 | 4.84 | -3.40 | -7.50 | 12.34 | 4.11 | 7.50 |
| Std. Error | 4.81 | 4.60 | 4.73 | 4.81 | 4.23 | 4.37 | 4.60 | 4.23 | 4.14 | 4.73 | 4.37 | 4.14 |
| Sig. | 0.330 | 0.720 | 0.058 | 0.330 | 0.853 | 0.783 | 0.720 | 0.853 | 0.280 | 0.058 | 0.783 | 0.280 |

| Treatment | 100% Non-AC CM | | | 100% AC CM | | | 100% Non-AC proline | | | 100% AC proline | | |
|---|---|---|---|---|---|---|---|---|---|---|---|---|
| | 100% AC CM | 100% Non-AC proline | 100% AC proline | 100% Non-AC CM | 100% Non-AC proline | 100% AC proline | 100% Non-AC CM | 100% AC CM | 100% AC proline | 100% Non-AC CM | 100% AC CM | 100% Non-AC proline |
| Mean Difference | -14.79 | -3.70 | -9.76 | 14.79 | 11.09 | 5.03 | 3.70 | -11.09 | -6.06 | 9.76 | -5.03 | 6.06 |
| Std. Error | 5.57 | 5.81 | 6.35 | 5.57 | 5.70 | 6.26 | 5.81 | 5.70 | 6.47 | 6.35 | 6.26 | 6.47 |
| Sig. | 0.053 | 0.92 | 0.426 | 0.053 | 0.226 | 0.852 | 0.92 | 0.226 | 0.785 | 0.426 | 0.852 | 0.785 |

**Supplementary Table S2** - Effect of exogenous proline and *N. muscorum* CM on *Arabidopsis* root hair viability at 50°C heat stress between wild-type and impaired proline transporter mutants (*atprot1-1::atprot2-3::atprot3-2*, *aap1* and *lht1*). *N. muscorum* CM properties: OD730 (1.43), chl-a (18.9 µg/ml) and carotenoid (4.67 µg/ml). (*) marks PCD levels significantly ($p<0.05$) different from the WT datasets as a control, using a one-way ANOVA Dunnett post-hoc test. Values are the average of $n \geqslant 12$ ($\pm$ SE) and represent the merged results of 3 experiments.

| Treatment | Genetic lines | PCD (%) | Mean difference from WT control (%) | *p*-value |
|---|---|---|---|---|
| BG11 | WT | 48.1 ± 2.92 | N/A | N/A |
| | *atprot* triple KO | 47.3 ± 3.73 | -0.76 | 0.996 |
| | *aap1* | 48.4 ± 2.54 | 0.32 | 1.000 |
| | *lht1* | 53.1 ± 2.82 | 5.06 | 0.549 |
| 1 µM pro | WT | 37.6 ± 2.77 | N/A | N/A |
| | *atprot* triple KO | 43.5 ± 3.47 | 5.94 | 0.461 |
| | *aap1* | 41.6 ± 2.43 | 3.98 | 0.728 |
| | *lht1* | 50.0 ± 4.32 | 12.5* | 0.027 |
| 2 µM pro | WT | 44.2 ± 3.08 | N/A | N/A |
| | *atprot* triple KO | 43.4 ± 5.22 | -0.79 | 0.998 |
| | *aap1* | 57.4 ± 2.98 | 13.3* | 0.038 |
| | *lht1* | 51.0 ± 2.92 | 6.88 | 0.416 |
| 5 µM pro | WT | 35.7 ± 2.54 | N/A | N/A |
| | *atprot* triple KO | 45.2 ± 4.64 | 9.52 | 0.153 |
| | *aap1* | 55.4 ± 3.35 | 19.7* | 0.001 |
| | *lht1* | 55.0 ± 3.41 | 19.3* | 0.001 |
| 100 µM pro | WT | 44.5 ± 3.15 | N/A | N/A |
| | *atprot* triple KO | 48.7 ± 3.78 | 4.15 | 0.764 |
| | *aap1* | 59.5 ± 3.59 | 15.0* | 0.015 |
| | *lht1* | 58.0 ± 4.22 | 13.5* | 0.033 |
| *N. muscorum* CM | WT | 26.7 ± 1.67 | N/A | N/A |
| | *atprot* triple KO | 38.1 ± 3.87 | 11.36 | 0.070 |
| | *aap1* | 39.0 ± 4.33 | 12.30 | 0.051 |
| | *lht1* | 37.6 ± 3.71 | 10.82 | 0.098 |

# Appendix II: Supplementary data for Chapter 3

**Supplementary Table S3** – Effect of heat stress on PCD levels in winter (WB) and spring (SB) barley varieties. Values are the average of n ≥ 8 (± SE) and represent the merged results of at least 2 experiments. A Dunnett *t*-test was used for statistical analysis which treated the 25 °C dataset as a control and compared all other group datasets against it. (*) indicates the mean difference is significant at the 0.05 level.

| Barley Variety | Temperature (°C) | % PCD | Mean difference from 25 °C dataset (%) | *p*-value |
|---|---|---|---|---|
| **WB1** | 25 | 43.38 ± 3.73 | N/A | N/A |
| | 35 | 86.47 ± 3.34 | 43.1* | 0.000 |
| | 45 | 86.90 ± 3.20 | 43.5* | 0.000 |
| | 50 | 97.84 ± 0.61 | 54.5* | 0.000 |
| | 55 | 96.46 ± 1.38 | 53.1* | 0.000 |
| **WB2** | 25 | 34.93 ± 4.85 | N/A | N/A |
| | 35 | 63.40 ± 5.37 | 28.5* | 0.000 |
| | 45 | 83.88 ± 5.14 | 48.9* | 0.000 |
| | 50 | 97.85 ± 0.53 | 62.9* | 0.000 |
| | 55 | 97.55 ± 0.56 | 62.6* | 0.000 |
| **WB3** | 25 | 39.94 ± 5.78 | N/A | N/A |
| | 35 | 42.92 ± 9.23 | 3.0 | 0.987 |
| | 45 | 82.53 ± 4.44 | 42.6* | 0.000 |
| | 50 | 97.21 ± 0.46 | 57.3* | 0.000 |
| | 55 | 91.11 ± 2.09 | 51.2* | 0.000 |
| **WB4** | 25 | 35.96 ± 3.62 | N/A | N/A |
| | 35 | 55.09 ± 5.45 | 19.1* | 0.001 |
| | 45 | 83.88 ± 4.07 | 47.9* | 0.000 |
| | 50 | 97.03 ± 0.73 | 61.1* | 0.000 |
| | 55 | 95.77 ± 0.83 | 59.8* | 0.000 |
| **SB1** | 25 | 10.21 ± 1.58 | N/A | N/A |
| | 35 | 12.94 ± 1.85 | 2.7 | 0.906 |
| | 45 | 68.62 ± 5.06 | 58.4* | 0.000 |
| | 50 | 93.40 ± 2.31 | 83.2* | 0.000 |
| | 55 | 93.47 ± 1.36 | 83.3* | 0.000 |
| **SB2** | 25 | 14.35 ± 2.98 | N/A | N/A |
| | 35 | 17.22 ± 2.45 | 2.9 | 0.834 |
| | 45 | 65.44 ± 3.33 | 51.1* | 0.000 |
| | 50 | 95.01 ± 0.96 | 80.7* | 0.000 |
| | 55 | 91.92 ± 1.43 | 77.6* | 0.000 |
| **SB3** | 25 | 11.27 ± 2.43 | N/A | N/A |
| | 35 | 10.04 ± 1.81 | -1.2 | 0.999 |
| | 45 | 56.56 ± 6.66 | 45.3* | 0.000 |
| | 50 | 96.03 ± 1.85 | 84.8* | 0.000 |
| | 55 | 87.06 ± 2.81 | 75.8* | 0.000 |

**Supplementary Table S4** - Effect of heat stress PCD levels in spring (SW) and winter (WW) wheat varieties. Values are the average of n ≥ 12 (± SE) and represent the merged results of 3 experiments. A Dunnett *t*-test was used for statistical analysis which treated the 25 °C dataset as a control and compared all other group datasets against it. (*) The mean difference is significant at the 0.05 level.

| Wheat Variety | Temperature (°C) | % PCD | Mean difference from 25 °C dataset (%) | *p*-value |
|---|---|---|---|---|
| **SW1** | 25 | 9.10 ± 2.36 | N/A | N/A |
| | 35 | 17.3 ± 2.94 | 8.200 | 0.229 |
| | 45 | 63.8 ± 4.70 | 54.7 * | 0.000 |
| | 50 | 91.3 ± 1.58 | 82.2 * | 0.000 |
| | 55 | 92.7 ± 1.67 | 83.6 * | 0.000 |
| **SW2** | 25 | 11.9 ± 3.06 | N/A | N/A |
| | 35 | 20.7 ± 1.80 | 8.89 | 0.085 |
| | 45 | 71.5 ± 4.86 | 59.6 * | 0.000 |
| | 50 | 90.9 ± 1.39 | 79.0 * | 0.000 |
| | 55 | 90.1 ± 1.46 | 78.3 * | 0.000 |
| **SW3** | 25 | 23.9 ± 1.90 | N/A | N/A |
| | 35 | 28.0 ± 2.64 | 4.1 | 0.482 |
| | 45 | 86.9 ± 3.03 | 63.0 * | 0.000 |
| | 50 | 91.5 ± 0.84 | 67.7 * | 0.000 |
| | 55 | 92.8 ± 0.94 | 69.0 * | 0.000 |
| **SW4** | 25 | 36.8 ± 4.20 | N/A | N/A |
| | 35 | 46.5 ± 6.14 | 9.63 | 0.238 |
| | 45 | 88.3 ± 2.92 | 51.5 * | 0.000 |
| | 50 | 93.0 ± 1.35 | 56.2 * | 0.000 |
| | 55 | 94.1 ± 0.55 | 57.3 * | 0.000 |
| **WW1** | 25 | 53.2 ± 3.80 | N/A | N/A |
| | 35 | 47.4 ± 3.58 | -5.82 | 0.425 |
| | 45 | 82.6 ± 2.95 | 29.4 * | 0.000 |
| | 50 | 93.8 ± 1.06 | 40.6 * | 0.000 |
| | 55 | 91.9 ± 1.25 | 38.7 * | 0.000 |
| **WW2** | 25 | 8.66 ± 2.00 | N/A | N/A |
| | 35 | 28.0 ± 3.13 | 19.3 * | 0.000 |
| | 45 | 84.5 ± 3.50 | 75.9 * | 0.000 |
| | 50 | 92.9 ± 1.54 | 84.2 * | 0.000 |
| | 55 | 88.0 ± 1.48 | 79.4 * | 0.000 |
| **WW3** | 25 | 13.7 ± 3.17 | N/A | N/A |
| | 35 | 32.7 ± 4.35 | 19.0 * | 0.000 |
| | 45 | 81.3 ± 2.73 | 67.6 * | 0.000 |
| | 50 | 93.2 ± 0.85 | 79.6 * | 0.000 |
| | 55 | 93.3 ± 0.88 | 79.7 * | 0.000 |
| **WW4** | 25 | 19.2 ± 2.13 | N/A | N/A |
| | 35 | 46.7 ± 3.12 | 27.5 * | 0.000 |
| | 45 | 70.3 ± 3.90 | 51.1 * | 0.000 |
| | 50 | 93.0 ± 1.27 | 73.8 * | 0.000 |
| | 55 | 93.0 ± 1.09 | 73.8 * | 0.000 |

**Supplementary Table S5** - Effect of salt stress on PCD levels in spring (SW) and winter (WW) wheat varieties. Values are the average of n ≥ 12 (± SE) and represent the merged results of 3 experiments. A Dunnett *t*-test was used for statistical analysis which treated the SDW dataset as a control and compared all other group datasets against it. (*) indicates the mean difference is significant at the 0.05 level.

| Wheat Variety | NaCl (mM) | % PCD | Mean difference from SDW dataset (%) | *p*-value |
|---|---|---|---|---|
| **SW1** | SDW | 15.53 ± 1.73 | N/A | N/A |
| | 50 | 20.44 ± 2.44 | 4.91 | 0.844 |
| | 100 | 20.12 ± 2.07 | 4.59 | 0.896 |
| | 150 | 22.52 ± 3.33 | 6.99 | 0.610 |
| | 200 | 63.77 ± 5.49 | 48.3* | 0.000 |
| | 250 | 85.27 ± 4.32 | 69.8* | 0.000 |
| **SW2** | SDW | 12.31 ± 1.61 | N/A | N/A |
| | 50 | 15.01 ± 1.27 | 2.70 | 0.995 |
| | 100 | 29.36 ± 5.10 | 17.0 | 0.054 |
| | 150 | 21.49 ± 2.56 | 9.17 | 0.527 |
| | 200 | 67.61 ± 6.57 | 55.3* | 0.000 |
| | 250 | 90.71 ± 3.14 | 78.4* | 0.000 |
| **SW3** | SDW | 15.64 ± 1.71 | N/A | N/A |
| | 50 | 26.00 ± 2.37 | 10.4* | 0.048 |
| | 100 | 24.57 ± 2.18 | 8.93 | 0.128 |
| | 150 | 28.50 ± 1.56 | 12.9* | 0.009 |
| | 200 | 80.10 ± 4.80 | 64.5* | 0.000 |
| | 250 | 86.15 ± 2.96 | 70.5* | 0.000 |
| **SW4** | SDW | 36.69 ± 4.07 | N/A | N/A |
| | 50 | 34.44 ± 3.78 | -2.25 | 0.997 |
| | 100 | 35.37 ± 3.20 | -1.31 | 1.000 |
| | 150 | 62.56 ± 5.78 | 25.9* | 0.000 |
| | 200 | 76.45 ± 5.03 | 39.78* | 0.000 |
| | 250 | 91.57 ± 2.03 | 54.9* | 0.000 |
| **WW1** | SDW | 26.89 ± 2.26 | N/A | N/A |
| | 50 | 28.96 ± 2.94 | 2.07 | 0.995 |
| | 100 | 32.70 ± 2.11 | 5.81 | 0.642 |
| | 150 | 44.27 ± 4.27 | 17.4* | 0.007 |
| | 200 | 71.09 ± 4.89 | 44.2* | 0.000 |
| | 250 | 89.96 ± 2.58 | 63.1* | 0.000 |
| **WW2** | SDW | 25.55 ± 1.92 | N/A | N/A |
| | 50 | 26.91 ± 1.98 | 1.36 | 0.998 |
| | 100 | 30.18 ± 3.04 | 4.63 | 0.773 |
| | 150 | 37.32 ± 4.66 | 11.8* | 0.037 |
| | 200 | 87.44 ± 2.89 | 61.9* | 0.000 |
| | 250 | 81.66 ± 3.21 | 56.1* | 0.000 |
| **WW3** | SDW | 18.01 ± 2.23 | N/A | N/A |
| | 50 | 14.99 ± 2.64 | -3.01 | 0.966 |
| | 100 | 16.81 ± 2.43 | -1.20 | 1.000 |
| | 150 | 29.39 ± 4.54 | 11.4 | 0.101 |
| | 200 | 80.49 ± 5.85 | 62.5* | 0.000 |
| | 250 | 91.04 ± 1.26 | 73.0* | 0.000 |
| **WW4** | SDW | 11.25 ± 2.42 | N/A | N/A |
| | 50 | 15.87 ± 2.31 | 4.62 | 0.649 |
| | 100 | 18.49 ± 2.29 | 7.24 | 0.219 |
| | 150 | 29.67 ± 4.32 | 18.4* | 0.000 |
| | 200 | 89.74 ± 2.60 | 78.5* | 0.000 |
| | 250 | 93.02 ± 2.16 | 81.8* | 0.000 |

**Supplementary Table S6** - Independent samples *t*-test of individual varieties examining the effects of applying different stress cues as the initial cue on PCD levels. Inputted data consisted of PCD levels scored across 0, 30, 60 and 120-mins.

**SW1**

| | **Group Statistics** | | | ***t*-test for Equality of Means** | | |
|---|---|---|---|---|---|---|
| Initial Stress cue | N | Mean | Std. Error Mean | Sig. (2-tailed) | Mean Difference | Std. Error Difference |
| H+S | 44 | 21.8 | 1.59 | 0.002* | -11.4 | 3.4 |
| S+H | 29 | 33.2 | 2.98 | | | |

**SW2**

| | **Group Statistics** | | | ***t*-test for Equality of Means** | | |
|---|---|---|---|---|---|---|
| Initial Stress cue | N | Mean | Std. Error Mean | Sig. (2-tailed) | Mean Difference | Std. Error Difference |
| H+S | 33 | 27.2 | 4.24 | 0.856 | -0.9 | 4.9 |
| S+H | 35 | 28.1 | 2.48 | | | |

**SW3**

| | **Group Statistics** | | | ***t*-test for Equality of Means** | | |
|---|---|---|---|---|---|---|
| Initial Stress cue | N | Mean | Std. Error Mean | Sig. (2-tailed) | Mean Difference | Std. Error Difference |
| H+S | 56 | 39.3 | 2.56 | 0.362 | -3.2 | 3.5 |
| S+H | 48 | 42.4 | 2.33 | | | |

**SW4**

| | **Group Statistics** | | | ***t*-test for Equality of Means** | | |
|---|---|---|---|---|---|---|
| Initial Stress cue | N | Mean | Std. Error Mean | Sig. (2-tailed) | Mean Difference | Std. Error Difference |
| H+S | 52 | 40.1 | 2.98 | 0.042* | -8.5 | 4.1 |
| S+H | 55 | 48.6 | 2.86 | | | |

**WW1**

| | **Group Statistics** | | | ***t*-test for Equality of Means** | | |
|---|---|---|---|---|---|---|
| Initial Stress cue | N | Mean | Std. Error Mean | Sig. (2-tailed) | Mean Difference | Std. Error Difference |
| H+S | 50 | 32.5 | 2.03 | 0.046* | -5.9 | 2.9 |
| S+H | 50 | 38.4 | 2.08 | | | |

**WW2**

| | Group Statistics | | | *t*-test for Equality of Means | | |
|---|---|---|---|---|---|---|
| Initial Stress cue | N | Mean | Std. Error Mean | Sig. (2-tailed) | Mean Difference | Std. Error Difference |
| H+S | 48 | 36.0 | 1.63 | 0.088 | -5.1 | 2.9 |
| S+H | 51 | 41.1 | 2.44 | | | |

**WW3**

| | Group Statistics | | | *t*-test for Equality of Means | | |
|---|---|---|---|---|---|---|
| Initial Stress cue | N | Mean | Std. Error Mean | Sig. (2-tailed) | Mean Difference | Std. Error Difference |
| H+S | 56 | 36.0 | 2.07 | 0.750 | -0.9 | 3.0 |
| S+H | 54 | 37.0 | 2.13 | | | |

**WW4**

| | Group Statistics | | | *t*-test for Equality of Means | | |
|---|---|---|---|---|---|---|
| Initial Stress cue | N | Mean | Std. Error Mean | Sig. (2-tailed) | Mean Difference | Std. Error Difference |
| H+S | 56 | 45.1 | 3.10 | 0.603 | 2.2 | 4.3 |
| S+H | 54 | 42.9 | 2.94 | | | |

# References:

**Abdel-Hafez SII, Abo-Elyousr KAM, Abdel-Rahim IR**. **2015**. Fungicidal activity of extracellular products of cyanobacteria against *Alternaria porri*. *European Journal of Phycology* **50**: 239–245.

**Abernethy RH, Thiel DS, Petersen NS, Helm K**. **1989**. Thermotolerance is developmentally dependent in germinating wheat seed. *Plant Physiology* **89**: 569–576.

**Abrahám E, Hourton-Cabassa C, Erdei L, Szabados L**. **2010**. Methods for determination of proline in plants. In: Sunkar R, ed. *Plant Stress Tolerance: Methods in Molecular Biology*. Totowa, NJ: Humana Press, 317–331.

**Adams DG, Bergman B, Nierzwicki-Bauer SA, Duggan PS, Rai AN, Schüßler A**. **2013**. Cyanobacterial-plant symbioses In: Rosenberg E, DeLong EF, Lory S, Stackebrandt E, Thompson F, eds. *The Prokaryotes*. Berlin, Heidelberg: Springer Berlin Heidelberg, 359–400.

**Adrain C, Martin SJ**. **2001**. The mitochondrial apoptosome: A killer unleashed by the cytochrome seas. *Trends in Biochemical Sciences* **26**: 390–397.

**Aggarwal M, Sharma S, Kaur N, Pathania D, Bhandhari K, Kaushal N, Kaur R, Singh K, Srivastava A, Nayyar H**. **2011**. Exogenous proline application reduces phytotoxic effects of selenium by minimising oxidative stress and improves growth in bean (*Phaseolus vulgaris* L.) seedlings. *Biological Trace Element Research* **140**: 354–367.

**Ahammed GJ, Li X, Zhou J, Zhou Y-H, Yu J-Q**. **2016**. Role of hormones in plant adaptation to heat stress In: Ahammed GJ, Yu J-Q, eds. *Plant Hormones under Challenging Environmental Factors*. Dordrecht: Springer Netherlands, 1–21.

**Ahmad P, Abdel Latef AAH, Rasool S, Akram NA, Ashraf M, Gucel S**. **2016**. Role of proteomics in crop stress tolerance. *Frontiers in Plant Science* **7**: 1336.

**Ahmad M, Zahir ZA, Nazli F, Akram F, Arshad M, Khalid M**. **2013**. Effectiveness of halo-tolerant, auxin producing *Pseudomonas* and *Rhizobium* strains to improve osmotic stress tolerance in mung bean (*Vigna radiata* L.). *Brazilian Journal of Microbiology* **44**: 1341–1348.

**Ahmed E, Holmström SJM**. **2014**. Siderophores in environmental research: Roles and applications. *Microbial Biotechnology* **7**: 196–208.

**Ahmed M, Stal LJ, Hasnain S**. **2010**. Association of non-heterocystous cyanobacteria with crop plants. *Plant and Soil* **336**: 363–375.

**Ainsworth E a, Gillespie KM**. **2007**. Estimation of total phenolic content and other oxidation substrates in plant tissues using Folin-Ciocalteu reagent. *Nature Protocols* **2**: 875–877.

**Alami Y, Achouak W, Marol C, Heulin T**. **2000**. Rhizosphere soil aggregation and plant growth promotion of sunflowers by an exopolysaccharide-producing *Rhizobium*

sp. strain isolated from sunflower roots. *Applied and Environmental Microbiology* **66**: 3393–3398.

**Alden KP, Dhondt-Cordelier S, McDonald KL, Reape TJ, Ng CK-Y, McCabe PF, Leaver CJ**. **2011**. Sphingolipid long chain base phosphates can regulate apoptotic-like programmed cell death in plants. *Biochemical and Biophysical Research Communications* **410**: 574–580.

**Ali Q, Anwar F, Ashraf M, Saari N, Perveen R**. **2013**. Ameliorating effects of exogenously applied proline on seed composition, seed oil quality and oil antioxidant activity of maize (*Zea mays* L.) under drought stress. *International Journal of Molecular Sciences* **14**: 818–835.

**Ali S, Charles TC, Glick BR**. **2014**. Amelioration of high salinity stress damage by plant growth-promoting bacterial endophytes that contain ACC deaminase. *Plant Physiology and Biochemistry* **80**: 160–167.

**Alia, Mohanty P, Matysik J**. **2001**. Effect of proline on the production of singlet oxygen. *Amino Acids* **21**: 195–200.

**Alori ET, Glick BR, Babalola OO**. **2017**. Microbial phosphorus solubilization and its potential for use in sustainable agriculture. *Frontiers in Microbiology* **8**: 971.

**Amat L, Traon D, du Jardin P, Zotz F**. **2014**. *A legal framework for plant biostimulants and agronomic fertiliser additives in the EU*. EU publications.

**Andreini C, Bertini I, Cavallaro G, Holliday GL, Thornton JM**. **2008**. Metal ions in biological catalysis: From enzyme databases to general principles. *JBIC Journal of Biological Inorganic Chemistry* **13**: 1205–1218.

**Angus AA, Hirsch AM**. **2013**. Biofilm formation in the rhizosphere: Multispecies interactions and implications for plant growth In: de Bruijn FJ, ed. *Molecular Microbial Ecology of the Rhizosphere*. Hoboken, NJ, USA: John Wiley & Sons, Inc., 701–712.

**Anjum NA, Aref IM, Duarte AC, Pereira E, Ahmad I, Iqbal M**. **2014**. Glutathione and proline can coordinately make plants withstand the joint attack of metal(loid) and salinity stresses. *Frontiers in Plant Science* **5**: 2010–2013.

**Anjum NA, Hasanuzzaman M, Hossain MA, Thangavel P, Roychoudhury A, Gill SS, Rodrigo MA, Adam V, Fujita M, Kizek R, Duarte AC, Pereira E, Ahmad I**. **2015**. Jacks of metal/metalloid chelation trade in plants: An overview. *Frontiers in Plant Science* **6**: 192.

**Annapurna K, Kumar A, Kumar LV, Govindasamy V, Bose P, Ramadoss D**. **2013**. PGPR-induced systemic resistance (ISR) in plant disease management In: *Bacteria in Agrobiology: Disease Management*. Berlin, Heidelberg: Springer Berlin Heidelberg, 405–425.

**Arbona V, Manzi M, Zandalinas SI, Vives-Peris V, Pérez-Clemente RM, Gómez-Cadenas A**. **2017**. Physiological, metabolic, and molecular responses of plants to abiotic stress In: Sarwat M, Ahmad A, Abdin MZ, Ibrahim MM, eds. *Stress Signaling in*

*Plants: Genomics and Proteomics Perspective, Volume 2*. Cham: Springer International Publishing, 1–35.

**Arif MS, Shahzad SM, Yasmeen T, Riaz M, Ashraf M, Ashraf MA, Mubarik MS, Kausar R**. **2017**. Improving plant phosphorus (P) acquisition by phosphate-solubilizing bacteria In: Naeem M, Ansari AA, Gill SS, eds. *Essential Plant Nutrients: Uptake, Use Efficiency, and Management*. Cham: Springer International Publishing, 513–556.

**Arkhipova TN, Prinsen E, Veselov SU, Martinenko EV, Melentiev AI, Kudoyarova GR**. **2007**. Cytokinin producing bacteria enhance plant growth in drying soil. *Plant and Soil* **292**: 305–315.

**Armengaud J, Christie-Oleza JA, Clair G, Malard V, Duport C**. **2012**. Exoproteomics: Exploring the world around biological systems. *Expert Review of Proteomics* **9**: 561–575.

**Arrigo AP**. **1998**. Small stress proteins: Chaperones that act as regulators of intracellular redox state and programmed cell death. *Biological Chemistry* **379**: 19–26.

**Asseng S, Ewert F, Rosenzweig C, Jones JW, Hatfield JL, Ruane AC, Boote KJ, Thorburn PJ, Rötter RP, Cammarano D, Brisson N, Basso B, Martre P, Aggarwal PK, Angulo C, Bertuzzi P, Biernath C, Challinor AJ, Doltra J, Gayler S, Goldberg R, Grant R, *et al.* 2013**. Uncertainty in simulating wheat yields under climate change. *Nature Climate Change* **3**: 827–832.

**Audenaert K, Pattery T, Cornelis P, Höfte M**. **2002**. Induction of systemic resistance to *Botrytis cinerea* in tomato by *Pseudomonas aeruginosa* 7NSK2: Role of salicylic acid, pyochelin, and pyocyanin. *Molecular Plant-Microbe Interactions* **15**: 1147–1156.

**Auton M, Rösgen J, Sinev M, Holthauzen LMF, Bolen DW**. **2011**. Osmolyte effects on protein stability and solubility: A balancing act between backbone and side-chains. *Biophysical Chemistry* **159**: 90–99.

**Aznar A, Dellagi A**. **2015**. New insights into the role of siderophores as triggers of plant immunity: What can we learn from animals? *Journal of Experimental Botany* **66**: 3001–3010.

**Balk J, Chew SK, Leaver CJ, McCabe PF**. **2003**. The intermembrane space of plant mitochondria contains a DNase activity that may be involved in programmed cell death. *Plant Journal* **34**: 573–583.

**Balk J, Leaver CJ**. **2001**. The PET1-CMS mitochondrial mutation in sunflower is associated with premature programmed cell death and cytochrome *c* release. *The Plant Cell* **13**: 1803–1818.

**Balk J, Leaver CJ, McCabe PF**. **1999**. Translocation of cytochrome *c* from the mitochondria to the cytosol occurs during heat-induced programmed cell death in cucumber plants. *FEBS Letters* **463**: 151–154.

**Barceló J, Poschenrieder C**. **1990**. Plant water relations as affected by heavy metal stress: A review. *Journal of Plant Nutrition* **13**: 1–37.

**Barker Jha, Slocombe SP, Ball KL, Hardie DG, Shewry PR, Halford NG**. **1996**. Evidence that barley 3-hydroxy-3-methylglutaryl-coenzyme a reductase kinase is a member of the sucrose nonfermenting-1-related protein kinase family. *Plant Physiology* **112**: 1141–1149.

**Barres BA, Hart IK, Coles HS, Burne JF, Voyvodic JT, Richardson WD, Raff MC**. **1992**. Cell death and control of cell survival in the oligodendrocyte lineage. *Cell* **70**: 31–46.

**Barreto V, Seldin L, Araujo FFD**. **2011**. Plant growth and health promoting bacteria. *Microbiology Monographs* **18**: 21–44.

**Bashan Y, De-Bashan LE, Prabhu SR, Hernandez JP**. **2014**. Advances in plant growth-promoting bacterial inoculant technology: Formulations and practical perspectives (1998-2013). *Plant and Soil* **378**: 1–33.

**Bashan Y, Hernandez JP, Leyva LA, Bacilio M**. **2002**. Alginate microbeads as inoculant carriers for plant growth-promoting bacteria. *Biology and Fertility of Soils* **35**: 359–368.

**Bastián F, Cohen A, Piccoli P, Luna V, Baraldi R, Bottini R**. **1998**. Production of indole-3-acetic acid and gibberellins A1 and A3 by *Acetobacter diazotrophicus* and *Herbaspirillum seropedicae* in chemically-defined culture media. *Plant Growth Regulation* **24**: 7–11.

**Bates LS, Waldren RP, Teare ID**. **1973**. Rapid determination of free proline for water-stress studies. *Plant and Soil* **39**: 205–207.

**Belimov AA, Hontzeas N, Safronova VI, Demchinskaya SV, Piluzza G, Bullitta S, Glick BR**. **2005**. Cadmium-tolerant plant growth-promoting bacteria associated with the roots of Indian mustard (*Brassica juncea* L. Czern.). *Soil Biology and Biochemistry* **37**: 241–250.

**Belimov AA, Safronova VI, Sergeyeva TA, Egorova TN, Matveyeva VA, Tsyganov VE, Borisov AY, Tikhonovich IA, Kluge C, Preisfeld A, Dietz KJ, Stepanok VV**. **2001**. Characterization of plant growth promoting rhizobacteria isolated from polluted soils and containing 1-aminocyclopropane-1-carboxylate deaminase. *Canadian Journal of Microbiology* **47**: 642–652.

**Berkey R, Bendigeri D, Xiao S**. **2012**. Sphingolipids and plant defense/disease: The “Death” connection and beyond. *Frontiers in Plant Science* **3**: 1–22.

**Bharti N, Pandey SS, Barnawal D, Patel VK, Kalra A**. **2016**. Plant growth promoting rhizobacteria *Dietzia natronolimnaea* modulates the expression of stress responsive genes providing protection of wheat from salinity stress. *Scientific Reports* **6**: 1.

**Bhaya D, Schwarz R, Grossman AR**. **2002**. Molecular responses to environmental stress In: Whitton BA, Potts M, eds. *The Ecology of Cyanobacteria*. Dordrecht: Kluwer Academic Publishers, 397–442.

**Bigirimana J, Höfte M**. **2002**. Induction of systemic resistance to *Colletotrichum lindemuthianum* in bean by a benzothiadiazole derivative and rhizobacteria. *Phytoparasitica* **30**: 159–168.

**Bistgani ZE, Siadat SA, Bakhshandeh A, Ghasemi Pirbalouti A, Hashemi M**. **2017**. Interactive effects of drought stress and chitosan application on physiological characteristics and essential oil yield of *Thymus daenensis* Celak. *The Crop Journal* **5**: 407–415.

**Blaha D, Prigent-Combaret C, Mirza MS, Moënne-Loccoz Y**. **2006**. Phylogeny of the 1-aminocyclopropane-1-carboxylic acid deaminase-encoding gene *acdS* in phytobeneficial and pathogenic *Proteobacteria* and relation with strain biogeography. *FEMS Microbiology Ecology* **56**: 455–470.

**Bodennec J, Koul O, Aguado I, Brichon G, Zwingelstein G, Portoukalian J**. **2000**. A procedure for fractionation of sphingolipid classes by solid-phase extraction on aminopropyl cartridges. *Journal of lipid research* **41**: 1524–1531.

**Bohlool BB, Ladha JK, Garrity DP, George T**. **1992**. Biological nitrogen fixation for sustainable agriculture: A perspective. *Plant and Soil* **141**: 1–11.

**Bolouri-Moghaddam MR, Roy KL, Xiang L, Rolland F, Van den Ende W**. **2010**. Sugar signalling and antioxidant network connections in plant cells. *The FEBS Journal* **277**: 2022–2037.

**Bolton MD, Kolmer JA, Garvin DF**. **2008**. Wheat leaf rust caused by *Puccinia triticina*. *Molecular Plant Pathology* **9**: 563–575.

**Bosch M, Franklin-Tong VE**. **2008**. Self-incompatibility in *Papaver*: Signalling to trigger PCD in incompatible pollen In: *Journal of Experimental Botany*.481–490.

**Bottini R, Fulchieri M, Pearce D, Pharis RP**. **1989**. Identification of gibberellins A1, A3, and iso-A3 in cultures of *Azospirillum lipoferum*. *Plant Physiology* **90**: 45–47.

**Boukhalfa H, Crumbliss AL**. **2002**. Chemical aspects of siderophore mediated iron transport. *Biometals* **15**: 325–339.

**Bowman SM, Free SJ**. **2006**. The structure and synthesis of the fungal cell wall. *BioEssays: News and Reviews in Molecular, Cellular and Developmental Biology* **28**: 799–808.

**Boyd V, Cholewa O, Papas K**. **2008**. Limitations in the use of fluorescein diacetate/propidium iodide (FDA/PI) and cell permeable nucleic acid stains for viability measurements of isolated islets of Langerhans. *Current Trends in Biotechnology and Pharmacy* **2**: 66–84.

**Braud A, Geoffroy V, Hoegy F, Mislin GLA, Schalk IJ**. **2010**. Presence of the siderophores pyoverdine and pyochelin in the extracellular medium reduces toxic metal accumulation in *Pseudomonas aeruginosa* and increases bacterial metal tolerance. *Environmental Microbiology Reports* **2**: 419–425.

**Braud A, Hannauer M, Mislin GLA, Schalk IJ**. **2009**. The *Pseudomonas aeruginosa* pyochelin-iron uptake pathway and its metal specificity. *Journal of Bacteriology* **191**: 3517–3525.

**Breitkreuz KE, Shelp BJ, Fischer WN, Schwacke R, Rentsch D**. **1999**. Identification and characterization of GABA, proline and quaternary ammonium compound transporters from *Arabidopsis thaliana*. *FEBS Letters* **450**: 280–284.

**Bresson J, Varoquaux F, Bontpart T, Touraine B, Vile D**. **2013**. The PGPR strain *Phyllobacterium brassicacearum* STM196 induces a reproductive delay and physiological changes that result in improved drought tolerance in *Arabidopsis*. *New Phytologist* **200**: 558–569.

**Breusegem FV, Dat JF**. **2006**. Reactive oxygen species in plant cell death. *Plant Physiology* **141**: 384–390.

**Burbridge E, Diamond M, Dix PJ, McCabe PF**. **2007**. Use of cell morphology to evaluate the effect of a peroxidase gene on cell death induction thresholds in tobacco. *Plant Science* **172**: 853–860.

**Buysens S, Heungens K, Poppe J, Hofte M**. **1996**. Involvement of pyochelin and pyoverdin in suppression of *Pythium*-induced damping-off of tomato by *Pseudomonas aeruginosa* 7NSK2. *Applied and Environmental Microbiology* **62**: 865–871.

**Cakmak I**. **2005**. Role of mineral nutrients in tolerance of crop plants to environmental stress factors. *Fertigation: Optimizing the Utilization of Water and Nutrients* **20**: 35.

**de Cano MMS, de Mulé MC, de Caire GZ, de Halperin DR**. **1990**. Inhibition of *Candida albicans* and *Staphylococcus aureus* by phenolic compounds from the terrestrial cyanobacterium *Nostoc muscorum*. *Journal of Applied Phycology* **2**: 79–81.

**Capiati DA, País SM, Téllez-Iñón MT**. **2006**. Wounding increases salt tolerance in tomato plants: Evidence on the participation of calmodulin-like activities in cross-tolerance signalling. *Journal of Experimental Botany* **57**: 2391–2400.

**Carr PW, Stoll DR, Wang X**. **2011**. Perspectives on recent advances in the speed of high performance liquid chromatography. *Analytical Chemistry* **83**: 1890–1900.

**Cassidy MB, Lee H, Trevors JT**. **1996**. Environmental applications of immobilized microbial cells: A review. *Journal of Industrial Microbiology* **16**: 79–101.

**Cattivelli L, Baldi P, Crosatti C, Di Fonzo N, Faccioli P, Grossi M, Mastrangelo AM, Pecchioni N, Stanca AM**. **2002**. Chromosome regions and stress-related sequences involved in resistance to abiotic stress in *Triticeae*. *Plant Molecular Biology* **48**: 649–665.

**Chandrasekara N, Shahidi F**. **2011**. Effect of roasting on phenolic content and antioxidant activities of whole cashew nuts, kernels, and testa. *Journal of Agricultural and Food Chemistry* **59**: 5006–5014.

**Chen J, Bellin D, Vandelle E**. **2018**. Measurement of cyclic GMP during plant hypersensitive disease resistance response In: De Gara L, Locato V, eds. *Plant Programmed Cell Death*. New York, NY: Springer New York, 143–151.

**Chen SL, Kao CH**. **1995**. Cd induced changes in proline level and peroxidase activity in roots of rice seedlings. *Plant Growth Regulation* **17**: 67–71.

**Chen YP, Rekha PD, Arun AB, Shen FT, Lai W-A, Young CC**. **2006**. Phosphate solubilizing bacteria from subtropical soil and their tricalcium phosphate solubilizing abilities. *Applied Soil Ecology* **34**: 33–41.

**Cherkasov N, Ibhadon AO, Fitzpatrick P**. **2015**. A review of the existing and alternative methods for greener nitrogen fixation. *Chemical Engineering and Processing: Process Intensification* **90**: 24–33.

**Chinnusamy V, Zhu J-K, Sunkar R**. **2010**. Gene regulation during cold stress acclimation in plants In: Sunkar R, ed. *Plant Stress Tolerance*. Totowa, NJ: Humana Press, 39–55.

**Choudhury ATMA, Kecskés ML, Kennedy IR**. **2014**. Utilization of BNF technology supplementing urea N for sustainable rice production. *Journal of Plant Nutrition* **37**: 1627–1647.

**Christenson L, Dionne K, Lysaught M**. **1993**. Biomedical application of immobilized cells In: Goosen MFA, ed. *Fundamentals of Animal Cell Encapsulation and Immobilization*. CRC Press, Boca Raton, FL: Taylor and Francis, 7–41.

**Christie-Oleza JA, Armengaud J, Guerin P, Scanlan DJ**. **2015**. Functional distinctness in the exoproteomes of marine *Synechococcus*. *Environmental Microbiology* **17**: 3781–3794.

**Christman HD, Campbell EL, Meeks JC**. **2011**. Global transcription profiles of the nitrogen stress response resulting in heterocyst or hormogonium development in *Nostoc punctiforme*. *Journal of Bacteriology* **193**: 6874–6886.

**Cimini S, Ronci MB, Barizza E, de Pinto MC, Locato V, Lo Schiavo F, De Gara L**. **2018**. Plant cell cultures as model systems to study programmed cell death In: De Gara L, Locato V, eds. *Plant Programmed Cell Death*. New York, NY: Springer New York, 173–186.

**Clarke SM, Cristescu SM, Miersch O, Harren FJM, Wasternack C, Mur LAJ**. **2009**. Jasmonates act with salicylic acid to confer basal thermotolerance in *Arabidopsis thaliana*. *New Phytologist* **182**: 175–187.

**Clarke SM, Mur LAJ, Wood JE, Scott IM**. **2004**. Salicylic acid dependent signaling promotes basal thermotolerance but is not essential for acquired thermotolerance in *Arabidopsis thaliana*. *The Plant Journal* **38**: 432–447.

**Cockram J, Chiapparino E, Taylor SA, Stamati K, Donini P, Laurie DA, O'Sullivan DM**. **2007**. Haplotype analysis of vernalization loci in European barley germplasm reveals novel *VRN-H1* alleles and a predominant winter *VRN-H1/VRN-H2* multi-locus haplotype. *Theoretical and Applied Genetics* **115**: 993–1001.

**Coello P, Hirano E, Hey SJ, Muttucumaru N, Martinez-Barajas E, Parry MAJ, Halford NG**. **2012**. Evidence that abscisic acid promotes degradation of SNF1-related protein kinase (SnRK) 1 in wheat and activation of a putative calcium-dependent SnRK2. *Journal of Experimental Botany* **63**: 913–924.

**Coffeen WC, Wolpert TJ**. **2004**. Purification and characterization of serine proteases that exhibit caspase-like activity and are associated with programmed cell death in *Avena sativa*. *The Plant Cell Online* **16**: 857–873.

**Cohen AC, Bottini R, Piccoli PN**. **2008**. *Azospirillum brasilense* Sp 245 produces ABA in chemically-defined culture medium and increases ABA content in *Arabidopsis* plants. *Plant Growth Regulation* **54**: 97–103.

**Cohen AC, Bottini R, Pontin M, Berli FJ, Moreno D, Boccanlandro H, Travaglia CN, Piccoli PN**. **2015**. *Azospirillum brasilense* ameliorates the response of *Arabidopsis thaliana* to drought mainly via enhancement of ABA levels. *Physiologia Plantarum* **153**: 79–90.

**Cohen AC, Travaglia CN, Bottini R, Piccoli PN**. **2009**. Participation of abscisic acid and gibberellins produced by endophytic *Azospirillum* in the alleviation of drought effects in maize. *Botany* **87**: 455–462.

**Coleman-Derr D, Tringe SG**. **2014**. Building the crops of tomorrow: Advantages of symbiont-based approaches to improving abiotic stress tolerance. *Frontiers in Microbiology* **5**: 1–6.

**Contran N, Cerana R, Crosti P, Malerba M**. **2007**. Cyclosporin A inhibits programmed cell death and cytochrome *c* release induced by fusicoccin in sycamore cells. *Protoplasma* **231**: 193–199.

**Cornelis P**. **2010**. Iron uptake and metabolism in pseudomonads. *Applied Microbiology and Biotechnology* **86**: 1637–1645.

**Cramer GR**. **2002**. Sodium-calcium interactions under salinity stress In: *Salinity: Environment - Plants - Molecules*. Springer, Dordrecht, 205–227.

**Curtis MJ, Wolpert TJ**. **2002**. The oat mitochondrial permeability transition and its implication in victorin binding and induced cell death. *Plant Journal* **29**: 295–312.

**Daly CT**. **2013**. Investigating the role of long-chain sphingoid bases in plant programmed cell death (Doctoral dissertation). *University College Dublin*.

**Daneva A, Gao Z, Van Durme M, Nowack MK**. **2016**. Functions and regulation of programmed cell death in plant development. *Annual Review of Cell and Developmental Biology* **32**: 441–468.

**De-Bashan LE, Bashan Y**. **2010**. Immobilized microalgae for removing pollutants: Review of practical aspects. *Bioresource Technology* **101**: 1611–1627.

**Deikman J**. **1997**. Molecular mechanisms of ethylene regulation of gene transcription. *Physiologia Plantarum* **100**: 561–566.

**Deuschle K, Funck D, Forlani G, Stransky H, Biehl A, Leister D, van der Graaff E, Kunze R, Frommer WB, Graaff EVD, Kunze R, Frommer WB**. **2004**. The role of $\Delta^1$-pyrroline-5-carboxylate dehydrogenase in proline degradation. *The Plant Cell* **16**: 3413–3425.

**Dimkpa CO, Merten D, Svatoš A, Büchel G, Kothe E**. **2009**. Metal-induced oxidative stress impacting plant growth in contaminated soil is alleviated by microbial siderophores. *Soil Biology and Biochemistry* **41**: 154–162.

**Doccula FG, Luoni L, Behera S, Bonza MC, Costa A**. **2018**. *In vivo* analysis of calcium levels and glutathione redox status in *Arabidopsis* epidermal leaf cells infected with the hypersensitive response-inducing bacteria *Pseudomonas syringae* pv. tomato *Avrb* (*PstAvrB*) In: De Gara L, Locato V, eds. *Plant Programmed Cell Death*. New York, NY: Springer New York, 125–141.

**Dodor DE, Tabatabai MA**. **2003**. Effect of cropping systems on phosphatases in soils. *J. Plant Nutr. Soil Sci.*: 7.

**van Doorn WG, Beers EP, Dangl JL, Franklin-Tong VE, Gallois P, Hara-Nishimura I, Jones AM, Kawai-Yamada M, Lam E, Mundy J, Mur LAJ, Petersen M, Smertenko A, Taliansky M, Van Breusegem F, Wolpert T, Woltering E, Zhivotovsky B, Bozhkov PV**. **2011**. Morphological classification of plant cell deaths. *Cell Death & Differentiation* **18**: 1241–1246.

**Doyle SM, Diamond M, McCabe PF**. **2010**. Chloroplast and reactive oxygen species involvement in apoptotic-like programmed cell death in *Arabidopsis* suspension cultures. *Journal of Experimental Botany* **61**: 473–482.

**Driessen AJM, Hellingwerf KJ, Konings WN**. **1987**. Mechanism of energy coupling to entry and exit of neutral and branched chain amino acids in membrane vesicles of *Streptococcus cremoris*. *Journal of Biological Chemistry* **262**: 12438–12443.

**Dubcovsky J, Luo M-C, Dvořák J**. **1995**. Linkage relationships among stress-induced genes in wheat. *Theoretical and Applied Genetics* **91**: 795–801.

**Duff SMG, Sarath G, Plaxton WC**. **1994**. The role of acid phosphatases in plant phosphorus metabolism. *Physiologia Plantarum* **90**: 791–800.

**Duggan PS, Gottardello P, Adams DG**. **2007**. Molecular analysis of genes in *Nostoc punctiforme* involved in pilus biogenesis and plant infection. *Journal of Bacteriology* **189**: 4547–4551.

**Ecker JR, Davis RW**. **1987**. Plant defense genes are regulated by ethylene. *Proceedings of the National Academy of Sciences of the United States of America* **84**: 5202–5206.

**Edinger AL, Thompson CB**. **2004**. Death by design: Apoptosis, necrosis and autophagy. *Current Opinion in Cell Biology* **16**: 663–669.

**Egamberdieva D, Wirth SJ, Alqarawi AA, Abd Allah EF, Hashem A**. **2017**. Phytohormones and beneficial microbes: Essential components for plants to balance stress and fitness. *Frontiers in Microbiology* **8**: 2104.

**Ekman M, Picossi S, Campbell EL, Meeks JC, Flores E**. **2013**. A *Nostoc punctiforme* sugar transporter necessary to establish a cyanobacterium-plant symbiosis. *Plant physiology* **161**: 1984–92.

**Elavarthi S, Martin B**. **2010**. Spectrophotometric assays for antioxidant enzymes in plants In: Sunkar R, ed. *Plant Stress Tolerance*. Totowa, NJ: Humana Press, 273–280.

**El-Sheekh MM, Osman MEH, Dyab MA, Amer MS**. **2006**. Production and characterization of antimicrobial active substance from the cyanobacterium *Nostoc muscorum*. *Environmental Toxicology and Pharmacology* **21**: 42–50.

**Erisman JW, Galloway JN, Seitzinger S, Bleeker A, Dise NB, Petrescu AMR, Leach AM, de Vries W**. **2013**. Consequences of human modification of the global nitrogen cycle. *Philosophical Transactions of the Royal Society B: Biological Sciences* **368**: 20130116–20130116.

**Esmaeilzadeh S, Valizadeh H, Zakeri-Milani P**. **2016**. A simple, fast, low cost, HPLC/UV validated method for determination of flutamide: Application to protein binding studies. *Advanced Pharmaceutical Bulletin* **6**: 251–256.

**Fahad S, Hussain S, Bano A, Saud S, Hassan S, Shan D, Khan FA, Khan F, Chen Y, Wu C, Tabassum MA, Chun MX, Afzal M, Jan A, Jan MT, Huang J**. **2015**. Potential role of phytohormones and plant growth-promoting rhizobacteria in abiotic stresses: Consequences for changing environment. *Environmental Science and Pollution Research* **22**: 4907–4921.

**Farago ME, Mullen WA**. **1981**. Plants which accumulate metals-V. Proline levels in the roots of seedlings of copper-tolerant and non-tolerant *Armeria maritima* (mill) willd. *Inorganic and Nuclear Chemistry Letters* **17**: 275–277.

**Felse PA, Panda T**. **2000**. Production of microbial chitinases – A revisit. *Bioprocess Engineering* **23**: 127–134.

**Ferreyra MLF, Casadevall R, D'Andrea L, Abd Elgawad H, Beemster GTS, Casati P**. **2016**. AtPDCD5 Plays a Role in Programmed Cell Death after UV-B Exposure in *Arabidopsis*. *Plant Physiology* **170**: 2444–2460.

**Fiedor L, Kania A, Myśliwa-Kurdziel B, Orzeł Ł, Stochel G**. **2008**. Understanding chlorophylls: Central magnesium ion and phytyl as structural determinants. *Biochimica et Biophysica Acta - Bioenergetics* **1777**: 1491–1500.

**Finkelstein R**. **2013**. Abscisic Acid Synthesis and Response. *The Arabidopsis Book* **11**: e0166.

**Finkelstein RA, Lankford CE**. **1957**. A bacteriotoxic substance in autoclaved culture media containing glucose and phosphate. *Applied Microbiology* **5**: 74–9.

**Flores E, Herrero A**. **2010**. Compartmentalized function through cell differentiation in filamentous cyanobacteria. *Nature Reviews Microbiology* **8**: 39–50.

**Flynn KJ, Gallon JR**. **1990**. Changes in intracellular and extracellular *α*-amino acids in *Gloeotheceie* during $N_2$-fixation and following addition of ammonium. *Archives of Microbiology* **153**: 574–579.

**Fogg GE**. **1952**. The production of extracellular nitrogenous substances by a blue-green alga. *Proceedings of the Royal Society of London. Series B - Biological Sciences* **139**: 372 –397.

**Fowler D, Coyle M, Skiba U, Sutton M a, Cape JN, Reis S, Sheppard LJ, Jenkins A, Grizzetti B, Galloway JN, Vitousek P, Leach A, Bouwman AF, Butterbach-Bahl K, Dentener F, Stevenson D, Amann M, Voss M**. **2013**. The global nitrogen cycle in the twenty-first century. *Philosophical transactions of the Royal Society of London. Series B, Biological sciences* **368**: 20130164.

**Frensch J, Hsiao TC**. **1995**. Rapid response of the yield threshold and turgor regulation during adjustment of root growth to water stress in *Zea mays*. *Plant Physiology* **108**: 303–312.

**Fridlender M, Inbar J, Chet I**. **1993**. Biological control of soilborne plant pathogens by a *β*-1,3 glucanase-producing *Pseudomonas cepacia*. *Soil Biology and Biochemistry* **25**: 1211–1221.

**Friedman M**. **2004**. Applications of the ninhydrin reaction for analysis of amino acids, peptides, and proteins to agricultural and biomedical sciences. *Journal of Agricultural and Food Chemistry* **52**: 385–406.

**Fujii H, Verslues PE, Zhu J-K**. **2011**. *Arabidopsis* decuple mutant reveals the importance of SnRK2 kinases in osmotic stress responses *in vivo*. *Proceedings of the National Academy of Sciences of the United States of America* **108**: 1717–1722.

**Fujita Y, Fujita M, Shinozaki K, Yamaguchi-Shinozaki K**. **2011**. ABA-mediated transcriptional regulation in response to osmotic stress in plants. *Journal of Plant Research* **124**: 509–525.

**Fujita Y, Nakashima K, Yoshida T, Katagiri T, Kidokoro S, Kanamori N, Umezawa T, Fujita M, Maruyama K, Ishiyama K, Kobayashi M, Nakasone S, Yamada K, Ito T, Shinozaki K, Yamaguchi-Shinozaki K**. **2009**. Three SnRK2 protein kinases are the main positive regulators of abscisic acid signaling in response to water stress in *Arabidopsis*. *Plant and Cell Physiology* **50**: 2123–2132.

**Gandhi NU, Chandra SB**. **2012**. A comparative analysis of three classes of bacterial non-specific acid phosphatases and archaeal phosphoesterases: Evolutionary perspective. *Acta Informatica Medica* **20**: 167–173.

**Ghosh A, Kushwaha HR, Hasan MR, Pareek A, Sopory SK, Singla-Pareek SL**. **2016**. Presence of unique glyoxalase III proteins in plants indicates the existence of shorter route for methylglyoxal detoxification. *Scientific Reports* **6**: 18358.

**Gill SS, Tuteja N**. **2010**. Reactive oxygen species and antioxidant machinery in abiotic stress tolerance in crop plants. *Plant Physiology and Biochemistry* **48**: 909–930.

**Gillespie KM, Chae JM, Ainsworth E a**. **2007**. Rapid measurement of total antioxidant capacity in plants. *Nature Protocols* **2**: 867–870.

**Glick BR**. **2005**. Modulation of plant ethylene levels by the bacterial enzyme ACC deaminase. *FEMS Microbiology Letters* **251**: 1–7.

**Glick BR**. **2012**. Plant growth-promoting bacteria: Mechanisms and applications. *Scientifica* **2012**: 1–15.

**Glick BR**. **2014**. Bacteria with ACC deaminase can promote plant growth and help to feed the world. *Microbiological Research* **169**: 30–39.

**Glick BR, Cheng Z, Czarny J, Duan J**. **2007**. Promotion of plant growth by ACC deaminase-producing soil bacteria. *European Journal of Plant Pathology* **119**: 329–339.

**Glick BR, Penrose DM, Li J**. **1998**. A model for the lowering of plant ethylene concentrations by plant growth-promoting bacteria. *Journal of Theoretical Biology* **190**: 63–68.

**Golden JW, Yoon H-S**. **2003**. Heterocyst development in *Anabaena*. *Current Opinion in Microbiology* **6**: 557–563.

**Grallath S, Weimar T, Meyer A, Gumy C, Suter-Grotemeyer M, Neuhaus J-M, Rentsch D**. **2005**. The AtProT family. Compatible solute transporters with similar substrate specificity but differential expression patterns. *Plant Physiology* **137**: 117–126.

**Gutiérrez J, González-Pérez S, García-García F, Daly CT, Lorenzo Ó, Revuelta JL, McCabe PF, Arellano JB**. **2014**. Programmed cell death activated by Rose Bengal in *Arabidopsis thaliana* cell suspension cultures requires functional chloroplasts. *Journal of Experimental Botany* **65**: 3081–3095.

**Gutierrez-Manero FJ, Ramos-Solano B, Probanza A, Mehouachi J, R. Tadeo F, Talon M**. **2001**. The plant-growth-promoting rhizobacteria *Bacillus pumilus* and *Bacillus licheniformis* produce high amounts of physiologically active gibberellins. *Physiologia Plantarum* **111**: 206–211.

**Halverson LJ, Jones TM, Firestone MK**. **2000**. Release of intracellular solutes by four soil bacteria exposed to dilution stress. *Soil Science Society of America Journal* **64**: 1630.

**Hamilton EW, Heckathorn SA**. **2001**. Mitochondrial adaptations to NaCl. Complex I is protected by anti-oxidants and small heat shock proteins, whereas Complex II is protected by proline and betaine. *Plant Physiology* **126**: 1266–1274.

**Hara-Nishimura I, Hatsugai N**. **2011**. The role of vacuole in plant cell death. *Cell death and differentiation* **18**: 1298–1304.

**Hare P, Cress W, Staden JV**. **2002**. Disruptive effects of exogenous proline on chloroplast and mitochondrial ultrastructure in *Arabidopsis* leaves. *South African Journal of Botany*: 393–396.

**Hare PD, Cress WA, van Staden J**. **1997**. The involvement of cytokinins in plant responses to environmental stress. *Plant Growth Regulation* **23**: 79–103.

**Hare PD, Cress WA, van Staden J**. **2001**. The effects of exogenous proline and proline analogues on *in vitro* shoot organogenesis in *Arabidopsis*. *Plant Growth Regulation* **34**: 203–207.

**Harris RF**. **1981**. Effect of water potential on microbial growth and activity. In: Parr JF, Gardner WR, Elliott LF, eds. Special Publication No. 9. *Water Potential Relations in Soil Microbiology*. Madison, Wisconsin: Soil Science Society of America, 23–95.

**Hasanuzzaman M, Nahar K, Alam Md, Roychowdhury R, Fujita M**. **2013**. Physiological, biochemical, and molecular mechanisms of heat stress tolerance in plants. *International Journal of Molecular Sciences* **14**: 9643–9684.

**Hasanuzzaman M, Nahar K, Hossain MA, Mahmud J, Rahman A, Inafuku M, Oku H, Fujita M**. **2017**. Coordinated actions of glyoxalase and antioxidant defense systems in conferring abiotic stress tolerance in plants. *International Journal of Molecular Sciences* **18**: 200.

**Hassen AI, Bopape FL, Sanger LK**. **2016**. Microbial inoculants as agents of growth promotion and abiotic stress tolerance in plants In: *Microbial Inoculants in Sustainable Agricultural Productivity*. New Delhi: Springer India, 23–36.

**Hatsugai N, Hara-Nishimura I**. **2018**. Measurement of the caspase-1-like activity of vacuolar processing enzyme in plants In: De Gara L, Locato V, eds. *Plant Programmed Cell Death*. New York, NY: Springer New York, 163–171.

**Hatsugai N, Kuroyanagi M, Nishimura M, Hara-Nishimura I**. **2006**. A cellular suicide strategy of plants: Vacuole-mediated cell death. *Apoptosis* **11**: 905–911.

**Hatsugai N, Yamada K, Goto-Yamada S, Hara-Nishimura I**. **2015**. Vacuolar processing enzyme in plant programmed cell death. *Frontiers in Plant Science* **6**: 1–11.

**Hayat S, Hayat Q, Alyemeni MN, Wani AS, Pichtel J, Ahmad A**. **2012**. Role of proline under changing environments. *Plant Signaling & Behavior* **7**: 1456–1466.

**Hedden P, Thomas SG**. **2012**. Gibberellin biosynthesis and its regulation. *Biochemical Journal* **444**: 11–25.

**Heinrikson RL, Meredith SC**. **1984**. Amino acid analysis by reverse-phase high-performance liquid chromatography: Precolumn derivatization with phenylisothiocyanate. *Analytical Biochemistry* **136**: 65–74.

**Herridge DF, Peoples MB, Boddey RM**. **2008**. Global inputs of biological nitrogen fixation in agricultural systems. *Plant and Soil* **311**: 1–18.

**Hirner A, Ladwig F, Stransky H, Okumoto S, Keinath M, Harms A, Frommer WB, Koch W**. **2006**. *Arabidopsis* LHT1 is a high-affinity transporter for cellular amino acid uptake in both root epidermis and leaf mesophyll. *Plant Cell* **18**: 1931–1946.

**Hoang TML, Moghaddam L, Williams B, Khanna H, Dale J, Mundree SG**. **2015**. Development of salinity tolerance in rice by constitutive-overexpression of genes involved in the regulation of programmed cell death. *Frontiers in Plant Science* **6**.

**Hoang TML, Williams B, Mundree SG**. **2016**. Manipulation of programmed cell death pathways enhances osmotic stress tolerance in plants: Physiological and molecular insights In: Hossain MA, Wani SH, Bhattacharjee S, Burritt DJ, Tran L-SP, eds. *Drought Stress Tolerance in Plants, Vol 1*. Cham: Springer International Publishing, 439–464.

**Hogg BV, Kacprzyk J, Molony EM, Reilly CO, Gallagher TF, Gallois P, Mccabe PF**. **2011**. An *in vivo* root hair assay for determining rates of apoptotic-like programmed cell death in plants. *Plant Methods* **7**: 45.

**Hoque MA, Banu MNA, Nakamura Y, Shimoishi Y, Murata Y**. **2008**. Proline and glycinebetaine enhance antioxidant defense and methylglyoxal detoxification systems and reduce NaCl-induced damage in cultured tobacco cells. *Journal of Plant Physiology* **165**: 813–824.

**Hoque TS, Hossain MA, Mostofa MG, Burritt DJ, Fujita M, Tran L-SP**. **2016**. Methylglyoxal: An emerging signaling molecule in plant abiotic stress responses and tolerance. *Frontiers in Plant Science* **7**: 1341.

**Hoque MA, Okuma E, Nasrin Akhter Banu M, Nakamura Y, Shimoishi Y, Murata Y**. **2007**. Exogenous proline mitigates the detrimental effects of salt stress more than exogenous betaine by increasing antioxidant enzyme activities. *Journal of Plant Physiology* **164**: 553–561.

**Hoque TS, Okuma E, Uraji M, Furuichi T, Sasaki T, Hoque MA, Nakamura Y, Murata Y**. **2012a**. Inhibitory effects of methylglyoxal on light-induced stomatal opening and inward $K^+$ channel activity in *Arabidopsis*. *Bioscience, Biotechnology, and Biochemistry* **76**: 617–619.

**Hoque MA, Uraji M, Banu MNA, Mori IC, Nakamura Y, Murata Y**. **2010**. The effects of methylglyoxal on glutathione S-transferase from *Nicotiana tabacum*. *Bioscience, Biotechnology, and Biochemistry* **74**: 2124–2126.

**Hoque MA, Uraji M, Torii A, Banu M, Akhter N, Mori IC, Nakamura Y, Murata Y**. **2012b**. Methylglyoxal inhibition of cytosolic ascorbate peroxidase from *Nicotiana tabacum*. *Journal of Biochemical and Molecular Toxicology* **26**: 315–321.

**Hossain MA, Burritt DJ, Fujita M**. **2016**. Cross-stress tolerance in plants: Molecular mechanisms and possible involvement of reactive oxygen species and methylglyoxal detoxification systems In: *Abiotic Stress Response in Plants*. John Wiley & Sons, Ltd, 327–380.

**Hossain MA, Fujita M**. **2010**. Evidence for a role of exogenous glycinebetaine and proline in antioxidant defense and methylglyoxal detoxification systems in mung bean seedlings under salt stress. *Physiology and Molecular Biology of Plants* **16**: 19–29.

**Hossain MA, Golam Mostofa M, Fujita M**. **2013**. Heat-shock positively modulates oxidative protection of salt and drought-stressed mustard (*Brassica campestris* L.) seedlings. *Journal of Plant Science and Molecular Breeding* **2**: 2.

**Hossain MA, Hasanuzzaman M, Fujita M**. **2010**. Up-regulation of antioxidant and glyoxalase systems by exogenous glycinebetaine and proline in mung bean confer tolerance to cadmium stress. *Physiology and Molecular Biology of Plants* **16**: 259–272.

**Hossain MA, Hasanuzzaman M, Fujita M**. **2011**. Coordinate induction of antioxidant defense and glyoxalase system by exogenous proline and glycinebetaine is correlated with salt tolerance in mung bean. *Frontiers of Agriculture in China* **5**: 1–14.

**Hossain MA, Hoque MA, Burritt DJ, Fujita M**. **2014a**. Proline protects plants against abiotic oxidative stress: Biochemical and molecular mechanisms In: *Oxidative Damage to Plants*. Elsevier, 477–522.

**Hossain MA, Mostofa MG, Burritt DJ, Fujita M**. **2014b**. Modulation of reactive oxygen species and methylglyoxal detoxification systems by exogenous glycinebetaine and proline improves drought tolerance in mustard (*Brassica juncea* l.). *International Journal of Plant Biology & Research* **2**: 1014.

**Huang Y-C, Niu C-Y, Yang C-R, Jinn T-L**. **2016**. The heat stress factor HSFA6b connects ABA signaling and ABA-mediated heat responses. *Plant Physiology* **172**: 1182–1199.

**Hussien MY, Abd El-All AAM, Mostafa SSM**. **2009**. Bioactivity of algal extracellular byproducts on *Cercospora* leaf spot disease, growth performance and quality of sugar beet In: *4th Conference on Recent Technologies in Agriculture*.119–129.

**Huysmans M, Lema A S, Coll NS, Nowack MK**. **2017**. Dying two deaths — Programmed cell death regulation in development and disease. *Current Opinion in Plant Biology* **35**: 37–44.

**Igual M, García-Martínez E, Camacho MM, Martínez-Navarrete N**. **2011**. Changes in flavonoid content of grapefruit juice caused by thermal treatment and storage. *Innovative Food Science and Emerging Technologies* **12**: 153–162.

**Ihara-Ohori Y, Nagano M, Muto S, Uchimiya H, Kawai-Yamada M**. **2007**. Cell death suppressor *Arabidopsis* Bax Inhibitor-1 is associated with calmodulin binding and ion homeostasis. *Plant Physiology* **143**: 650–660.

**Illmer P, Schinner F**. **1995**. Solubilization of inorganic calcium phosphates—Solubilization mechanisms. *Soil Biology and Biochemistry* **27**: 257–263.

**Ingram J, Bartels D**. **1996**. The molecular basis of dehydration tolerance in plants. *Annual Review of Plant Physiology and Plant Molecular Biology* **47**: 377–403.

**Irina I, Mohamed G**. **2012**. Biological activities and effects of food processing on flavonoids as phenolic antioxidants In: *Advances in Applied Biotechnology*. Rijeka: IntechOpen, 25.

**Ishikawa T, Watanabe N, Nagano M, Kawai-Yamada M, Lam E**. **2011**. Bax inhibitor-1: a highly conserved endoplasmic reticulum-resident cell death suppressor. *Cell death and differentiation* **18**: 1271–1278.

**Issa AA, Abd-Alla MH, Ohyama T**. **2014**. Nitrogen fixing cyanobacteria: Future prospect In: Ohyama T, ed. *Advances in Biology and Ecology of Nitrogen Fixation*. InTech, .

**Jabs T**. **1999**. Reactive oxygen intermediates as mediators of programmed cell death in plants and animals. *Biochemical Pharmacology* **57**: 231–245.

**Jacobs JW, Niall HD**. **1975**. High sensitivity automated sequence determination of polypeptides. *The Journal of Biological Chemistry* **250**: 3629–3636.

**Jacobson CB, Pasternak JJ, Glick BR**. **1994**. Partial purification and characterization of 1-aminocyclopropane-1-carboxylate deaminase from the plant growth promoting rhizobacterium *Pseudomonas putida* GR12-2. *Canadian Journal of Microbiology* **40**: 1019–1025.

**Jadhav HP, Shaikh SS, Sayyed RZ**. **2017**. Role of hydrolytic enzymes of rhizoflora in biocontrol of fungal phytopathogens: An overview In: *Rhizotrophs: Plant Growth Promotion to Bioremediation*. Singapore: Springer Singapore, 183–203.

**Jaiswal P, Singh PK, Prasanna R**. **2008**. Cyanobacterial bioactive molecules: An overview of their toxic properties. *Canadian Journal of Microbiology* **54**: 701–717.

**Jambunathan N**. **2010**. Determination and detection of reactive oxygen species (ROS), lipid peroxidation, and electrolyte leakage in plants In: Sunkar R, ed. Methods in Molecular Biology. *Plant Stress Tolerance*. Totowa, NJ: Humana Press, 291–297.

**Janz D, Behnke K, Schnitzler J-P, Kanawati B, Schmitt-Kopplin P, Polle A**. **2010**. Pathway analysis of the transcriptome and metabolome of salt sensitive and tolerant poplar species reveals evolutionary adaption of stress tolerance mechanisms. *BMC Plant Biology* **10**: 150.

**du Jardin P**. **2015**. Plant biostimulants: Definition, concept, main categories and regulation. *Scientia Horticulturae* **196**: 3–14.

**Jia X, Meng Q, Zeng H, Wang W, Yin H**. **2016**. Chitosan oligosaccharide induces resistance to *Tobacco mosaic virus* in *Arabidopsis* via the salicylic acid-mediated signalling pathway. *Scientific Reports* **6**.

**Jiang Y, Huang B**. **2001**. Effects of calcium on antioxidant activities and water relations associated with heat tolerance in two cool-season grasses. *Journal of experimental botany* **52**: 341–349.

**John RP, Tyagi RD, Brar SK, Surampalli RY, Prévost D**. **2011**. Bio-encapsulation of microbial cells for targeted agricultural delivery. *Critical reviews in biotechnology* **31**: 211–26.

**Joo G-J, Kang S-M, Hamayun M, Kim S-K, Na C-I, Shin D-H, Lee I-J**. **2009**. *Burkholderia* sp. KCTC 11096BP as a newly isolated gibberellin producing bacterium. *The Journal of Microbiology* **47**: 167–171.

**Judy E, Kishore N**. **2016**. Biological wonders of osmolytes: The need to know more. *Biochemistry & Analytical Biochemistry* **05**: 1000304.

**Kacprzyk J, Brogan NP, Daly CT, Doyle SM, Diamond M, Molony EM, McCabe PF**. **2017**. The retraction of the protoplast during PCD is an active, and interruptible, calcium-flux driven process. *Plant Science* **260**: 50–59.

**Kacprzyk J, Daly CT, McCabe PF**. **2011**. The botanical dance of death: Programmed cell death in plants In: *Advances in Botanical Research*. Elsevier, 169–261.

**Kacprzyk J, Devine A, McCabe PF**. **2014**. The root hair assay facilitates the use of genetic and pharmacological tools in order to dissect multiple signalling pathways that lead to programmed cell death (I De Smet, Ed.). *PLoS ONE* **9**: e94898.

**Kang S-M, Joo G-J, Hamayun M, Na C-I, Shin D-H, Kim HY, Hong J-K, Lee I-J**. **2009**. Gibberellin production and phosphate solubilization by newly isolated strain of *Acinetobacter calcoaceticus* and its effect on plant growth. *Biotechnology Letters* **31**: 277–281.

**Kang S-M, Radhakrishnan R, Khan AL, Kim M-J, Park J-M, Kim B-R, Shin D-H, Lee I-J**. **2014a**. Gibberellin secreting rhizobacterium, *Pseudomonas putida* H-2-3 modulates the hormonal and stress physiology of soybean to improve the plant growth under saline and drought conditions. *Plant Physiology and Biochemistry* **84**: 115–124.

**Kang S-M, Waqas M, Hamayun M, Asaf S, Khan AL, Kim A-Y, Park Y-G, Lee I-J**. **2017**. Gibberellins and indole-3-acetic acid producing rhizospheric bacterium *Leifsonia xyli* SE134 mitigates the adverse effects of copper-mediated stress on tomato. *Journal of Plant Interactions* **12**: 373–380.

**Kang S-M, Waqas M, Khan AL, Lee I-J**. **2014b**. Plant-growth-promoting rhizobacteria: Potential candidates for gibberellins production and crop growth promotion In: Miransari M, ed. *Use of Microbes for the Alleviation of Soil Stresses, Volume 1*. New York, NY: Springer New York, 1–19.

**Karadeniz A, Topcuoğlu SF, Inan S**. **2006**. Auxin, gibberellin, cytokinin and abscisic acid production in some bacteria. *World Journal of Microbiology and Biotechnology* **22**: 1061–1064.

**Karthikeyan N, Prasanna R, Sood A, Jaiswal P, Nayak S, Kaushik BD**. **2009**. Physiological characterization and electron microscopic investigation of cyanobacteria associated with wheat rhizosphere. *Folia Microbiologica* **54**: 43–51.

**Kashyap PL, Xiang X, Heiden P**. **2015**. Chitosan nanoparticle based delivery systems for sustainable agriculture. *International Journal of Biological Macromolecules* **77**: 36–51.

**Kasuga M, Liu Q, Miura S, Yamaguchi-Shinozaki K, Shinozaki K**. **1999**. Improving plant drought, salt, and freezing tolerance by gene transfer of a single stress-inducible transcription factor. *Nature Biotechnology* **17**: 287–291.

**Katiyar V, Goel R**. **2004**. Siderophore mediated plant growth promotion at low temperature by mutant of fluorescent *Pseudomonad*. *Plant Growth Regulation* **42**: 239–244.

**Kaur C, Kushwaha HR, Mustafiz A, Pareek A, Sopory SK, Singla-Pareek SL**. **2015**. Analysis of global gene expression profile of rice in response to methylglyoxal indicates its possible role as a stress signal molecule. *Frontiers in Plant Science* **6**: 682.

**Kaushal N, Gupta K, Bhandhari K, Kumar S, Thakur P, Nayyar H**. **2011**. Proline induces heat tolerance in chickpea (*Cicer arietinum* L.) plants by protecting vital enzymes of carbon and antioxidative metabolism. *Physiology and Molecular Biology of Plants* **17**: 203–213.

**Kaushik BD**. **2014**. Developments in cyanobacterial biofertilizer. *Proceedings of the Indian National Science Academy* **80**: 379.

**Kavi Kishor PB, Sangam S, Amrutha RN, Sri Laxmi P, Naidu KR, Rao KRSS, Rao S, Reddy KJ, Theriappan P, Sreenivasulu N**. **2005**. Regulation of proline biosynthesis, degradation, uptake and transport in higher plants: Its implications in plant growth and abiotic stress tolerance. *Current Science* **88**: 424–438.

**Kavi Kishor PB, Sreenivasulu N**. **2014**. Is proline accumulation per se correlated with stress tolerance or is proline homeostasis a more critical issue? *Plant, Cell and Environment* **37**: 300–311.

**Kawai-Yamada M, Hori Z, Ogawa T, Ihara-Ohori Y, Tamura K, Nagano M, Ishikawa T, Uchimiya H**. **2009**. Loss of calmodulin binding to Bax Inhibitor-1 affects *Pseudomonas*-mediated hypersensitive response-associated cell death in *Arabidopsis thaliana*. *Journal of Biological Chemistry* **284**: 27998–28003.

**Kawai-Yamada M, Jin L, Yoshinaga K, Hirata A, Uchimiya H**. **2001**. Mammalian Bax-induced plant cell death can be down-regulated by overexpression of *Arabidopsis* Bax Inhibitor-1 (AtBI-1). *Proceedings of the National Academy of Sciences of the United States of America* **98**: 12295–12300.

**Kawasaki S, Borchert C, Deyholos M, Wang H, Brazille S, Kawai K, Galbraith D, Bohnert HJ**. **2001**. Gene Expression Profiles during the Initial Phase of Salt Stress in Rice. *The Plant Cell* **13**: 889.

**Kazan K**. **2015**. Diverse roles of jasmonates and ethylene in abiotic stress tolerance. *Trends in Plant Science* **20**: 219–229.

**Kelly VA**. **2006**. *Factors Affecting Demand for Fertilizer in Sub-Saharan Africa*. 1818 H Street, NW Washington, DC 20433: Agriculture & Rural Development Department World Bank.

**Kende H**. **1993**. Ethylene Biosynthesis. *Annual Review of Plant Physiology and Plant Molecular Biology* **44**: 283–307.

**Kennedy I**. **2008**. *Efficient nutrient use in rice production in Vietnam achieved using inoculant biofertilisers*. Canberra, ACT: Australian Centre for International Agricultural Research.

**Keshishian EA, Rashotte AM**. **2015**. Plant cytokinin signalling. *Essays in Biochemistry* **58**: 13–27.

**Khamar HJ, Breathwaite EK, Prasse CE, Fraley ER, Secor CR, Chibane FL, Elhai J, Chiu W-L**. **2010**. Multiple roles of soluble sugars in the establishment of *Gunnera-Nostoc* endosymbiosis. *Plant physiology* **154**: 1381–1389.

**Khan MS, Zaidi A, Ahmad E**. **2014**. Mechanism of phosphate solubilization and physiological functions of phosphate-solubilizing microorganisms In: Khan MS, Zaidi A, Musarrat J, eds. *Phosphate Solubilizing Microorganisms*. Cham: Springer International Publishing, 31–62.

**Kim JS**. **2013**. Antioxidant activity of Maillard reaction products derived from aqueous and ethanolic glucose-glycine and its oligomer solutions. *Food Science and Biotechnology* **22**: 39–46.

**Kim Y, Wang M, Bai Y, Zeng Z, Guo F, Han N, Bian H, Wang J, Pan J, Zhu M**. **2014**. Bcl-2 suppresses activation of VPEs by inhibiting cytosolic $Ca^{2+}$ level with elevated $K^{+}$ efflux in NaCl-induced PCD in rice. *Plant Physiology and Biochemistry* **80**: 168–175.

**Kleinhenz MD, Palta JP**. **2002**. Root zone calcium modulates the response of potato plants to heat stress. *Physiologia Plantarum* **115**: 111–118.

**Kolupaev YE, Akinina GE, Mokrousov A V. 2005**. Induction of heat tolerance in wheat coleoptiles by calcium ions and its relation to oxidative stress. *Russian Journal of Plant Physiology* **52**: 199–204.

**Kosová K, Vítámvás P, Urban M, Klíma M, Roy A, Prášil I**. **2015**. Biological networks underlying abiotic stress tolerance in temperate crops—A proteomic perspective. *International Journal of Molecular Sciences* **16**: 20913–20942.

**Krämer R**. **1994**. Secretion of amino acids by bacteria: Physiology and mechanism. *FEMS Microbiology Reviews* **13**: 75–93.

**Kramer DM, Evans JR**. **2011**. The importance of energy balance in improving photosynthetic productivity. *Plant Physiology* **155**: 70–8.

**Kruse E, Liu Z, Kloppstech K**. **1993**. Expression of heat shock proteins during development of barley. *Plant Molecular Biology* **23**: 111–122.

**Kůdela V**. **2010**. Potential impact of climate change on geographic distribution of plant pathogenic bacteria in Central Europe. *Plant Protection Science* **45**: S27–S32.

**Kulik A, Wawer I, Krzywińska E, Bucholc M, Dobrowolska G**. **2011**. SnRK2 protein kinases—Key regulators of plant response to abiotic stresses. *OMICS* **15**: 859–872.

**Kumar P, Dubey RC, Maheshwari DK**. **2012**. *Bacillus strains* isolated from rhizosphere showed plant growth promoting and antagonistic activity against phytopathogens. *Microbiological Research* **167**: 493–499.

**Kumar K, Mella-Herrera RA, Golden JW**. **2010**. Cyanobacterial heterocysts. *Cold Spring Harbor Perspectives in Biology* **2**: a000315–a000315.

**Kumar V, Yadav SK**. **2009**. Proline and betaine provide protection to antioxidant and methylglyoxal detoxification systems during cold stress in *Camellia sinensis* (L.) O. Kuntze. *Acta Physiologiae Plantarum* **31**: 261–269.

**Kurepin LV, Zaman M, Pharis RP**. **2014**. Phytohormonal basis for the plant growth promoting action of naturally occurring biostimulators. *Journal of the Science of Food and Agriculture* **94**: 1715–1722.

**Kuroyanagi M, Yamada K, Hatsugai N, Kondo M, Nishimura M, Hara-Nishimura I**. **2005**. Vacuolar processing enzyme is essential for mycotoxin-induced cell death in *Arabidopsis thaliana*. *Journal of Biological Chemistry* **280**: 32914–32920.

**Kwanyuen P, Burton JW**. **2010**. A modified amino acid analysis using PITC derivatization for soybeans with accurate determination of cysteine and half-cystine. *Journal of the American Oil Chemists' Society* **87**: 127–132.

**Lacomme C, Santa Cruz S**. **1999**. Bax-induced cell death in tobacco is similar to the hypersensitive response. *Proceedings of the National Academy of Sciences of the United States of America* **96**: 7956–7961.

**Lam E**. **2008**. Programmed cell death in plants: Orchestrating an intrinsic suicide program within walls. *Critical Reviews in Plant Sciences* **27**: 413–423.

**Lam E, Kato N, Lawton M**. **2001**. Programmed cell death, mitochondria and the plant hypersensitive response. *Nature* **411**: 848–853.

**Larkindale J, Hall JD, Knight MR, Vierling E**. **2005**. Heat stress phenotypes of *Arabidopsis* mutants implicate multiple signaling pathways in the acquisition of thermotolerance. *Plant Physiology* **138**: 882–897.

**Laude AJ, Simpson AWM**. **2009**. Compartmentalized signalling: $Ca2^{+}$compartments, microdomains and the many facets of $Ca2^{+}$ signalling. *FEBS Journal* **276**: 1800–1816.

**Laurie DA**. **1997**. Comparative genetics of flowering time. *Plant Molecular Biology* **35**: 167–177.

**Lee Y-H, Foster J, Chen J, Voll LM, Weber APM, Tegeder M**. **2007**. AAP1 transports uncharged amino acids into roots of *Arabidopsis*. *The Plant Journal* **50**: 305–319.

**Lehman AP, Long SR**. **2013**. Exopolysaccharides from *Sinorhizobium meliloti* can protect against $H_2O_2$-dependent damage. *Journal of Bacteriology* **195**: 5362–5369.

**Lehmann S, Funck D, Szabados L, Rentsch D**. **2010**. Proline metabolism and transport in plant development. *Amino Acids* **39**: 949–962.

**Lehmann S, Gumy C, Blatter E, Boeffel S, Fricke W, Rentsch D**. **2011**. *In planta* function of compatible solute transporters of the AtProT family. *Journal of Experimental Botany* **62**: 787–796.

**Lennon SV, Martin SJ, Cotter TG**. **1991**. Dose-dependent induction of apoptosis in human tumour cell lines by widely diverging stimuli. *Cell proliferation* **24**: 203–214.

**Lenochová Z, Soukup A, Votrubová O**. **2009**. Aerenchyma formation in maize roots. *Biologia Plantarum* **53**: 263–270.

**Levine A, Pennell RI, Alvarez ME, Palmer R, Lamb C**. **1996**. Calcium-mediated apoptosis in a plant hypersensitive disease resistance response. *Current biology: CB* **6**: 427–437.

**Levy K, Woster AP, Goldstein RS, Carlton EJ**. **2016**. Untangling the impacts of climate change on waterborne diseases: A systematic review of relationships between diarrheal diseases and temperature, rainfall, flooding, and drought. *Environmental science & technology* **50**: 4905–4922.

**Liang H, Yao N, Song JT, Luo S, Lu H, Greenberg JT**. **2003**. Ceramides modulate programmed cell death in plants. *Genes and Development* **17**: 2636–2641.

**Liang X, Zhang L, Natarajan SK, Becker DF**. **2013**. Proline mechanisms of stress survival. *Antioxidants & Redox Signaling* **19**: 998–1011.

**Licht S, Cui B, Wang B, Li F-F, Lau J, Liu S**. **2014**. Ammonia synthesis by $N_2$ and steam electrolysis in molten hydroxide suspensions of nanoscale $Fe_2O_3$. *Science* **345**: 637–640.

**Linde-Laursen I, Heslop-Harrison JS, Shepherd KW, Taketa S**. **2004**. The barley genome and its relationship with the wheat genomes. A survey with an internationally agreed recommendation for barley chromosome nomenclature. *Hereditas* **126**: 1–16.

**Liu J, Feng L, Li J, He Z**. **2015**. Genetic and epigenetic control of plant heat responses. *Frontiers in Plant Science* **06**.

**Liu F, Xing S, Ma H, Du Z, Ma B**. **2013**. Cytokinin-producing, plant growth-promoting rhizobacteria that confer resistance to drought stress in *Platycladus orientalis* container seedlings. *Applied Microbiology and Biotechnology* **97**: 9155–9164.

**Lockshin RA, Zakeri Z**. **2004**. Apoptosis, autophagy, and more. *The International Journal of Biochemistry & Cell Biology* **36**: 2405–2419.

**Lord CEN, Gunawardena AHLAN**. **2012**. Programmed cell death in *C. elegans*, mammals and plants. *European Journal of Cell Biology* **91**: 603–613.

**Lu W, Deng M, Guo F, Wang M, Zeng Z, Han N, Yang Y, Zhu M, Bian H**. **2016**. Suppression of *OsVPE3* enhances salt tolerance by attenuating vacuole rupture during programmed cell death and affects stomata development in rice. *Rice* **9**: 65.

**Lu Y, Xu J**. **2015**. Phytohormones in microalgae: A new opportunity for microalgal biotechnology? *Trends in Plant Science* **20**: 273–282.

**Lv W-T, Lin B, Zhang M, Hua X-J**. **2011**. Proline accumulation is inhibitory to *Arabidopsis* seedlings during heat stress. *Plant physiology* **156**: 1921–1933.

**Madhaiyan M, Poonguzhali S, Ryu J, Sa T**. **2006**. Regulation of ethylene levels in canola (*Brassica campestris*) by 1-aminocyclopropane-1-carboxylate deaminase-containing *Methylobacterium fujisawaense*. *Planta* **224**: 268–278.

**Maestri E, Klueva N, Perrotta C, Gulli M, Nguyen HT, Marmiroli N**. **2002**. Molecular genetics of heat tolerance and heat shock proteins in cereals. *Plant Molecular Biology* **48**: 667–681.

**Magnuson A, Krassen H, Stensjö K, Ho FM, Styring S**. **2011**. Modeling Photosystem I with the alternative reaction center protein PsaB2 in the nitrogen fixing cyanobacterium *Nostoc punctiforme*. *Biochimica et Biophysica Acta* **1807**: 1152–1161.

**Malusá E, Vassilev N**. **2014**. A contribution to set a legal framework for biofertilisers. *Applied Microbiology and Biotechnology* **98**: 6599–6607.

**Mammone T, Gan D, Collins D, Lockshin RA, Marenus K, Maes D**. **2000**. Successful separation of apoptosis and necrosis pathways in HaCaT keratinocyte cells induced by UVB irradiation. *Cell Biology and Toxicology* **16**: 293–302.

**Maness N**. **2010**. Extraction and analysis of soluble carbohydrates. *Methods in Molecular Biology (Clifton, N.J.)* **639**: 341–370.

**Mano J, Biswas MdS**. **2018**. Analysis of reactive carbonyl species generated under oxidative stress In: De Gara L, Locato V, eds. *Plant Programmed Cell Death*. New York, NY: Springer New York, 117–124.

**Markham JE, Li J, Cahoon EB, Jaworski JG**. **2006**. Separation and identification of major plant sphingolipid classes from leaves. *Journal of Biological Chemistry* **281**: 22684–22694.

**Marmiroli N, Maestri E, Terzi V, Gulli M, Pavesi A, Raho G, Lupotto E, Di Cola G, Sinibaldi R, Perrotta C**. **1994**. Genetic and molecular evidences of the regulation of gene expression during heat shock in plants In: Cherry JH, ed. NATO ASI Series. *Biochemical and Cellular Mechanisms of Stress Tolerance in Plants*. Springer Berlin Heidelberg, 157–190.

**Marmiroli N, Malcevschi A, Maestri E**. **1998**. Application of stress responsive genes RFLP analysis to the evaluation of genetic diversity in plants In: Karp A, Isaac PG, Ingram DS, eds. *Molecular Tools for Screening Biodiversity: Plants and Animals*. Dordrecht: Springer Netherlands, 464–470.

**Maršálek B, Zahradníčková H, Hronková M**. **1992**. Extracellular abscisic acid produced by cyanobacteria under salt stress. *Journal of Plant Physiology* **139**: 506–508.

**Martínez JP, Araya H**. **2010**. Ascorbate-glutathione cycle: Enzymatic and non-enzymatic integrated mechanisms and its biomolecular regulation In: Anjum NA, Chan M-T, Umar S, eds. *Ascorbate-Glutathione Pathway and Stress Tolerance in Plants*. Dordrecht: Springer Netherlands, 303–322.

**Marulanda A, Barea JM, Azcón R**. **2009**. Stimulation of plant growth and drought tolerance by native microorganisms (AM Fungi and bacteria) from dry environments: Mechanisms related to bacterial effectiveness. *Journal of Plant Growth Regulation* **28**: 115–124.

**Masalha J, Kosegarten H, Elmaci Ö, Mengel K**. **2000**. The central role of microbial activity for iron acquisition in maize and sunflower. *Biology and Fertility of Soils* **30**: 433–439.

**Matyash V, Liebisch G, Kurzchalia T V., Shevchenko A, Schwudke D**. **2008**. Lipid extraction by methyl-tert-butyl ether for high-throughput lipidomics. *The Journal of Lipid Research* **49**: 1137–1146.

**Matysik J, Alia, Bhalu B, Mohanty P**. **2002**. Molecular mechanisms of quenching of reactive oxygen species by proline under stress in plants. *Current Science* **82**: 525–532.

**McCabe PF, Levine A, Meijer PJ, Tapon NA, Pennell RI**. **1997**. A programmed cell death pathway activated in carrot cells cultured at low cell density. *Plant Journal* **12**: 267–280.

**McLoughlin AJ**. **1994**. Controlled release of immobilized cells as a strategy to regulate ecological competence of inocula In: *Biotechnics/Wastewater*. Berlin, Heidelberg: Springer Berlin Heidelberg, 1–45.

**Medeiros MJL, Silva MMDA, Granja MMC, Júnior GDSES, Camara T, Willadino L**. **2015**. Effect of exogenous proline in two sugarcane genotypes grown *in vitro* under salt stress. *Acta biol. Colomb* **20**: 57–63.

**Meeks JC**. **1990**. Cyanobacterial-bryophyte associations In: Rai AN, ed. *CRC Handbook of Symbiotic Cyanobacteria*. CRC Press, Boca Raton, 43–63.

**Meeks JC, Campbell E, Summers M, Wong F**. **2002**. Cellular differentiation in the cyanobacterium *Nostoc punctiforme*. *Archives of Microbiology* **178**: 395–403.

**Meeks JC, Elhai J**. **2002**. Regulation of cellular differentiation in filamentous cyanobacteria in free-living and plant-associated symbiotic growth states. **66**: 94–121.

**Meeks JC, Enderlin CS, Joseph CM, Chapman JS, Lollar MWL**. **1985**. Fixation of [$^{13}$N] $N_2$ and transfer of fixed nitrogen in the *Anthoceros-Nostoc* symbiotic association. *Planta* **164**: 406–414.

**Meena KK, Sorty AM, Bitla UM, Choudhary K, Gupta P, Pareek A, Singh DP, Prabha R, Sahu PK, Gupta VK, Singh HB, Krishanani KK, Minhas PS**. **2017**. Abiotic stress responses and microbe-mediated mitigation in plants: The omics strategies. *Frontiers in Plant Science* **8**: 172.

**Mehta VB, Vaidya BS**. **1978**. Cellular and extracellular polysaccharides of the blue green alga *Nostoc*. *Journal of Experimental Botany* **29**: 1423–1430.

**Millaleo R, Reyes- Diaz M, Ivanov AG, Mora ML, Alberdi M**. **2010**. Manganese as essential and toxic element for plants: Transport, accumulation and resistance mechanisms. *Journal Of Soil Science And Plant Nutrition* **10**: 470–481.

**Mirsa S, Kaushik BD**. **1989**. Growth promoting substances of cyanobacteria, II. Detections of amino acids, sugars and auxin. *Proceedings of the Indian National Science Academy* **B55**: 499–504.

**Mishra S, Dubey RS**. **2006**. Heavy metal uptake and detoxification mechanisms in plants. *International Journal of Agricultural Research* **1**: 122–141.

**Mitsuhara I, Malik KA, Miura M, Ohashi Y**. **1999**. Animal cell-death suppressors Bcl-$x_L$ and Ced-9 inhibit cell death in tobacco plants. *Current Biology* **9**: 775-S1.

**Mittler R**. **2006**. Abiotic stress, the field environment and stress combination. *Trends in Plant Science* **11**: 15–19.

**Mittler R, Blumwald E**. **2010**. Genetic engineering for modern agriculture: Challenges and perspectives. *Annual Review of Plant Biology* **61**: 443–462.

**Montesinos ML, Herrero A, Flores E**. **1995**. Amino acid transport systems required for diazotrophic growth in the cyanobacterium *Anabaena* sp. strain PCC 7120. *Journal of Bacteriology* **177**: 3150–3157.

**Mordor Intelligence**. *Biofertilizers Market | Growth, Trends & Forecast (2019–2024)*. https://www.mordorintelligence.com/industry-reports/global-biofertilizers-market-industry. 12 Jun. 2019.

**Munns R**. **2010**. Approaches to identifying genes for salinity tolerance and the importance of timescale. *Methods in Molecular Biology (Clifton, N.J.)* **639**: 25–38.

**Munns R, Guo J, Passioura JB, Cramer GR**. **2000**. Leaf water status controls day-time but not daily rates of leaf expansion in salt-treated barley. *Functional Plant Biology* **27**: 949.

**Munns R, Schachtman D, Condon A**. **1995**. The significance of a two-phase growth response to salinity in wheat and barley. *Functional Plant Biology* **22**: 561.

**Munns R, Wallace PA, Teakle NL, Colmer TD**. **2010**. Measuring soluble ion concentrations ($Na^+$, $K^+$, $Cl^-$) in salt-treated plants In: Sunkar R, ed. *Plant Stress Tolerance*. Totowa, NJ: Humana Press, 371–382.

**Mustafiz A, Sahoo KK, Singla-Pareek SL, Sopory SK**. **2010**. Metabolic engineering of glyoxalase pathway for enhancing stress tolerance in plants. *Methods in molecular biology (Clifton, N.J.)* **639**: 95–118.

**Myers JA, Curtis BS, Curtis WR**. **2013**. Improving accuracy of cell and chromophore concentration measurements using optical density. *BMC Biophysics* **6**: 4.

**Nadeem SM, Zahir ZA, Naveed M, Ashraf M**. **2010**. Microbial ACC-Deaminase: Prospects and applications for inducing salt tolerance in plants. *Critical Reviews in Plant Sciences* **29**: 360–393.

**Naseem H, Bano A**. **2014**. Role of plant growth-promoting rhizobacteria and their exopolysaccharide in drought tolerance of maize. *Journal of Plant Interactions* **9**: 689–701.

**Natarajan SK, Zhu W, Liang X, Zhang L, Demers AJ, Zimmerman MC, Simpson MA, Becker DF**. **2012**. Proline dehydrogenase is essential for proline protection against hydrogen peroxide-induced cell death. *Free Radical Biology and Medicine* **53**: 1181–1191.

**Naureen Z, Price AH, Hafeez FY, Roberts MR**. **2009**. Identification of rice blast disease-suppressing bacterial strains from the rhizosphere of rice grown in Pakistan. *Crop Protection* **28**: 1052–1060.

**Nemhauser JL, Hong F, Chory J**. **2006**. Different plant hormones regulate similar processes through largely nonoverlapping transcriptional responses. *Cell* **126**: 467–475.

**Nguyen GN, Hailstones DL, Wilkes M, Sutton BG**. **2009**. Drought-induced oxidative conditions in rice anthers leading to a programmed cell death and pollen abortion. *Journal of Agronomy and Crop Science* **195**: 157–164.

**Nicolas M, Munns R, Samarakoon A, Gifford R**. **1993**. Elevated $CO_2$ improves the growth of wheat under salinity. *Functional Plant Biology* **20**: 349.

**Nilsson M, Rasmussen U, Bergman B**. **2006**. Cyanobacterial chemotaxis to extracts of host and nonhost plants. *FEMS Microbiology Ecology* **55**: 382–390.

**Nogales J, Gudmundsson S, Knight EM, Palsson BO, Thiele I**. **2012**. Detailing the optimality of photosynthesis in cyanobacteria through systems biology analysis. *Proceedings of the National Academy of Sciences of the United States of America* **109**: 2678–83.

**Obata T, Fernie AR**. **2012**. The use of metabolomics to dissect plant responses to abiotic stresses. *Cellular and Molecular Life Sciences* **69**: 3225–3243.

**Oldroyd GED, Dixon R**. **2014**. Biotechnological solutions to the nitrogen problem. *Current Opinion in Biotechnology* **26**: 19–24.

**Oliveira P, Martins N, Santos M, Couto N, Wright P, Tamagnini P**. **2015**. The *Anabaena* sp. PCC 7120 exoproteome: Taking a peek outside the box. *Life* **5**: 130–163.

**Oukarroum A, El Madidi S, Strasser RJ**. **2012**. Exogenous glycine betaine and proline play a protective role in heat-stressed barley leaves (*Hordeum vulgare* L.): A chlorophyll *a* fluorescence study. *Plant Biosystems - An International Journal Dealing with all Aspects of Plant Biology* **146**: 1037–1043.

**Ow SY, Noirel J, Cardona T, Taton A, Lindblad P, Stensjö K, Wright PC**. **2009**. Quantitative overview of $N_2$ fixation in *Nostoc punctiforme* ATCC 29133 through cellular enrichments and itraq shotgun proteomics. *Journal of Proteome Research* **8**: 187–198.

**Pandey P, Irulappan V, Bagavathiannan MV, Senthil-Kumar M**. **2017**. Impact of combined abiotic and biotic stresses on plant growth and avenues for crop improvement by exploiting physio-morphological traits. *Frontiers in Plant Science* **8**: 537.

**Park Y-G, Mun B-G, Kang S-M, Hussain A, Shahzad R, Seo C-W, Kim A-Y, Lee S-U, Oh KY, Lee DY, Lee I-J, Yun B-W**. **2017**. *Bacillus aryabhattai* SRB02 tolerates

oxidative and nitrosative stress and promotes the growth of soybean by modulating the production of phytohormones (R Aroca, Ed.). *PLOS ONE* **12**: e0173203.

**Passioura JB, Munns R**. **2000**. Rapid environmental changes that affect leaf water status induce transient surges or pauses in leaf expansion rate. *Functional Plant Biology* **27**: 941.

**Pavlů J, Novák J, Koukalová V, Luklová M, Brzobohatý B, Černý M**. **2018**. Cytokinin at the crossroads of abiotic stress signalling pathways. *International Journal of Molecular Sciences* **19**: 2450.

**Penninckx IA, Eggermont K, Terras FR, Thomma BP, De Samblanx GW, Buchala A, Métraux JP, Manners JM, Broekaert WF**. **1996**. Pathogen-induced systemic activation of a plant defensin gene in *Arabidopsis* follows a salicylic acid-independent pathway. *The Plant Cell* **8**: 2309–2323.

**Penrose DM, Glick BR**. **2001**. Levels of ACC and related compounds in exudate and extracts of canola seeds treated with ACC deaminase-containing plant growth-promoting bacteria. *Canadian Journal of Microbiology* **47**: 368–372.

**Penrose DM, Glick BR**. **2003**. Methods for isolating and characterizing ACC deaminase-containing plant growth-promoting rhizobacteria. *Physiologia Plantarum* **118**: 10–15.

**Perchlik M, Foster J, Tegeder M**. **2014**. Different and overlapping functions of *Arabidopsis* LHT6 and AAP1 transporters in root amino acid uptake. *Journal of Experimental Botany* **65**: 5193–5204.

**Pernil R, Picossi S, Herrero A, Flores E, Mariscal V**. **2015**. Amino acid transporters and release of hydrophobic amino acids in the heterocyst-forming cyanobacterium *Anabaena* sp. Strain PCC 7120. *Life* **5**: 1282–1300.

**Pernil R, Picossi S, Mariscal V, Herrero A, Flores E**. **2008**. ABC-type amino acid uptake transporters Bgt and N-II of *Anabaena* sp. strain PCC 7120 share an ATPase subunit and are expressed in vegetative cells and heterocysts. *Molecular Microbiology* **67**: 1067–1080.

**Petrov V, Hille J, Mueller-Roeber B, Gechev TS**. **2015**. ROS-mediated abiotic stress-induced programmed cell death in plants. *Frontiers in Plant Science* **6**: 1–16.

**Pham VT, Vu TN, Luong HT**. **2008**. Adoption and regulation of biofertiliser technology for rice production In: *ACIAR Proceedings No. 130, pp. 92-96, Canberra ACT*. Canberra, ACT: Australian Centre for International Agricultural Research, .

**Picossi S, Montesinos ML, Pernil R, Lichtlé C, Herrero A, Flores E**. **2005**. ABC-type neutral amino acid permease N-I is required for optimal diazotrophic growth and is repressed in the heterocysts of *Anabaena* sp. strain PCC 7120. *Molecular Microbiology* **57**: 1582–1592.

**Piszczek E, Gutman W**. **2007**. Caspase-like proteases and their role in programmed cell death in plants. *Acta Physiologiae Plantarum* **29**: 391–398.

**Porter JR, Semenov MA**. **2005**. Crop responses to climatic variation. *Philosophical Transactions of the Royal Society B: Biological Sciences* **360**: 2021–2035.

**Porter JR, Xie L, Challinor A, Cochrane K, Howden S, Iqbal MM, Lobell DB, Travasso MI, Aggarwal PK, Hakala K, Jordan J**. **2015**. Food security and food production systems In: 485–534.

**Posmyk MM, Janas KM**. **2007**. Effects of seed hydropriming in presence of exogenous proline on chilling injury limitation in *Vigna radiata* L. seedlings. *Acta Physiologiae Plantarum* **29**: 509–517.

**Prasanna R, Kumar A, Babu S, Chawla G, Chaudhary V, Singh S, Gupta V, Nain L, Saxena AK**. **2013**. Deciphering the biochemical spectrum of novel cyanobacterium-based biofilms for use as inoculants. *Biological Agriculture & Horticulture* **29**: 145–158.

**Prasanna R, Nain L, Tripathi R, Gupta V, Chaudhary V, Middha S, Joshi M, Ancha R, Kaushik BD**. **2008**. Evaluation of fungicidal activity of extracellular filtrates of cyanobacteria - Possible role of hydrolytic enzymes. *Journal of Basic Microbiology* **48**: 186–194.

**Prasanna R, Sood A, Jaiswal P, Nayak S, Gupta V, Chaudhary V, Joshi M, Natarajan C**. **2010**. Rediscovering cyanobacteria as valuable sources of bioactive compounds. *Applied Biochemistry and Microbiology* **46**: 119–134.

**Qin D, Wu H, Peng H, Yao Y, Ni Z, Li Z, Zhou C, Sun Q**. **2008**. Heat stress-responsive transcriptome analysis in heat susceptible and tolerant wheat (*Triticum aestivum* L.) by using Wheat Genome Array. *BMC Genomics* **9**: 432.

**Qin X, Zeevaart JAD**. **2002**. Overexpression of a 9-*cis*-epoxycarotenoid dioxygenase gene in *Nicotiana plumbaginifolia* increases abscisic acid and phaseic acid levels and enhances drought tolerance. *Plant Physiology* **128**: 544–551.

**Quarrie SA, Gulli M, Calestani C, Steed A, Marmiroli N**. **1994**. Location of a gene regulating drought-induced abscisic acid production on the long arm of chromosome 5A of wheat. *Theoretical and Applied Genetics* **89**: 794–800.

**Queval G, Noctor G**. **2007**. A plate reader method for the measurement of NAD, NADP, glutathione, and ascorbate in tissue extracts: Application to redox profiling during Arabidopsis rosette development. *Analytical Biochemistry* **363**: 58–69.

**Qurashi AW, Sabri AN**. **2012**. Bacterial exopolysaccharide and biofilm formation stimulate chickpea growth and soil aggregation under salt stress. *Brazilian Journal of Microbiology* **43**: 1183–1191.

**Rabea EI, Badawy MEI, Rogge TM, Stevens CV, Höfte M, Steurbaut W, Smagghe G**. **2005**. Insecticidal and fungicidal activity of new synthesized chitosan derivatives. *Pest Management Science* **61**: 951–960.

**Radzki W, Gutierrez Mañero FJ, Algar E, Lucas García JA, García-Villaraco A, Ramos Solano B**. **2013**. Bacterial siderophores efficiently provide iron to iron-starved tomato plants in hydroponics culture. *Antonie Van Leeuwenhoek* **104**: 321–330.

**Rais A, Jabeen Z, Shair F, Hafeez FY, Hassan MN**. **2017**. *Bacillus* spp., a bio-control agent enhances the activity of antioxidant defense enzymes in rice against *Pyricularia oryzae* (M-J Virolle, Ed.). *PLOS ONE* **12**: e0187412.

**Rais A, Shakeel M, Hafeez FY, Hassan MN**. **2016**. Plant growth promoting rhizobacteria suppress blast disease caused by *Pyricularia oryzae* and increase grain yield of rice. *BioControl* **61**: 769–780.

**Rasheed R, Ashraf MA, Hussain I, Haider MZ, Kanwal U, Iqbal M**. **2014**. Exogenous proline and glycinebetaine mitigate cadmium stress in two genetically different spring wheat (*Triticum aestivum* L.) cultivars. *Brazilian Journal of Botany* **37**: 399–406.

**Rasmussen S, Barah P, Suarez-Rodriguez MC, Bressendorff S, Friis P, Costantino P, Bones AM, Nielsen HB, Mundy J**. **2013**. Transcriptome responses to combinations of stresses in *Arabidopsis*. *Plant Physiology* **161**: 1783–1794.

**Rasmussen U, Bergman B, Johansson C**. **1994**. Early communication in the *Gunnera-Nostoc* symbiosis plant-induced cell differentiation and protein synthesis in the cyanobacterium. *Molecular Plant-Microbe Interactions* **7**: 696–702.

**Rathore S, Desai PM, Liew CV, Chan LW, Heng PWS**. **2013**. Microencapsulation of microbial cells. *Journal of Food Engineering* **116**: 369–381.

**Reape TJ, Brogan NP, McCabe PF**. **2015**. Mitochondrion and chloroplast regulation of plant programmed cell death In: Gunawardena AN, McCabe PF, eds. *Plant Programmed Cell Death*. Cham: Springer International Publishing, 33–53.

**Reape TJ, McCabe PF**. **2008**. Apoptotic-like programmed cell death in plants. *New Phytologist* **180**: 13–26.

**Reape TJ, McCabe PF**. **2010**. Apoptotic-like regulation of programmed cell death in plants. *Apoptosis* **15**: 249–256.

**Reape TJ, McCabe PF**. **2013**. Commentary: The cellular condensation of dying plant cells: Programmed retraction or necrotic collapse? *Plant Science* **207**: 135–139.

**Reape TJ, Molony EM, McCabe PF**. **2008**. Programmed cell death in plants: Distinguishing between different modes. *Journal of Experimental Botany* **59**: 435–444.

**Rejeb KB, Abdelly C, Savouré A**. **2014a**. How reactive oxygen species and proline face stress together. *Plant Physiology and Biochemistry* **80**: 278–284.

**Rejeb I, Pastor V, Mauch-Mani B**. **2014b**. Plant responses to simultaneous biotic and abiotic stress: Molecular mechanisms. *Plants* **3**: 458–475.

**Ren D-B, Yang Z-H, Liang Y-Z, Fan W, Ding Q**. **2013**. Effects of injection volume on chromatographic features and resolution in the process of counter-current chromatography. *Journal of Chromatography. A* **1277**: 7–14.

**Rentsch D, Hirner B, Schmelzer E, Frommer WB**. **1996**. Salt stress-induced proline transporters and salt stress-repressed broad specificity amino acid permeases identified

by suppression of a yeast amino acid permease-targeting mutant. *The Plant Cell* **8**: 1437–1446.

**Reynolds MP, Quilligan E, Aggarwal PK, Bansal KC, Cavalieri AJ, Chapman SC, Chapotin SM, Datta SK, Duveiller E, Gill KS, Jagadish KSV, Joshi AK, Koehler A-K, Kosina P, Krishnan S, Lafitte R, Mahala RS, Muthurajan R, Paterson AH, Prasanna BM, Rakshit S, Rosegrant MW, *et al.* 2016**. An integrated approach to maintaining cereal productivity under climate change. *Global Food Security* **8**: 9–18.

**Richert L, Golubic S, Guédès RL, Ratiskol J, Payri C, Guezennec J**. **2005**. Characterization of exopolysaccharides produced by cyanobacteria isolated from polynesian microbial mats. *Current Microbiology* **51**: 379–384.

**Rivero RM, Mestre TC, Mittler R, Rubio F, Garcia-Sanchez F, Martinez V**. **2014**. The combined effect of salinity and heat reveals a specific physiological, biochemical and molecular response in tomato plants: Stress combination in tomato plants. *Plant, Cell & Environment* **37**: 1059–1073.

**Robertson D**. **2013**. Modulating plant calcium for better nutrition and stress tolerance. *ISRN Botany* **2013**: 1–22.

**Robison MM, Griffith M, Pauls KP, Glick BR**. **2001**. Dual role for ethylene in susceptibility of tomato to *Verticillium* wilt. *Journal of Phytopathology* **149**: 385–388.

**Rock KL, Kono H**. **2008**. The inflammatory response to cell death. *Annual Review of Pathology: Mechanisms of Disease* **3**: 99–126.

**Rodriguez MM, Heyser JW**. **1988**. Growth inhibition by exogenous proline and its metabolism in saltgrass (*Distichlis spicata*) suspension cultures. *Plant Cell Reports* **7**: 305–308.

**Rodríguez H, Fraga R**. **1999**. Phosphate solubilizing bacteria and their role in plant growth promotion. *Biotechnology Advances* **17**: 319–339.

**Roesser M, Müller V**. **2001**. Osmoadaptation in bacteria and archaea: Common principles and differences. *Environmental Microbiology* **3**: 743–754.

**Rogers C, Oldroyd GED**. **2014**. Synthetic biology approaches to engineering the nitrogen symbiosis in cereals. *Journal of Experimental Botany* **65**: 1939–46.

**Rojo E, Martín R, Carter C, Zouhar J, Pan S, Plotnikova J, Jin H, Paneque M, Sánchez-Serrano JJ, Baker B, Ausubel FM, Raikhel NV**. **2004**. VPEγ exhibits a caspase-like activity that contributes to defense against pathogens. *Current Biology* **14**: 1897–1906.

**Rossi F, De Philippis R**. **2015**. Role of cyanobacterial exopolysaccharides in phototrophic biofilms and in complex microbial mats. *Life* **5**: 1218–1238.

**Sah SK, Reddy KR, Li J**. **2016**. Abscisic acid and abiotic stress tolerance in crop plants. *Frontiers in Plant Science* **7**.

**Saidi Y, Finka A, Muriset M, Bromberg Z, Weiss YG, Maathuis FJM, Goloubinoff P**. **2009**. The heat shock response in moss plants is regulated by specific calcium-permeable channels in the plasma membrane. *The Plant Cell* **21**: 2829–2843.

**Saikia S, Jain V**. **2007**. Biological nitrogen fixation with non-legumes: An achievable target or a dogma? *Current Science* **92**: 317–322.

**Saikia J, Sarma RK, Dhandia R, Yadav A, Bharali R, Gupta VK, Saikia R**. **2018**. Alleviation of drought stress in pulse crops with ACC deaminase producing rhizobacteria isolated from acidic soil of Northeast India. *Scientific Reports* **8**: 3560.

**Sakakibara H, Takei K, Hirose N**. **2006**. Interactions between nitrogen and cytokinin in the regulation of metabolism and development. *Trends in Plant Science* **11**: 440–448.

**Salamone IEGD, Hynes RK, Nelson LM**. **2005**. Role of cytokinins in plant growth promotion by rhizosphere bacteria In: *PGPR: Biocontrol and Biofertilization*. Dordrecht: Springer Netherlands, 173–195.

**Salazar-Cerezo S, Martínez-Montiel N, García-Sánchez J, Pérez-y-Terrón R, Martínez-Contreras RD**. **2018**. Gibberellin biosynthesis and metabolism: A convergent route for plants, fungi and bacteria. *Microbiological Research* **208**: 85–98.

**Salomé PA**. **2017**. Manganese is a plant's best friend: Intracellular Mn transport by the transporter NRAMP2. *The Plant Cell* **29**: 2953–2954.

**Sandhya V, Ali SKZ, Grover M, Reddy G, Venkateswarlu B**. **2009**. Alleviation of drought stress effects in sunflower seedlings by the exopolysaccharides producing *Pseudomonas putida* strain GAP-P45. *Biology and Fertility of Soils* **46**: 17–26.

**Sanmartín M, Jaroszewski L, Raikhel NV, Rojo E**. **2005**. Caspases. Regulating Death Since the Origin of Life. *Plant Physiology* **137**: 841–847.

**Santi C, Bogusz D, Franche C**. **2013**. Biological nitrogen fixation in non-legume plants. *Annals of Botany* **111**: 743–767.

**Santos R, Hérouart D, Sigaud S, Touati D, Puppo A**. **2001**. Oxidative burst in alfalfa-*Sinorhizobium meliloti* symbiotic interaction. *Molecular Plant-Microbe Interactions* **14**: 86–89.

**Saraf M, Jha CK, Patel D**. **2010**. The role of ACC deaminase producing PGPR in sustainable agriculture In: *Plant Growth and Health Promoting Bacteria*. Berlin, Heidelberg: Springer Berlin Heidelberg, 365–385.

**Satoh R, Nakashima K, Seki M, Shinozaki K, Yamaguchi-Shinozaki K**. **2002**. ACTCAT, a novel cis-acting element for proline- and hypoosmolarity-responsive expression of the ProDH gene encoding proline dehydrogenase in *Arabidopsis*. *Plant Physiology* **130**: 709–719.

**Savill J, Fadok V**. **2000**. Corpse clearance defines the meaning of cell death. *Nature* **407**: 784–8.

**Sayyed R, Jadhav H**. **2016**. Hydrolytic enzymes of rhizospheric microbes in crop protection. *MOJ Cell Science & Report* **3**: 135–136.

**Schachtman DP, Reid RJ, Ayling SM**. **1998**. Phosphorus uptake by plants: From soil to cell. *Plant Physiology* **116**: 447–453.

**Schalk IJ, Hannauer M, Braud A**. **2011**. New roles for bacterial siderophores in metal transport and tolerance: Siderophores and metals other than iron. *Environmental Microbiology* **13**: 2844–2854.

**Schoebitz M, López MD, Roldán A**. **2013**. Bioencapsulation of microbial inoculants for better soil-plant fertilization. A review. *Agronomy for Sustainable Development* **33**: 751–765.

**Schoebitz M, Simonin H, Poncelet D**. **2012**. Starch filler and osmoprotectants improve the survival of rhizobacteria in dried alginate beads. *Journal of Microencapsulation* **29**: 532–538.

**Schrock RR**. **2005**. Catalytic reduction of dinitrogen to ammonia at a single molybdenum center. *Accounts of Chemical Research* **38**: 955–962.

**Schwacke R, Grallath S, Breitkreuz KE, Stransky E, Stransky H, Frommer WB, Rentsch D**. **1999**. LeProT1, a transporter for proline, glycine betaine, and γ-amino butyric acid in tomato pollen. *The Plant Cell* **11**: 377–92.

**Sekar J, Raj R, Prabavathy VR**. **2016**. Microbial consortial products for sustainable agriculture: Commercialization and regulatory issues in India In: *Agriculturally Important Microorganisms*. Springer, Singapore, 107–132.

**Seneviratne G, Thilakaratne R, Jayasekara A, Seneviratne K, Padmathilake KRE, De Silva M**. **2009**. Developing beneficial microbial biofilms on roots of non legumes: A novel biofertilizing technique In: Khan MS, Zaidi A, Musarrat J, eds. *Microbial Strategies for Crop Improvement*. Berlin, Heidelberg: Springer Berlin Heidelberg, 51–62.

**Servet C, Ghelis T, Richard L, Zilberstein A, Savoure A**. **2012**. Proline dehydrogenase: A key enzyme in controlling cellular homeostasis. *Frontiers in Bioscience* **17**: 607–620.

**Shabala S**. **2009**. Salinity and programmed cell death: Unravelling mechanisms for ion specific signalling. *Journal of Experimental Botany* **60**: 709–712.

**Shahid MA, Balal RM, Pervez MA, Abbas T, Aqeel MA, Javaid MM, Garcia-Sanchez F**. **2014**. Exogenous proline and proline-enriched *Lolium perenne* leaf extract protects against phytotoxic effects of nickel and salinity in *Pisum sativum* by altering polyamine metabolism in leaves. *Turkish Journal of Botany* **38**: 914–926.

**Sharma SS, Dietz KJ**. **2006**. The significance of amino acids and amino acid-derived molecules in plant responses and adaptation to heavy metal stress. *Journal of Experimental Botany* **57**: 711–726.

**Sharma P, Gujral HS**. **2011**. Effect of sand roasting and microwave cooking on antioxidant activity of barley. *Food Research International* **44**: 235–240.

**Sharma P, Jha AB, Dubey RS, Pessarakli M**. **2012**. Reactive oxygen species, oxidative damage, and antioxidative defense mechanism in plants under stressful conditions. *Journal of Botany* **2012**: 1–26.

**Sharma SB, Sayyed RZ, Trivedi MH, Gobi TA**. **2013**. Phosphate solubilizing microbes: Sustainable approach for managing phosphorus deficiency in agricultural soils. *SpringerPlus* **2**: 587.

**Sharma SS, Schat H, Vooijs R**. **1998**. *In vitro* alleviation of heavy metal-induced enzyme inhibition by proline. *Phytochemistry* **49**: 1531–1535.

**Sharma S, Verslues PE**. **2010**. Mechanisms independent of abscisic acid (ABA) or proline feedback have a predominant role in transcriptional regulation of proline metabolism during low water potential and stress recovery. *Plant, Cell & Environment* **33**: 1838–1851.

**Shen J, Yuan L, Zhang J, Li H, Bai Z, Chen X, Zhang W, Zhang F**. **2011**. Phosphorus dynamics: From soil to plant. *Plant Physiology* **156**: 997–1005.

**Shetty K**. **1997**. Biotechnology to harness the benefits of dietary phenolics; focus on *Lamiaceae*. *Asia Pacific Journal of Clinical Nutrition* **6**: 162–171.

**Shetty K, Wahlqvist M**. **2004**. A model for the role of the proline-linked pentose phosphate pathway in phenolic phytochemical biosynthesis and mechanism of action for human health and environmental applications. *Asia Pacific Journal of Clinical Nutrition* **13**: 1–24.

**Shi L, Bielawski J, Mu J, Dong H, Teng C, Zhang J, Yang X, Tomishige N, Hanada K, Hannun YA, Zuo J**. **2007**. Involvement of sphingoid bases in mediating reactive oxygen intermediate production and programmed cell death in *Arabidopsis*. *Cell Research* **17**: 1030–1040.

**Shimizu S, Narita M, Tsujimoto Y**. **1999**. Bcl-2 family proteins regulate the release of apoptogenic cytochrome *c* by the mitochondrial channel VDAC. *Nature* **399**: 483–487.

**Sigma-Aldrich**. **2019**. *Growth Regulators - Plant Tissue Culture Protocol*. https://www.sigmaaldrich.com/technical-documents/protocols/biology/growth-regulators.html. 6 May 2019.

**Signorelli S, Arellano JB, Melø TB, Borsani O, Monza J**. **2013**. Proline does not quench singlet oxygen: Evidence to reconsider its protective role in plants. *Plant Physiology and Biochemistry* **64**: 80–83.

**da Silva Conceicão A, Marty-Mazars D, Raikhel NV, Marty F**. **1999**. The formation of the plant vacuolar system. In: Altman A, Ziv M, Izhar S, eds. Current Plant Science and Biotechnology in Agriculture. *Plant Biotechnology and In Vitro Biology in the 21st Century*. Dordrecht: Springer Netherlands, 369–372.

**Silvester WB, Parsons R, Watt PW**. **1996**. Direct measurement of release and assimilation of ammonia in the *Gunnera- Nostoc* symbiosis. *The New Phytologist* **132**: 617–625.

**Singh S, Kate BN, Banerjee UC**. **2005**. Bioactive compounds from cyanobacteria and microalgae: An overview. *Critical Reviews in Biotechnology* **25**: 73–95.

**Singh B, Mishra S, Bohra A, Joshi R, Siddique KHM**. **2018**. Crop phenomics for abiotic stress tolerance in crop plants In: Wani SH, ed. *Biochemical, Physiological and Molecular Avenues for Combating Abiotic Stress Tolerance in Plants*. Academic Press, 277–296.

**Singh B, Satyanarayana T**. **2011**. Microbial phytases in phosphorus acquisition and plant growth promotion. *Physiology and Molecular Biology of Plants* **17**: 93–103.

**Smirnoff N, Cumbes QJ**. **1989**. Hydroxyl radical scavenging activity of compatible solutes. *Phytochemistry* **28**: 1057–1060.

**Sohlenkamp C, Geiger O**. **2016**. Bacterial membrane lipids: Diversity in structures and pathways (F Narberhaus, Ed.). *FEMS Microbiology Reviews* **40**: 133–159.

**Stael S, Wurzinger B, Mair A, Mehlmer N, Vothknecht UC, Teige M**. **2012**. Plant organellar calcium signalling: An emerging field. *Journal of Experimental Botany* **63**: 1525–1542.

**Stal LJ**. **2012**. Cyanobacterial mats and stromatolites. *Springer* **Ecology of**: 65–125.

**Stankovich J, Gritti F, Stevenson P, Guiochon G**. **2013**. The impact of column connection on band broadening in very high pressure liquid chromatography. *Journal of Separation Science* **36**: 2709–2717.

**Stewart WDP**. **1963**. Liberation of extracellular nitrogen by two nitrogen-fixing blue-green algae. *Nature* **200**: 1020–1021.

**Stiens M, Schneiker S, Keller M, Kuhn S, Pühler A, Schlüter A**. **2006**. Sequence analysis of the 144-kilobase accessory plasmid *pSmeSM11a*, isolated from a dominant *Sinorhizobium meliloti* strain identified during a long-term field release experiment. *Applied and Environmental Microbiology* **72**: 3662–3672.

**Stratonovitch P, Semenov MA**. **2015**. Heat tolerance around flowering in wheat identified as a key trait for increased yield potential in Europe under climate change. *Journal of Experimental Botany* **66**: 3599–3609.

**Svennerstam H, Jämtgård S, Ahmad I, Huss-Danell K, Näsholm T, Ganeteg U**. **2011**. Transporters in *Arabidopsis* roots mediating uptake of amino acids at naturally occurring concentrations. *The New Phytologist* **191**: 459–467.

**Svenning MM, Eriksson T, Rasmussen U**. **2005**. Phylogeny of symbiotic cyanobacteria within the genus *Nostoc* based on 16S rDNA sequence analyses. *Archives of Microbiology* **183**: 19–26.

**Swarnalakshmi K, Prasanna R, Kumar A, Pattnaik S, Chakravarty K, Shivay YS, Singh R, Saxena AK**. **2013**. Evaluating the influence of novel cyanobacterial biofilmed biofertilizers on soil fertility and plant nutrition in wheat. *European Journal of Soil Biology* **55**: 107–116.

**Tabatabai MA**. **1994**. Soil Enzymes In: Bottomley PS, Angle JS, Weaver RW, eds. SSSA. *Methods of Soil Analysis: Part 2—Microbiological and Biochemical Properties*. Soil Science Society of America, .

**Tanaka T, Kawasaki K, Daimon S, Kitagawa W, Yamamoto K, Tamaki H, Tanaka M, Nakatsu CH, Kamagata Y**. **2014**. A hidden pitfall in the preparation of agar media undermines microorganism cultivability. *Applied and Environmental Microbiology* **80**: 7659–7666.

**Tarafdar JC, Yadav RS, Meena SC**. **2001**. Comparative efficiency of acid phosphatase originated from plant and fungal sources. *Journal of Plant Nutrition and Soil Science* **164**: 279–282.

**Tausz M, Šircelj H, Grill D**. **2004**. The glutathione system as a stress marker in plant ecophysiology: Is a stress-response concept valid? *Journal of Experimental Botany* **55**: 1955–1962.

**Taylor RC, Cullen SP, Martin SJ**. **2008**. Apoptosis: Controlled demolition at the cellular level. *Nature Reviews Molecular Cell Biology* **9**: 231–241.

**Terrón-Camero LC, Molina-Moya E, Sanz-Fernández M, Sandalio LM, Romero-Puertas MC**. **2018**. Detection of reactive oxygen and nitrogen species (ROS/RNS) during hypersensitive cell death In: De Gara L, Locato V, eds. *Plant Programmed Cell Death*. New York, NY: Springer New York, 97–105.

**Thomson KJ**. **2003**. World agriculture: Towards 2015/2030: An FAO perspective. *Land Use Policy* **20**: 375.

**Tripathi M, Munot HP, Shouche Y, Meyer JM, Goel R**. **2005**. Isolation and functional characterization of siderophore-producing lead- and cadmium-resistant *Pseudomonas putida* KNP9. *Current Microbiology* **50**: 233–237.

**Triveni S, Prasanna R, Shukla L, Saxena AK**. **2013**. Evaluating the biochemical traits of novel *Trichoderma*-based biofilms for use as plant growth-promoting inoculants. *Annals of Microbiology* **63**: 1147–1156.

**Trofimova MS, Andreev IM, Kuznetsov VV**. **1999**. Calcium is involved in regulation of the synthesis of HSPs in suspension-cultured sugar beet cells under hyperthermia. *Physiologia Plantarum* **105**: 67–73.

**Tsavkelova EA, Klimova SYu, Cherdyntseva TA, Netrusov AI**. **2006**. Microbial producers of plant growth stimulators and their practical use: A review. *Applied Biochemistry and Microbiology* **42**: 117–126.

**Tsegaye Y, Richardson CG, Bravo JE, Mulcahy BJ, Lynch DV, Markham JE, Jaworski JG, Chen M, Cahoon EB, Dunn TM**. **2007**. *Arabidopsis* mutants lacking

long chain base phosphate lyase are fumonisin-sensitive and accumulate trihydroxy-18:1 long chain base phosphate. *Journal of Biological Chemistry* **282**: 28195–28206.

**Tuteja N**. **2007**. Abscisic Acid and Abiotic Stress Signaling. *Plant Signaling & Behavior* **2**: 135–138.

**Ueda A, Shi W, Sanmiya K, Shono M, Takabe T**. **2001**. Functional analysis of salt-inducible proline transporter of barley roots. *Plant Cell Physiology* **42**: 1282–1289.

**Ueda A, Yamamoto-Yamane Y, Takabe T**. **2007**. Salt stress enhances proline utilization in the apical region of barley roots. *Biochemical and Biophysical Research Communications* **355**: 61–66.

**United Nations D of E and SA Population Division (2017)**. **2017**. *World Population Prospects: The 2017 Revision, Key Findings and Advance Tables.*

**Upadhyay A, Kochar M, Rajam MV, Srivastava S**. **2017**. Players over the surface: Unraveling the role of exopolysaccharides in zinc biosorption by fluorescent *Pseudomonas* Strain Psd. *Frontiers in Microbiology* **8**: 284.

**Upadhyay SK, Singh JS, Singh DP**. **2011**. Exopolysaccharide-producing plant growth-promoting rhizobacteria under salinity condition. *Pedosphere* **21**: 214–222.

**Vacca RA, de Pinto MC, Valenti D, Passarella S, Marra E, De Gara L**. **2004**. Production of reactive oxygen species, alteration of cytosolic ascorbate peroxidase, and impairment of mitochondrial metabolism are early events in heat shock-induced programmed cell death in tobacco bright-yellow 2 cells. *Plant Physiology* **134**: 1100–1112.

**Vacca RA, Valenti D, Bobba A, Merafina RS, Passarella S, Marra E**. **2006**. Cytochrome *c* is released in a reactive oxygen species-dependent manner and is degraded via caspase-like proteases in tobacco bright-yellow 2 cells en route to heat shock-induced cell death. *Plant Physiology* **141**: 208–219.

**Van Doorn WG, Woltering EJ**. **2005**. Many ways to exit? Cell death categories in plants. *Trends in Plant Science* **10**: 117–122.

**Van Loon LC, Bakker PAHM**. **2005**. Induced systemic resistance as a mechanism of disease suppression by rhizobacteria In: *PGPR: Biocontrol and Biofertilization*. Dordrecht: Springer Netherlands, 39–66.

**Van Zee K, Chen FQ, Hayes PM, Close TJ, Chen THH**. **1995**. Cold-specific induction of a dehydrin gene family member in barley. *Plant Physiology* **108**: 1233–1239.

**Vartapetian AB, Tuzhikov AI, Chichkova NV, Taliansky M, Wolpert TJ**. **2011**. A plant alternative to animal caspases: Subtilisin-like proteases. *Cell Death and Differentiation* **18**: 1289–1297.

**Verslues PE**. **2010**. Quantification of water stress-induced osmotic adjustment and proline accumulation for *Arabidopsis thaliana* molecular genetic studies In: Sunkar R,

ed. Methods in Molecular Biology. *Plant Stress Tolerance*. Totowa, NJ: Humana Press, 301–315.

**Verslues PE, Sharma S**. **2010**. Proline metabolism and its implications for plant-environment interaction. *The Arabidopsis Book / American Society of Plant Biologists* **8**: e0140.

**Verslues PE, Sharp RE**. **1999**. Proline accumulation in maize (*Zea mays* L.) primary roots at low water potentials. II. Metabolic source of increased proline deposition in the elongation zone. *Plant Physiology* **119**: 1349–1360.

**Vessey J**. **2003**. Plant growth promoting rhizobacteria as biofertilizers. *Plant and soil* **255**: 571–586.

**Vhangani LN, Van Wyk J**. **2013**. Antioxidant activity of Maillard reaction products (MRPs) derived from fructose-lysine and ribose-lysine model systems. *Food Chemistry* **137**: 92–98.

**Volk RB**. **2007**. Studies on culture age versus exometabolite production in batch cultures of the cyanobacterium *Nostoc insulare*. *Journal of Applied Phycology* **19**: 491–495.

**Vurukonda SSKP, Vardharajula S, Shrivastava M, SkZ A**. **2016**. Enhancement of drought stress tolerance in crops by plant growth promoting rhizobacteria. *Microbiological Research* **184**: 13–24.

**Vyas P, Gulati A**. **2009**. Organic acid production in vitro and plant growth promotion in maize under controlled environment by phosphate-solubilizing fluorescent *Pseudomonas*. *BMC Microbiology* **9**: 174.

**Wada N, Sakamoto T, Matsugo S**. **2013**. Multiple roles of photosynthetic and sunscreen pigments in cyanobacteria focusing on the oxidative stress. *Metabolites* **3**: 463–483.

**Waditee R, Hibino T, Tanaka Y, Nakamura T, Incharoensakdi A, Hayakawa S, Suzuki S, Futsuhara Y, Kawamitsu Y, Takabe T, Takabe T**. **2002**. Functional characterization of betaine/proline transporters in betaine-accumulating mangrove. *Journal of Biological Chemistry* **277**: 18373–18382.

**Walker V, Mills GA**. **1995**. Quantitative methods for amino acid analysis in biological fluids. *Annals of Clinical Biochemistry* **32**: 28–57.

**Walter J, Jentsch A, Beierkuhnlein C, Kreyling J**. **2013**. Ecological stress memory and cross stress tolerance in plants in the face of climate extremes. *Environmental and Experimental Botany* **94**: 3–8.

**Wang X**. **2001**. The expanding role of mitochondria in apoptosis. *Genes & development* **15**: 2922–2933.

**Wang XJ, Hsiao KC**. **1995**. Sugar degradation during autoclaving: Effects of duration and solution volume on breakdown of glucose. *Physiologia Plantarum* **94**: 415–418.

**Wang H, Li J, Bostock R, Gilchrist D**. **1996**. Apoptosis: A functional paradigm for programmed plant cell death induced by a host-selective phytotoxin and invoked during development. *The Plant Cell* **8**: 375–391.

**Wang Y, Loake GJ, Chu C**. **2013a**. Cross-talk of nitric oxide and reactive oxygen species in plant programed cell death. *Frontiers in Plant Science* **4**.

**Wang P, Lombi E, Zhao F-J, Kopittke PM**. **2016**. Nanotechnology: A new opportunity in plant sciences. *Trends in Plant Science* **21**: 699–712.

**Wang MC, Peng ZY, Li CL, Li F, Liu C, Xia GM**. **2008**. Proteomic analysis on a high salt tolerance introgression strain of *Triticum aestivum*/*Thinopyrum ponticum*. *Proteomics* **8**: 1470–1489.

**Wang J, Vanga S, Saxena R, Orsat V, Raghavan V**. **2018**. Effect of climate change on the yield of cereal crops: A review. *Climate* **6**: 41.

**Wang W, Vinocur B, Altman A**. **2003**. Plant responses to drought, salinity and extreme temperatures: towards genetic engineering for stress tolerance. *Planta* **218**: 1–14.

**Wang W, Vinocur B, Shoseyov O, Altman A**. **2004**. Role of plant heat-shock proteins and molecular chaperones in the abiotic stress response. *Trends in Plant Science* **9**: 244–252.

**Wang M, Zheng Q, Shen Q, Guo S**. **2013b**. The critical role of potassium in plant stress response. *International Journal of Molecular Sciences* **14**: 7370–7390.

**Wang X, Zhuang L, Shi Y, Huang B**. **2017**. Up-regulation of HSFA2c and HSPs by ABA contributing to improved heat tolerance in tall fescue and *Arabidopsis*. *International Journal of Molecular Sciences* **18**.

**Waraich EA, Ahmad R, Halim A, Aziz T**. **2012**. Alleviation of temperature stress by nutrient management in crop plants: a review. *Journal of soil science and plant nutrition* **12**: 221–244.

**Warren CR**. **2008**. Rapid measurement of chlorophylls with a microplate reader. *Journal of Plant Nutrition* **31**: 1321–1332.

**Watanabe A**. **1951**. Production in cultural solution of some amino acids by the atmospheric nitrogen-fixing blue-green algae. *Archives of Biochemistry and Biophysics* **34**: 50–55.

**Watanabe N, Lam E**. **2008**. *Arabidopsis* Bax Inhibitor-1: A rheostat for ER stress-induced programmed cell death. *Plant Signaling & Behavior* **3**: 564–566.

**Watanabe N, Lam E**. **2009**. Programmed cell death in plants: Apoptotic but not quite In: Dong Z, Yin X-M, eds. *Essentials of Apoptosis*. Totowa, NJ: Humana Press, 301–324.

**Wituszynska W, Karpinski S**. **2013**. Programmed cell death as a response to high light, UV and drought stress in plants In: Vahdati K, ed. *Abiotic Stress - Plant Responses and Applications in Agriculture*. InTech, .

**Wood CC, Islam N, Ritchie RJ, Kennedy IR**. **2001**. A simplified model for assessing critical parameters during associative $^{15}N_2$ fixation between *Azospirillum* and wheat. *Functional Plant Biology* **28**: 969.

**Wu Z, Guo L, Qin S, Li C**. **2012**. Encapsulation of *R. planticola* Rs-2 from alginate-starch-bentonite and its controlled release and swelling behavior under simulated soil conditions. *Journal of Industrial Microbiology & Biotechnology* **39**: 317–327.

**Wu Q, Jackson D**. **2018**. Detection of MAPK3/6 phosphorylation during hypersensitive response (HR)-associated programmed cell death in plants In: De Gara L, Locato V, eds. *Plant Programmed Cell Death*. New York, NY: Springer New York, 153–161.

**Xiao D, He H, Huang W, Oo TL, Wang A, He L-F**. **2018**. Analysis of mitochondrial markers of programmed cell death. *Methods in Molecular Biology (Clifton, N.J.)* **1743**: 65–71.

**Xu H, Xu W, Xi H, Ma W, He Z, Ma M**. **2013**. The ER luminal binding protein (BiP) alleviates $Cd^{2+}$-induced programmed cell death through endoplasmic reticulum stress-cell death signaling pathway in tobacco cells. *Journal of Plant Physiology* **170**: 1434–1441.

**Yadav R, Flowers TJ, Yeo AR**. **1996**. The involvement of the transpirational bypass flow in sodium uptake by high- and low-sodium-transporting lines of rice developed through intravarietal selection. *Plant, Cell and Environment* **19**: 329–336.

**Yamanouchi U, Yano M, Lin H, Ashikari M, Yamada K**. **2002**. A rice spotted leaf gene, *Spl7*, encodes a heat stress transcription factor protein. *Proceedings of the National Academy of Sciences* **99**: 7530–7535.

**Yancey PH**. **2001**. Water stress, osmolytes and proteins. *American Zoologist* **41**: 699–709.

**Yancey PH**. **2005**. Organic osmolytes as compatible, metabolic and counteracting cytoprotectants in high osmolarity and other stresses. *Journal of Experimental Biology* **208**: 2819–2830.

**Yang J, Liu X, Bhalla K, Kim CN, Ibrado AM, Cai J, Peng TI, Jones DP, Wang X**. **1997**. Prevention of apoptosis by Bcl-2: release of cytochrome *c* from mitochondria blocked. *Science* **275**: 1129–1132.

**Yeo AR, Yeo ME, Flowers TJ**. **1987**. The contribution of an apoplastic pathway to sodium uptake by rice roots in saline conditions. *Journal of Experimental Botany* **38**: 1141–1153.

**Yi Y, Huang W, Ge Y**. **2008**. Exopolysaccharide: A novel important factor in the microbial dissolution of tricalcium phosphate. *World Journal of Microbiology and Biotechnology* **24**: 1059–1065.

**You J, Hu H, Xiong L**. **2012**. An ornithine δ-aminotransferase gene OsOAT confers drought and oxidative stress tolerance in rice. *Plant Science* **197**: 59–69.

**Youle RJ, Strasser A**. **2008**. The BCL-2 protein family: Opposing activities that mediate cell death. *Nature Reviews Molecular Cell Biology* **9**: 47–59.

**Yurekli F, Porgali ZB, Turkan I**. **2004**. Variations in abscisic acid, indole-3-acetic acid, gibberellic acid and zeatin concentrations in two bean species subjected to salt stress. *Acta Biologica Cracoviensia Series Botanica* **46:201-212**: 12.

**Zavřel T, Sinetova M, Červený J**. **2015**. Measurement of chlorophyll *a* and carotenoids concentration in cyanobacteria. *Bio-Protocol* **5**: 1–5.

**Zeeshan M, Suhail S, Biswas D, Farooqui A, Arif JM**. **2010**. Screening of selected cyanobacterial strains for phycochemical compounds and biological activities *in vitro*. *Biochemical and Cellular Archives* **10**: 163–168.

**Zhang Y, Andralojc PJ, Hey SJ, Primavesi LF, Specht M, Koehler J, Parry MAJ, Halford NG**. **2008**. *Arabidopsis* sucrose non-fermenting-1-related protein kinase-1 and calcium-dependent protein kinase phosphorylate conserved target sites in ABA response element binding proteins. *Annals of Applied Biology* **153**: 401–409.

**Zhang M, Chen H, Li J, Pei Y, Liang Y**. **2010**. Antioxidant properties of tartary buckwheat extracts as affected by different thermal processing methods. *LWT - Food Science and Technology* **43**: 181–185.

**Zhang X-Z, Zhang Y-HP**. **2013**. Cellulases: Characteristics, sources, production, and applications In: *Bioprocessing Technologies in Biorefinery for Sustainable Production of Fuels, Chemicals, and Polymers*. Hoboken, NJ, USA: John Wiley & Sons, Inc., 131–146.

**Zhang B, Zhang T, Wang Q, Ren T**. **2015**. Microorganism-based monodisperse microcapsules: Encapsulation of the fungicide tebuconazole and its controlled release properties. *RSC Advances* **5**: 25164–25170.

**Zheng CJ, Yoo J-S, Lee T-G, Cho H-Y, Kim Y-H, Kim W-G**. **2005**. Fatty acid synthesis is a target for antibacterial activity of unsaturated fatty acids. *FEBS letters* **579**: 5157–5162.

**Zhu JK**. **2016**. Abiotic Stress Signaling and Responses in Plants. *Cell* **167**: 313–324.

**Zhu YP, Su ZW, Li CH**. **1989**. Growth-inhibition effects of oleic-acid, linoleic-acid, and their methyl-esters on transplanted tumors in mice. *Journal of the National Cancer Institute* **81**: 1302–1306.

**Zhu Z, Sun B, Xu X, Chen H, Zou L, Chen G, Cao B, Chen C, Lei J**. **2016**. Overexpression of *AtEDT1*/*HDG11* in Chinese kale (*Brassica oleracea* var. *alboglabra*) enhances drought and osmotic stress tolerance. *Frontiers in Plant Science* **7**: 1–16.

**Zulpa G, Zaccaro MC, Boccazzi F, Parada JL, Storni M**. **2003**. Bioactivity of intra and extracellular substances from cyanobacteria and lactic acid bacteria on “wood blue stain” fungi. *Biological Control* **27**: 345–348.

**Zuther E, Koehl K, Kopka J**. **2007**. Comparative metabolome analysis of the salt response in breeding cultivars of rice In: Jenks MA, Hasegawa PM, Jain SM, eds.

*Advances in Molecular Breeding Toward Drought and Salt Tolerant Crops*. Dordrecht: Springer Netherlands, 285–315.

**Zwack PJ, Rashotte AM**. **2015**. Interactions between cytokinin signalling and abiotic stress responses. *Journal of Experimental Botany* **66**: 4863–4871.